

2-1-2006

Evaluation of Displacements and Stresses in Horizontally Curved Beams

Ben T. Yen

Dongjoo Kim

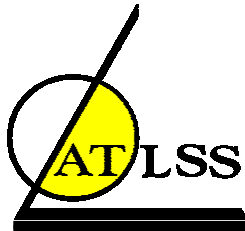
John L. Wilson

Follow this and additional works at: <http://preserve.lehigh.edu/engr-civil-environmental-atlss-reports>

Recommended Citation

Yen, Ben T.; Kim, Dongjoo; and Wilson, John L., "Evaluation of Displacements and Stresses in Horizontally Curved Beams" (2006).
ATLSS Reports. ATLSS report number 06-05:
<http://preserve.lehigh.edu/engr-civil-environmental-atlss-reports/74>

This Technical Report is brought to you for free and open access by the Civil and Environmental Engineering at Lehigh Preserve. It has been accepted for inclusion in ATLSS Reports by an authorized administrator of Lehigh Preserve. For more information, please contact preserve@lehigh.edu.



**Evaluation of Displacements and Stresses in
Horizontally Curved Beams**

by

Dongjoo Kim

Ben T. Yen

John L. Wilson

ATLSS Report No. 06-05

February 2006

**ATLSS is a National Center for Engineering Research
on Advanced Technology for Large Structural Systems**

117 ATLSS Drive
Bethlehem, PA 18015-4729

Phone: (610)758-3525
Fax: (610)758-5902

www.atlss.lehigh.edu
Email: inatl@lehigh.edu

Acknowledgments

The study presented in this report was supported by the federal Highway Administration (FHWA), Pennsylvania Infrastructure Technology Alliance (PITA) and the Engineering Research Center for Advanced Technology for Large Structural Systems (ATLSS) and the Department of Civil and Environmental Engineering of Lehigh University. The support is highly appreciated.

The advise and assistance of Dr. Charles G. Culver, consulting engineer; Dr. William J. Wright, FHWA; Mr. John M. Yadlosky, HDR, Inc. and Dr. Le-wu Lu and Dr. Alex Ostapenko of Lehigh University are sincerely acknowledged.

TABLE OF CONTENTS

	Page
Acknowledgments	ii
Table of Contents	iii
Abstract	1
1. Introduction	2
1.1 Background	2
1.2 Objective and Scope	3
2. Brief Review of Previous Studies	3
2.1 Background	3
2.2 Studies on Behavior of Arches	3
2.2.1 In-plane behavior of Arches	3
2.2.2 Out-of-Plane Behavior of Arches	5
2.3 The Behavior of Horizontally Curved Beam	7
2.3.1 Buckling Analyses of Horizontally Curved Beam	7
2.3.2 Amplification Analysis of Horizontally Curved Beam	9
2.3.3. Flexural Strength of Horizontally Curved Beam	12
3. Strain and Displacement Relationships	18
3.1 Introduction	18
3.2 Strains and Displacement	18
3.2.1 Assumptions	18
3.2.2 Longitudinal and Shear Strains	19
3.2.3 Comparison of longitudinal strains	26
4. Formulation of Differential Equations for Curved Beams	36
4.1 Introduction	36
4.2 Application of the Principle of Stationary Total Potential Energy to Curved Beams	36
4.3 Derivation of Components for Differential Equations	38
4.3.1 Variation of Strain Energy	38
4.3.2 Variation of Potential Energy due to Applied Load	48
4.3.3 Components of Governing Differential Equations and Boundary Forces	49
4.4 Differential Equations for Curved Beams	53
4.4.1 Linear and nonlinear Components	54
4.4.2 Exact Solution for Linear Differential Equations	61

4.4.3 Comparison of Results	62
4.5 Method of Solution by Incremental Total Lagrangian Formulation	63
4.5.1 Derivation of Equilibrium Equation in Incremental Formulation	63
4.5.2. Incremental Strain of Large Total Rotation	66
4.6 Formulation with Respect to One Reference Line	71
4.6.1 Reference Lines	71
4.6.2 Reference Line in Cross Section	72
4.6.3 Formulation for One-reference Line not in Cross Section	73
4.7 Effect of Sectional Deformation of I-Beams	74
4.7.1. Slander and Stocky Cross Sections	74
4.7.2 Strains from Deformation	75
4.7.3 Differential Equations Incorporating Sectional Deformation	78
5. Development of Line Element	101
5.1 Introduction	101
5.2 Shape Function and Displacement Field	101
5.2.1 Nodal Degree of Freedom	102
5.2.2 Shape Function	104
5.2.3 Nodal Load Vector	111
5.2.4 Calculation of Stresses	114
5.3. Stiffness Matrix	115
5.3.1 Linear, Stress and Geometric Stiffness Matrixes	115
5.3.2 Unbalanced Matrix	127
5.4 Numerical Solution Technique for Incremental Analysis	128
6. Load and Deflection Curves	145
6.1 Introduction	145
6.2 3D Finite Element Analysis (3DFEA)	145
6.2.1 Finite Element Model	145
6.2.2. Boundary Conditions	146
6.2.3 Comparison with Experimental Results	147
6.2.3.1 Comparison with Results of Beams Tested as a Pair	147
6.2.3.2 Comparison with Results of Beam Tested individually	148
6.3 Effects of Simplification of Strains	149
6.4 Comparison of Deflections by 3DFEA and FLEA	150
6.4.1 Doubly Symmetric Section	151
6.4.1.1 Load and Deflection response	151
6.4.1.2 Stress Distribution	152
6.4.2 Singly Symmetric Section (I-Shape)	153
6.4.3 Singly Symmetric Section about x-axis (Channel Section)	154
6.4.4 Unsymmetrical Cross Section	155
6.4.4.1 Deflections	155
6.4.4.2 Stress distribution	156
6.4.5 Comparison of Results form FLEA and Test Data	156
6.5 Evaluation of Exact Solution of Some Cases	156

7. Sources of Nonlinearity	208
7.1 Introduction	208
7.2 Large Rotation	208
7.3 P-Delta Effect	208
7.4 Sectional Deformation	209
8. Equation for Maximum Stress of Symmetrical I-Beams	220
8.1 Need for an Equation	220
8.2 Selection of independent Parameters	220
8.3 Parametric Study	222
8.4 Equation for Maximum Stress	222
9. Summary and Conclusion	239
9.1 Summary	239
9.2 Conclusions	240
9.3 Potential Future Work	241
10. References	242

Abstract

The formulation of large strains and displacement relations and equilibrium equations for evaluating nonlinear behavior of horizontally curved beams is presented. An examination is conducted to investigate the effects of approximations used in existing studies on curved beams. Justification of simplified approach is reviewed based on results from this study. Solution of equations is obtained by the development and use of a line element which incorporates the characteristics of displacement field and shape function of curved beams. The results from analysis are compared with those from three-dimensional finite element models of example beams and from test data. Beams with doubly and singly symmetric I-section, symmetric C-section and general cross sectional shape are examined. It is determined that analyses considering only small displacements and small rotations or large displacements and small rotations underestimate deflections and stresses. The effects of p-delta and cross sectional deformation on the load-displacement behavior and stresses of horizontally curved beams are investigated with the result that nonlinearity due to these effects is significant. An equation for maximum stress in curved beams is developed through a parametric study using the line element incorporating the effects of large displacements, large rotations and sectional deformations.

1. Introduction

1.1 Background

Current practice of designing horizontal curved beams is based on the concept of amplification. That is the application of a multiplication factor to stresses of straight beams provides adequate values for horizontally curved beams. This concept is derived from the correlation between flexural and shearing strengths in the plane of loading and out of plane, lateral torsional buckling of straight beams.

However, there is a strong difference between the behavior of straight and curved beams. For straight beams, the in plane behavior and the out of plane buckling are considered independent in the theory of small displacement. For horizontally curved beams, the primary loading is perpendicular to the plane of curvature of the beam. The vertical or out of plane displacement starts at the onset of load application. The vertical displacement is coupled with a horizontal displacement and twisting of the beam, making the behavior of the beam nonlinear with respect to the applied load. Therefore the evaluation of displacement and stresses of horizontally curved beams should take into consideration of vertical displacement, horizontal displacement and twisting of the beam simultaneously.

There have been numerous studies on the buckling and deflection of curved members. Some considered the in-plane and out of plane behavior of arches with the applied loads in the plane of the arch curvature. Some evaluated the out of plane nonlinear behavior of horizontally curved beams. All of these studies used various degrees of simplifying assumptions, rendering most of these studies as nonlinear analysis which incorporated large displacement in the derivation of governing differential equations. But none of these studies has been evaluated analytically for accuracy.

1.2 Objective and Scope

The objectives of this study are 1) to develop a procedure for examining the results of existing studies; 2) to formulate equations for calculating accurately the displacement and stresses of horizontally curved beams; and 3) to explore the development of an equation, or a set of equations for estimating maximum stresses in the beams for design purposes. To achieve these goals, the following steps were followed in the course of this research.

- (1) investigate the effects of simplifying assumptions used by previous studies.
- (2) derive equations for analyzing the effects of large displacement, of large rotation and of other possible factors such as cross sectional deformation and p-delta effect.
- (3) examine the difference equations for beams with doubly symmetric, singly symmetric and unsymmetrical or general cross section.
- (4) develop a procedure for solving the derived differential equations for displacement and stresses
- (5) check the accuracy of the solution

- (6) explore the procedure for developing an equation of maximum stresses in horizontally curved beams

2. Brief Review of Previous Studies

2.1 Background

Previous studies on curved structural members can be categorized as buckling analyses, deflection analyses and strength analyses of arches and horizontally curved beams. Arches and horizontally curved beams are characterized by the loading condition. When loads are applied in the plane of curvature, a member is an arch, and horizontally curved beam can be subjected to any load transverse to the plane. Arches resist applied loads by longitudinal axial forces and in-plane bending moments. Horizontally curved beams resist external loads by torsion about the longitudinal axis and bending about the strong axis and the weak axis. In analysis, whether a member is horizontally curved beam or an arch, the fundamental principles leading to the governing differential equations are the same. The formulation of equilibrium has to handle both in plane and out of plane forces. However, since previous studies were mainly conducted either on arches or curved beams, these studies are reviewed presently in two different section; behavior of arches and behavior of horizontally curved beams. Even though previous studies have dealt with several subjects in the analysis, the work on specific aspects are extracted and reviewed for convenience.

2.2 Studies on Behavior of Arches

2.2.1 In-plane behavior of Arches

Previous studies related to in-plane behavior of arches mostly concentrated on global buckling and large displacement behavior. Global buckling can be defined as when an arch moves from one equilibrium position to an adjacent equilibrium position without load change and cross-sectional deformation. The early stages of studies were done by Timoshenko and Gere (1961). They studied the instability of arches in bifurcation and snap-through buckling by formulations of equilibrium in-plane. Warping of the arch cross section was not considered. The bifurcation buckling associates with inextensibility of the centroidal axis under internal axial force whereas the snap-through buckling is analyzed assuming extensibility of the centroidal axis. Since the effects of prebuckling displacement are not included in their studies, the results are approximate solutions.

The nonlinear load and displacement behavior of deep circular arches was investigated by Huddleston (1968). Using a numerical analysis based on a standard predict-and-correction method, the characteristics of bifurcation and snap-through buckling were investigated. Several parametric studies were conducted to examine the effects of height-to-span ratio and of the compressibility on the load and in-plane large displacement.

Austin (1971) studied extensively the buckling of symmetric, circular, two-hinged arches with concentrated vertical load at the crown. It was found that the critical axial thrust for a symmetrically loaded arch is rather insensitive to the type of loading and unsymmetrical loading produces instability at a much lower value of thrust than does symmetrical loading. In 1976, he extended his previous study of in-plane buckling to include the prebuckling effects. Numerical analysis was conducted for an accurate solution of the “exact” theory in which moments were computed for the displaced configuration and displacement was computed from changes in curvature by a numerical technique considering large deflection. Comparison was made with the classical theory. The critical load was calculated in either a symmetrical buckling mode or an antisymmetrical buckling mode by both the “exact” method and the classical method. It was founded that the critical loads and the corresponding horizontal reactions for antisymmetrical modes are rather insensitive to the prebuckling displacements and the classical theory provides a practical way to estimate the buckling load for the symmetrical modes.

DaDeppo and Schmidt (1974) studied the buckling behavior subsequent to large prebuckling deflection of hingeless circular arches subjected to a downward load at the crown as well as their own dead weight. Euler’s nonlinear theory of the inextensible curved elastica was used. Interaction curves of the critical values of the two loads were developed. It was founded that non-shallow hingeless arches buckle in-plane by either asymmetrical sideway or symmetrical snap-through, depending on the relative magnitudes of the point load and the weight of the arches.

A study of the in-plane inelastic strength of steel arches was studied by Harrison (1970). He investigated analytically the ultimate strength of pin-ended parabolic steel arches of rectangular and circular cross section and considered the effects of the prebuckling deformation and the spread of yielding.

Shinke et al. (1975) investigated analytically the effects of residual stresses and initial crookedness on the in-plane strengths of arch ribs. He concluded that the effects of initial crookedness are not important on the in-plane strengths.

Pi and Trahair (1996) investigate the in-plane inelastic buckling and strength of circular steel I-section arches using a finite element method for nonlinear inelastic analysis. The elastic-plastic-strain-hardening character of steel was considered. The behavior of arches was analyzed by considering the effects of the arch curvature, large deformations, material inelasticity, initial crookedness, and residual stresses. Radial loads uniformly distributed along the arch axis, concentrated loads, and loads distributed along the horizontal projection of the arch were investigated. For the numerical method, the total Lagrangian formulation was used for nonlinear elastic large-deformation analysis.

2.2.2 Out-of-Plane Behavior of Arches

The early pioneering work for buckling analysis of thin-walled curved members was done by Saint-Venant (1843). Since then, a number of others have contributed to the understanding of behavior of curved beam. Timoshenko and Gere (1961) investigated the behavior of arches and derived linear differential equation for in-plane and out-of-plane buckling. In their analysis, warping effects was not considered.

A more through analysis was given by Vlasov (1961). He derived linear differential equations for curved member with a thin-walled open cross section subjected to warping. From a unit length of the line of centroid, six equilibrium equations were developed. Three differential equations are for the axial force and the perpendicular forces in the directions of axis normal to the longitudinal direction. The other three equations are for the moment about axis normal to the longitudinal axis and the total torsional moment. The total torsional moment is composed of St. Venant torsion and the warping torsion. In order to drive a set of differential equations, Eq. 2.1, Vlasov used constitutive relationship of straight beam, Eq. 2.2. He replaced kinematic terms of a straight beams with those of curved beams.

- Differential equation

$$E I_y \left(u^{iv} + 2 \frac{u''}{R^2} + \frac{u'}{R^4} \right) - f_x + \frac{f_z}{R} = 0 \quad 2.1a$$

$$-E \left(I_x + \frac{I_\omega}{R^2} \right) v^{iv} + \frac{G K_T}{R^2} v'' - \frac{E I_\omega}{R} \beta^{iv} + \frac{E I_x + G K_T}{R} \beta'' + f_y = 0 \quad 2.1b$$

$$- \left(E \frac{I_\omega}{R} \right) v^{iv} + \frac{E I_x + G K_T}{R} v'' - (E I_\omega) \beta^{iv} + G K_T \beta'' - E \frac{I_x}{R^2} \beta + m_z = 0 \quad 2.1c$$

(The terms in the equation are defined later in Chapter3)

- Constitutive relationship of a straight beam

$$F_z = E \varepsilon_z \quad 2.2a$$

$$M_x = E I_x \kappa_x \quad 2.2b$$

$$M_y = -E I_y \kappa_y \quad 2.2c$$

$$M_z = -E I_\omega \kappa_z'' + G K_T \kappa' \quad 2.2d$$

In comparison of the kinematic terms, corresponding strain and curvature terms are listed in Table 2.1. With the developed linear differential equation, Eq. 2.1, Vlasov derived buckling strength of curved member.

Vacharajittiphan and Porpan (1975) derived differential equations for analyzing the flexural-torsional buckling of curved member by extending the methods established for straight members and plane frames. They presented numerical solutions obtained by a finite integral method.

In all the aforementioned studies on out-of-plane buckling of curved members, the equilibrium approach was used. By the equilibrium method, a equilibrium equation is derived with the curved member in a displaced position. Another approach for obtaining equilibrium equation is to use the method of minimum total potential energy. In the energy method, equilibrium equation is obtained by the calculus of variation of total potential energy.

Yoo (1982) presented a set of stability equation derived by the energy approach in which the curvature terms of curved member were incorporated into the energy functional expressions. The closed form solutions of critical loads for some specific loading and boundary conditions were presented. Yoo compared his critical loads with those of Timoshenko and Vlasov. His results were different from Vlasov's and Timoshenko's in certain loading cases. Yoo suspected that the differential equation of Vlasov may have an error. The error may be attributed to the fact that Vlasov substituted the curvature terms of curved members (Table 2.1) into differential equation for stability of straight members. This contradiction triggered a lot of controversy and called attention to the study of curved members.

Trahair and Papangelis (1987, 1987a, and 1987b) published a series of papers on flexural-torsional buckling and experiment of buckling of curved members with doubly symmetric and mono-symmetric I-shaped cross section. Nonlinear expressions for the axial and shear strains were derived from the consideration of displaced geometry. By using the second variation of total potential energy, the buckling equation was obtained. Closed-form solutions were derived for critical loads for arches in uniform bending and uniform compression. They compared their numerical results with the results of Vlasov (1964), Yoo (1982) and the experiment, and showed that the experimental results agreed better with their theory than with those by Yoo (1982) and Vlasov (1964). They concluded that the disagreement is caused by the substitution of curvature terms of curved members into the governing equation of straight members.

Usami and Koh (1980) developed a large displacement theory in which the displacement components of an arbitrary point on a cross section was derived by integrating the nonlinear strain-displacement equation for thin-walled curved members expressed in the cylindrical coordinates. They derived the governing equation for lateral-torsional buckling of arches by using the derived strain-displacement relations through the Euler method in a variational principal.

Another important contribution on the buckling analysis on the curved members was made by Yang and Kuo (1987). Nonlinear differential equation based on the principle of virtual displacements was derived. The effect of curvature was included on the sectional properties, stress resultants and radial stresses. They showed that each of these factors affects the critical loads significantly and concluded that for correct results, all the factors have to be included in the buckling analysis of curved members under general loading.

Later the concept of radial stress factor used by Yang was critiqued by Kang (1994). Kang pointed out that the radial stress has to vanish when the fundamental assumption is considered. The mathematical interpretation of the assumption that cross sections do not distorted is that the transverse strain and shear strain in the plane of a cross section equal to zero. The radial stress associated with transverse strain and shear strain therefore has to vanish. Also he doubted about using two shear forces, noting that Saint Venant shear stresses do not form shear forces.

Pi and Trahair (1994) presented the effects of prebuckling in-plane displacement on the elastic buckling of mono-symmetric arches. Nonlinear displacement-strain relationship was derived by using position vectors. They studied the discrepancies among theoretical solution of Yoo (1984), Yang and Kuo (1986) and Rajasekaran and Padmanabhan (1989). They found out that an inconsistency in the treatments of the effects of the initial curvature and the using of different displacement transformations in deriving the displacement-strain relationship caused the discrepancies. The rotational transformation matrix $[T_R]$ has to satisfy the condition $[T_R] \times [T_R]^T = [T_R]^T \times [T_R] = I$ and $Det[T_R] = 1$.

2.3 The Behavior of Horizontally Curved Beam

Previous studies on the behavior of horizontally curved beams can be categorized as buckling analysis, amplification analysis and strength studies. Buckling analyses has been conducted to understand the buckling characteristic of small curvature curved beam through an eigenvalue analysis of the linear differential equations. Amplification analyses of horizontally curved beams have been conducted for studying nonlinear behavior of horizontally curved beam, either by the assumption of small deflection or large deflection. Strength studies have been made to investigate the relationship between the strength and curved beam parameters which includes the geometry of beam cross section, span length, boundary conditions and material properties. From parametric studies, simplified equations for estimating the strength have been derived for designing horizontally curved beams.

2.3.1 Buckling Analyses of Horizontally Curved Beams

When horizontally curved beams with small curvature are subjected to external forces out-of-plane of the curvature, out-of-plane displacement in the vertical direction and twist-rotation takes place (the in-plane displacement is not considered in many previous studies). This condition implies that bifurcation type of out-of-plane buckling can happen.

Ojalvo (1968) presented differential equations and boundary conditions from which the small-deflection static instability analysis for arbitrary cross beam sections and loads can be accomplished. He considered two different stages of equilibrium, the reference stage and the departure stage. These stages can be interpreted as the undeformed stage and the pre-buckling stage under load. Because of the displacement from the reference stage due to loading, the equilibrium equations at the stage of departure become nonlinear. In order to solve the nonlinear equilibrium equations,

linearization is necessary. Linearization was accomplished by the assumption that in the departure or perturbation stage, the variation from the reference stage is small and the coupling terms associated with the variation are negligible. Similar linearization can be applied to the associated boundary condition, displacement-curvature relations and the constitutive equations which relate the internal stress resultants to deformation quantities. The equilibrium equations in the departure stage are expressed as

$$\frac{d(\Delta F_x)}{dz} - k_z \Delta F_y - \bar{F}_y \Delta k_z + k_y \Delta F_z + \bar{F}_z \Delta k_y + \Delta f_x = 0 \quad \mathbf{2.3a}$$

$$\frac{d(\Delta F_y)}{dz} + k_z \Delta F_x + \bar{F}_x \Delta k_z - k_x \Delta F_z - \bar{F}_z \Delta k_x + \Delta f_y = 0 \quad \mathbf{2.3b}$$

$$\frac{d(\Delta F_z)}{dz} - k_y \Delta F_x - \bar{F}_x \Delta k_y + k_x \Delta F_y + \bar{F}_y \Delta k_x + \Delta f_z = 0 \quad \mathbf{2.3c}$$

$$\frac{d(\Delta M_x)}{dz} - k_z \Delta M_y - \bar{M}_y \Delta k_z + k_y \Delta M_z + \bar{M}_z \Delta k_y - \Delta f_y - \Delta m_x = 0 \quad \mathbf{2.3d}$$

$$\frac{d(\Delta M_y)}{dz} + k_z \Delta M_x + \bar{M}_x \Delta k_z - k_x \Delta M_z - \bar{M}_z \Delta k_x + \Delta f_x + \Delta m_y = 0 \quad \mathbf{2.3e}$$

$$\frac{d(\Delta M_z)}{dz} + k_y \Delta M_y + \bar{M}_y \Delta k_x - k_y \Delta M_x - \bar{M}_x \Delta k_y + \Delta m_z = 0 \quad \mathbf{2.3f}$$

Where k_x , k_y , k_z are curvature about x, y and z axis. F_x , F_y and F_z are concentrated internal forces. M_x , M_y and M_z are internal moments. f_x , f_y and f_z are distributed internal forces, and m_x , m_y and m_z are distributed internal moments. The terms with Δ and $\bar{}$ are quantities representing the departure stage and the reference stage. For the constitutive relationship between stress resultants and displacement, Equation, Eq.2.4 was used.

$$\Delta M_x = E I_x (\Delta k_x) \quad \mathbf{2.4a}$$

$$\Delta M_y = E I_y (\Delta k_y) \quad \mathbf{2.4b}$$

$$\Delta M_z = E K_T (\Delta k_z) \quad \mathbf{2.4c}$$

The curvature terms in Equation 2.4 and the longitudinal strains were derived by the position vector and the assumption of inextensibility conditions. The moment ΔM_z in Equation 2.4c represents the twisting moment about longitudinal direction. As seen in Eq. 2.4, only one sectional property, Saint-Venant constant K_T was used; warping torsion was not included. For thin-walled-open-sections, torsional resistance is primarily through warping torsional rigidity and has to be considered. This task was accomplished by McManus and Culver (1971).

McManus and Culver derived second order differential equations for thin-walled open sections under normal stresses due to bending and torsion by using the method of

Ojalvo. In the formulation by McManus, constitutive relationship of force-displacement was derived by replacing curvature terms of straight beam with corresponding curvature terms of curved beam, Table 2.1. For buckling analysis, the second order differential equations were linearized by ignoring higher-than first order terms under the assumption that the variation from the reference stage is small. In order to investigate the effect of the significant parameters on the critical loads, they conducted numerical analysis by using the finite difference method. They found that “the buckling loads determined for a curved beam loaded normal to the plane of curvature are essentially the same as those for a corresponding straight beam”.

Kang and Yoo (1992) studied buckling behavior of horizontally curved beam and found that large variations of torsional rigidity have little effect on the buckling strength of horizontally curved beams loaded by vertical bending moment and that the subtended angle is the main parameter for buckling strength. From the parametric study accomplished by finite element analysis, a reduction factor was developed which reduces the buckling strengths for an equivalent straight beam to that of the curved beam.

Pi and Trahair (1996) investigated the bifurcation buckling strength of horizontally curved beam. Using a strain-displacement relationship derived by position vector and the energy method, they derived nonlinear governing differential equations. Buckling load was obtained by solving nonlinear differential equation numerically. Among the numerical methods, finite element method was used. They compared their result with that of Yoo et al and found that their buckling moments are lower than those obtained by Kang and Yoo (1992), particularly for curved beam with large subtended angles.

2.3.2 Amplification Analysis of Horizontally Curved Beam

For any horizontally curved beam, the buckling load provides a reference but the analysis does not predict the behavior of curved beam. As soon as a load is applied to a curved beam, the beam undergoes out-of-plane displacement, rotation and associated in-plane displacement. Thus, bifurcation type of out-of-plane buckling does not happen. For a meaningful study on the strength of curved beam, amplification analysis characterized by load-deflection behavior is necessary. The amplification analysis of curved beams can be classified as small displacement-small rotation analysis, large displacement-small rotation analysis and large rotation-large displacement analysis.

A theoretical treatment on amplification analysis is traced back to Gottfeld (1932). He studied two beams supported by cross bracings and subjected to loads transverse to the plane of curvature on both beams. Umanskii (1948) investigated a curved beam with a doubly symmetrical I-shaped cross section with a more complete analysis which included the bi-moment in the I-beam which was supported by point-type bearings and was subjected to a load perpendicular to the plane of curvature.

Early big contribution on the amplification analysis of curved beams was made by Dabrowski (1968). He studied the bending and non-uniform torsion of continuous

curved beams of thin-walled, singly symmetric, open cross section. He derived the fundamental equations for the non-uniform torsion of curved box girders with non-deformable asymmetric cross section. He also derived closed-form solution to the first order linear differential equations for curved beam of thin-walled, non-deformable, doubly and mono symmetric open cross-section, with different loads perpendicular to the plane of curvature and “basic boundary condition”. The bi-moment and deflection of beams were derived by linear differential equations. Because his studies on load-deflection behavior were based on linear differential equations in which the out-of-plane displacement is not coupled with the in-plane of displacement, lateral displacement was not generated by the vertical loads.

All the studies done by Gottfeld (1932), Umanskii (1948) and Dabrowski (1969) were based on the assumption of small displacement and small rotation.

With the assumption of large displacements and small rotations, McManus (1971) derived linearized differential equation for curved beam by superimposing two differential equations representing the reference stage and the departure state. Using the “basic boundary system”, McManus investigated the amplification behavior of horizontally curved beams under flexural bending and bi-moment loads. He interpreted restraint provided by lateral bracing in bridge system as a bi-moment loading to a beam. With various combination of vertical bending moment and bi-moment and different curvature of beams, several numerical case studies were conducted by using the finite difference method. He compared his results with those of Dabrowski and showed that the lateral deflection and lateral bending moment occurred immediately upon loading of a curved beam and grew nonlinearly and quite rapidly as the magnitude of load increased. He also showed that the flange stresses caused by bi-moment were higher than those computed by linear analysis. To take into account the results that the angle of twist and the bi-moment increased nonlinearly as the applied end moment was increased, he developed an amplification factor.

$$Amp = \frac{1 - 0.86M^* + 0.4M^{*2}}{1 - M^*} \quad 2.5$$

Where:

$$M^* = \frac{M_x}{(M_{cr})_{st}} \quad 2.6a$$

$$(M_{cr})_{st} = \frac{\pi}{L} \sqrt{E I_y \left(\pi^2 \frac{E I_\omega}{L^2} + G K_T \right)} \quad 2.6b$$

This amplification factor can be applied to the bi-moment at the mid-span and at the end sections, M_ω , and to the lateral bending moment, M_{y2} .

$$M_{\omega} = -R\eta \left[M_L \left(\frac{\sin \varphi}{\sin \Gamma} - \frac{\sinh(k R \varphi)}{\sin(k L)} \right) + M_R \left(\frac{\sin \varphi'}{\sin \Gamma} - \frac{\sinh(k R \varphi')}{\sin(k L)} \right) \right] \quad 2.8a$$

$$M_{y2} = \beta_1 M_{x1} + \nu_1 M_{z1} \quad 2.8b$$

$$k = \sqrt{\frac{G K_T}{E I_{\omega}}} \quad \eta = \frac{1}{1 + (k R)^2} \quad 2.8c$$

The notations in the Eq. 2.8 are shown in Figures 2.1 and 2.2. The subscript 1 and 2 in Eq. 2.8b indicate the quantities at the reference stage and the departure stage. Equation 2.8b is the simplified equation derived by using the direction cosine. The fundamental assumption and its application will be presented in next section for strength analysis.

A series of extensive investigations on the behavior of horizontally curved beam considering large rotations and large displacements was made by Fukumoto and Nishida (1981). They derived second-order equilibrium equations for curved beams based on the nonlinear strains derived by adopting assumption for classical thin-walled open section. By using a transfer matrix, they presented the nonlinear elastic loads and deflection of a curved beam with the basic boundary condition and under a point load and constant moment. Six welded, curved I-beams were tested under point loading to investigate the load and deflection behavior and the ultimate load. The ratio of span length to radius, L/R , was a parameter of study. They compared their test results and the results of their large-displacement analysis. The agreement was quite good. The interesting phenomenon of their analytical result is the lateral deflection. As the lateral deflection at the mid-span increased with load and became large, the direction of lateral displacement was reversed. This phenomenon has been used for checking the outcome of many subsequent finite element analyses by others. It is noted that in the formulation by Fukumoto and Nishida, the effects of curvature on the sectional properties, e.g. $R/(R-x)$ were not included and only doubly symmetric cross section was considered.

Gendy (1992) conducted a study for developing equation based on one reference line for curved beams. He developed a finite element formulation for non-symmetric cross sections based on generalized strains. Rotation about the radial axis and the vertical axis were treated independently with vertical and lateral displacement. His numerical results were compared with those generated from strains used by Yoo (1980) for doubly symmetric cross sections. In order to use the strains of doubly symmetric cross sections for non-symmetric cross sections, transformation was needed: from two-reference lines to one-reference line. He used rigid body rotation for transformation, which is not generally applicable. Furthermore, even though single reference line formulation is derived based on the generalized strain, transformations for radial and vertical displacements are still needed.

With the assumption of large displacement and small rotation, Kang and Yoo (1994) developed equilibrium differential equations using the nonlinear strains that were developed from similar procedure by Usami and Roh (1980). In the formulation of finite line element to solve the equations and to investigate the large deflection behavior of horizontally curved beams, Kang and Yoo used the theory of Total Lagrange. In order to simplify the complexity of nonlinear strains associated with large rotations, conventionally only the first term of Taylor's expansion of trigonometric functions is used. On the other hand, they used the first and second term to improve accuracy of their differential equation.

Another important contribution to the static analysis of horizontally curved beams was made by Pi and Trahair (1996). They investigated the second-order coupling between the vertical and horizontal deflection and twist rotation in the nonlinear range of behavior of doubly symmetric cross section. By using a finite line element formulation base on the nonlinear strains developed from the position vector, they studied the linear and nonlinear elastic equilibrium of horizontally curved I-beam under vertical loading. They found that when the curvature of a curved beam is small and the beam is nearly straight, the primary coupling is small and bending is the major action. If the curvature of curved beam is not small, torsion is a major component of deflection. The nonlinear behavior develops very early and no flexural torsional buckling behaviors occur.

Most of the previous amplification analyses were on doubly symmetric cross sections. In the cases of large displacement and rotation analysis, consideration of singly or general cross section were very rare. Because of the complexity of the nonlinear differential equations, simplification was always made for solution. However little study on the effect of simplification on the behavior of horizontally curved beam was conducted. Nor was the contribution of sectional deformation or P- Δ effect on load-deflection behavior included in any of these previous studies.

2.3.3. Flexural Strength of Horizontally Curved Beam

No guideline or equation for design of curved beam is based on the ultimate carrying capacity of these beams. Buckling and limiting stresses are the references. The current AASHTO Guide Specifications provide equation for computing the flexural stress of horizontally curved beams with rectangular flanges and a vertical or inclined web attached at mid-width of the top flange. The span length is between lateral bracing points. For design load, factored constant moment and bi-moment at the end sections are considered. The equations for curved beams are modified from that for an equivalent straight beam by using the reduction factors. Two reduction factors, $\bar{\rho}_b \bar{\rho}_w$ and $\rho_b \rho_w$, are specified for compact and non-compact cross sections.

For a Compact section:

$$F_{cr} = F_{bs} \bar{\rho}_b \bar{\rho}_w \tag{2.9}$$

Where:

$$F_{bs} = F_y (1 - 3\lambda^2) \quad 2.10$$

$$\lambda = \frac{1}{\pi} \frac{L}{b} \sqrt{\frac{F_y}{E}} \quad 2.11$$

$$\bar{\rho}_b = \frac{1}{1 + \frac{12L}{b_f} \left(1 + \frac{2L}{b_f}\right) \left(\frac{L}{R} - 0.01\right)^2} \quad 2.12a$$

$$\bar{\rho}_w = 0.95 + 18 \left(0.1 - \frac{L}{R}\right)^2 + \frac{f_l}{f_b} \frac{\left(0.3 - 1.2 \frac{L}{R} \frac{L}{b_f}\right)}{1 + \frac{12L}{b_f} \left(1 + \frac{2L}{b_f}\right) \left(\frac{L}{R} - 0.01\right)^2} \quad 2.12b$$

$$\bar{\rho}_b \bar{\rho}_w \leq 1.0 \quad 2.12c$$

F_{bs} is ultimate bending stress of a curved beam compression flange

F_{cr} is maximum average stress in curved flange

ρ_b is curved beam reduction factor to account for bending

ρ_w is curved beam reduction factor to account for warping

L = distance between brace points

R = radius of curvature

f_l = total factored lateral flange bending stress

f_b = factored average flange stress

For a non-compact section:

$$F_{cr} = F_{bs} \rho_b \rho_w \quad 2.13$$

where:

$$\rho_b = \frac{1}{1 + \frac{L}{R} \frac{12L}{b_f}} \quad 2.14a$$

$$\rho_{w1} = \frac{1}{1 - \frac{f_l}{f_b} \left(1 - \frac{12L}{75b_f}\right)} \quad 2.14b$$

$$\rho_{w2} = \frac{0.95 + \frac{\frac{12L}{b_f}}{30 + 8000 \left(0.1 - \frac{L}{R}\right)^2}}{1 + 0.6 \frac{f_l}{f_b}} \quad 2.14c$$

when: $\frac{f_l}{f_b} \geq 0$, $\rho_w = \rho_{w1}$ or ρ_{w2} , whichever is smaller

when: $\frac{f_l}{f_b} \leq 0$, $\rho_w = \rho_{w1}$

These flexural design criteria are based on the analytical work of McManus (1971) who developed an amplification model based on small rotation and large displacement. He conducted a parametric study for the relationship between sectional properties and flange stress with warping moment increased by amplification factors. In the derivation of the reduction factors, secondary moment (lateral bending moment) was considered. Lateral bending moment generated by the coupling effect was calculated by the simplified Equation 2.8b. The un-simplified or complete form of Equation 2.8b is Equation 2.15.

$$M_{y2} = \beta_2 M_{x1} + v_2 M_{z1} \quad 2.15$$

Where v_2 and β_2 are displacement and rotation calculated from the departure stage, Figure 2.2. The symbols v_1 and β_1 in Eq. 2.8b are displacement and rotation obtained from the reference stage. With this approximation, the coupling between in-plane displacement and out-of-displacement is eliminated. This approximation is valid within small rotation and small displacement.

An interaction formula for allowable stress design of horizontally curved I-beams was proposed by the Hanshin Expressway Public Corporation of Japan (1988).

$$\frac{f_b}{F_{sa}\psi_1} + \frac{f_w}{F_{ua}} \leq 1.0 \quad 2.16$$

Where $F_{sa}\psi_1$ is the allowable lateral torsional buckling stress, F_{ua} is the allowable upper limit flexural stress and f_b and f_w are bending and warping stress. This equation represents interaction between the warping stress and lateral buckling strength of the beam which is reduced by the curvature effect. The specification is derived from the theoretical and experimental study of Nakai et al (1988).

Fukumoto and Nishida (1985) presented an approximate strength equation based on the second order deflection of the compression flange. The equation takes into consideration the plastic moment capacity, the elastic buckling moment of equivalent straight and the elastic buckling load with respect to weak axis of the curved beam.

Yoo and Davidson (1996) proposed an interaction equation based on the static analysis of I-shape beams under vertical end-moments. This equation can be used for singly symmetric composite and non-composite I-shape in both the positive and negative region of beam bending moment. For compact sections, complete plastification is the

limit and for non-compact section, first yielding at mid-span or end-section is the reference.

As a summary of the review on previous studies, it is determined that although a number of buckling analyses related to in-plane and out-of-plane behavior of curved members have been conducted, investigation considering large rotation and large displacement of horizontally curved beams is needed. The treatment of the nonlinear terms in the strains is inconsistent, and no numerical study on this effect has been done. For horizontally curved beams with moderate curvature, the behavior is not governed by the buckling phenomenon but by the relatively large out of plane and lateral deflection or the flange stresses. An adequate procedure for calculating flange stresses associated with large displacement, large rotation and cross sectional deformation is needed.

Table 2.1 the longitudinal strain and curvature of straight and curved beams

	ϵ_z	κ_x	κ_y	κ_z
Straight Beam	w'	$-v''$	u''	β'
Curved Beam	$w' - \frac{u}{R}$	$-v'' + \frac{\beta}{R}$	$u'' + \frac{u}{R^2}$	$-\beta' - \frac{v'}{R}$

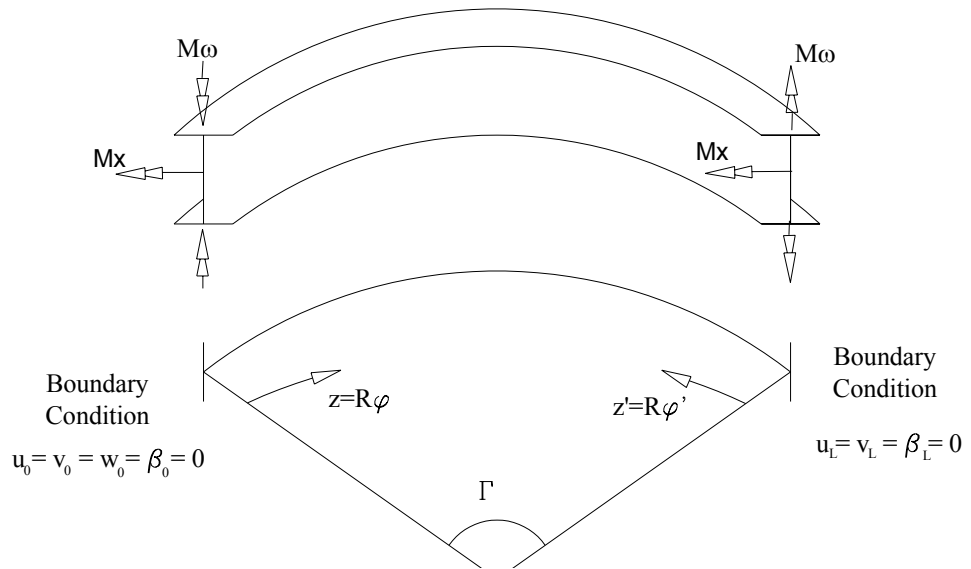


Figure2.1. the curved beam subjected with constant moment and bi-moment with basic boundary condition system.

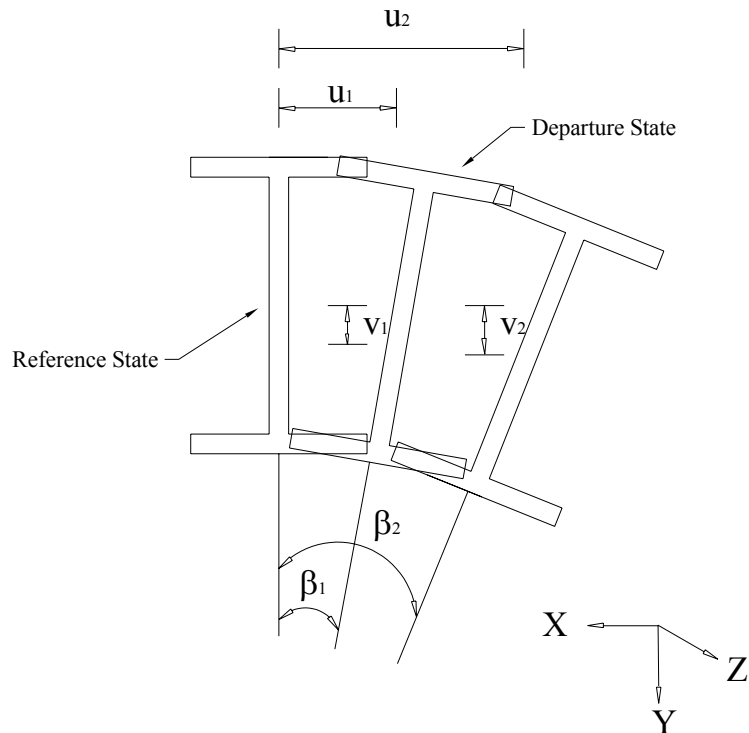


Figure 2.2 the deflection of the beam in x, y and z direction and twist rotation

3. Strain and displacement relationship

3.1 Introduction

In the previous chapter, literature on the analysis of a curved member was reviewed. Many studies on the behavior of horizontally curved beams dealt with the buckling strength. Since horizontally curved beams subjected to vertical loads sustain vertical, horizontal and rotation of beam cross sections, the behavior is three dimensional and nonlinear even in the elastic range of material properties. As soon as an external force is applied to a curved beam, all displacements take place. Bifurcation type of buckling does not happen. Therefore it is necessary to study the behavior of horizontally curved beams based on an analysis considering large displacement and rotation. This task can be started with developing the relationship between strains and displacements of the beams. Because of the coupling between displacement and twist (rotation of cross sections), complex nonlinear strain-displacement relation is inevitable. The development of a strain and displacement relationship for the spatial behavior of a horizontally curved beam with an arbitrary prismatic cross section is accomplished by conducting the following two stages.

- a) The development of the kinematics and strain-displacement relationship which include fourth order terms of displacement and strains. In this stage, no approximation is attempted.
- b) The simplification of the complex fourth-order strain equation based on different levels of approximation.

3.2 Strains and Displacement

3.2.1 Assumptions

In order to derive a strain-displacement relationship, several assumptions are adopted in the present study, and are listed below.

1. The shear strains due to change of normal stresses (flexural and warping normal stresses) are negligibly small.
2. The displacements are finite.
3. The thin-walled cross section retains its original shape (cross sectional deformation is treated in Chapter 4)
4. The span length of beam is much larger than any cross sectional dimension.
5. Shear strains in planes normal to the middle surface of the thin wall can be neglected.

The longitudinal displacement of the reference line of the beam cross section can be derived by the assumption 5. The displacement at any point on the beam cross section can be expressed in terms of the reference line displacement and rigid cross sectional rotation and warping, based on the assumption that the cross section retains its shape.

3.2.2 Longitudinal and Shear Strains

A cross section of a curved beam is shown in Fig 3.1. The general strain-displacement relations, in curvilinear coordinate system, are given by the following equations [73].

$$\varepsilon_x = \frac{\partial u}{\partial x} + \frac{1}{2} \left[\left(\frac{\partial u}{\partial x} \right)^2 + \left(\frac{\partial w}{\partial x} \right)^2 + \left(\frac{\partial v}{\partial x} \right)^2 \right] \quad 3.1a$$

$$\varepsilon_y = \frac{\partial v}{\partial y} + \frac{1}{2} \left[\left(\frac{\partial u}{\partial y} \right)^2 + \left(\frac{\partial w}{\partial y} \right)^2 + \left(\frac{\partial v}{\partial y} \right)^2 \right] \quad 3.1b$$

$$\varepsilon_z = \left(\frac{R}{R-x} \right) \frac{\partial w}{\partial z} - \frac{u}{R-x} + \frac{1}{2} \left(\frac{R}{R-x} \right)^2 \left[\left(\frac{\partial u}{\partial z} + \frac{w}{R} \right)^2 + \left(\frac{\partial w}{\partial z} - \frac{u}{R} \right)^2 + \left(\frac{\partial v}{\partial z} \right)^2 \right] \quad 3.1c$$

$$\varepsilon_{zy} = \frac{\partial w}{\partial y} + \frac{R}{R-x} \frac{\partial v}{\partial z} + \left[\frac{R}{R-x} \frac{\partial u}{\partial y} \frac{\partial u}{\partial z} + \frac{w}{R-x} \frac{\partial u}{\partial y} + \frac{R}{R-x} \frac{\partial w}{\partial y} \frac{\partial w}{\partial z} - \frac{u}{R-x} \frac{\partial w}{\partial y} + \frac{R}{R-x} \frac{\partial v}{\partial y} \frac{\partial v}{\partial z} \right] \quad 3.1d$$

$$\varepsilon_{xy} = \frac{\partial v}{\partial x} + \frac{\partial u}{\partial y} + \left[\frac{\partial u}{\partial x} \frac{\partial u}{\partial y} + \frac{\partial v}{\partial x} \frac{\partial v}{\partial y} + \frac{\partial w}{\partial x} \frac{\partial w}{\partial y} \right] \quad 3.1e$$

$$\varepsilon_{zx} = \frac{R}{R-x} \frac{\partial u}{\partial z} + \frac{w}{R-x} + \frac{\partial w}{\partial x} + \left[\frac{R}{R-x} \frac{\partial u}{\partial x} \frac{\partial u}{\partial z} + \frac{w}{R-x} \frac{\partial u}{\partial x} + \frac{R}{R-x} \frac{\partial w}{\partial x} \frac{\partial w}{\partial z} - \frac{u}{R-x} \frac{\partial w}{\partial x} + \frac{R}{R-x} \frac{\partial v}{\partial x} \frac{\partial v}{\partial z} \right] \quad 3.1f$$

Where u , v and w are the displacement in the horizontal, vertical and longitudinal direction of an arbitrary point (x, y, z) of the cross section; ε_x , ε_y , ε_z are normal strains; ε_{xy} , ε_{zx} and ε_{zy} are the shear strains and R is the radius of curvature of the beam.

From the assumption that span length is much larger than any cross sectional dimension, it is implied that the displacement of u and v are much large than w and nonlinear terms associated with derivation of longitudinal displacement can be ignored. Thus, Eq. 3.1 can be expressed as the following equation.

$$\varepsilon_x = \frac{\partial u}{\partial x} + \frac{1}{2} \left[\left(\frac{\partial u}{\partial x} \right)^2 + \left(\frac{\partial v}{\partial x} \right)^2 \right] \quad 3.2a$$

$$\varepsilon_y = \frac{\partial v}{\partial y} + \frac{1}{2} \left[\left(\frac{\partial u}{\partial y} \right)^2 + \left(\frac{\partial v}{\partial y} \right)^2 \right] \quad 3.2b$$

$$\varepsilon_z = \left(\frac{R}{R-x} \right) \frac{\partial w}{\partial z} - \frac{u}{R-x} + \frac{1}{2} \left(\frac{R}{R-x} \right)^2 \left[\left(\frac{\partial u}{\partial z} + \frac{w}{R} \right)^2 + \left(\frac{u}{R} \right)^2 + \left(\frac{\partial v}{\partial z} \right)^2 \right] \quad 3.2c$$

$$\varepsilon_{zy} = \frac{\partial w}{\partial y} + \frac{R}{R-x} \frac{\partial v}{\partial z} + \left[\frac{R}{R-x} \frac{\partial u}{\partial y} \frac{\partial u}{\partial z} + \frac{w}{R-x} \frac{\partial u}{\partial y} + \frac{R}{R-x} \frac{\partial v}{\partial y} \frac{\partial v}{\partial z} \right] \quad 3.2d$$

$$\varepsilon_{xy} = \frac{\partial v}{\partial x} + \frac{\partial u}{\partial y} + \left[\frac{\partial u}{\partial x} \frac{\partial u}{\partial y} + \frac{\partial v}{\partial x} \frac{\partial v}{\partial y} \right] \quad 3.2e$$

$$\varepsilon_{zx} = \frac{R}{R-x} \frac{\partial u}{\partial z} + \frac{w}{R-x} + \frac{\partial w}{\partial x} + \left[\frac{R}{R-x} \frac{\partial u}{\partial x} \frac{\partial u}{\partial z} + \frac{w}{R-x} \frac{\partial u}{\partial x} + \frac{R}{R-x} \frac{\partial v}{\partial x} \frac{\partial v}{\partial z} \right] \quad 3.2f$$

Based on the assumption that the cross section retains its original shape, the strains ε_x , ε_y and ε_{xy} are zero.

$$\varepsilon_x = \frac{\partial u}{\partial x} + \frac{1}{2} \left[\left(\frac{\partial u}{\partial x} \right)^2 + \left(\frac{\partial v}{\partial x} \right)^2 \right] = 0 \quad 3.2g$$

$$\varepsilon_y = \frac{\partial v}{\partial y} + \frac{1}{2} \left[\left(\frac{\partial u}{\partial y} \right)^2 + \left(\frac{\partial v}{\partial y} \right)^2 \right] = 0 \quad 3.2h$$

$$\varepsilon_{xy} = \frac{\partial v}{\partial x} + \frac{\partial u}{\partial y} + \left[\frac{\partial u}{\partial x} \frac{\partial u}{\partial y} + \frac{\partial v}{\partial x} \frac{\partial v}{\partial y} \right] = 0 \quad 3.2i$$

The solution of differential Eq. 3.2g and Eq. 3.2h leads to the following lateral and vertical displacement equations.

$$u = u_s - (y - y_s) \sin \beta - (x - x_s) (1 - \cos \beta) \quad 3.3a$$

$$v = v_s + (x - x_s) \sin \beta - (y - y_s) (1 - \cos \beta) \quad 3.3b$$

where x_s and y_s are centroid distances of the shear center, u_s and v_s are the horizontal and vertical displacement of shear center and β is the angle of rotation about z-axis as defined in Figure 3.1.

The shear strains on surfaces parallel to the middle surface of the cross section, ϵ_{zs} , and the shear strain on the planes normal to the middle surface, ϵ_{zn} , in a curvilinear coordinate system can be related to the shear strains ϵ_{zx} and ϵ_{zy} , by the following formulas.

$$\epsilon_{zs} = \frac{\partial y}{\partial s} \epsilon_{zy} + \frac{\partial x}{\partial s} \epsilon_{zx} \quad 3.4a$$

$$\epsilon_{zn} = \frac{\partial y}{\partial s} \epsilon_{zx} - \frac{\partial x}{\partial s} \epsilon_{zy} \quad 3.4b$$

where s is contour ordinate along the middle surface of thin-wall shown in Figure 3.1 and n is the axis normal to s

The mathematical interpretation of the assumption that the shear strains due to change of normal stresses and shear strains in planes normal to the middle surface of thin wall are small and negligible is the following:

$$\hat{\epsilon}_{zs} = 0 \quad 3.5a$$

$$\epsilon_{zn} = 0 \quad 3.5b$$

where $\hat{\epsilon}_{zs}$ denotes the shear strain at middle surface of z - s plane.

With Eq. 3.4 and Eq. 3.5, and Eq. 3.2, the longitudinal displacement can be solved and is expressed by the following equation:

$$w = w_c + x \left(\tilde{u}'_s \cos \beta + v'_s \sin \beta + \frac{y_s}{R} \left(\tilde{u}'_s \sin \beta - v'_s \cos \beta \right) \right) - y \left(v'_s \cos \beta - \tilde{u}'_s \sin \beta \right) - \omega \left(\beta' + \frac{v'_s}{R} \cos \beta - \frac{\tilde{u}'_s}{R} \sin \beta \right) \quad 3.6a$$

Where w is the longitudinal displacement of an arbitrary point on the section.

w_c is the displacement of centroid.

$$\tilde{u}'_s = u'_s + \frac{w_c}{R} \quad 3.6b$$

$$\omega = \int_0^s \rho ds \quad 3.6c$$

The terms ω and ρ are the normalized sectorial area and distance of contour tangent from the reference point. The normalized sectorial area satisfies the condition $\int_A \omega dA = 0$. In Equation 3.6a, two reference lines (shear center and centroid) are used. If only the centroidal axis is used as the reference line, all displacement components must refer to the centroid.

By substituting the above displacement field of Eqs. 3.3 and 3.6 into the non-zero strains in Eq. 3.1, the following equations for longitudinal and shear strain are obtained.

$$\varepsilon_z = \gamma_0 + x\gamma_x + y\gamma_y + \omega\gamma_\omega + x^2\gamma_{xx} + y^2\gamma_{yy} + xy\gamma_{xy} + x\omega\gamma_{x\omega} + y\omega\gamma_{y\omega} \quad \mathbf{3.7a}$$

$$\varepsilon_{zs} = 2n\gamma_n \quad \mathbf{3.7b}$$

Where:

$$\gamma_0 = a \left(\tilde{w}'_c - \frac{\sin\beta y_s}{R} - \frac{(1-\cos\beta)x_s}{R} \right) + \frac{1}{2} a^2 \left(\begin{array}{l} (\tilde{u}'_s + \cos\beta y_s \beta' + \sin\beta x_s \beta')^2 + \\ (v'_s - \cos\beta x_s \beta' + \sin\beta y_s \beta')^2 + \\ (u_s + \sin\beta y_s + (1-\cos\beta)x_s)^2 / R^2 \end{array} \right) \quad \mathbf{3.8a}$$

$$\begin{aligned} \gamma_x = & \frac{a}{R} - \frac{a^2}{R^2} (u_s + x_s) \\ & + \cos\beta \left(a \left(-\tilde{u}''_s - \frac{1}{R} + \frac{y_s}{R} (v''_s - \tilde{u}'\beta') - v'_s \beta' \right) + \right. \\ & \left. a^2 \left(-\frac{\tilde{u}_s'^2}{R} + y_s \frac{\tilde{u}'_s v'_s}{R^2} + \frac{(u_s + 2x_s)}{R^2} + v'_s \beta' \right) \right) \\ & + \sin\beta \left(a \left(\beta' \tilde{u}'_s - v''_s - \frac{y_s}{R} (\tilde{u}''_s - v'_s \beta') \right) + a^2 \left(-\tilde{u}'_s \tilde{\beta}' - \frac{y_s}{R^2} \tilde{u}_s'^2 \right) \right) \\ & + \cos^2\beta \left(a^2 \left(-\frac{y_s}{R} \beta' \tilde{u}'_s + \frac{y_s^2}{R^2} \beta'_s v'_s - \frac{x_s}{R^2} - x_s \beta'^2 \right) \right) \\ & + \sin^2\beta \left(a^2 \left(x_s \left(-\beta' \tilde{\beta}' - \frac{y_s}{R^2} \tilde{u}'_s \beta' \right) \right) \right) \end{aligned}$$

$$+ \sin \beta \cos \beta \left(a^2 \left(-y_s \beta' \tilde{\beta}' - \frac{y_s^2}{R^2} \tilde{u}'_s \beta'_s - \frac{x_s}{R} \beta'_s \tilde{u}'_s + \right) \right. \\ \left. \left(\frac{x_s y_s}{R} \beta'_s v'_s + \frac{y_s}{R^2} + y_s \beta'^2 \right) \right) \quad 3.8b$$

$$\gamma_y = \cos \beta \left(a(-v''_s + \tilde{u}'_s \beta') + a^2(-\tilde{u}'_s \tilde{\beta}') \right) \\ + \sin \beta \left(a \left(\tilde{u}''_s + v'_s \beta' + \frac{1}{R} \right) + a^2 \left(\frac{\tilde{u}'_s{}^2}{R} - \frac{u_s + x_s}{R^2} - \beta' v'_s \right) \right) \\ + \cos^2 \beta a^2 (-y_s \beta' \tilde{\beta}') + \sin^2 \beta a^2 \left(\frac{x_s}{R} \tilde{u}'_s \beta' - y_s \beta'^2 \right) \\ + \sin \beta \cos \beta a^2 \left(-x_s \beta' \tilde{\beta}' + \frac{y_s}{R} \tilde{u}'_s \beta' + \frac{x_s}{R^2} + x_s \beta'^2 \right) \quad 3.8c$$

$$\gamma_\omega = -a\beta'' - a^2 \frac{\tilde{u}'_s \beta'}{R} \\ + \cos \beta \left(a \left(-\frac{v''_s}{R} + \frac{\tilde{u}'_s \beta'}{R} \right) + a^2 \left(-\frac{\tilde{u}'_s v'_s}{R^2} - \frac{y_s}{R} \beta'^2 \right) \right) \\ + \sin \beta \left(a \left(\frac{\tilde{u}''_s}{R} + \frac{v'_s \beta'}{R} \right) + a^2 \left(\frac{\tilde{u}'_s{}^2}{R^2} - \frac{x_s}{R} \beta'^2 \right) \right) \\ + \cos^2 \beta \left(a^2 \left(-\frac{y_s}{R^2} v'_s \beta' \right) \right) + \sin^2 \beta \left(a^2 \left(\frac{x_s}{R^2} \tilde{u}'_s \beta' \right) \right) \\ + \cos \beta \sin \beta \frac{a^2}{R^2} (y_s \tilde{u}'_s \beta' - x_s v'_s \beta') \quad 3.8d$$

$$\gamma_{xx} = \frac{a^2}{2R^2} - \cos \beta \frac{a^2}{R^2} \\ + \cos^2 \beta \left(\frac{a^2}{2} \left(\left(-\frac{\tilde{u}'_s}{R} + \frac{y_s}{R^2} v'_s \right)^2 + \frac{1}{R^2} + \beta'^2 \right) \right) \\ + \sin^2 \beta \left(\frac{a^2}{2} \left(-\tilde{\beta}' - \frac{y_s}{R^2} \tilde{u}'_s \right)^2 \right) \\ + \cos \beta \sin \beta \left(\frac{a^2}{R} \left(-\tilde{\beta}' - \frac{y_s}{R^2} \tilde{u}'_s \right) \left(-\tilde{u}'_s + \frac{y_s}{R} v'_s \right) \right) \quad 3.8f$$

$$\begin{aligned}\gamma_{yy} = & \cos^2 \beta \frac{a^2}{2} (\tilde{\beta}'^2) + \sin^2 \beta \frac{a^2}{2} \left(\frac{\tilde{u}_s'^2}{R^2} + \frac{1}{R^2} + \beta'^2 \right) \\ & + \cos \beta \sin \beta a^2 \left(-\frac{\tilde{u}_s' \tilde{\beta}'}{R} \right)\end{aligned}\quad \mathbf{3.8e}$$

$$\begin{aligned}\gamma_{xy} = & \cos^2 \beta \frac{a^2}{R} \left(\tilde{\beta}' \left(\tilde{u}_s' - \frac{y_s}{R} v_s' \right) \right) + \sin^2 \beta \frac{a^2}{R} \left(\tilde{u}_s' \left(-\tilde{\beta}' - \frac{y_s}{R^2} \tilde{u}_s' \right) \right) \\ & + \cos \beta \sin \beta \left(a^2 \left(\tilde{\beta}'^2 + \frac{y_s}{R^2} \tilde{\beta}' \tilde{u}_s' - \frac{\tilde{u}_s'^2}{R^2} + \frac{y_s}{R^3} \tilde{u}_s' v_s' - \frac{1}{R^2} - \beta'^2 \right) \right)\end{aligned}\quad \mathbf{3.8g}$$

$$\begin{aligned}\gamma_{x\omega} = & \cos \beta \frac{a^2}{R^2} \left(\beta' \tilde{u}_s' - \frac{y_s}{R} \beta' v_s' \right) + \sin \beta \frac{a^2}{R} \left(\beta' \tilde{\beta}' + \frac{y_s}{R^2} \beta' \tilde{u}_s' \right) \\ & + \cos^2 \beta \frac{a^2}{R^3} \left(v_s' \tilde{u}_s' - \frac{y_s}{R} v_s'^2 \right) + \sin^2 \beta \frac{a^2}{R^2} \left(-\tilde{u}_s' \tilde{\beta}' - \frac{y_s}{R^2} \tilde{u}_s'^2 \right) \\ & + \cos \beta \sin \beta \left(\frac{a^2}{R^2} \left(v_s' \tilde{\beta}' + \frac{y_s}{R^2} v_s' \tilde{u}_s' - \frac{\tilde{u}_s'^2}{R} + \frac{y_s}{R^2} \tilde{u}_s' v_s' \right) \right)\end{aligned}\quad \mathbf{3.8h}$$

$$\begin{aligned}\gamma_{y\omega} = & \cos \beta \frac{a^2}{R} (\beta' \tilde{\beta}') + \sin \beta \frac{a^2}{R^2} (-\beta' \tilde{u}_s') \\ & + \cos^2 \beta \frac{a^2}{R^2} (v_s' \tilde{\beta}') + \sin^2 \beta \frac{a^2}{R^3} (\tilde{u}_s'^2) + \cos \beta \sin \beta \left(a^2 \left(-\frac{v_s' \tilde{u}_s'}{R^3} - \frac{\tilde{u}_s' \tilde{\beta}'}{R^2} \right) \right)\end{aligned}\quad \mathbf{3.8i}$$

$$\gamma_n = a \left(\beta' + \frac{v_s'}{R} \cos \beta - \frac{\tilde{u}_s'}{R} \sin \beta \right)\quad \mathbf{3.8j}$$

Where

$$a = \frac{R}{R - x}\quad \mathbf{3.8k}$$

$$\tilde{w}'_c = w'_c - \frac{u_s}{R}\quad \mathbf{3.8L}$$

$$\tilde{\beta} = \beta + \frac{v_s}{R}\quad \mathbf{3.8m}$$

n is direction coordinate which is normal to the middle surface and defined in Figure 3.1

The strains in Equation 3.8 are too complicated to use. Various levels of simplification have been made in different studies based on the assumption that nonlinear terms

which are believed to have minor effects can be ignored. These approximations can be categorized as the following.

- a) The nonlinear terms divided by R^2 and higher can be ignored.
- b) $R / (R-x)$ can be approximated to be unity.
- c) All nonlinear terms divided by R can be ignored
- d) With the assumption of small rotation and displacement, trigonometric functions can be approximated by the first term of Taylor expansions
- e) The inextensible conditions: $\frac{\partial w}{\partial z} - \frac{u}{R} \cong 0$ or $\frac{\partial w}{\partial z} \cong 0$, depending on interpretation of the inextensible condition.

Although simplifications based on these approximations have been made, not much effort has been attempted to examine their effects on the behavior of load and deflection of horizontally curved beams because the complete strain and corresponding differential equation are too complicate. In order to examine the effects, the longitudinal and shear strain of Equation 3.7 are simplified based on each category of approximation above.

If approximation a) is adopted that the nonlinear terms divided by R^2 can be ignored, the strains of Equation 3.8 can be simplified as listed in Table 3.1. It is to be noted that by adopting the approximation that the nonlinear term divided by R^2 can be ignored, the difference on the interpretation of inextensible conditions; $\frac{\partial w}{\partial z} - \frac{u}{R} \cong 0$ or

$\frac{\partial w}{\partial z} \cong 0$ in Eq. 3.1c and 3.2c vanishes. Thus, approximation e) is at the same level as approximation a). Therefore no examination is needed on approximation e). The next approximation is on $R/(R-x)$. There are two ways of treatment. One is that $R/(R-x)$ is approximated as $1+x/R$. The other one is that x/R is much smaller than 1 and $R/(R-x)$ can be approximated as one. The former makes the differential equation of curved beams more complicated. So, the latter, which is approximation b), is adopted. With that, the strain equations in Table 3.1 are simplified to those of Table 3.2. Another level of simplification can be made by using the approximation that nonlinear terms divided by R are small and can be ignored. The terms of strains in Table 3.2 are then further simplified and are shown in Table 3.3. Finally if the assumption of small rotation and small displacement is adopted, the strains may be further simplified. Table 3.4 show the simplified terms of strains based on this approximation. The equations in Table 3.4 are of 4th order. If only 2nd order terms are considered, the equations are simplified as listed in Table 3.5.

Equation 3.8 contains fourth order nonlinear differential terms for the longitudinal strain and shear strain of Equation 3.7. This set of equations is formulated with two reference lines, which are the centroidal axis and the axis of shear center. The derivation of longitudinal and shear strains based on one reference line (centroid) can be done by simply replacing the terms associated with x_s and y_s . Special care is needed

when the reference line is not on the cross section of the beam. This will be discussed in chapter 4. In the one-reference-line system, the differential equation for longitudinal and shear strains for both doubly symmetric and non-symmetric cross sections have identical terms except that the sectional properties are different. Table 3.6 shows the strains associated with the one reference line formulation, corresponding to those given in Eq. 3.8 for two reference lines. The simplification of the equations associated with one reference line formulation can be done with the same procedure adopted in the two reference line formulation.

3.2.3 Comparison of longitudinal strains

The simplification of longitudinal strains for doubly symmetric cross sections was done in all previous studies based on the interpretation of insignificant contribution of the nonlinear terms. Dabrowski (1968) derived the longitudinal and shear strains with the assumption of small rotations and small displacements. Fukumoto and Nishida (1981) derived the equation for longitudinal strains based on large rotation theory and incorporated no higher than second order terms. Kang and Yoo (1994) developed the equation for longitudinal strains by using first and second terms of Taylor's expansion of trigonometric function. These equations and that of the current study are compared below.

(1) Current Study

The simplified equation for longitudinal (normal) strains in beams with a doubly symmetric cross section is shown as Equation 3.9. It is derived from longitudinal strains listed in Table 3.1 by considering the approximating level a) through e) on page 39 and ignoring the third and fourth order terms.

$$\varepsilon_z = \left(\begin{array}{l} \tilde{w}'_c + \frac{1}{2}\tilde{u}_s'^2 + \frac{1}{2}v_s'^2 + x(-\tilde{u}_s'' - \beta v_s'') \\ + y\left(-v_s'' + \beta \tilde{u}_s'' + \frac{\beta}{R}\right) + \omega\left(-\beta'' - \frac{v_s''}{R} + \frac{\beta \tilde{u}_s''}{R}\right) \\ + x^2\left(\frac{1}{2}(\beta'^2)\right) + y^2\left(\frac{1}{2}(\beta'^2)\right) \end{array} \right) \quad 3.9$$

(2) By Dabrowski (1968)

$$\varepsilon_z = \tilde{w}' + x\left(-\tilde{u}_s'' - \frac{u_s}{R^2} - \frac{\beta}{R^2}\right) + y\left(-v'' + \beta \tilde{u}_s'' + \frac{\beta}{R}\right) + \omega\left(-\beta'' + \frac{v_s''}{R}\right) \quad 3.10$$

Equation 3.10 is developed with the basic assumption that beam cross sections can not deform and the shear strain at the middle surface of the thin-walled beam can be

ignored. The simplification was accomplished by a mixture of approximations a) through e). In comparison to Equation 3.9, it can be seen that terms with R^2 in the denominator exists in Equation 3.10 while many other terms in Equation 3.9 are missing in Equation 3.10.

(3) By Fukumoto (1981)

$$\begin{aligned} \varepsilon_z = & \left[\tilde{w}'_c + \frac{1}{2} \tilde{u}'_s{}^2 + \frac{1}{2} v'_s{}^2 + x \left(\frac{1}{R} + \cos \beta \left(-\tilde{u}''_s - \frac{1}{R} \right) + \sin \beta (-v''_s) \right) \right. \\ & + y \left(\cos \beta (-v''_s) + \sin \beta \left(\tilde{u}''_s + \frac{1}{R} \right) \right) + \omega \left(-\beta'' - \frac{v''_s}{R} \right) \\ & \left. + x^2 \left(\frac{1}{2} (\beta'^2) \right) + y^2 \left(\frac{1}{2} (\beta'^2) \right) \right] \end{aligned} \quad 3.11$$

The equation for longitudinal and shear strains by Fukumoto are the basis for Japanese specifications for curved beams. Equation 3.11 is derived from last assumption in Section 3.2.1 and using approximation a) through c). All strain terms by Fukumoto are the same as those from the current study simplified by a) through c) except the terms related to warping:

- Current study

$$\gamma_{\omega} = -\beta'' + \cos \beta \left(-\frac{v''_s}{R} \right) + \sin \beta \left(\frac{\tilde{u}''_s}{R} \right) \quad 3.12a$$

- Fukumoto

$$\gamma_{\omega} = \left(-\beta'' - \frac{v''_s}{R} \right) \quad 3.12b$$

If approximation d) is imposed on the Equation 3.11, it results in an equation almost identical to Equation 3.9 except the underlined term ($\beta \tilde{u}''_s$) in Eq. 3.9 is missing.

(4) Kang (1994)

$$\begin{aligned} \varepsilon_z = & \tilde{w}'_c + x(-\tilde{u}''_s) + y \left(-v''_s + \frac{\beta}{R} \right) + \omega \left(-\beta'' + \frac{v''_s}{R} \right) \\ & + \frac{1}{2} \tilde{u}'_s{}^2 + x \left(\frac{\beta^2}{2R} - \beta' v'_s - \beta \beta'' \right) + y \left(\tilde{u}''_s \beta - \frac{v'_s}{R} \tilde{u}'_s \right) + \frac{\omega}{R} \left(\tilde{u}''_s \beta - \frac{v''_s}{R} \tilde{u}'_s \right) \\ & + \frac{1}{2} \left(\left(y + \frac{\omega}{R} \right)^2 \beta'^2 + (v'_s + x\beta')^2 + (u_s - y\beta)^2 \right) \end{aligned} \quad 3.13$$

With the inclusion of the first and second terms of Taylor's expansions in the derivation, Equation 3.13 contains more terms than Equation 3.9 of the current study. The effects of the approximations for simplifying the equations for complex and nonlinear longitudinal and shear strains are examined later in Chapter 6.

Table 3.1 Simplified Strain Terms by Neglecting Nonlinear Terms Divided by R^2

Approx- imation	Value	Equation *
a)	γ_0	$a\left(\frac{\tilde{w}'_c}{R} - \frac{s y_s}{R} - \frac{(1-c)x_s}{R}\right) + \frac{1}{2}a^2\left(\frac{(\tilde{u}'_s + c y_s \beta' + s x_s \beta')^2}{+ (v'_s - c x_s \beta' + s y_s \beta')^2}\right)$
	γ_x	$\begin{aligned} & \frac{a}{R} + c\left(a\left(-\tilde{u}''_s - \frac{1}{R} + \frac{y_s}{R}(v''_s - \tilde{u}'_s \beta') - v'_s \beta'\right) + a^2\left(-\frac{\tilde{u}'_s{}^2}{R} + v'_s \beta'\right)\right) \\ & + s\left(a\left(\beta' \tilde{u}'_s - v''_s - \frac{y_s}{R}(\tilde{u}''_s - v'_s \beta')\right) + a^2(-\tilde{u}'_s \tilde{\beta}')\right) \\ & + c^2\left(a^2\left(-\frac{y_s}{R} \beta' \tilde{u}'_s - x_s \beta'^2\right)\right) + s^2\left(a^2(-x_s \beta' \tilde{\beta}')\right) \\ & + s c\left(a^2\left(-y_s \beta' \tilde{\beta}' - \frac{x_s}{R} \beta' \tilde{u}'_s + \frac{x_s y_s}{R} \beta' v'_s + y_s \beta'^2\right)\right) \end{aligned}$
	γ_y	$\begin{aligned} & c\left(a(-v''_s + \tilde{u}'_s \beta') + a^2(-\tilde{u}'_s \tilde{\beta}')\right) \\ & + s\left(a\left(\tilde{u}''_s + v'_s \beta' + \frac{1}{R}\right) + a^2\left(\frac{\tilde{u}'_s{}^2}{R} - \beta' v'_s\right)\right) \\ & + c^2 a^2(-y_s \beta' \tilde{\beta}') + s^2 a^2\left(\frac{x_s}{R} \tilde{u}'_s \beta' - y_s \beta'^2\right) \\ & + s c a^2\left(-x_s \beta' \tilde{\beta}' + \frac{y_s}{R} \tilde{u}'_s \beta' + x_s \beta'^2\right) \end{aligned}$
	γ_ω	$\begin{aligned} & -a\beta'' - a^2 \frac{\tilde{u}'_s \beta'}{R} + c\left(a\left(-\frac{v''_s}{R} + \frac{\tilde{u}'_s \beta'}{R}\right) + a^2\left(-\frac{y_s}{R} \beta'^2\right)\right) \\ & + s\left(a\left(\frac{\tilde{u}''_s}{R} + \frac{v'_s \beta'}{R}\right) + a^2\left(-\frac{x_s}{R} \beta'^2\right)\right) \end{aligned}$
	γ_{xx}	$\begin{aligned} & c^2\left(\frac{a^2}{2}\left(\left(-\frac{\tilde{u}'_s}{R}\right)^2 + \beta'^2\right)\right) + s^2\left(\frac{a^2}{2}(-\tilde{\beta}')^2\right) \\ & + c s\left(\frac{a^2}{R}(-\tilde{\beta}')\left(-\tilde{u}'_s + \frac{y_s}{R} v'_s\right)\right) \end{aligned}$
a)	γ_{yy}	$c^2 \frac{a^2}{2} (\tilde{\beta}'^2) + s^2 \frac{a^2}{2} (\beta'^2) + c s a^2 \left(-\frac{\tilde{u}'_s \tilde{\beta}'}{R}\right)$
	γ_{xy}	$c^2 \frac{a^2}{R} \left(\tilde{\beta}' \tilde{u}'_s - \frac{y_s}{R} \tilde{\beta}' v'_s\right) + s^2 \frac{a^2}{R} (-\tilde{u}'_s \tilde{\beta}') + c s \left(a^2 (\tilde{\beta}'^2 - \beta'^2)\right)$

	$\gamma_{x\omega}$	$s \frac{a^2}{R} (\beta' \tilde{\beta}')$
	$\gamma_{y\omega}$	$s \frac{a^2}{R} (\beta' \tilde{\beta}')$
	γ_n	$a \left(\beta' + \frac{v'_s}{R} c + \frac{\tilde{u}'_s}{R} s \right)$

* “c” and “s” represent $\cos \beta$ and $\sin \beta$

Table 3.2 Simplified Strain Terms by Approximation a) and b)

Approx- imation	Value	Equation *
a) b)	γ_0	$(\tilde{w}'_c - \frac{s y_s}{R} - \frac{(1-c)x_s}{R}) + \frac{1}{2} \left(\frac{(\tilde{u}'_s + c y_s \beta' + s x_s \beta')^2}{(v'_s - c x_s \beta' + s y_s \beta')^2} + \right)$
	γ_x	$\frac{1}{R} + c \left(-\tilde{u}''_s - \frac{1}{R} + \frac{y_s}{R} (v''_s - \tilde{u}'_s \beta') - \frac{\tilde{u}'^2_s}{R} \right) +$ $s \left(\frac{v'_s \tilde{u}'_s}{R} - v''_s - \frac{y_s}{R} (\tilde{u}''_s - v'_s \beta') \right) +$ $c^2 \left(-\frac{y_s}{R} \beta' \tilde{u}'_s - x_s \beta'^2 \right) + s^2 \left(-x_s \beta' \tilde{\beta}' \right) +$ $s c \left(-y_s \beta' \tilde{\beta}' - \frac{x_s}{R} \beta' \tilde{u}'_s + \frac{x_s y_s}{R} \beta' v'_s + y_s \beta'^2 \right)$
	γ_y	$c \left(-v''_s - \frac{\tilde{u}'_s v_s}{R} \right) + s \left(\tilde{u}''_s + \frac{1}{R} + \frac{\tilde{u}'^2_s}{R} \right)$ $+ c^2 \left(-y_s \beta' \tilde{\beta}' \right) + s^2 \left(\frac{x_s}{R} \tilde{u}'_s \beta' - y_s \beta'^2 \right)$ $+ s c \left(-x_s \beta' \tilde{\beta}' + \frac{y_s}{R} \tilde{u}'_s \beta' + x_s \beta'^2 \right)$
	γ_ω	$-\beta'' - \frac{\tilde{u}'_s \beta'}{R} +$ $c \left(-\frac{v''_s}{R} + \frac{\tilde{u}'_s \beta'}{R} - \frac{y_s}{R} \beta'^2 \right) + s \left(\frac{\tilde{u}''_s}{R} + \frac{v'_s \beta'}{R} - \frac{x_s}{R} \beta'^2 \right)$
	γ_{xx}	$c^2 \left(\frac{1}{2} \beta'^2 \right) + s^2 \left(\frac{1}{2} \tilde{\beta}'^2 \right) + c s \left(-\frac{\tilde{\beta}'}{R} \left(-\tilde{u}'_s + \frac{y_s}{R} v'_s \right) \right)$

	γ_{yy}	$c^2 \frac{1}{2}(\tilde{\beta}'^2) + s^2 \frac{1}{2}(\beta'^2) + c s \left(-\frac{\tilde{u}'_s \tilde{\beta}'}{R} \right)$
	γ_{xy}	$c^2 \frac{1}{R} \left(\tilde{\beta}' \tilde{u}'_s - \frac{y_s}{R} \tilde{\beta}' v'_s \right) + s^2 \frac{1}{R} (-\tilde{u}'_s \tilde{\beta}') + c s (\tilde{\beta}'^2 - \beta'^2)$
	$\gamma_{x\omega}$	$s \left(\frac{\beta' \tilde{\beta}'}{R} \right)$
	$\gamma_{y\omega}$	$c \left(\frac{\beta' \tilde{\beta}'}{R} \right)$
	γ_n	$\beta' + c \frac{v'_s}{R} + s \frac{\tilde{u}'_s}{R}$

* “c” and “s” represent cos β and sin β

Table 3.3 Simplified Strain Terms by Approximation a), b) and c)

Approx- imation	Value	Equation
a) b) c)	γ_0	$(\tilde{w}'_c - \frac{s y_s}{R} - \frac{(1-c)x_s}{R}) + \frac{1}{2} \left((\tilde{u}'_s + c y_s \beta' + s x_s \beta')^2 + (v'_s - c x_s \beta' + s y_s \beta')^2 \right)$
	γ_x	$\frac{1}{R} + c \left(-\tilde{u}''_s - \frac{1}{R} + \frac{y_s}{R} (v''_s) \right) + s \left(-v''_s - \frac{y_s}{R} (\tilde{u}''_s) \right) - x_s \beta'^2$
	γ_y	$c(-v''_s) + s \left(\tilde{u}''_s + \frac{1}{R} \right) - y_s \beta'^2$
	γ_ω	$-\beta'' + c \left(-\frac{v''_s}{R} \right) + s \left(\frac{\tilde{u}''_s}{R} \right)$
	γ_{xx}	$\frac{\beta'^2}{2}$
	γ_{yy}	$\frac{\beta'^2}{2}$
	γ_{xy}	0
	$\gamma_{x\omega}$	0
	$\gamma_{y\omega}$	0
	γ_n	$\left(\beta' + \frac{v'_s}{R} c + \frac{\tilde{u}'_s}{R} s \right)$

* “c” and “s” represent cos β and sin β

Table 3.4 Simplified Strain Terms Approximated by a), b), c) and d)

Approx- imation	Value	Equation*
a) b) c) d)	γ_0	$(\tilde{w}'_c - \frac{y_s \beta}{R}) + \frac{1}{2}((\tilde{u}'_s + y_s \beta' + x_s \beta \beta')^2 + (v'_s - x_s \beta' + y_s \beta \beta')^2)$
	γ_x	$-\tilde{u}''_s + \frac{y_s}{R}(v''_s) - \beta v''_s - x_s \beta'^2$
	γ_y	$-v''_s + \frac{\beta}{R} + \beta \tilde{u}''_s - y_s \beta'^2$
	γ_ω	$-\beta'' - \frac{v''_s}{R}$
	γ_{xx}	$\frac{\beta'^2}{2}$
	γ_{yy}	$\frac{\beta'^2}{2}$
	γ_{xy}	0
	$\gamma_{x\omega}$	0
	$\gamma_{y\omega}$	0
γ_n	$\beta' + \frac{v'_s}{R}$	

* “c” and “s” represent cos β and sin β

Table 3.5 Simplified Strain Terms Considering only 2nd Order Terms

Approx- imation	Value	Equation*
2 nd order	γ_0	$(\tilde{w}'_c - \frac{y_s \beta}{R}) + \frac{1}{2}((\tilde{u}'_s + y_s \beta')^2 + (v'_s - x_s \beta')^2)$
	γ_x	$-\tilde{u}''_s + \frac{y_s}{R}(v''_s) - \beta v''_s - x_s \beta'^2$
	γ_y	$-v''_s + \frac{\beta}{R} + \beta \tilde{u}''_s - y_s \beta'^2$
	γ_ω	$-\beta'' - \frac{v''_s}{R}$
	γ_{xx}	$\frac{\beta'^2}{2}$
	γ_{yy}	$\frac{\beta'^2}{2}$

	γ_{xy}	0
	$\gamma_{x\omega}$	0
	$\gamma_{y\omega}$	0
	γ_n	$\beta' + \frac{v'_s}{R}$

* “c” and “s” represent $\cos \beta$ and $\sin \beta$

Table 3.6 Strain Term Based on One Reference Line

Approx- imation	Value	Equation*
	γ_0	$a(\tilde{w}'_c) + \frac{1}{2}a^2\left(\tilde{u}'_c{}^2 + v'_c{}^2 + \frac{u_c{}^2}{R^2}\right)$
	γ_x	$\frac{a}{R} - \frac{a^2}{R^2}u_c + c\left(a\left(-\tilde{u}''_c - \frac{1}{R} - v'_c\beta'\right) + a^2\left(-\frac{\tilde{u}'_c{}^2}{R} + v'_c\beta' + \frac{u_c}{R^2}\right)\right) +$ $s\left(a(\beta'\tilde{u}'_c - v''_c) + a^2(-\tilde{u}'_c\tilde{\beta}')\right)$
	γ_y	$c\left(a(-v''_c + \tilde{u}'_c\beta') + a^2(-\tilde{u}'_c\tilde{\beta}')\right) +$ $s\left(a\left(\tilde{u}''_c + v'_c\beta' + \frac{1}{R}\right) + a^2\left(\frac{\tilde{u}'_c{}^2}{R} - \frac{u_c}{R^2} - \beta'v'_c\right)\right)$
	γ_ω	$-a\beta'' - a^2\frac{\tilde{u}'_c\beta'}{R} + c\left(a\left(-\frac{v''_c}{R} + \frac{\tilde{u}'_c\beta'}{R}\right) + a^2\left(-\frac{\tilde{u}'_c v'_c}{R^2}\right)\right) +$ $s\left(a\left(\frac{\tilde{u}''_c}{R} + \frac{v'_c\beta'}{R}\right) + a^2\left(\frac{\tilde{u}'_c{}^2}{R^2}\right)\right)$
	γ_{xx}	$\frac{a^2}{2R^2} - c\frac{a^2}{R^2} + c^2\left(\frac{a^2}{2}\left(\left(\frac{\tilde{u}'_c}{R}\right)^2 + \frac{1}{R^2} + \beta'^2\right)\right) + s^2\left(\frac{a^2}{2}(\tilde{\beta}')^2\right) +$ $c\,s\left(\frac{a^2}{R}\tilde{\beta}'\tilde{u}'_c\right)$
	γ_{yy}	$c^2\frac{a^2}{2}(\tilde{\beta}'^2) + s^2\frac{a^2}{2}\left(\frac{\tilde{u}'_c{}^2}{R^2} + \frac{1}{R^2} + \beta'^2\right) + c\,s\,a^2\left(-\frac{\tilde{u}'_c\tilde{\beta}'}{R}\right)$
	γ_{xy}	$c^2\frac{a^2}{R}(\tilde{\beta}'\tilde{u}'_c) + s^2\frac{a^2}{R}(-\tilde{\beta}'\tilde{u}'_c) + c\,s\left(a^2\left(\tilde{\beta}'^2 - \frac{\tilde{u}'_c{}^2}{R^2} - \frac{1}{R^2} - \beta'^2\right)\right)$

	$e_{x\omega}$	$c \frac{a^2}{R^2} (\beta' \tilde{u}'_c) + s \frac{a^2}{R} (\beta' \tilde{\beta}') + c^2 \frac{a^2}{R^3} (v'_c \tilde{u}'_c) + s^2 \frac{a^2}{R^2} (-\tilde{u}'_c \tilde{\beta}') +$ $c s \left(\frac{a^2}{R^2} \left(v'_c \tilde{\beta}' - \frac{\tilde{u}'_c{}^2}{R} \right) \right)$
	$\gamma_{y\omega}$	$c \frac{a^2}{R} (\beta' \tilde{\beta}') + s \frac{a^2}{R^2} (-\beta' \tilde{u}'_c) + c^2 \frac{a^2}{R^2} (v'_c \tilde{\beta}') + s^2 \frac{a^2}{R^3} (\tilde{u}'_c{}^2) +$ $c s \left(a^2 \left(-\frac{v'_c \tilde{u}'_c}{R^3} - \frac{\tilde{u}'_c \tilde{\beta}'}{R^2} \right) \right)$
	γ_n	$\beta' + \frac{v'}{R} c + \frac{\tilde{u}'_c}{R} s$

* “c” and “s” represent cos β and sin β

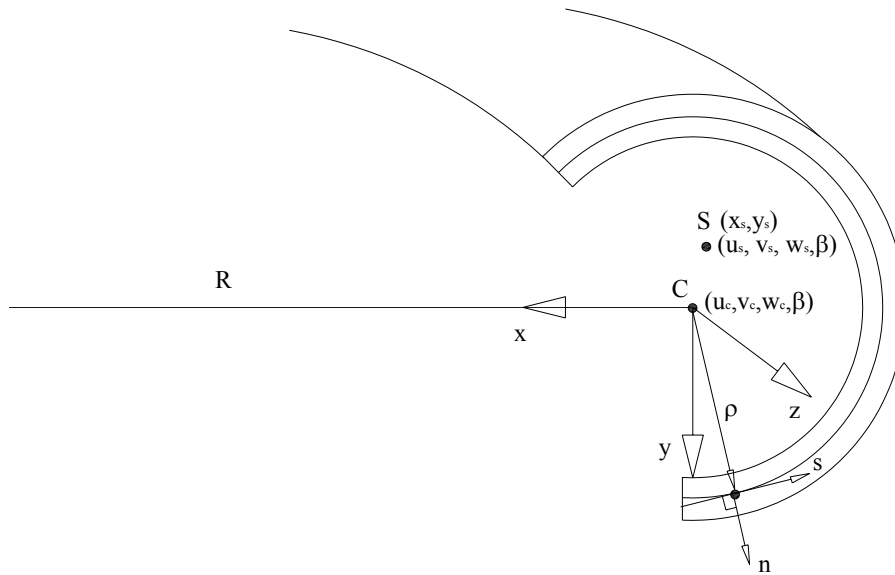


Figure 3.1 Coordinate System of Curved Beam

C and S are centroid and shear center
 u_s, v_s, w_s are displacement of shear center in x, y, z direction
 u_c, v_c, w_c are displacement of centroid in x, y, z direction
 β is rotation of the cross section about z axis

4. Formulation of Differential Equation for A Curved Beam

4.1 Introduction

In this chapter, a formulation of differential equation for the analysis of arbitrary thin-walled spatial curved beams under general loading and boundary condition is derived by using the principle of minimum total potential energy. The formulation includes six modes of stretching, shearing, twisting and bending with non-uniform warping being an important mode of displacement. Flexural behavior of horizontally curved beams represented by large rotations and large displacements is modeled on the basis of incremental formulation for un-deformable cross-sections.

For the singly-symmetric and non-symmetric cross sections, two reference lines (the axes of centroid and shear center) are needed in the conventional beam theory. Two-reference-line system generates many disadvantages caused by the coupling associated with the distance between the two reference points. In order to overcome these difficulties, one-reference-line system is developed by transferring all displacements to one-reference point.

For investigating the effects of sectional deformation of I-shaped cross sections, a formulation is derived based on the assumption that the flanges retain their original shape and the web can deform. The shape of web deformation depends on the external load. In-plane loading and out of plane loading generate different shape. In this study, only the shape of web deformation by out-of-plane loading is considered. The formulation of differential equation with sectional deformation starts with introducing a relative rotation between the flanges and the web. The additional strain terms associated with sectional deformation are derived from the relative rotation. For large rotation and displacement analysis, formulation is modified for incremental step analysis.

Solving linear differential equation for arbitrary boundary conditions with specific loading is difficult. Dabrowski (1968) derived the exact solution for one specific boundary condition, which is defined here as the “basic boundary system”. With similar approach, exact solutions of linear differential equation are derived for a set of different boundary conditions including those of free-free and fixed-fixed against warping at the ends of a curved beam.

4.2 Application of the Principle of Stationary Total Potential Energy to Curved Beams

When an elastic system is subjected to conservative forces and is in equilibrium, the total potential energy of the system must be stationary. The essence of using the principle of stationary total potential energy to solve problems of load and displacement is to calculate the total potential energy Π at different stages and to invoke stationary Π .

In a linear elastic continuum with zero initial stresses, the total potential energy of the system is the following:

$$\Pi = \int_V \frac{1}{2} \bar{\varepsilon}^T [C] \bar{\varepsilon} dV - \int_V \bar{u}^T \bar{f}^B dV - \int_{S_f} \bar{u}^{s_f T} \bar{f}^{s_f} dS \quad 4.1$$

Where: $\bar{\varepsilon}$ is strain vector

T is transpose

V is volume of curved beam

$[C]$ is material stiffness matrix;

\bar{u} is displacement vector;

\bar{f}^B is body force vector per unit volume;

S_f is surface area of beam

\bar{u}^{s_f} is displacement vector of u corresponding to surface S_f

\bar{f}^{s_f} is surface traction vector per unit surface area (S_f)

The first term in Equation 4.1 for the total potential energy is the strain energy stored in the elastic body. The Second and third terms are the loss of potential energy of the system.

The mathematical statement of the principle of stationary total potential energy can be expressed as $\delta\Pi = 0$. By invoking the stationary total potential energy with respect to the displacements, the equilibrium equation can be obtained as the following equation;

$$\delta\Pi = \int_V \bar{S}^T \delta\bar{\varepsilon} dV - \int_V \delta\bar{u}^T \bar{f}^B dV - \int_{S_f} \delta\bar{u}^{s_f T} \bar{f}^{s_f} dS = 0 \quad 4.2$$

For equilibrium Equation 4.2, it is assumed that constitutive law in Equation 4.3a, the strain-displacement relationship in Equation 4.3b and the displacement boundary conditions in Equation 4.3c are satisfied.

$$\bar{S} = [C] \bar{\varepsilon} \quad \text{in Volume } V \quad 4.3a$$

$$\bar{\varepsilon} = \partial\bar{u} \quad \text{in Volume } V \quad 4.3b$$

$$\bar{u}^{s_u} - \bar{u} = 0 \quad \text{on the surface } S_u \quad 4.3c$$

Where S_u is surface area of support, \bar{u}^{s_u} is displacement component corresponding to the surface S_u , \bar{u} is the prescribed displacement components and \bar{S} is stress vector. Since in this study, the non-zero strains and stresses are ε_z , ε_{zs} and σ_z , σ_{zs} , the strain and stress vectors in Eq. 4.2 can be expressed by the following equations.

$$\bar{\varepsilon} = \{\varepsilon_z, \varepsilon_{sz}\}^T \quad 4.3d$$

$$\bar{S} = \{\sigma_z, \sigma_{sz}\}^T \quad 4.3e$$

For the horizontally curved beam, only homogeneous material is considered. Thus, material matrix $[C]$ is

$$[C] = \begin{bmatrix} E & 0 \\ 0 & G \end{bmatrix} \quad 4.3f$$

In order to account for the effect of curvature of curved beam on the volume, the differential of volume, dV , is expressed in cylindrical coordinate as:

$$dV = \rho d\phi d\rho dy \quad 4.4$$

Where: ρ is $R-x$

ϕ is enclosed angle defined in Figure 2.1

In Cartesian coordinates, Equation 4.4 can be transformed to the following equation;

$$dV = \frac{R-x}{R} dx dy dz = \frac{R-x}{R} dA dz \quad 4.5$$

Where dA is the differential area of the beam cross section A

It should be noted that integration of the term $[(R-x)/R] dA$ causes new sectional properties for the curved beams. These new properties generally can be expressed by

the two conventional sectional properties, i.e., $Q_y^c = \int_A x \left(\frac{R-x}{R} \right) dA = Q_y - \frac{I_y}{R}$ where

Q_y^c is first moment of area about y-axis for curved beams. Q_y and I_y are first moment of area about y-axis and moment of inertial about y-axis respectively. The effect of sectional properties associated with x/R can be examined by comparing the results of ignoring and including x/R in the calculation.

4.3 Derivation of Components for Differential Equations

The individual components of the equilibrium equation, Eq 4.2, need to be expressed in strains and displacements for solution. Any of the simplified strains from Chapter 3 can be used. With more elaborate expression for strains, better solution of load-displacement relationship will be the outcome. However, solving of complicated differential equation is still often not achievable. The equilibrium equation based on the assumption of small rotation is derived in this section and further simplified as linear differential equation from which exact solution is derived for a specific loading and boundary condition in the following section. The governing differential equation based on large rotation and displacement will be derived in Chapter 5 and solved for specific loading and boundary conditions using the numerical procedure in Chapter 6.

4.3.1 Variation of Strain Energy

In the variational formulation, the symbol δ is used for variation of variables. The expression δF is similar to the differential dF . The law of variational sum and products are the following:

$$\delta(F(z) + G(z)) = \delta F(z) + \delta G(z) \quad 4.6a$$

$$\delta(F G) = G \delta F + F \delta G \quad 4.6b$$

$$\delta(F)^n = n(F)^{n-1} \delta F \quad 4.6c$$

One of the important laws of variation is that the operator of variation can be translated in and out of an integral sign:

$$\delta \int F(z) dz = \int \delta F(z) dz \quad 4.7$$

A simplified nonlinear equilibrium differential equation for small displacement and rotation is derived using the longitudinal strain and shear strain in Eq. 4.8. which is simplification of Eq. 3.7 based on the the assumption of ignoring the terms with $1/R^2$ and higher than 2nd order.

$$\varepsilon_z = \gamma_0 + x\gamma_x + y\gamma_y + \omega\gamma_\omega + x^2\gamma_{xx} + y^2\gamma_{yy} + xy\gamma_{xy} + x\omega\gamma_{x\omega} + y\omega\gamma_{y\omega} \quad 4.8a$$

$$\varepsilon_{zs} = 2n\gamma_n \quad 4.8b$$

Where n is direction coordinate which is normal to the middle surface and defined in the Figure 3.1

For convenience, the components of strains are divided into linear and nonlinear terms, e and η .

$$\begin{aligned} \varepsilon_z &= e_z + \eta_z \\ &= \left((e_0 + \eta_0) + x(e_x + \eta_x) + y(e_y + \eta_y) + \omega(e_\omega + \eta_\omega) + x^2(e_{xx} + \eta_{xx}) + \right. \\ &\quad \left. y^2(e_{yy} + \eta_{yy}) + xy(e_{xy} + \eta_{xy}) + x\omega(e_{x\omega} + \eta_{x\omega}) + y\omega(e_{y\omega} + \eta_{y\omega}) \right) \end{aligned} \quad 4.9a$$

$$\varepsilon_{zs} = e_{zs} + \eta_{zs} = 2n(e_n + \eta_n) \quad 4.9b$$

where

$$e_0 + \eta_0 = \left(a\left(\tilde{w}'_c - \frac{\beta y_s}{R}\right) + \left(\frac{1}{2} a^2 \left((\tilde{u}'_s + y_s \beta')^2 + (v'_s - x_s \beta')^2 \right) \right) \right) \quad 4.10a$$

$$e_x + \eta_x = a \left(-\tilde{u}''_s + \frac{y_s v''_s}{R} \right) + \left(a \left(\frac{y_s}{R} (-\tilde{u}'_s \beta' - \beta \tilde{u}''_s) - v'_s \beta' - \beta v''_s \right) + a^2 \left(-\frac{u'^2_s}{R} + v'_s \beta' - \frac{y_s}{R} \beta' u'_s - x_s \beta'^2 \right) \right) \quad 4.10b$$

$$e_y + \eta_y = \left(a \left(-v''_s + \frac{\beta}{R} \right) \right) + \left(a(\tilde{u}'_s \beta' + \beta \tilde{u}''_s) + a^2(-\tilde{u}'_s \tilde{\beta}' - y_s \beta' \tilde{\beta}') \right) \quad 4.10c$$

$$e_\omega + \eta_\omega = \left(a \left(-\beta'' - \frac{v''_s}{R} \right) \right) + \left(a \left(\frac{u'_s \beta'}{R} + \frac{\beta u''_s}{R} \right) + a^2 \left(-\frac{u'_s \beta'}{R} - \frac{y_s}{R} \beta'^2 \right) \right) \quad 4.10d$$

$$e_{xx} + \eta_{xx} = 0 + \left(\frac{a^2}{2} (\beta'^2) \right) \quad 4.10e$$

$$e_{yy} + \eta_{yy} = 0 + \left(\frac{a^2}{2} (\beta'^2) \right) \quad 4.10f$$

$$e_{xy} + \eta_{xy} = 0 + \left(\frac{a^2}{R} (\beta' u'_s) \right) \quad 4.10g$$

$$e_{x\omega} + \eta_{x\omega} = 0 + 0 \quad 4.10h$$

$$e_{y\omega} + \eta_{y\omega} = 0 + \left(\frac{a^2}{2} (\beta'^2) \right) \quad 4.10i$$

$$e_n + \eta_n = a \left(\beta' + \frac{v'_s}{R} \right) + a \left(\frac{u'_s \beta}{R} \right) \quad 4.10j$$

e_z and e_{zs} are linear parts of longitudinal and shear strain

η_z and η_{zs} are nonlinear parts of longitudinal and shear strain

$a = R/(R-x)$

With the strains in Eq. 4.9, the first term in Eq. 4.2 can be expressed as the following:

$$\begin{aligned} \int_V \bar{S}^T \delta \bar{\epsilon} dV &= \int_V [\bar{S}^T \delta (\bar{\epsilon} + \bar{\eta})] dV \\ &= \int_V [\sigma_z \delta (e_z + \eta_z)] dV + \int_V [\sigma_{zs} \delta (e_{zs} + \eta_{zs})] dV \end{aligned} \quad 4.11a$$

Where

$$\bar{S} = \{ \sigma_z, \sigma_{zs} \}^T \quad 4.11b$$

$$\bar{\epsilon} = \{ e_z, e_{zs} \}^T \quad 4.11c$$

$$\bar{\eta} = \{ \eta_z, \eta_{zs} \}^T \quad 4.11d$$

The strain energy, Eq. 4.11a is composed of longitudinal and shear strain energy. The strain energy associated with longitudinal strain can be expressed as the following equation

$$\begin{aligned} &\int_V [\sigma_z \delta (e_0 + x e_x + y e_y + \omega e_\omega)] dV \\ &+ \int_V [\sigma_z \delta (\eta_0 + x \eta_x + y \eta_y + \omega \eta_\omega + x^2 \eta_{xx} + y^2 \eta_{yy} + xy \eta_{xy} + y\omega \eta_{y\omega})] dV \end{aligned} \quad 4.11d$$

Equation 4.11d is expanded by using the stress resultants defined in the following equations.

$$F_z = \int_A \sigma_z dA \quad 4.12a$$

$$M_x = \int_A \sigma_z y dA \quad 4.12b$$

$$M_y = -\int_A \sigma_z x dA \quad 4.12c$$

$$M_\omega = \int_A \sigma_z \omega dA \quad 4.12d$$

$$K_{xx} = \int_A \sigma_z x^2 dA \quad 4.12e$$

$$K_{yy} = \int_A \sigma_z y^2 dA \quad 4.12f$$

$$K_{xy} = \int_A \sigma_z xy dA \quad 4.12g$$

$$K_{x\omega} = \int_A \sigma_z x\omega dA \quad 4.12h$$

$$K_{y\omega} = \int_A \sigma_z y\omega dA \quad 4.12i$$

Equation 4.12 applies to two groups. One group of resultant is from the traditional form of $F = \int \sigma(x, y, \omega) dA$. The other is associated with curvature of the curved beam.

$F^a = \int \sigma(x, y, \omega) R / (R - x) dA$. Those resultants with the superscript ‘‘a’’ can be expressed by just multiplying the additional term $R / (R - x)$ to those shown in Eq. 4.12. With the stress resultants, Eq. 4.11 associated with longitudinal strain is expanded to the following.

$$\int_V [\sigma_z \delta(e_z + \eta_z)] dV = \int_V \left[\begin{array}{l} F_z \delta e_0 - M_y \delta e_x + M_x \delta e_y + M_\omega \delta e_\omega + K_{xx} \delta e_{xx} + K_{yy} \delta e_{yy} + \\ K_{xy} \delta e_{xy} + K_{y\omega} \delta e_{y\omega} \end{array} \right] dV$$

$$+ \int_V \left[\begin{array}{l} F_z \delta \eta_0 + M_y \delta \eta_x - M_x \delta \eta_y + M_\omega \delta \eta_\omega + K_{xx} \delta \eta_{xx} + \\ K_{yy} \delta \eta_{yy} + K_{xy} \delta \eta_{xy} + K_{y\omega} \delta \eta_{y\omega} \end{array} \right] dV \quad 4.13$$

Using Eq. 4.5 and substituting the expression for linear and nonlinear strains, Equation 4.13 can be expressed as the following equation:

$$\int_V \left[\begin{array}{l} F_z \delta e_0 - M_y \delta e_x + M_x \delta e_y + M_\omega \delta e_\omega + K_{xx} \delta e_{xx} + K_{yy} \delta e_{yy} + \\ K_{xy} \delta e_{xy} + K_{y\omega} \delta e_{y\omega} \end{array} \right] dV =$$

$$\begin{aligned}
& \int_L \left[F_z \delta \left(w'_c - \frac{u_s}{R} - \frac{\beta y_s}{R} \right) - M_y \delta \left(-u''_s - \frac{w'_c}{R} + \frac{y_s v''_s}{R} \right) \right] dz \\
& + \int_L \left[M_x \delta \left(-v''_s + \frac{\beta}{R} \right) + M_\omega \delta \left(-\beta'' - \frac{v''_s}{R} \right) \right] dz \\
& + \int_L \left[F_z^a \delta \left(\frac{1}{2} \left((\tilde{u}'_s + y_s \beta')^2 + (v'_s - x_s \beta')^2 \right) \right) \right] dz \\
& - \int_L \left[M_y \delta \left(\frac{y_s}{R} (-\tilde{u}'_s \beta' - \beta \tilde{u}''_s) - v'_s \beta' - \beta v''_s \right) \right] dz \\
& - \int_L \left[M_y^a \delta \left(-\frac{u'^2}{R} + v'_s \beta' - \frac{y_s}{R} \beta' u'_s - x_s \beta'^2 \right) \right] dz \\
& + \int_L \left[M_x \delta (\tilde{u}'_s \beta' + \beta \tilde{u}''_s) + M_x^a \delta (-\tilde{u}'_s \tilde{\beta}' - y_s \beta' \tilde{\beta}') \right] dz \\
& + \int_L \left[K_{xx}^a \delta \left(\frac{a}{2} (\beta'^2) \right) + K_{yy}^a \delta \left(\frac{a}{2} (\beta'^2) \right) \right] dz \\
& + \int_L \left[K_{xy}^a \delta \left(\frac{a}{R} (\beta' u'_s) \right) + K_{yw}^a \delta \left(\frac{a}{2} (\beta'^2) \right) \right] dz
\end{aligned} \tag{4.14}$$

By using Eq. 4.15, the expansion of variation for the nonlinear longitudinal strain terms of Eq. 4.14 results in the following:

$$\begin{aligned}
& \int_V \left[F_z \delta \eta_0 + M_y \delta \eta_x - M_x \delta \eta_y + M_\omega \delta \eta_\omega + K_{xx} \delta \eta_{xx} + \right. \\
& \left. K_{yy} \delta \eta_{yy} + K_{xy} \delta \eta_{xy} + K_{y\omega} \delta \eta_{y\omega} \right] dV = \\
& \int_L \left[F_z^a \left(\left(u'_s + \frac{w_c}{R} + y_s \beta' \right) \delta \left(u'_s + \frac{w_c}{R} + y_s \beta' \right) + (v'_s - x_s \beta') \delta (v'_s - x_s \beta') \right) \right] dz \\
& - \int_L \left[M_y \frac{y_s}{R} \left(-\delta \left(u'_s + \frac{w_c}{R} \right) \beta' - \beta \delta \left(u''_s + \frac{w'_c}{R} \right) - \delta \beta' \left(u'_s + \frac{w_c}{R} \right) - \delta \beta \left(u''_s + \frac{w'_c}{R} \right) \right) \right] dz \\
& - \int_L \left[M_y (-\delta v'_s \beta' - \delta \beta v''_s - v'_s \delta \beta' - \beta \delta v''_s) \right] dz \\
& + \int_L \left[M_x \left(\delta \left(u'_s + \frac{w_c}{R} \right) \beta' + \left(u'_s + \frac{w_c}{R} \right) \delta \beta' + \delta \beta \left(u''_s + \frac{w'_c}{R} \right) + \beta \delta \left(u''_s + \frac{w'_c}{R} \right) \right) \right] dz
\end{aligned}$$

$$\begin{aligned}
& + \int_L \left[M_x^a \left(-\delta \left(u'_s + \frac{w_c}{R} \right) \left(\beta' + \frac{v'_s}{R} \right) - \left(u'_s + \frac{w_c}{R} \right) \delta \left(\beta' + \frac{v'_s}{R} \right) \right. \right. \\
& \quad \left. \left. - y_s \delta \beta' \left(\beta' + \frac{v'_s}{R} \right) - y_s \beta' \delta \left(\beta' + \frac{v'_s}{R} \right) \right) \right] dz \\
& + \int_L \left[M_\omega \left(\frac{\delta u'_s \beta'}{R} + \frac{u'_s \delta \beta'}{R} + \frac{\delta \beta u''_s}{R} + \frac{\beta \delta u''_s}{R} \right) \right] dz \\
& + \int_L \left[M_\omega^a \left(-\frac{\delta u'_s \beta'}{R} - \frac{u'_s \delta \beta'}{R} - 2 \frac{y_s}{R} \delta \beta' \beta' \right) \right] dz \\
& + \int_L \left[K_{xx}^a (\delta \beta' \beta') + K_{yy}^a (\delta \beta' \beta') + \frac{K_{xy}^a}{R} (\delta \beta' u'_s + \beta' \delta u'_s) + K_{yw}^a (\delta \beta' \beta') \right] dz \quad \mathbf{4.15}
\end{aligned}$$

Equation 4.14 can be divided into two groups of variational strain energy. One is for the strain energy associated with linear strains. The other one is for the strain energy associated with nonlinear strains. From this separation, linear and nonlinear terms for the equilibrium differential equation can be developed. By integrating by parts and grouping the strain energy with the same variational terms, the strain energy associated with linear strains can be expanded as the following.

- Variational energy strain terms associated with δu_s is

$$\int_L \left[-\frac{F_z}{R} \delta u_s + M_y \delta u''_s \right] dz \quad \mathbf{4.16}$$

Integration by parts:

$$\left(M_y \delta u'_s \Big|_0^L - M_y' \delta u_s \Big|_0^L + \int_0^L M_y'' \delta u_s dz \right) - \int_0^L \frac{F_z}{R} \delta u_s dz \quad \mathbf{4.17}$$

- Variational energy strain terms associated with δw_c is

$$\int_L \left(F_z + \frac{M_y}{R} \right) \delta w'_c dz \quad \mathbf{4.18}$$

Integration by parts:

$$\left(F_z + \frac{M_y}{R} \right) \delta w_c \Big|_0^L - \int_0^L \left(F_z' + \frac{M_y'}{R} \right) \delta w_c dz \quad \mathbf{4.19}$$

- Variational energy strain terms associated with δv_s is

$$\int_L \left(-M_x - y_s \frac{M_y}{R} - \frac{M_\omega}{R} \right) \delta v''_s dz \quad \mathbf{4.20}$$

Integration by parts:

$$\begin{aligned}
& - \left(M_x + y_s \frac{M_y}{R} + \frac{M_\omega}{R} \right) \delta v_s \Big|_0^L + \left(M_x' + y_s \frac{M_y'}{R} + \frac{M_\omega'}{R} \right) \delta v_s \Big|_0^L \\
& - \int_0^L \left(M_x'' + y_s \frac{M_y''}{R} + \frac{M_\omega''}{R} \right) \delta v_s dz
\end{aligned} \tag{4.21}$$

- Variational energy strain terms associated with $\delta\beta$ is

$$\int_L \left[- \left(y_s \frac{F_z}{R} - \frac{M_x}{R} \right) \delta\beta - M_\omega \delta\beta'' \right] dz \tag{4.22}$$

Integration by parts:

$$- \int_0^L \left(y_s \frac{F_z}{R} - \frac{M_x}{R} \right) \delta\beta - M_\omega \delta\beta' \Big|_0^L + M_\omega' \delta\beta \Big|_0^L - \int_0^L M_\omega'' \delta\beta dz \tag{4.23}$$

Similarly, the strain energy associated with nonlinear strains can be expanded as the following:

- Variational energy strain terms associated with δu_s is

$$\begin{aligned}
& \left(F_z^a \left(u_s' + \frac{w_c}{R} + y_s \beta' \right) \delta(u_s') \right) - \left(M_y \left(\frac{y_s}{R} (-2\delta u_s' \beta') \right) + M_y^a \left(-2 \frac{\delta u_s' u_s'}{R} - \frac{y_s}{R} \beta' \delta u_s' \right) \right) \\
& + \left(M_x (\delta u_s' \beta' + \beta \delta(u_s'')) + M_x^a \left(-\delta u_s' \left(\beta' + \frac{v_s'}{R} \right) \right) \right) \\
& + \left(M_\omega \left(\frac{\delta u_s' \beta'}{R} + \frac{\beta \delta u_s''}{R} \right) + M_\omega^a \left(-\frac{\delta u_s' \beta'}{R} \right) \right) + K_{xy}^a \left(\frac{(\beta' \delta u_s')}{R} \right)
\end{aligned} \tag{4.24}$$

Integration by parts:

$$\begin{aligned}
& F_z^a \left(u_s' + \frac{w_c}{R} + y_s \beta' \right) \delta u_s \Big|_0^L - \int_0^L \left(F_z^a \left(u_s' + \frac{w_c}{R} + y_s \beta' \right) \right)' \delta u_s dz \\
& \left(M_y \left(2 \frac{y_s}{R} \beta' \delta u_s' \right) + M_y^a \left(2 \frac{u_s'}{R} + \frac{y_s}{R} \beta' \right) \right) \delta u_s \Big|_L^L
\end{aligned}$$

$$\begin{aligned}
& - \int_L^0 \left(M_y \left(2 \frac{y_s}{R} \beta' \delta u'_s \right) + M_y^a \left(2 \frac{u'_s}{R} + \frac{y_s}{R} \beta' \right) \right)' \delta u_s dz \\
& + \left(M_x \beta' - M_x^a \tilde{\beta}' \right) \delta u'_s \Big|_0^L + \left(M_x \beta \right) \delta u'_s \Big|_0^L - \left(M_x \beta \right)' \delta u_s \Big|_0^L \\
& - \int_0^L \left(\left(M_x \beta' - M_x^a \tilde{\beta}' \right)' - \left(M_x \beta \right)'' \right) \delta u_s dz \\
& + \left(M_\omega - M_\omega^a \right) \frac{\beta'}{R} \delta u_s \Big|_0^L - \int_0^L \left(M_\omega - M_\omega^a \right) \frac{\beta'}{R} \delta u_s dz \\
& + M_\omega \frac{\beta}{R} \delta u'_s \Big|_0^L - \left(M_\omega \frac{\beta}{R} \right)' \delta u_s \Big|_0^L + \int_0^L \left(M_\omega \frac{\beta}{R} \right)'' \delta u_s dz \\
& + K_{xy}^a \frac{\beta'}{R} \delta u_s \Big|_0^L - \int_0^L \left(K_{xy}^a \frac{\beta'}{R} \right)' \delta u_s dz
\end{aligned} \tag{4.25}$$

- Variational energy strain terms associated with δw_c is

$$\int_L^0 \left[\begin{aligned} & \left(F_z^a \left(u'_s + \frac{w_c}{R} + y_s \beta' \right) \delta \frac{w_c}{R} \right) + M_y \left(\frac{y_s}{R} \left(2 \beta' \delta \frac{w_c}{R} + 2 \beta \delta \frac{w'_c}{R} \right) \right) \\ & + \left(M_x \left(\delta \frac{w_c}{R} \beta' + \beta \delta \frac{w'_c}{R} \right) - M_x^a \left(\beta' + \frac{v'_s}{R} \right) \delta \frac{w_c}{R} \right) \end{aligned} \right] dz \tag{4.26}$$

Integration by parts:

$$\int_0^L F_z^a \left(\frac{u'_s}{R} + y_s \frac{\beta'}{R} \right) \delta w_c dz \tag{4.27}$$

$$\int_0^L \left(M_x - M_x^a \right) \frac{\beta'}{R} \delta w_c dz + M_x \frac{\beta}{R} \delta w_c \Big|_0^L - \int_0^L \left(M_x \frac{\beta}{R} \right)' \delta w_c dz$$

- Variational energy strain terms associated with δv_s is

$$\int_L^0 \left[\begin{aligned} & \left(F_z^a (v'_s - x_s \beta') \delta v'_s \right) + M_y (\delta v'_s \beta' + \beta \delta v''_s) - M_y^a \beta' \delta v'_s \\ & + \left(M_x^a \left(- \left(u'_s + \frac{w_c}{R} \right) \delta \frac{v'_s}{R} - y_s \beta' \delta \frac{v'_s}{R} \right) \right) \end{aligned} \right] dz \tag{4.28}$$

Integration by parts:

$$\begin{aligned}
& F_z^a (v'_s - x_s \beta') \delta v_s \Big|_0^L - \int_0^L \left\{ F_z^a (v'_s - x_s \beta') \right\}' \delta v_s dz \\
& - \beta' (M_y^a - M_y) \delta v_s \Big|_0^L + \int_0^L \left(\beta' (M_y^a - M_y) \right)' \delta v_s dz \\
& + M_y \beta \delta v'_s \Big|_0^L - (M_y \beta)' \delta v_s \Big|_0^L + \int_0^L \left\{ M_y \beta \right\}'' \delta v_s dz \\
& - M_x^a \left(\frac{u'_s}{R} + y_s \frac{\beta'}{R} \right) \delta v_s \Big|_0^L + \int_0^L \left\{ M_x^a \left(\frac{u'_s}{R} + y_s \frac{\beta'}{R} \right) \right\}' \delta v_s dz
\end{aligned} \tag{4.29}$$

- Variational energy strain terms associated with $\delta\beta$ is

$$\begin{aligned}
& \int_L \left[F_z^a \left(y_s \left(u'_s + \frac{w_c}{R} \right) - x_s v'_s + (x_s^2 + y_s^2) \beta' \right) \delta\beta' \right. \\
& \quad - M_y \left(-\delta\beta v_s'' - v'_s \delta\beta' \right) - M_y^a \left(v'_s \delta\beta' - \frac{y_s}{R} (u'_s + 2x_s \beta') \delta\beta' \right) \\
& \quad + \left(M_x \left(\left(u'_s + \frac{w_c}{R} \right) \delta\beta' + \left(u_s'' + \frac{w'_c}{R} \right) \delta\beta \right) - \left(u'_s + \frac{w_c}{R} + y_s \beta' + y_s \frac{v'_s}{R} + y_s \beta' \right) \delta\beta' \right) \\
& \quad + M_\omega \left(\frac{u'_s \delta\beta'}{R} + \frac{u_s'' \delta\beta}{R} \right) + M_\omega^a \left(-\frac{u'_s \delta\beta'}{R} - 2 \frac{y_s}{R} \beta' \delta\beta' \right) \\
& \quad \left. + \left(K_{xx}^a + K_{yy}^a + K_{y\omega}^a \right) (\beta' \delta\beta') + K_{xy}^a \left(\frac{u'_s}{R} \delta\beta' \right) \right] dz
\end{aligned} \tag{4.30}$$

Integration by parts:

$$\begin{aligned}
& F_z^a \left(y_s (\tilde{u}'_s) - x_s v'_s + (x_s^2 + y_s^2) \beta' \right) \delta\beta \Big|_0^L \\
& - \int_0^L \left(F_z^a \left(y_s (\tilde{u}'_s) - x_s v'_s + (x_s^2 + y_s^2) \beta' \right) \right)' \delta\beta dz \\
& + \int_0^L \left\{ M_y v_s'' \right\} \delta\beta dz - \left((M_y^a - M_y) v'_s - M_y \frac{y_s}{R} (u'_s + 2x_s \beta') \right) \delta\beta \Big|_0^L \\
& + \int_0^L \left\{ \left((M_y^a - M_y) v'_s - M_y \frac{y_s}{R} (u'_s + 2x_s \beta') \right) \right\}' \delta\beta dz \\
& - \int_0^L \left\{ -M_x \tilde{u}_s'' \right\} \delta\beta dz - \left((M_x^a - M_x) \tilde{u}'_s + M_x^a y_s (\tilde{\beta}' + \beta') \right) \delta\beta \Big|_0^L \\
& + \int_0^L \left\{ \left((M_x^a - M_x) \tilde{u}'_s + M_x^a y_s (\tilde{\beta}' + \beta') \right) \right\}' \delta\beta dz
\end{aligned}$$

$$\begin{aligned}
& + \int_0^L \left\{ M_\omega \frac{u_s''}{R} \right\} \delta\beta \, dz + \left((M_\omega - M_\omega^a) \frac{u_s'}{R} - 2M_\omega^a y_s \frac{\beta'}{R} \right) \delta\beta \Big|_0^L \\
& - \int_0^L \left\{ \left((M_\omega - M_\omega^a) \frac{u_s'}{R} - 2M_\omega^a y_s \frac{\beta'}{R} \right)' \right\} \delta\beta \, dz \\
& + \left(K_{xx}^a + K_{yy}^a + K_{y\omega}^a \right) \beta' \delta\beta \Big|_0^L + K_{xy}^a \frac{u_s'}{R} \delta\beta \Big|_0^L \\
& - \int_0^L \left(\left(K_{xx}^a + K_{yy}^a + K_{y\omega}^a \right) \beta' \right)' \delta\beta \, dz - \int_0^L \left(K_{xy}^a \frac{u_s'}{R} \right)' \delta\beta \, dz
\end{aligned} \tag{4.31}$$

In a similar way with regard to shear strains, the last term of Equation 4.11a can be expressed as the following:

$$\int_V [\sigma_{zs} \delta(e_{zs} + \eta_{zs})] dV = \int_V [\sigma_{zs} 2n \delta(e_n)] dV + \int_V [\sigma_{zs} 2n \delta(\eta_n)] dV \tag{4.32}$$

By using the definition of stress resultants, Equation 4.32 can be expanded as the following:

$$\int_V (M_{sv} \delta e_n) dV + \int_V (M_{sv} \delta \eta_n) dV \tag{4.33a}$$

$$\text{Where } M_{sv} = \int_A 2n (\sigma_{zs}) dA \tag{4.33b}$$

Substituting the expression for linear and nonlinear strains from Eq. 4.10j and sorting out same displacement field, Equation 4.33a can be expressed as the following:

$$\int_L \left[M_{sv} \left(\delta\beta' + \frac{\delta v_s'}{R} \right) \right] dz + \int_L \left[M_{sv} \left(\frac{\delta u_s' \beta}{R} + \frac{u_s' \delta\beta}{R} \right) \right] dz \tag{4.34}$$

- From variational energy strain terms associated with δu_s and integration by parts;

$$M_{sv} \frac{\beta}{R} \delta u_s \Big|_0^L - \int_0^L \left(M_{sv} \frac{\beta}{R} \right)' \delta u_s \, dz \tag{4.35}$$

- Variational energy strain terms associated with δv_s :

$$\frac{M_{sv}}{R} \delta v_s \Big|_0^L - \int_0^L \frac{M_{sv}'}{R} \delta v_s \, dz \tag{4.36}$$

- From variational energy strain terms associated with $\delta\beta$ and integration by parts, the expression associated with linear and nonlinear strains are the following

$$M_{sv} \delta\beta \Big|_0^L - \int_0^L M_{sv}' \delta\beta dz \quad 4.37a$$

$$M_{sv} \frac{u_s'}{R} \delta\beta \Big|_0^L - \int_0^L \left(M_{sv} \frac{u_s'}{R} \right)' \delta\beta dz \quad 4.37b$$

4.3.2 Variation of Potential Energy due to Applied Load

For the analysis of load and deflection behavior of curved beams in this study, the external loads include distributed loads and concentrated loads. The body forces are not included. The variation of potential energy due to applied loads, as expressed by the third term of Eq. 4.2, can be expressed as the following:

$$\int_L \delta \bar{u}^T \bar{f} dz + \sum_j \delta \bar{q}_j^T \bar{F}_j \quad 4.38$$

Where \bar{f} and \bar{u} are the vector of distributed loads and displacements along the span length L as defined in Figure 4.1, and have the following components:

$$\bar{f} = \left\{ f_x, f_y, f_z, m_x, m_y, m_z, m_\omega \right\}^T \quad 4.39a$$

$$\bar{u} = \left\{ u_s, v_s, w_s, \theta_x, \theta_y, \beta, \theta_\omega \right\}^T \quad 4.39b$$

$$\theta_x = v_s' \quad 4.39c$$

$$\theta_y = u_s' + \frac{w_c}{R} \quad 4.39d$$

$$\theta_\omega = \beta' + \frac{v_s'}{R} \quad 4.39e$$

Where:

f_x is distribute shear loads applied to shear center in direction x-axis

f_y is distribute shear loads applied to shear center in direction y-axis

f_z is distribute axial loads applied to centroid in z-axis

m_x and m_y are distribute moment applied to centroid

m_z and m_ω are torsional and warping moment applied to shear center

w_c is longitudinal displacement of the centroid

θ_x and θ_y are rotation about x- and y-axis

θ_ω is warping rotation

\bar{F}_j of Eq. 4.38 is the equivalent concentrate force vector defined in Figure 4.2, and \bar{q}_j is the displacement vector at the location of the applied loads \bar{F}_j .

$$\bar{F}_j = \left\{ F_{xj}, F_{yj}, F_{zj}, M_{xj}, M_{yj}, M_{zj}, M_{\omega j} \right\}^T \quad 4.40a$$

$$\bar{q}_j = \left\{ u_{sj}, v_{sj}, w_{cj}, \theta_{xj}, \theta_{yj}, \beta_j, \theta_{\omega j} \right\}^T \quad 4.40b$$

where j is load number

With the orthogonal condition and by integration by parts, Equation 4.38 can be expanded as the following expression:

$$\begin{aligned} & \int_0^L \left[\left(f_x - m_y' \right) \delta u_s + \left(f_y - m_x' - \frac{m_\omega'}{R} \right) \delta v_s + \left(f_z + \frac{m_y}{R} \right) \delta w_c + \left(m_z - m_\omega' \right) \delta \beta \right] dz \\ & + \left(m_x \delta v_s + m_y \delta u_s + m_\omega \delta \beta + \frac{m_\omega}{R} \delta v_s \right) \Big|_0^L \\ & + \sum_j \left(F_{xj} \delta u_{sj} + F_{yj} \delta v_{sj} + F_{zj} \delta w_{cj} + M_{xj} \delta \theta_{xj} + M_{yj} \delta \theta_{yj} + M_{zj} \delta \beta_j + M_{\omega j} \delta \theta_{\omega j} \right) \Big|_{L_j} \end{aligned} \quad 4.41$$

Where L_j is the location of applied load number j

4.3.3 Components of Governing Differential Equations and Boundary Forces

The governing differential equation can be derived by substituting the strain energy expressions developed in preceding sections into the equation of total potential energy.

For axial deformation δw_c :

$$\begin{aligned} & \int_0^L \left(-F_z' - \frac{M_y'}{R} + F_z^a \left(\frac{u_s'}{R} + y_s \frac{\beta'}{R} \right) + \left(M_x - M_x^a \right) \frac{\beta'}{R} - \left(M_x \frac{\beta}{R} \right)' \right) \delta w_c dz \\ & = \int_0^L \left(p_z + \frac{m_y}{R} \right) \delta w_c dz \end{aligned} \quad 4.42$$

For in-plane deformation δu_s :

$$\begin{aligned}
& \int_0^L \left[\begin{aligned}
& M_y'' - \frac{F_z}{R} - \left(F_z^a \left(u'_s + \frac{w_c}{R} + y_s \beta' \right) \right)' \\
& + \left(M_y \left(-2 \frac{y_s}{R} \beta' \delta u'_s \right) - M_y^a \left(2 \frac{u'_s}{R} + \frac{y_s}{R} \beta' \right) \right)' \\
& - \left(M_x \beta' - M_x^a \left(\beta' + \frac{v'_s}{R} \right) \right)' + (M_x \beta)'' - \left((M_\omega - M_\omega^a) \frac{\beta'}{R} \right)' \\
& + \left(M_\omega \frac{\beta}{R} \right)'' - \left(K_{xy}^a \frac{\beta'}{R} \right)' - \left(M_{sv} \frac{\beta}{R} \right)'
\end{aligned} \right] \delta u_s dz \\
& = \int_0^L \left(p_x - m_y' \right) \delta w_c dz
\end{aligned} \tag{4.43}$$

For out-of-plane deformation δv_s :

$$\begin{aligned}
& \int_0^L \left\{ \begin{aligned}
& \left(-M_x'' - y_s \frac{M_y''}{R} - \frac{M_\omega''}{R} \right) - \left(F_z^a (v'_s - x_s \beta') \right)' + \left(\beta' (M_y^a - M_y) \right)' \\
& + (M_y \beta)'' + \left(M_x^a \left(\frac{u'_s}{R} + y_s \frac{\beta'}{R} \right) \right)' - \frac{M_{sv}'}{R}
\end{aligned} \right\} \delta v_s dz \\
& = \int_0^L \left(f_y - m_x' - \frac{m_\omega'}{R} \right) \delta v_s dz
\end{aligned} \tag{4.44}$$

For twist rotation $\delta \beta$:

$$\begin{aligned}
& \int_0^L \left\{ \begin{aligned}
& -M_\omega'' - \left(y_s \frac{F_z}{R} - \frac{M_x}{R} \right) - M_{sv} - \left(F_z^a (y_s (\tilde{u}'_s) - x_s v'_s + (x_s^2 + y_s^2) \beta') \right)' \\
& + M_y v'_s + \left((M_y^a - M_y) v'_s - M_y \frac{y_s}{R} (u'_s + 2x_s \beta') \right)' + M_x \tilde{u}_s'' - \left(K_{xy}^a \frac{u'_s}{R} \right)' \\
& + \left((M_x^a - M_x) \tilde{u}'_s + M_x y_s (\tilde{\beta}' + \beta') \right)' + M_\omega \frac{u_s''}{R} - \left((K_{xx}^a + K_{yy}^a + K_{y\omega}^a) \beta' \right)' \\
& - \left(M_{sv} \frac{u'_s}{R} \right)'
\end{aligned} \right\} \delta\beta \, dz \\
& = \int_0^L (m_z - m_\omega') \delta\beta \, dz \tag{4.45}
\end{aligned}$$

Since the displacements δu_s , δv_s , δw_c and $\delta\beta$ are arbitrary, the terms in the brackets on both sides of Eq. 4.42 to 4.45 must be equal. The resulting differential equations for horizontally curved beams are the following.

$$-F_z' - \frac{M_y'}{R} + F_z^a \left(\frac{u'_s}{R} + y_s \frac{\beta'}{R} \right) + (M_x - M_x^a) \frac{\beta'}{R} - \left(M_x \frac{\beta'}{R} \right)' - \left(f_z + \frac{m_y}{R} \right) = 0 \tag{4.46a}$$

$$\begin{aligned}
& M_y'' - \frac{F_z}{R} + (M_x \beta)'' - \left(F_z^a \left(u'_s + \frac{w_c}{R} + y_s \beta' \right) \right)' + \left(M_\omega \frac{\beta}{R} \right)'' - \left(K_{xy}^a \frac{\beta'}{R} \right)' \\
& - \left((M_\omega - M_\omega^a) \frac{\beta'}{R} \right)' - \left(M_{sv} \frac{\beta}{R} \right)' - (f_x - m_y') = 0 \tag{4.46b}
\end{aligned}$$

$$\begin{aligned}
& \left(-M_x'' - y_s \frac{M_y''}{R} - \frac{M_\omega''}{R} \right) - \left(F_z^a (v'_s - x_s \beta') \right)' + \left(\beta' (M_y^a - M_y) \right)' \\
& + (M_y \beta)'' + \left(M_x^a \left(\frac{u'_s}{R} + y_s \frac{\beta'}{R} \right) \right)' - \frac{M_{sv}'}{R} - \left(f_y - m_x' - \frac{m_\omega'}{R} \right) = 0 \tag{4.46c}
\end{aligned}$$

$$-M_\omega'' - \left(y_s \frac{F_z}{R} - \frac{M_x}{R} \right) - M_{sv} - \left(F_z^a (y_s (\tilde{u}'_s) - x_s v'_s + (x_s^2 + y_s^2) \beta') \right)'$$

$$\begin{aligned}
& + M_y v'' + \left((M_y^a - M_y) v'_s - M_y \frac{y_s}{R} (u'_s + 2x_s \beta') \right)' + M_x \tilde{u}_s'' - \left(K_{xy}^a \frac{u'_s}{R} \right)' \\
& + \left((M_x^a - M_x) \tilde{u}'_s + M_x y_s (\tilde{\beta}' + \beta') \right)' + M_\omega \frac{u''_s}{R} - \left((K_{xx}^a + K_{yy}^a + K_{y\omega}^a) \beta' \right) \\
& - \left(M_{sv} \frac{u'_s}{R} \right)' - \left(m_z - m_\omega \right)' = 0
\end{aligned} \tag{4.46d}$$

As a check of correctness of Eq. 4.46, a set of differential equation is reduced from it for a straight beam with a doubly symmetrical cross section. By letting the radius of curvature R approaching infinity and centroidal distance x_s and y_s of the shear center equal to zero, Equation 4.46 is simplified to the following set of equations.

$$F_z' + f_z = 0 \tag{4.47a}$$

$$M_y'' + (M_x \beta)'' - (F_z u'_s)' - (f_x - m_y)' = 0 \tag{4.47b}$$

$$\left(-M_x'' \right) - (F_z v'_s)' + (M_y \beta)'' - (f_y - m_x)' = 0 \tag{4.47c}$$

$$-M_\omega'' + M_y v''_s + M_x u''_s - (m_z - m_\omega)' = 0 \tag{4.47d}$$

This set of equations is that of straight beams given by Galambos (1968). Further verification of the adequacy of Eq. 4.46 will be conducted in Chapter 6 with a numerical examples.

The application of the principle of variation of total potential energy generates boundary forces at both ends of the curved beam in association with the equilibrium equations. The force boundary conditions related to the differential displacement components are:

- For δw_c

$$F_z + \frac{M_y}{R} + F_z^a \left(\frac{u'_s}{R} + y_s \frac{\beta'}{R} \right) + M_x \frac{\beta}{R} = 0 \tag{4.48}$$

- For δu_s

$$-M_y' + F_z^a \left(u'_s + \frac{w_c}{R} + y_s \beta' \right) + M_y \left(2 \frac{y_s}{R} \beta' \delta u'_s \right) + M_y^a \left(2 \frac{u'_s}{R} + \frac{y_s}{R} \beta' \right)$$

$$+ \left(M_x \beta' - M_x^a \tilde{\beta}' \right) - (M_x \beta)' + \left((M_\omega - M_\omega^a) \frac{\beta'}{R} \right) - \left(M_\omega \frac{\beta}{R} \right)'$$

$$+ K_{xy}^a \frac{\beta'}{R} + M_{sv} \frac{\beta}{R} - m_y = 0 \quad 4.49$$

- For δv_s

$$\begin{aligned} M_x' + y_s \frac{M_y'}{R} + \frac{M_\omega'}{R} + F_z^a (v_s' - x_s \beta') - \beta' (M_y^a - M_y) \\ - (M_y \beta)' - M_x^a \left(\frac{u_s'}{R} + y_s \frac{\beta'}{R} \right) + \frac{M_{sv}}{R} - m_x + \frac{m_\omega}{R} = 0 \end{aligned} \quad 4.50$$

- For $\delta \theta_y$

$$M_y + (M_x \beta' - M_x^a \tilde{\beta}' + M_x \beta) + M_\omega \frac{\beta}{R} + \frac{F_z}{R} = 0 \quad 4.51$$

- For $\delta \theta_x$

$$- \left(M_x + y_s \frac{M_y}{R} + \frac{M_\omega}{R} - M_y \beta \right) = 0 \quad 4.52$$

- For $\delta \beta$

$$\begin{aligned} M_\omega' + M_{sv} + F_z^a (y_s (\tilde{u}_s') - x_s v_s' + (x_s^2 + y_s^2) \beta') + \left(M_{sv} \frac{u_s'}{R} \right)' \\ + \left((M_y^a - M_y) v_s' - M_y \frac{y_s}{R} (u_s' + 2x_s \beta') \right) - \left((M_x^a - M_x) \tilde{u}_s' + M_x^a y_s (\tilde{\beta}' + \beta') \right) \\ + \left((M_\omega - M_\omega^a) \frac{u_s'}{R} - 2M_\omega^a y_s \frac{\beta'}{R} \right) + (K_{xx}^a + K_{yy}^a + K_{y\omega}^a) \beta' + K_{xy}^a \frac{u_s'}{R} - m_\omega = 0 \end{aligned} \quad 4.53$$

- For warping $\delta \theta_\omega$

$$- M_\omega - \frac{M_x}{R} + \frac{M_y}{R} = 0 \quad 4.54$$

The above force boundary conditions are in addition to the geometric boundary conditions.

$$\delta w_s = \delta u_s = \delta v_s = \delta \theta_y = \delta \theta_x = \delta \beta = \delta \theta_\omega = 0 \quad 4.55$$

With regard to each of the differential displacement, either the force boundary condition or the geometric boundary condition should be satisfied.

4.4 Differential Equations for Curved Beams

4.4.1 Linear and nonlinear Components

Solving of the governing differential equations with complicated terms of stress resultants is very tedious if at all possible. Even when relatively simplified forms of strain-displacement relationship are used, Eqs 4.46 are still unmanageable when there are linear and nonlinear strain terms in the stress resultants. While a solution technique is to be presented later in this study for general cases, the solving of linear parts of the differential equations is made here for a few load cases.

The linear differential equations expressed in terms of stress resultants can be derived from Equation 4.46 by mealy removing the coupling terms.

$$-F_z' - \frac{M_y'}{R} = f_z + \frac{m_y}{R} \quad 4.56a$$

$$M_y'' - \frac{F_z^a}{R} = f_x - m_y' \quad 4.56b$$

$$-M_x'' - y_s \frac{M_y''}{R} - \frac{M_z'}{R} = f_y - m_x' - \frac{m_\omega'}{R} \quad 4.56c$$

$$-M_z' - \left(y_s \frac{F_z}{R} - \frac{M_x}{R} \right) = m_z - m_\omega' \quad 4.56d$$

The total torsion-moment, M_z , is the summation of Saint-Venant torsion and the warping torsion, which can be expressed as the derivative of warping moment.

$$M_z = M_\omega' + M_{sv} \quad 4.57$$

By using the constitutive laws, cross sectional properties and the complete strain-displacement relationship, the stress resultants in Equation 4.56 can be expressed by the displacement field.

The constitutive laws expressed in Eq. 4.3a can be decomposed as the following equations:

$$\sigma_z = E(\varepsilon_z) = E(e_z + \eta_z) \quad 4.58a$$

$$\tau_{sz} = G(\varepsilon_{sz}) = G 2n(e_{sz} + \eta_{sz}) \quad 4.58b$$

Where E and G are the elastic modulus and the shear modulus.

By substituting Equation 4.58 and the strain-displacement relationship of Equation 4.8 into equation 4.12, the stress resultants can be expressed in the following forms.

$$F_z = \int_A \sigma_z dA = \int_A E(e_z + \eta_z) dA = F_z^e + F_z^n$$

$$F_z^e = E \left[A^a \left(\tilde{w}'_c - \frac{\beta y_s}{R} \right) + Q_y^a \left(-\tilde{u}''_s + \frac{y_s v_s''}{R} \right) - Q_x^a (\tilde{v}''_s) - Q_\omega^a (\tilde{\beta}'') \right]$$

$$F_z^n = E \left[A^a \frac{(\tilde{u}'_s + y_s \beta')^2 + (v'_s - x_s \beta')^2}{2} + Q_y^a \left(-\frac{y_s}{R} (-\tilde{u}'_s \beta)' - (v'_s \beta)' \right) \right. \\ \left. + Q_y^q \left(-\frac{u_s'^2}{R} + v'_s \beta' - \frac{y_s}{R} \beta' u'_s - x_s \beta'^2 \right) + Q_x^a (\tilde{u}'_s \beta)' - Q_x^q (\tilde{u}'_s + y_s \beta') \tilde{\beta}' \right. \\ \left. + Q_\omega^a \left(\frac{u'_s \beta}{R} \right)' + Q_\omega^q \left(-\frac{u'_s \beta'}{R} - \frac{y_s}{R} \beta'^2 \right) + \left(\frac{I_y^q + I_x^q + I_{y\omega}^q}{2} \right) \beta'^2 + I_{xy}^q \frac{\beta' u'_s}{R} \right]$$

4.59a

$$M_x = \int_A \sigma_z y dA = \int_A E(e_z + \eta_z) y dA = M_x^e + M_x^n$$

$$M_x^e = E \left[Q_x^a \left(\tilde{w}'_c - \frac{\beta y_s}{R} \right) + I_{xy}^a \left(-\tilde{u}''_s + \frac{y_s v_s''}{R} \right) + I_x^a \left(-v''_s + \frac{\beta''}{R} \right) + I_{y\omega}^a \left(-\beta'' - \frac{v_s''}{R} \right) \right]$$

$$M_x^n = E \left[Q_x^a \frac{(\tilde{u}'_s + y_s \beta')^2 + (v'_s - x_s \beta')^2}{2} + I_{xy}^a \left(-\frac{y_s}{R} (-\tilde{u}'_s \beta)' - (v'_s \beta)' \right) \right. \\ \left. + I_{xy}^q \left(-\frac{u_s'^2}{R} + v'_s \beta' - \frac{y_s}{R} \beta' u'_s - x_s \beta'^2 \right) + I_x^a (\tilde{u}'_s \beta)' - I_x^q (\tilde{u}'_s + y_s \beta') \tilde{\beta}' \right. \\ \left. + I_{y\omega}^a \left(\frac{u'_s \beta}{R} \right)' + I_{y\omega}^q \left(-\frac{u'_s \beta'}{R} - \frac{y_s}{R} \beta'^2 \right) + \left(\frac{I_{xxy}^q + I_{yyy}^q + I_{yy\omega}^q}{2} \right) \beta'^2 \right. \\ \left. + I_{xyy}^q \frac{\beta' u'_s}{R} \right]$$

4.59b

$$M_y = \int_A -\sigma_z x dA = -\int_A E(e_z + \eta_z) x dA = M_y^e + M_y^n$$

$$M_y^e = -E \left[Q_y^a \left(\tilde{w}'_c - \frac{\beta y_s}{R} \right) + I_y^a \left(-\tilde{u}''_s + \frac{y_s v_s''}{R} \right) \right. \\ \left. + I_{xy}^a \left(-v''_s + \frac{\beta''}{R} \right) + I_{x\omega}^a \left(-\beta'' - \frac{v_s''}{R} \right) \right]$$

$$M_y^n = \left[Q_y^a \frac{(\tilde{u}'_s + y_s \beta')^2 + (v'_s - x_s \beta')^2}{2} + I_y^a \left(-\frac{y_s}{R} (-\tilde{u}'_s \beta)' - (v'_s \beta)' \right) \right]$$

$$\begin{aligned}
& + I_y^q \left(-\frac{u_s'^2}{R} + v_s' \beta' - \frac{y_s}{R} \beta' u_s' - x_s \beta'^2 \right) + I_{xy}^a (\tilde{u}' \beta)' - I_{xy}^q (\tilde{u}' + y_s \beta') \tilde{\beta}' \\
& + I_{x\omega}^a \left(\frac{u_s' \beta}{R} \right)' + I_{x\omega}^q \left(-\frac{u_s' \beta'}{R} - \frac{y_s}{R} \beta'^2 \right) + \left(\frac{I_{xxx}^q + I_{xyy}^q + I_{xy\omega}^q}{2} \right) \beta'^2 \\
& + I_{xy}^q \frac{\beta' u_s'}{R} \quad \left. \right] \quad \quad \quad \mathbf{4.59c}
\end{aligned}$$

$$M_\omega = \int_A \sigma_z \omega \, dA = \int_A E(e_z + \eta_z) \omega \, dA = M_\omega^e + M_\omega^n$$

$$\begin{aligned}
M_\omega^e = E \left[\right. & Q_\omega^a \left(\tilde{w}'_c - \frac{\beta y_s}{R} \right) + I_{x\omega}^a \left(-\tilde{u}_s'' + \frac{y_s v_s''}{R} \right) \\
& \left. + I_{y\omega}^a \left(-v_s'' + \frac{\beta}{R} \right) + I_\omega^a \left(-\beta'' - \frac{v_s''}{R} \right) \right]
\end{aligned}$$

$$\begin{aligned}
M_\omega^n = E \left[\right. & Q_\omega^a \frac{(\tilde{u}'_s + y_s \beta')^2 + (v'_s - x_s \beta')^2}{2} + I_{x\omega}^a \left(-\frac{y_s}{R} (-\tilde{u}'_s \beta)' - (v'_s \beta)' \right) \\
& + I_{x\omega}^q \left(-\frac{u_s'^2}{R} + v_s' \beta' - \frac{y_s}{R} \beta' u_s' - x_s \beta'^2 \right) + I_{y\omega}^a (\tilde{u}' \beta)' - I_{y\omega}^q (\tilde{u}' + y_s \beta') \tilde{\beta}' \\
& + I_\omega^a \left(\frac{u_s' \beta}{R} \right)' + I_\omega^q \left(-\frac{u_s' \beta'}{R} - \frac{y_s}{R} \beta'^2 \right) + \left(\frac{I_{xx\omega}^q + I_{yy\omega}^q + I_{x\omega\omega}^q}{2} \right) \beta'^2 \\
& \left. + I_{xy\omega}^q \frac{\beta' u_s'}{R} \right] \quad \quad \quad \mathbf{4.59d}
\end{aligned}$$

$$K_{xx} = \int_A \sigma_z x^2 \, dA = \int_A E(e_z + \eta_z) x^2 \, dA = K_{xx}^e + K_{xx}^n$$

$$K_{xx}^e = E \left[\right. I_y^a \left(\tilde{w}'_c - \frac{\beta y_s}{R} \right) + I_{xxx}^a \left(-\tilde{u}_s'' + \frac{y_s v_s''}{R} \right) + I_{xy}^a \left(-v_s'' + \frac{\beta}{R} \right) + I_{xx\omega}^a \left(-\beta'' - \frac{v_s''}{R} \right) \left. \right]$$

$$\begin{aligned}
K_{xx}^n = E \left[\right. & I_y^a \frac{(\tilde{u}'_s + y_s \beta')^2 + (v'_s - x_s \beta')^2}{2} + I_{xxx}^a \left(-\frac{y_s}{R} (-\tilde{u}'_s \beta)' - (v'_s \beta)' \right) \\
& + I_{xxx}^q \left(-\frac{u_s'^2}{R} + v_s' \beta' - \frac{y_s}{R} \beta' u_s' - x_s \beta'^2 \right) + I_{xy}^a (\tilde{u}' \beta)' - I_{xy}^q (\tilde{u}' + y_s \beta') \tilde{\beta}'
\end{aligned}$$

$$\begin{aligned}
& + I_{xx\omega}^a \left(\frac{u'_s \beta}{R} \right)' + I_{xx\omega}^q \left(-\frac{u'_s \beta'}{R} - \frac{y_s}{R} \beta'^2 \right) + \left(\frac{I_{xxxx}^q + I_{yyxx}^q + I_{xxx\omega}^q}{2} \right) \beta'^2 \\
& + I_{xxy}^q \frac{\beta' u'_s}{R} \Big] \quad \mathbf{4.59f}
\end{aligned}$$

$$K_{yy} = \int_A \sigma_z y^2 dA = \int_A E(e_z + \eta_z) y^2 dA = K_{yy}^e + K_{yy}^n$$

$$\begin{aligned}
K_{yy}^e = E \Big[& I_x^a \left(\tilde{w}'_c - \frac{\beta y_s}{R} \right) + I_{yyx}^a \left(-\tilde{u}''_s + \frac{y_s v''_s}{R} \right) \\
& + I_{yy}^a \left(-v''_s + \frac{\beta}{R} \right) + I_{yy\omega}^a \left(-\beta'' - \frac{v''_s}{R} \right) \Big]
\end{aligned}$$

$$\begin{aligned}
K_{yy}^n = E \Big[& I_x^a \frac{(\tilde{u}'_s + y_s \beta')^2 + (v'_s - x_s \beta')^2}{2} + I_{xy}^a \left(-\frac{y_s}{R} (-\tilde{u}'_s \beta)' - (v'_s \beta)' \right) \\
& + I_{xy}^q \left(-\frac{u'^2_s}{R} + v'_s \beta' - \frac{y_s}{R} \beta' u'_s - x_s \beta'^2 \right) + I_{yyy}^a (\tilde{u}'_s \beta)' - I_{yyy}^q (\tilde{u}'_s + y_s \beta') \tilde{\beta}' \\
& + I_{yy\omega}^a \left(\frac{u'_s \beta}{R} \right)' + I_{yy\omega}^q \left(-\frac{u'_s \beta'}{R} - \frac{y_s}{R} \beta'^2 \right) + \left(\frac{I_{xxyy}^q + I_{yyyy}^q + I_{xyy\omega}^q}{2} \right) \beta'^2 \\
& + I_{xyy}^q \frac{\beta' u'_s}{R} \Big] \quad \mathbf{4.59g}
\end{aligned}$$

$$K_{xy} = \int_A \sigma_z xy dA = \int_A E(e_z + \eta_z) xy dA = K_{xy}^e + K_{xy}^n$$

$$K_{xy}^e = E \left[I_{xy}^a \left(\tilde{w}'_c - \frac{\beta y_s}{R} \right) + I_{xxy}^a \left(-\tilde{u}''_s + \frac{y_s v''_s}{R} \right) + I_{xy}^a \left(-v''_s + \frac{\beta}{R} \right) + I_{xy\omega}^a \left(-\beta'' - \frac{v''_s}{R} \right) \right]$$

$$\begin{aligned}
K_{xy}^n = E \Big[& I_{xy}^a \frac{(\tilde{u}'_s + y_s \beta')^2 + (v'_s - x_s \beta')^2}{2} + I_{xxy}^a \left(-\frac{y_s}{R} (-\tilde{u}'_s \beta)' - (v'_s \beta)' \right) \\
& + I_{xxy}^q \left(-\frac{u'^2_s}{R} + v'_s \beta' - \frac{y_s}{R} \beta' u'_s - x_s \beta'^2 \right) + I_{xyy}^a (\tilde{u}'_s \beta)' - I_{xyy}^q (\tilde{u}'_s + y_s \beta') \tilde{\beta}' \\
& + I_{xy\omega}^a \left(\frac{u'_s \beta}{R} \right)' + I_{xy\omega}^q \left(-\frac{u'_s \beta'}{R} - \frac{y_s}{R} \beta'^2 \right) + \left(\frac{I_{xxyy}^q + I_{xyyy}^q + I_{xyy\omega}^q}{2} \right) \beta'^2
\end{aligned}$$

$$\left. + I_{xxyy}^q \frac{\beta' u'_s}{R} \right] \quad 4.59h$$

$$K_{x\omega} = \int_A \sigma_z x \omega dA = \int_A E(e_z + \eta_z) x \omega dA = K_{x\omega}^e + K_{x\omega}^n$$

$$K_{x\omega}^e = E \left[I_{x\omega}^a \left(\tilde{w}'_c - \frac{\beta y_s}{R} \right) + I_{xx\omega}^a \left(-\tilde{u}''_s + \frac{y_s v''_s}{R} \right) + I_{xy\omega}^a \left(-v''_s + \frac{\beta}{R} \right) + I_{x\omega\omega}^a \left(-\beta'' - \frac{v''_s}{R} \right) \right]$$

$$\begin{aligned} K_{x\omega}^n = E & \left[I_{x\omega}^a \frac{(\tilde{u}'_s + y_s \beta')^2 + (v'_s - x_s \beta')^2}{2} + I_{xx\omega}^a \left(-\frac{y_s}{R} (-\tilde{u}'_s \beta)' - (v'_s \beta)' \right) \right. \\ & + I_{xx\omega}^q \left(-\frac{u'^2_s}{R} + v'_s \beta' - \frac{y_s}{R} \beta' u'_s - x_s \beta'^2 \right) + I_{xy\omega}^a (\tilde{u}'_s \beta)' - I_{xy\omega}^q (\tilde{u}'_s + y_s \beta') \tilde{\beta}' \\ & + I_{x\omega\omega}^a \left(\frac{u'_s \beta}{R} \right)' + I_{x\omega\omega}^q \left(-\frac{u'_s \beta'}{R} - \frac{y_s}{R} \beta'^2 \right) + \left(\frac{I_{xxx\omega}^q + I_{xyy\omega}^q + I_{xx\omega\omega}^q}{2} \right) \beta'^2 \\ & \left. + I_{xxy\omega}^q \frac{\beta' u'_s}{R} \right] \quad 4.59i \end{aligned}$$

$$M_{sv} = \int_A \tau_{sv} 2n dA = \int_A G(e_{sv} + \eta_{sv}) 2n dA = M_{sv}^e + M_{sv}^n$$

$$M_{sv}^e = G K_T^a \left(\beta' + \frac{v'_s}{R} \right)$$

$$M_{sv}^n = G K_T^a \left(\frac{u'_s \beta}{R} \right) \quad 4.59j$$

The superscript “e” and “n” in the stress resultants denote linear and nonlinear. In Equation 4.59, the sectional properties associated with second and third order units are defined as

$$A = \int_{A_0} dA \quad 4.60a$$

$$Q_x = \int_{A_0} y dA \quad 4.60b$$

$$Q_y = \int_{A_0} x dA \quad 4.60c$$

A, Q_x and Q_y are the area and the first moment of area about the x-axis and the y-axis respectively.

The sectional properties associated with fourth order units are;

$$I_x = \int_{A_0} y^2 dA \quad 4.61a$$

$$I_y = \int_{A_0} x^2 dA \quad 4.61b$$

$$I_{xy} = \int_{A_0} x y dA \quad 4.61c$$

$$K_T = \int_S (2n)^2 t ds \quad 4.61d$$

$$Q_\omega = \int_{A_0} \omega dA \quad 4.61e$$

I_x , I_y and I_{xy} are moment of inertia about the x-axis and the y-axis and the cross product of inertia. K_T is the Saint-Venant torsional constant and Q_ω is the warping static moment. Since normalized warping function is used in this study, the warping static moment of 4.61e vanishes.

The sectional properties associated with fifth and sixth order unit are;

$$I_{x\omega} = \int_{A_0} x \omega dA \quad 4.62a$$

$$I_{y\omega} = \int_{A_0} y \omega dA \quad 4.62b$$

$$I_\omega = \int_{A_0} \omega^2 dA \quad 4.62c$$

The $I_{x\omega}$, $I_{y\omega}$ and I_ω are warping product of inertia about the x-axis and the y-axis and the warping moment inertia. It is to be noted that in the differential equations based on two reference lines, (shear center and centroid), the quantity of $I_{x\omega}$ or $I_{y\omega}$ can be made to vanish by using normalized warping function for singly symmetric cross section, but this can not be done in the equation based on a single reference line at the centroid. This fact also applies to other sectional properties associated with warping sectorials.

The other sectional properties in equation 4.59 are defined by the following equations.

The sectional properties associated with fifth order units are:

$$I_{xxx} = \int_{A_0} x^3 dA \quad 4.63a$$

$$I_{xxy} = \int_{A_0} x^2 y dA \quad 4.63b$$

$$I_{yyy} = \int_{A_0} y^3 dA \quad 4.63c$$

The sectional properties associated with sixth order units are:

$$I_{xy\omega} = \int_{A_0} xy\omega dA \quad 4.64a$$

$$I_{yy\omega} = \int_{A_0} y^2\omega dA \quad 4.64b$$

$$I_{xxxx} = \int_{A_0} x^4 dA \quad 4.64c$$

$$I_{xxxy} = \int_{A_0} x^3 y dA \quad 4.64d$$

$$I_{xxyy} = \int_{A_0} x^2 y^2 dA \quad 4.64e$$

$$I_{yyyy} = \int_{A_0} y^4 dA \quad 4.64f$$

$$I_{yyy\omega} = \int_{A_0} y^3\omega dA \quad 4.64g$$

$$I_{xyyy} = \int_{A_0} xy^3 dA \quad 4.64h$$

The sectional properties associated with higher than sixth order units are:

$$I_{y\omega\omega} = \int_{A_0} y\omega^2 dA \quad 4.65a$$

$$I_{\omega\omega\omega} = \int_{A_0} \omega^3 dA \quad 4.65b$$

$$I_{xxx\omega} = \int_{A_0} x^3\omega dA \quad 4.65c$$

$$I_{xx\omega\omega} = \int_{A_0} x^2\omega^2 dA \quad 4.65d$$

$$I_{xyy\omega} = \int_{A_0} xy^2\omega dA \quad 4.65e$$

$$I_{xy\omega\omega} = \int_{A_0} xy\omega^2 dA \quad 4.65f$$

$$I_{x\omega\omega\omega} = \int_{A_0} x\omega^3 dA \quad 4.65g$$

$$I_{yy\omega\omega} = \int_{A_0} y^2\omega^2 dA \quad 4.65h$$

$$I_{y\omega\omega\omega} = \int_{A_0} y\omega^3 dA \quad 4.65i$$

$$I_{\omega\omega\omega\omega} = \int_{A_0} \omega^4 dA \quad 4.65j$$

In Eq 4.59, the sectional properties have super script a, q or r, which represent multiplying $\frac{R}{R-x}$, $\left(\frac{R}{R-x}\right)^2$ or $\left(\frac{R}{R-x}\right)^3$ to the integrand in Equations 4.60 to 4.65.

e.g. $I_x^a = \int_{A_0} \left(\frac{R}{R-x}\right) y^2 dA$, $I_x^q = \int_{A_0} \left(\frac{R}{R-x}\right)^2 y^2 dA$ and $I_x^r = \int_{A_0} \left(\frac{R}{R-x}\right)^3 y^2 dA$. Because of these terms, the quantity of Q_x , Q_y , Q_ω , I_{xy} , $I_{x\omega}$ and $I_{y\omega}$ can not be made to vanishe in formulation; the orthogonal condition can not even be applied to a symmetrical cross section.

The linear differential equations in terms of displacement can be derived by substituting Equation 4.59 into Equation 4.56. If the approximation a) and b) in Section 3.2.2 is adopted, the resulting equations are the following.

$$E \left[-A \left(\tilde{w}_c'' - \frac{y_s}{R} \beta' \right) + \frac{I_y}{R} u_s'' + \frac{I_{xy}}{R} v_s'' + \frac{I_{x\omega}}{R} \beta'' \right] = f_z + \frac{m_y}{R} \quad 4.66a$$

$$E \left[I_y \tilde{u}_s^{iv} - \frac{I_{xy}}{R} \beta'' + I_{x\omega} \beta^{iv} - \left(\frac{y_s I_y}{R} - I_{xy} - \frac{I_{x\omega}}{R} \right) v_s^{iv} - \frac{A}{R} w_c' \right] = f_x - m_y' \quad 4.66b$$

$$E \left(y_s \frac{I_y}{R} + I_{xy} - \frac{I_{x\omega}}{R} \right) u_s^{iv} + E I_{xy} w_c'' + E \left(I_x + \frac{I_{y\omega}}{R} - \frac{I_{y\omega}}{R} \right) v_s^{iv} + E \left(I_{y\omega} + y_s \frac{I_{x\omega}}{R} + \frac{I_{y\omega}}{R} - \frac{I_\omega}{R} \right) \beta^{iv} - \left(E \frac{I_x}{R} + G \frac{K_T}{R} \right) \beta'' = f_y - m_x' - \frac{m_\omega'}{R} \quad 4.66c$$

$$E I_{x\omega} \tilde{u}_s^{iv} + \left(E I_{y\omega} - E y_s \frac{I_{x\omega}}{R} + E \frac{I_\omega}{R} \right) v_s^{iv} + (E I_\omega) \beta^{iv} - E \frac{I_{xy}}{R} u_s'' - \left(E \frac{I_x}{R} + G \frac{K_T}{R} \right) v_s'' - \left(E \frac{I_{y\omega}}{R} + G K_T + E \frac{I_{y\omega}}{R} \right) \beta'' - E y_s \frac{A}{R} w_c' = m_z - m_\omega' \quad 4.66d$$

4.4.2 Exact Solution for Linear Differential Equations

For some loading and boundary conditions and cross sectional shapes, the stress resultants for horizontally curved beams can be clearly derived based on the first order analysis. Conventionally the “basic” loading and boundary condition of Figure 4.3(b) were used for deriving exact solution of stress resultants along the beam span. In the two dimensional beam model of Figure 4.3(b), u and v are lateral and vertical displacement of the shear center, w is the longitudinal displacement of the centroid, θ_x , θ_y , β are rotation about x, y and z axis, θ_ω is warping rotation, Φ and Φ' are angles to

the point load measured from the left and the right end, z' is the longitudinal coordinate from the right end and Γ is the enclosed angle of the curved beam.

From static equilibrium, the vertical flexural bending moment M_x and the axial force F_z along the span for any cross sectional shape can be determined. Thus, Eq 4.56d are independent with the other differential equations, Eq. 4.56a, Eq. 4.56b and Eq 4.56c. With the assumption of small displacement and small rotation, the approximation $R/(R-x) = 1$ and the orthogonal condition of singly symmetric cross sections about y -axis, the linear part of M_ω and M_{sv} of Eq. 4.59 can be simplified as

$$M_\omega = -E I_\omega (\tilde{\beta}''') \quad 4.67a$$

$$M_{sv} = G K_T (\tilde{\beta}') \quad 4.67b$$

and Eq. 4.56d becomes

$$E I_\omega \tilde{\beta}^{iv} - G K_T (\tilde{\beta}''') = \left(y_s \frac{F_z}{R} - \frac{M_x}{R} \right) + m_z - m_\omega' \quad 4.68$$

This equation is identical to that derived by Dabrowski (1964). The torsional moment and bi-moment in a curved beam must be determined by solving the differential equations in conjunction with boundary conditions. The determination of stress resultants for seven example cases is considered in this section. The loading and warping boundary conditions of these cases are the following. The curved beam is simply supported for flexural loading.

1. Point loads and equal end moment, P and M	Fixed – Fixed
2. P and M	Fixed – Free
3. Distributed vertical load and moment, p and m	Fixed – Fixed
4. p and m	Fixed – Free
5. Moment at one End, M	Fixed – Fixed
6. Moment and both ends, M_L and M_R	Fixed – Free
7. Bi-moment at one End, Bi	Fixed – Free

The resulting expressions for stress resultants are listed in Table 4.1 to 4.7 for the above seven example cases. The expression of stress resultants for the seven loading cases and free-free warping boundary condition can be founded in Dabrowski (1968). With given numerical values of beam dimension and applied loads, the expressions in Table 4.1 to 4.7 permit the calculation of forces, stresses and displacements under the assumption of linear behavior

4.4.3 Comparison of Results

There are no available analytical results for evaluating the exact solution listed in Table 4.1 to 4.7. Only an approximate solution has been derived by simplified analysis, (Xanthakos, 1994). The evaluation of solution is conducted by comparing the results from exact solution and approximate solution.

Figure 4.4 shows the procedure of the simplified analysis in which the Bi-moment of the horizontally curved beam under point load P is calculated. The first step of the simplified analysis is to isolate a flange from the curved beam and treat it as a straight beam which has length $L=R\Gamma$. The boundary condition of the equivalent straight beam is in compliance with the warping boundary condition of curved beam. Figure 4.4(b) shows the example of fixed-fixed warping boundary condition. The next step is to derive the lateral distributed loads along the span. These loads can be obtained from the beam bending moment diagram by equilibrium of a free body of a small segment of the curved flange, Figure 4.4(a). The last step is to calculate lateral bending moment from the laterally distributed loads. Then, the bi-moments can be obtained by multiplying web-depth to the obtained lateral bending moment, e.g., $M_{\omega(0)}=M_A h$, $M_{\omega(L)}=M_B h$, $M_{\omega(L/2)}=M_C h$. These approximated bi-moments $M_{\omega(0)}$, $M_{\omega(L/2)}$ and $M_{\omega(L)}$ for a curved beam with the cross sectional geometry shown in Figure 4.5 are compared with those calculated from the equations presented in Table 4.1 in which exact solution of bi-moment for fixed-fixed boundary condition is listed. Table 4.8 shows the results for computation. The approximated bi-moments are fairly close to the exact value at the end sections. But at the mid-span, the results are quite different. So, the evaluation of the equations in Table 4.1 to 4.7 can not be achieved by comparing with the approximate solution. Evaluation of solution will be made by using the finite line element for the curved beams, which is developed in Chapter 5, and by using the numerical method in Chapter 6.

4.5 Method of Solution by Incremental Total Lagrangian Formulation

4.5.1 Derivation of Equilibrium Equation in Incremental Formulation

In preceding sections, linear and nonlinear differential equations are developed with the assumption of small rotations and displacements. For certain loading and boundary conditions, closed form solutions of linear differential equation are also developed. Since in general curved beams can undergo large displacement and large rotation, precise load-deflection behavior can only be obtained from solving nonlinear differential equation. An approximate solution of nonlinear differential equation for large displacement and rotation analysis can be derived by the incremental analysis. In incremental analysis, the governing equations in each incremental step are linearized and equilibrium is maintained at the beginning and the end of each discrete increase of displacement.

Three equilibrium positions are schematically shown in Figure 4.6 - the initial and two consecutive positions. For convenience, these are designated as position 0, t and $t+\Delta t$, although no dynamic effect is considered. In each incremental step, it is assumed that the displacement, rotation and strains are small enough for the adoption of conventional small displacement beam theory, with high order terms ignored and trigonometric functions represented by the first term of Taylor expansions. Depending on the choice of reference position and configuration, two formulations can be made; total Lagrangian and updated Lagrangian formulation. In the total Lagrangian formulation, all static and kinematic variables are referred to the initial position and

undeformed configuration. The updated Lagrangian formulation uses the last position and configuration of equilibrium. Both the total Lagrangian and updated Lagrangian formulation include all kinematic nonlinear effects due to large displacement and large rotation. In practice, these two formulations give identical results. The only advantage of one over the other is in the numerical efficiency (Bathe 1982)

In this study of horizontally curved beams, the total Lagrangian formulation is adopted. The updated Lagrangian formulation needs the modification of beam configuration based on the character of external forces which are displacement and rotation dependant. Also, to update the beam configuration, an equivalent stiffness matrix has to be added to the beam stiffness of the last step. This causes the system stiffness matrix to be non-symmetric when non-conservative moment is considered and require more processing time.

One disadvantage of the total Lagrangian formulation is the complexity of the geometric stiffness matrix and the stress stiffness matrix. Each stiffness matrix includes the total displacement and trigonometric expression associated with large rotation which can not be simplified by taking only the first term of Taylor series.

To deriving the equilibrium equation of the curved beam at a discrete position by using minimum total potential energy, the first step is to evaluating the incremental displacement and rotation. Minimum total potential energy at the position $t+ \Delta t$ is expressed as the following.

$$\delta \Pi^{t+\Delta t} = \int_{V_0} (\delta \bar{\epsilon}^{t+\Delta t})^T \bar{S}^{t+\Delta t} dV - \bar{H}^{t+\Delta t} = 0 \quad 4.69$$

$$\bar{H}^{t+\Delta t} = \int_{V_0}^{t+\Delta t} (\bar{f}^B)^T \delta \bar{u} dV + \int_{S_0}^{t+\Delta t} (\bar{f}^{s_f})^T \delta \bar{u}^{s_f} dS \quad 4.70$$

Where V_0 and S_0 are the volume and surface of the undeformed body, $\bar{S}^{t+\Delta t}$ is the stress tensor at position $t+ \Delta t$, H is the loss of potential energy, and \bar{f}^B and \bar{f}^{s_f} are components of the externally applied forces per unit volume and externally applied surface traction per unit surface.

The following relations can be expressed between two adjacent positions.

$$\bar{u}^{t+\Delta t} = \bar{u}^t + \Delta \bar{u} \quad 4.71a$$

$$\bar{\epsilon}^{t+\Delta t} = \bar{\epsilon}^t + \Delta \bar{\epsilon} \quad 4.71b$$

$$\bar{S}^{t+\Delta t} = \bar{S}^t + \Delta \bar{S} \quad 4.71c$$

The incremental form of the principal of minimum total potential is

$$\delta \Delta \Pi = \delta \Pi^{t+\Delta t} - \delta \Pi^t \quad 4.72$$

In the configuration position $t+\Delta t$, $\delta\Pi^t$ is already satisfied. That is, the variation of total potential energy at position t is equal to zero.

$$\delta\Pi^t = \int_{V_0} (\delta \bar{\varepsilon}^t)^T \bar{S}^t dV - \bar{H}^t = 0 \quad 4.73$$

By substituting the incremental values of Eq. 4.71 into Eq. 4.69 and using Eq. 4.73, the variation of incremental total potential energy is

$$\delta \Delta\Pi = \int_{V_0} (\delta \bar{\varepsilon}^{t+\Delta t})^T \Delta \bar{S} dV + \int_{V_0} (\delta \Delta \bar{\varepsilon})^T \bar{S}^t dV - \bar{H}^{t+\Delta t} = 0 \quad 4.74$$

Equation 4.74 can be further decomposed by noting that a strain tensor can be expressed in linear and nonlinear terms, $\bar{\varepsilon} = \bar{\varepsilon} + \bar{\eta}$, and that the variation of total strain, $\delta \bar{\varepsilon}^{t+\Delta t}$, equals to $\delta \Delta \bar{\varepsilon}$;

$$\int_{V_0} \Delta \bar{S} \delta \Delta \bar{\varepsilon} dV + \int_{V_0} \bar{S}^t \delta \Delta \bar{\eta} dV = \bar{H}^{\Delta t} + \left(\bar{H}^t - \int_{V_0} \bar{S}^t \delta \Delta \bar{\varepsilon} dV \right) \quad 4.75a$$

where:

$$\bar{H}^{\Delta t} = \int_{V_0}^{t+\Delta t} (\Delta \bar{f}^B)^T \delta(\Delta \bar{u}) dV + \int_{S_0}^{t+\Delta t} (\Delta \bar{f}^{s_f})^T \delta(\Delta \bar{u}^{s_f}) dS \quad 4.75b$$

$$\bar{H}^t = \int_{V_0}^{t+\Delta t} (\bar{f}^B)^T \delta(\Delta \bar{u}) dV + \int_{S_0}^{t+\Delta t} (\bar{f}^{s_f})^T \delta(\Delta \bar{u}^{s_f}) dS \quad 4.75c$$

By considering the equilibrium state at position t , the terms within the parentheses on the right hand side of equation 4.75a can be removed.

No approximation has been made in the formulation of Eq 4.75a. However, because the first term on the right hand side of the equation is nonlinear, thus no solution can be derived directly. Approximation must be introduced. By neglecting the high order terms, and using the linear constitutive law between incremental stress and strain tensor, $\bar{S} = C \Delta \bar{\varepsilon}$, the following linear equation is obtained.

$$\int_{V_0} \delta(\Delta \bar{\varepsilon})^T [C] \delta(\Delta \bar{\varepsilon}) dV + \int_{V_0} S^T \delta(\Delta \bar{\eta}) dV = \bar{H}^{\Delta t} \quad 4.76$$

Where $[C]$ is the material stiffness vector

Equation 4.76 is the governing equation at position $t+\Delta t$ for incremental loading $H^{\Delta t}$. The incremental displacement can be obtained from Equation 4.76 corresponding to position $t+\Delta t$. The total displacement, total stress and total strain at that position can easily be calculated by adding incremental displacement, stress and strain onto the respective values which have been evaluated at position t .

Because of the approximation used in linearization to arrive at Eq. 4.76, the incremental displacement may not be correct. Therefore it is necessary to check the difference between the exact solution and approximated solution. With the computed approximate displacement, stresses and external forces at position $t+\Delta t$, the error can be defined as the following equation.

$$error = \bar{H}^{(t+\Delta t)k} - \int_{V_0} \left(\delta \bar{\varepsilon}^{(t+\Delta t)k} \right)^T \bar{S}^{(t+\Delta t)k} dV \quad 4.77$$

Where k is an iteration number

Iteration will be performed until the error is negligible. Several iteration schemes will be exam and employed in the next chapter.

4.5.2. Incremental Strain of Large Total Rotation

The procedure to develop large rotation incremental strain is basically the same as that for small rotation. The difference is in handling the trigonometric functions. In large rotation incremental analysis, the total rotation can't be approximated by the first term of Taylor series. But the incremental rotation $\Delta\beta$ at each incremental load step can be made small so the higher order terms of Taylor series of cosine function can be ignored. Thus, the trigonometric functions may be assumed as the following.

$$\cos(\beta + \Delta\beta) = \cos(\beta) - \sin(\beta)\Delta\beta \quad 4.78a$$

$$\sin(\beta + \Delta\beta) = \sin(\beta) + \cos(\beta)\Delta\beta \quad 4.78b$$

$$\cos(\beta + \Delta\beta)^2 = \cos(\beta)^2 - 2\cos(\beta)\sin(\beta)\Delta\beta \quad 4.78c$$

$$\sin(\beta + \Delta\beta)^2 = \sin(\beta)^2 + 2\cos(\beta)\sin(\beta)\Delta\beta \quad 4.78d$$

$$\sin(\beta + \Delta\beta)\cos(\beta + \Delta\beta) = \sin(\beta)\cos(\beta) + \cos(\beta)^2\Delta\beta - \sin(\beta)^2\Delta\beta \quad 4.78e$$

Consequently, the incremental strains of large rotation can be derived by using the following relation;

$$\Delta\varepsilon_z = \varepsilon_z^{t+\Delta t} - \varepsilon_z^t \quad 4.79a$$

$$\Delta\varepsilon_{zs} = \varepsilon_{zs}^{t+\Delta t} - \varepsilon_{zs}^t \quad 4.79b$$

By substituting the total displacement at positions $t+\Delta t$ and t , $\bar{u}^{t+\Delta t}$ and \bar{u}^t , into any strain-displacement equation derived in Chapter 3, the incremental strain Eq. 4.74 can be expressed in terms of the displacement. In this chapter, incremental strains based on Eq. 3.8 only are derived. Because Eq. 3.8 has not undergone simplification, the derived

incremental strain will be used for developing the complete incremental stiffness matrix later in Chapter 5.

The incremental strain can be decomposed into three parts; linear incremental strain, incremental strain associated with initial displacement at the beginning of the increment and quadric incremental strain terms. However, in all the strain parts, certain terms are coupled with trigonometric functions (as seen later in Eq. 4.81, 4.82 and 4.83). Thus, strictly, dividing incremental strain into three parts can not be done. But for comparison with the results from considering only small rotation and for the convenience of examining the contribution of initial displacement and stress at the beginning of the increment on the total behavior of horizontally curved beams, the incremental strain is decomposed.

$$\Delta \varepsilon_z = \Delta e_z + \Delta \eta_z = (\Delta e_z^0 + \Delta e_z^i) + \Delta \eta_z \quad 4.80a$$

$$\Delta \varepsilon_{zs} = \Delta e_{zs} + \Delta \eta_{zs} = (\Delta e_{zs}^0 + \Delta e_{zs}^i) + \Delta \eta_{zs} \quad 4.80b$$

$$\begin{aligned} \Delta e_z^0 = & \Delta e_{(0)}^0 + (\Delta e_{(x)}^0)x + (\Delta e_{(y)}^0)y + (\Delta e_{(\omega)}^0)\omega \\ & + (\Delta e_{(xx)}^0)x^2 + (\Delta e_{(yy)}^0)y^2 + (\Delta e_{(xy)}^0)xy + (\Delta e_{(x\omega)}^0)x\omega + (\Delta e_{(y\omega)}^0)y\omega \end{aligned} \quad 4.80c$$

$$\begin{aligned} \Delta e_z^i = & \Delta e_{(0)}^i + (\Delta e_{(x)}^i)x + (\Delta e_{(y)}^i)y + (\Delta e_{(\omega)}^i)\omega \\ & + (\Delta e_{(xx)}^i)x^2 + (\Delta e_{(yy)}^i)y^2 + (\Delta e_{(xy)}^i)xy + (\Delta e_{(x\omega)}^i)x\omega + (\Delta e_{(y\omega)}^i)y\omega \end{aligned} \quad 4.80d$$

$$\begin{aligned} \Delta \eta_z = & \Delta \eta_{(0)} + (\Delta \eta_{(x)})x + (\Delta \eta_{(y)})y + (\Delta \eta_{(\omega)})\omega \\ & + (\Delta \eta_{(xx)})x^2 + (\Delta \eta_{(yy)})y^2 + (\Delta \eta_{(xy)})xy + (\Delta \eta_{(x\omega)})x\omega + (\Delta \eta_{(y\omega)})y\omega \end{aligned} \quad 4.80e$$

$$\Delta e_{zs}^0 = 2n \Delta e_n^0 \quad 4.80f$$

$$\Delta e_{zs}^i = 2n \Delta e_n^i \quad 4.80g$$

$$\Delta \eta_{zs} = 2n \Delta \eta_n \quad 4.80h$$

Where: Δe_z^0 is linear longitudinal incremental strain

Δe_z^i is incremental strain associated with initial displacement

$\Delta \eta_z$ is quadric longitudinal incremental strain

Δe_{zs}^0 is linear incremental shear strain

Δe_{zs}^i is incremental shear strain associated with initial displacement

$\Delta \eta_{zs}$ is quadric incremental shear strain

The linear incremental strain terms in Equation 4.80 are as expressed by Equations 4.81a to 4.81e for doubly symmetric cross sections. The additional incremental strain terms associated with non-symmetric cross section are listed in Table 4.9.

$$\Delta e_{(0)}^0 = a \left(\Delta w'_c - \frac{\Delta u_s}{R} \right) \quad 4.81a$$

$$\Delta e_{(x)}^0 = \left(\frac{a^2}{R^2} \Delta u_s (c-1) + c a (-\Delta \tilde{u}_s'') \right) \quad 4.81b$$

$$\Delta e_{(y)}^0 = c a \left(-\Delta v_s'' + \frac{\Delta \beta}{R} \right) \quad 4.81c$$

$$\Delta e_{(\omega)}^0 = a \left(-\Delta \beta'' + c \left(-\frac{\Delta v_s''}{R} \right) \right) \quad 4.81d$$

$$\Delta e_{(n)}^0 = a \left(\Delta \beta' + c \frac{\Delta v_s'}{R} \right) \quad 4.81e$$

The incremental strains associated with initial displacement in equation 4.80 are given below as Eqs. 4.82a to 4.82j for doubly symmetric cross section. The corresponding additional incremental strain terms associated with non-symmetric cross section are listed in Table 4.10.

$$\Delta e_{(0)}^i = a \left(s x_s \frac{\Delta \beta}{R} \right) + a^2 \left(+ 2 \Delta \tilde{u}'_s \tilde{u}'_s + \Delta v'_s v'_s + \frac{\Delta u_s u_s}{R^2} \right) \quad 4.82a$$

$$\begin{aligned} \Delta e_{(x)}^i = & -s \Delta \beta \left(a \left(-\tilde{u}_s'' - \frac{1}{R} - v'_s \beta' \right) + a^2 \left(-\frac{\tilde{u}_s'^2}{R} + \frac{u_s}{R^2} + v'_s \beta' \right) \right) \\ & + c \left(a \left(-\Delta v'_s \beta' - v'_s \Delta \beta' \right) + a^2 \left(-\frac{2 \tilde{u}'_s \Delta \tilde{u}'_s}{R} + \Delta v'_s \beta' + v'_s \Delta \beta' \right) \right) \\ & + s \left(a \left(\Delta \beta' \tilde{u}'_s + \beta' \Delta \tilde{u}'_s - \Delta v_s'' \right) + a^2 \left(-\Delta \tilde{u}'_s \tilde{\beta}' - \tilde{u}'_s \Delta \tilde{\beta}' \right) \right) \end{aligned} \quad 4.82b$$

$$\begin{aligned} \Delta e_{(y)}^i = & c a \left(\Delta \tilde{u}'_s \beta' + \tilde{u}'_s \Delta \beta' \right) - a^2 \left(\Delta \tilde{u}'_s \tilde{\beta}' + \tilde{u}'_s \Delta \tilde{\beta}' \right) - s \Delta \beta a \left(-v_s'' + \tilde{u}'_s \beta' \right) \\ & + s \Delta \beta a^2 \tilde{u}'_s \tilde{\beta}' + s a \left(\Delta \tilde{u}_s'' + \left(\Delta v'_s \beta' + v'_s \Delta \beta' \right) \right) + s a^2 \left(\frac{2 \Delta \tilde{u}'_s \tilde{u}'_s}{R} \right) \\ & - s a^2 \frac{\Delta u_s}{R^2} - \left(\Delta v'_s \beta' + v'_s \Delta \beta' \right) + c \Delta \beta \left(a \left(\tilde{u}_s'' + v'_s \beta' \right) + a^2 \left(\frac{\tilde{u}_s'^2}{R} - \frac{u_s}{R^2} - \beta' v'_s \right) \right) \end{aligned} \quad 4.82c$$

$$\Delta e_{(\omega)}^i = -a^2 \frac{\Delta \tilde{u}'_s \beta' + \tilde{u}'_s \Delta \beta'}{R} + c a \left(\frac{\Delta \tilde{u}'_s \beta' + \tilde{u}'_s \Delta \beta'}{R} \right) + a^2 \left(-\frac{\Delta \tilde{u}'_s v'_s + \tilde{u}'_s \Delta v'_s}{R^2} \right)$$

$$\begin{aligned}
& -s\Delta\beta\left(a\left(-\frac{v_s''}{R}+\frac{\tilde{u}'_s\beta'}{R}\right)+a^2\left(-\frac{\tilde{u}'_sv'_s}{R^2}\right)\right)+c\Delta\beta\left(a\left(\frac{\tilde{u}_s''}{R}+\frac{v'_s\beta'}{R}\right)+a^2\left(\frac{\tilde{u}_s'^2}{R^2}\right)\right) \\
& + (s)\left(a\left(\frac{\Delta\tilde{u}_s''}{R}+\frac{\Delta v'_s\beta'+v'_s\Delta\beta'}{R}\right)+a^2\left(\frac{2\tilde{u}'_s\Delta\tilde{u}'_s}{R^2}\right)\right) \tag{4.82d}
\end{aligned}$$

$$\begin{aligned}
\Delta e^i_{(xx)} & = c^2\left(a^2\left(\left(-\frac{\tilde{u}'_s}{R}\right)\left(-\frac{\Delta\tilde{u}'_s}{R}\right)+\Delta\beta'\beta'\right)\right)+s^2\left(a^2(-\tilde{\beta}')(-\Delta\tilde{\beta}')\right) \\
& + cs\left(\frac{a^2}{R}\left(\Delta\tilde{\beta}'\tilde{u}'_s+\tilde{\beta}'\Delta\tilde{u}'_s\right)\right) \tag{4.82e}
\end{aligned}$$

$$\Delta e^i_{(yy)} = c^2a^2(\Delta\tilde{\beta}'\tilde{\beta}')+s^2a^2\left(\frac{\tilde{u}'_s\Delta\tilde{u}'_s}{R^2}+\Delta\tilde{\beta}'\tilde{\beta}'\right)+csa^2\left(-\frac{\tilde{u}'_s\Delta\tilde{\beta}'+\Delta\tilde{u}'_s\tilde{\beta}'}{R}\right) \tag{4.82f}$$

$$\begin{aligned}
\Delta e^i_{(xy)} & = c^2\frac{a^2}{R}\Delta\tilde{\beta}'\tilde{u}'_s+\tilde{\beta}'\Delta\tilde{u}'_s-s^2\frac{a^2}{R}\left(\Delta\tilde{u}'_s\tilde{\beta}'+\tilde{u}'_s\Delta\tilde{\beta}'\right) \\
& + cs a^2\left(2\tilde{\beta}'\Delta\tilde{\beta}'-\frac{2\tilde{u}'_s\Delta\tilde{u}'_s}{R^2}-2\beta'\Delta\tilde{\beta}'\right) \tag{4.82g}
\end{aligned}$$

$$\begin{aligned}
\Delta e^i_{(x\omega)} & = c\frac{a^2}{R^2}(\Delta\beta'\tilde{u}'_s+\beta'\Delta\tilde{u}'_s)+s\frac{a^2}{R}(\Delta\beta'\tilde{\beta}'+\beta'\Delta\tilde{\beta}')-s\frac{a^2}{R^2}(\beta'\tilde{u}'_s)\Delta\beta \\
& + c\Delta\beta\frac{a^2}{R}(\beta'\tilde{\beta}')+c^2\frac{a^2}{R^3}(\Delta v'_s\tilde{u}'_s+v'_s\Delta\tilde{u}'_s)+s^2\frac{a^2}{R^2}(-\Delta\tilde{u}'_s\tilde{\beta}'-\tilde{u}'_s\Delta\tilde{\beta}') \\
& + cs\frac{a^2}{R^2}\left(\Delta v'_s\tilde{\beta}'+v'_s\Delta\tilde{\beta}'-\frac{2\tilde{u}'_s\Delta\tilde{u}'_s}{R}\right) \tag{4.82h}
\end{aligned}$$

$$\begin{aligned}
\Delta e^i_{(y\omega)} & = c\frac{a^2}{R}(\Delta\beta'\tilde{\beta}'+\beta'\Delta\tilde{\beta}')+s\frac{a^2}{R^2}(-\Delta\beta'\tilde{u}'_s-\beta'\Delta\tilde{u}'_s)-\frac{s}{R}a^2(\beta'\tilde{\beta}')\Delta\beta \\
& + \frac{c}{R^2}a^2(-\beta'\tilde{u}'_s)\Delta\beta+c^2\frac{a^2}{R^2}(v'_s\Delta\tilde{\beta}'+\Delta v'_s\tilde{\beta}')+s^2\frac{a^2}{R^3}(2\tilde{u}'_s\Delta\tilde{u}'_s) \\
& - cs a^2\left(\frac{\Delta v'_s\tilde{u}'_s+v'_s\Delta\tilde{u}'_s}{R^3}+\frac{\Delta\tilde{u}'_s\tilde{\beta}'+\tilde{u}'_s\Delta\tilde{\beta}'}{R^2}\right) \tag{4.82i}
\end{aligned}$$

$$\Delta e^i_{(n)} = a\left(-s\frac{v'_s}{R}\Delta\beta+c\frac{\tilde{u}'_s}{R}\Delta\beta-s\frac{\Delta\tilde{u}'_s}{R}\right) \tag{4.82j}$$

The quadric incremental strain terms are shown in Eq. 4.83a to 4.83j. The corresponding additional incremental strain terms associated with non-symmetric cross

section are listed in Table 4.11. The 4th order terms are included in the quadric incremental strain, for later examination of effects of high order terms on the load-displacement behavior.

$$\Delta\eta_{(0)} = \frac{1}{2}a^2 \left(\Delta\tilde{u}'_s \Delta\tilde{u}'_s + \Delta v'_s \Delta v'_s + \frac{1}{R^2} \Delta u_s \Delta u_s \right) \quad 4.83a$$

$$\begin{aligned} \Delta\eta_{(x)} = & c \left(-a \Delta v'_s \Delta\beta' + a^2 \left(\frac{\Delta\tilde{u}'_s \Delta\tilde{u}'_s}{R} + \Delta v'_s \Delta\beta' \right) \right) + s \Delta\beta a (\Delta\tilde{u}''_s + \Delta v'_s \beta' + v'_s \Delta\beta') \\ & + s \Delta\beta a^2 \left(\frac{2\tilde{u}'_s \Delta\tilde{u}'_s}{R} - \frac{\Delta u_s}{R^2} - \Delta v'_s \beta' - v'_s \Delta\beta' \right) + s a (\Delta\beta' \Delta\tilde{u}'_s - \Delta v'_s \Delta\beta') \\ & - s a^2 \Delta\tilde{u}'_s \Delta\tilde{\beta}' c \Delta\beta + \left(a (\Delta\beta' \tilde{u}'_s + \beta' \Delta\tilde{u}'_s - \Delta v'_s) + a^2 (-\Delta\tilde{u}'_s \tilde{\beta}' - \tilde{u}'_s \Delta\tilde{\beta}') \right) \end{aligned} \quad 4.83b$$

$$\begin{aligned} \Delta\eta_{(y)} = & -s \Delta\beta \left(a (-\Delta v''_s + (\Delta\tilde{u}'_s \beta' + \tilde{u}'_s \Delta\beta')) - a^2 (\Delta\tilde{u}'_s \tilde{\beta}' + \tilde{u}'_s \Delta\tilde{\beta}') \right) \\ & + c \left(a (\Delta\tilde{u}'_s \Delta\beta') + a^2 (-\Delta\tilde{u}'_s \Delta\tilde{\beta}') \right) + s \left(a (\Delta v'_s \Delta\beta') + a^2 \left(\frac{\Delta\tilde{u}'_s \tilde{u}'_s}{R} - \Delta\beta' \Delta v'_s \right) \right) \\ & + c \Delta\beta \left(a (\Delta\tilde{u}''_s + \Delta v'_s \beta' + v'_s \Delta\beta') + a^2 \left(\frac{2\Delta\tilde{u}'_s \tilde{u}'_s}{R} - \frac{\Delta u_s}{R^2} - \Delta v'_s \beta' - v'_s \Delta\beta' \right) \right) \end{aligned} \quad 4.83c$$

$$\begin{aligned} \Delta\eta_{(\omega)} = & -s \Delta\beta \left(a \left(-\frac{\Delta v''_s}{R} + \frac{\Delta\tilde{u}'_s \beta' + \tilde{u}'_s \Delta\beta'}{R} \right) - a^2 \frac{\Delta\tilde{u}'_s v'_s + \tilde{u}'_s \Delta v'_s}{R^2} \right) \\ & + c \left(a \left(\frac{\Delta\tilde{u}'_s \Delta\beta'}{R} \right) - a^2 \frac{\Delta\tilde{u}'_s \Delta v'_s}{R^2} \right) + s \left(a \left(\frac{\Delta v'_s \Delta\beta'}{R} \right) + a^2 \frac{\Delta\tilde{u}'_s \Delta\tilde{u}'_s}{R^2} \right) \\ & + (c \Delta\beta) \left(a \left(\frac{\Delta\tilde{u}''_s}{R} + \frac{\Delta v'_s \beta' + v'_s \Delta\beta'}{R} \right) + a^2 \frac{2\tilde{u}'_s \Delta\tilde{u}'_s}{R^2} \right) \end{aligned} \quad 4.83d$$

$$\Delta\eta_{(xx)} = c^2 \frac{a^2}{2} \left(\frac{\Delta\tilde{u}'_s \Delta\tilde{u}'_s}{R^2} + \Delta\beta' \Delta\beta' \right) + s^2 \frac{a^2}{2} \Delta\tilde{\beta}' \Delta\tilde{\beta}' + c s \frac{a^2}{R} \Delta\tilde{\beta}' \Delta\tilde{u}'_s \quad 4.83e$$

$$\Delta\eta_{(yy)} = c^2 \frac{a^2}{2} \Delta\tilde{\beta}' \Delta\tilde{\beta}' + s^2 \frac{a^2}{2} \left(\frac{\Delta\tilde{u}'_s \Delta\tilde{u}'_s}{R^2} + \Delta\tilde{\beta}' \Delta\tilde{\beta}' \right) - c s a^2 \frac{\Delta\tilde{u}'_s \Delta\tilde{\beta}'}{R} \quad 4.83f$$

$$\Delta\eta_{(xy)} = c^2 \frac{a^2}{R} \Delta\tilde{\beta}' \Delta\tilde{u}'_s - s^2 \frac{a^2}{R} \Delta\tilde{u}'_s \Delta\tilde{\beta}' + c s a^2 \left(\Delta\tilde{\beta}' \Delta\tilde{\beta}' - \frac{\Delta\tilde{u}'_s \Delta\tilde{u}'_s}{R^2} - \Delta\beta'^2 \right) \quad 4.83g$$

$$\begin{aligned}
\Delta\eta_{(x\omega)} = & c \frac{a^2}{R^2} \Delta\beta' \Delta\tilde{u}'_s + s \frac{a^2}{R} \Delta\beta' \Delta\tilde{\beta}' - s \Delta\beta \frac{a^2}{R^2} (\Delta\beta' \tilde{u}'_s + \beta' \Delta\tilde{u}'_s) \\
& + c \Delta\beta \frac{a^2}{R} (\Delta\beta' \tilde{\beta}' + \beta' \Delta\tilde{\beta}') + c^2 \frac{a^2}{R^3} \Delta v'_s \Delta\tilde{u}'_s - s^2 \frac{a^2}{R^2} \Delta\tilde{u}'_s \Delta\tilde{\beta}' \\
& + c s \frac{a^2}{R^2} \left(\Delta v'_s \Delta\tilde{\beta}' - \frac{\Delta\tilde{u}'_s \Delta\tilde{u}'_s}{R} \right)
\end{aligned} \tag{4.83h}$$

$$\begin{aligned}
\Delta\eta_{(y\omega)} = & c \frac{a^2}{R} (\Delta\beta' \Delta\tilde{\beta}') - s \frac{a^2}{R^2} \Delta\beta' \Delta\tilde{u}'_s - s \Delta\beta \frac{a^2}{R} (\Delta\beta' \tilde{\beta}' + \beta' \Delta\tilde{\beta}') \\
& - c \Delta\beta \frac{a^2}{R^2} (\Delta\beta' \tilde{u}'_s + \beta' \Delta\tilde{u}'_s) + c^2 \frac{a^2}{R^2} (\Delta v'_s \Delta\tilde{\beta}') + s^2 \frac{a^2}{R^3} (\Delta\tilde{u}'_s \Delta\tilde{u}'_s) \\
& - c a^2 \left(\frac{\Delta v'_s \Delta\tilde{u}'_s}{R^3} + \frac{\Delta\tilde{u}'_s \Delta\tilde{\beta}'}{R^2} \right)
\end{aligned} \tag{4.83i}$$

$$\Delta\eta_{(n)} = a \left(-s \Delta\beta \frac{\Delta v'_s}{R} - c \Delta\beta \frac{\Delta\tilde{u}'_s}{R} \right) \tag{4.83j}$$

Incremental strains from simplified strain-displacement equations, Table 3.1 to Table 3.8, can be obtained from Eq. 4.81, 4.82 and 4.83 by using the approximation a) to e) shown in Section 3.2.2.

4.6 Formulation with Respect to One Reference Line

4.6.1 Reference Lines

Conventionally, the beam theories have been formulated based on two reference lines: the centroidal axis and the axis of shear center. In previous sections, the equation for curved beams were also developed using two reference lines. Using two reference lines has the advantage of making the governing differential equations independent and utilizing the orthogonal condition for symmetric cross sections. However, this advantage disappears in analysis with large displacement and rotation or in analysis of non-symmetrical cross sections. Furthermore, there are apparent disadvantages. First, in the two-reference line formulation, external loads act through two different points of beam cross section: torsional moment and shear force on the shear center and flexural moment and longitudinal axial force on the centroid. Because of this, coupling between external loads and the distance of two reference points in deformed configuration can be occurred. With small rotations, the coupling is easily expressed by rigid-rotation. But with large rotations, the uncoupling may not be possible. Secondly, there are degenerate cases where the shear center is not defined or is difficult to find. Therefore, there is strong advantage in developing a formulation based on one reference line.

The reference line could be any line that passes through the plane of cross section. The centroidal axis is chosen as the reference line in this study, because it utilizes sectional properties corresponding to those for conventional beam theory and provides orthogonal character in the formulation. The centroidal axis is within the cross section for doubly and singly symmetric I-sections and is out side of the cross section for un-symmetric cross sections. Depending on whether the location of the centroidal axis as the reference line is inside or outside of the cross section, different procedure is needed for the deriving differential equation of curved beams.

4.6.2 Reference Line in Cross Section

When the single reference line is in the cross section, Figure 4.7, the longitudinal and shear strains can be derived by modifying the corresponding ones of two-reference lines. The terms associated with distances x_s and y_s in the strains of the two-reference line formulation are replaced. Thus, the set of equations in Eq. 4.9 is modified as the following equations.

$$\varepsilon_z = \left(w_c' - \frac{u_c}{R} \right) - x \left(u_c'' + \frac{w_c'}{R} \right) - y \left(v_c'' - \frac{\beta}{R} \right) - \omega \left(\beta'' + \frac{v_c''}{R} \right) \quad 4.84a$$

$$\varepsilon_{zs} = 2n \left(\beta' + \frac{v_c'}{R} \right) \quad 4.84b$$

Where u_c , v_c and w_c are the displacement at the centroid. For simplicity and convenience, only the linear parts of strains are presented.

By using the longitudinal strain and the shear strain of Eq. 4.84, the variation of strain energy in minimum total potential energy, Eq. 4.2, can be expressed as the following equations.

$$\begin{aligned} \int_V \sigma_z \delta \varepsilon_z dV = \int_0^L E \left[A \left(w_c' - \frac{u_c}{R} \right) \delta \left(w_c' - \frac{u_c}{R} \right) + I_y \left(u_c'' + \frac{w_c'}{R} \right) \delta \left(u_c'' + \frac{w_c'}{R} \right) \right. \\ \left. + I_{xy} \left(u_c'' + \frac{w_c'}{R} \right) \delta \left(v_c'' - \frac{\beta}{R} \right) + I_{x\omega} \left(u_c'' + \frac{w_c'}{R} \right) \delta \left(\beta'' + \frac{v_c''}{R} \right) \right. \\ \left. + I_{xy} \left(v_c'' - \frac{\beta}{R} \right) \delta \left(u_c'' + \frac{w_c'}{R} \right) + I_x \left(v_c'' - \frac{\beta}{R} \right) \delta \left(v_c'' - \frac{\beta}{R} \right) \right. \\ \left. + I_{y\omega} \left(v_c'' - \frac{\beta}{R} \right) \delta \left(\beta'' + \frac{v_c''}{R} \right) + I_{x\omega} \left(\beta'' + \frac{v_c''}{R} \right) \delta \left(u_c'' + \frac{w_c'}{R} \right) \right] \end{aligned}$$

$$+ I_{y\omega} \left(\beta'' + \frac{v_c''}{R} \right) \delta \left(v_c'' - \frac{\beta}{R} \right) + I_{\omega} \left(\beta'' + \frac{v_c''}{R} \right) \delta \left(\beta'' + \frac{v_c''}{R} \right) \Big] dA \quad 4.85a$$

$$\int_V \sigma_{zs} \delta \varepsilon_{zs} dV = G K_T \int_0^L \left[\left(\beta' + \frac{v_c}{R} \right) \delta \left(\beta' + \frac{v_c}{R} \right) \right] dz \quad 4.85b$$

The loss of potential energy expressed by Eq. 4.38 can be modified as the following equation;

$$\int_L \delta \bar{u}_c^T \bar{f} dz + \sum_j \delta \bar{q}_{cj}^T \bar{F}_j \quad 4.86a$$

Where:

$$\bar{u}_c = \left\{ u_c, v_c, w_c, \theta_x \left(= \frac{v_c'}{R} \right), \theta_y \left(= u_c' + \frac{w_c}{R} \right), \beta, \theta_\omega \left(= \beta + \frac{v_c'}{R} \right) \right\}^T \quad 4.86b$$

$$\bar{q}_{cj} = \left\{ u_{cj}, v_{cj}, w_{cj}, \theta_{xj} \left(= \frac{v_{cj}'}{R} \right), \theta_{yj} \left(= u_{cj}' + \frac{w_{cj}}{R} \right), \beta_j, \theta_{\omega j} \left(= \beta_j + \frac{v_{cj}'}{R} \right) \right\}^T \quad 4.86d$$

It is noted that all external forces (\bar{f} and \bar{F}_j) in Eq. 4.86a are applied through the centroidal axis.

4.6.3 Formulation for One-reference Line not in Cross Section

When the reference line is not in the cross section, Figure 4.8, one-reference line formulation cannot be developed by merely replacing terms containing x_s and y_s as it is done in the previous section. This situation comes from the condition that cross sectional rotation is composed of two parts. One is associated with Saint-Venant torsion and the other one, with warping torsion. If the centroidal reference line is in the cross section, rotation of the reference line includes the contribution from both warping and pure torsion. When the reference point is not in the cross section, warping displacement does not occur at the reference point and only Saint-Venant torsion contributes to the rotation. The magnitudes of rotation angles θ_x , θ_y , β and θ_ω of shear center and the centroid in Fig. 4.8 have to be same respectively. In Figure 4.8 the fictitious wall linking the centroidal line to a longitudinal line at a point in the cross section is not subjected to warping displacement. Consequently, the equations of the minimum total potential energy expressed in Eq. 4.85 and 4.86 have to be examined. For the strain energy in the total potential energy, Equation 4.85 can be used. However, the loss of potential energy as expressed by Eq. 4.86 has to be changed. In Eq. 4.86, the reference point rotation of θ_x , θ_y and warping rotation θ_ω contain the β' term which represents warping torsion, as shown below

$$\theta_x = v'_c = v'_s - x_s \beta' \quad 4.87a$$

$$\theta_y = u'_c + \frac{w_c}{R} = (u'_s + y_s \beta') + \frac{w_c}{R} \quad 4.87b$$

$$\theta_\omega = \beta + \frac{v'_c}{R} = \beta + \frac{(v'_s - x_s \beta')}{R} \quad 4.87c$$

Because the reference point is outside of the cross section and only rigid body rotation is contributing, the rotation generated by warping should be removed. Otherwise the magnitudes of rotation angle θ_x , θ_y , β and θ_ω at shear center and centroid in Fig. 4.8 are different. Therefore, the proper expression for rotation of any point in the cross section can be expressed as the following set of equations.

$$\theta_x = v'_c + x_s \beta' \quad 4.88a$$

$$\theta_y = u'_c - y_s \beta' + \frac{w_c}{R} \quad 4.88b$$

$$\theta_\omega = \beta + \frac{(v'_c + x_s \beta')}{R} \quad 4.88c$$

By using Eq. 4.88, the complete nonlinear equation of a horizontally curved beam can be formulated based on centroidal reference line, and is used for formulating the finite line element for solution in next chapter.

4.7 Effect of Sectional Deformation of I-Beams

4.7.1. Slender and Stocky Cross Sections

When a horizontally curved beam is subjected to vertical load, the beam deflects vertically, laterally and twists. Associated with these displacement are internal radial forces between the flanges and the web. Figure 4.9 shows schematically the distributed internal radial forces in the top flange of a curved beam under equal end moment. In conventional beam theory, the sectional deformation is not considered, implying stocky beam cross section and that the web can resist the distributed internal radial load without deformation. For the slender cross sections with relatively high slenderness ratio of web depth to web thickness, deformation of the cross section is inevitable. The upper flange deflects outward in the plane of beam curvature and the bottom flange deflects inward corresponding to the radially distributed loads on the flanges. The shape of the deformed cross section is sketched in Fig. 4.10. The internal bending moment associated with the deformed web is shown in Fig. 4.11. The amount of web deformation depends on the rigidity of the web. If the web is rigid, it deforms very little, the torsional moment associated with twisting is resisted by Saint-Venant torsion and warping torsion as assumed in conventional beam theory. If the web is very flexible and deforms, the contribution of the web in resisting torsional moment is small and it can be assumed that torsional moment is only resisted by the warping action.

In this section, strains based on web deformation and associated flange rotations are derived. By using the variation of total potential energy, nonlinear differential equation including the effect of sectional deformation will be developed.

4.7.2 Strains from Deformation

Strains based on sectional deformation can be formulated by modifying the third assumption in Section 3.2.1 as “the cross section of I-beam can deform but the amount of deformation is small”. It is assumed that the flanges are rigid enough to remain flat and that only the web deforms as shown in Figures 4.10 and 4.11. The strains in the web in the direction of its depth can be expressed in terms of rotation α , between the flanges and the web.

$$\varepsilon_w = \alpha \left(\frac{12}{d^2} \right) x y \quad 4.89$$

where: ε_w is strain of web in direction of y-axis
 d is the depth of web

α is relative rotation of flange as defined in Fig. 4.11

The relative twist rotation of flanges, α , generates additional shear strains in the flanges. The total shear strains, including the additional strains by web deformation, are expressed by the following equations:

$$\varepsilon_{sz_f} = 2n \left(\beta' + \frac{v'_s}{R} - \alpha' \right) + 2n \left(\frac{u'_s \beta}{R} - \frac{u'_s \alpha}{R} \right) \quad 4.90a$$

$$\varepsilon_{sz_w} = 2n \left(\beta' + \frac{v'_s}{R} \right) + 2n \left(\frac{u'_s \beta}{R} \right) \quad 4.90b$$

where:

ε_{sz_f} is shear strain of flange associated with web deformation

ε_{sz_w} is shear strain of web associated with web deformation

The additional longitudinal strain can be derived from the assumption that shear strain in planes normal to the middle surface of the thin wall can be neglected. By the same procedure that is used in Chapter 3, the additional longitudinal strain associated with web deformation is derived as the following.

$$\varepsilon_z = - \left(\frac{d}{2} \cos \alpha \alpha' \right) x - \left(\frac{d}{2} \sin \alpha \alpha' \right) y + \left(\frac{\frac{d}{2} \sin \alpha \alpha'}{R} + \alpha' \right) \omega \quad 4.90c$$

The sectional rotation, α , is considered to be small based on the assumption that the amount of deformation is small. Therefore, Equation 4.90c can be simplified as the following.

$$\varepsilon_z = -\left(\frac{d}{2} \alpha'\right)x + (\alpha')\omega \quad 4.90d$$

Because the sectorial area of flange for thin-walled I sections can be expressed as $\omega = (d/2)x$ at flange, and x and ω equal to zero at web, the right hand side of Equation 4.90d vanishes. Therefore no additional longitudinal strain is generated from web deformation.

With the shear strains of the web and flanges, Eq. 4.90a and 4.90b, the first term of the equation for variational total potential energy, Eq. 4.2, can be expressed as the following.

$$\begin{aligned} & \int_V \sigma_{zs} \delta \varepsilon_{zs} dV \\ &= \int_{V_f} \left[\sigma_{zs_f} 2n \left(\delta \left(\beta' + \frac{v'_s}{R} - \alpha' \right) + \delta_s \left(\frac{u'_s \beta}{R} - \frac{u'_s \alpha}{R} \right) \right) \right] dV \\ &+ \int_{V_w} \left[\sigma_{zs_w} 2n \left(\delta \left(\beta' + \frac{v'_s}{R} \right) + \delta \left(\frac{u'_s \beta}{R} \right) \right) \right] dV \\ &= \int_L \left[M_{sv_f} \left(\delta \left(\beta' + \frac{v'_s}{R} - \alpha' \right) + \delta \left(\frac{u'_s \beta}{R} - \frac{u'_s \alpha}{R} \right) \right) \right] dz \\ &+ \int_L \left[M_{sv_w} \left(\delta \left(\beta' + \frac{v'_s}{R} \right) + \delta \left(\frac{u'_s \beta}{R} \right) \right) \right] dz \end{aligned} \quad 4.91a$$

Where:

$$M_{sv_f} = \int_{A_f} \left[\sigma_{zs_f} 2n \right] dA \quad 4.91b$$

$$M_{sv_w} = \int_{A_w} \left[\sigma_{zs_w} 2n \right] dA \quad 4.91c$$

V_f, A_f is the volume and area of flange

V_w, A_w is the volume and area of web

By integration by parts, Equation 4.91a is re-organized as the following.

For variation δv_s

$$\left(\frac{M_{sv_f} + M_{sv_w}}{R} \right) \delta v_s \Big|_0^L - \int_0^L \left(\frac{M_{sv_f} + M_{sv_w}}{R} \right)' \delta v_s dz \quad 4.92a$$

For variation $\delta\beta$

$$\left(M_{sv_f} + M_{sv_w} \right) \delta\beta \Big|_0^L - \int_0^L \left(M_{sv_f} + M_{sv_w} \right) \delta\beta dz - \int_0^L \frac{M_{sv_f}}{R} u_s' \delta\beta dz \quad 4.92b$$

For variation $\delta\alpha$

$$- M_{sv_f} \delta\alpha \Big|_0^L + \int_0^L M_{sv_f}' \delta\alpha dz + \int_0^L \frac{M_{sv_f}}{R} u_s' \delta\alpha dz \quad 4.92c$$

For variation δu_s

$$M_{sv_f} \left(\frac{\beta - \alpha}{R} \right) \delta u_s \Big|_0^L - \int_0^L \left(M_{sv_f} \frac{\beta - \alpha}{R} \right)' \delta u_s dz \quad 4.92d$$

$$+ M_{sv_w} \frac{\beta}{R} \delta u_s \Big|_0^L - \int_0^L \left(M_{sv_w} \frac{\beta}{R} \right)' \delta u_s dz$$

The strain energy of the web and its variation form are expressed as the following.

$$\int_V \sigma_w \delta \varepsilon_w dV = \int_V \left[\sigma_w \left(12 \frac{y}{d^2} \right) x \delta\alpha \right] dV = \int_0^L [M_\alpha \delta\alpha] dz \quad 4.93a$$

Where:

$$M_\alpha = \int_A \left[\sigma_w \left(12 \frac{y}{d^2} \right) x \right] dA \quad 4.93b$$

σ_w is the stress in direction of y-axis at the web

Because the variation terms associated with rotation α are additional terms, the modified differential equation for horizontally curved beams including web deformation can be developed by just adding the additional terms into the original differential equation.

With this incorporation of the additional terms for the variation of $\delta\alpha$, $\delta\beta$, δu_s and δv_s , the differential equations for deformable curved beam are the following.

$$-F_z' - \frac{M_y'}{R} = f_z + \frac{m_y}{R} \quad 4.94a$$

$$M_y'' - \frac{F_z^a}{R} = f_x - m_y' \quad 4.94b$$

$$-M_x'' - y_s \frac{M_y''}{R} - \frac{M_z^\alpha'}{R} = f_y - m_x' - \frac{m_\omega'}{R} \quad 4.94c$$

$$-M_z^\alpha' - \left(y_s \frac{F_z}{R} - \frac{M_x}{R} \right) = m_z - m_\omega' \quad 4.94d$$

$$M_{sv_f}' + M_\alpha = 2 m_\alpha \quad 4.94e$$

Where:

$$M_z^\alpha = M_\omega' + M_{sv_f} + M_{sv_w} \quad 4.94f$$

m_α is distribute moment from sectional deformation, Figure 4.11

In Equation 4.94, the sectional rotation, α , due to web deformation is considered being the same for the flanges. However, because of the arch effect and the direction of the internal distributed radial forces, the rotation at the top and bottom flanges is slightly different. In the present study, the effect of this difference is not considered.

4.7.3 Differential Equations Incorporating Sectional Deformation

The constitutive laws associated with sectional deformation can be expressed by the following equations.

$$\sigma_w = E\alpha \left(\frac{12}{d^2} \right) x y \quad 4.95a$$

$$\sigma_{sz_f} = G \left[2n \left(\beta' + \frac{v_s'}{R} - \alpha' \right) + 2n \left(\frac{u_s' \beta}{R} - \frac{u_s' \alpha}{R} \right) \right] \quad 4.95b$$

$$\sigma_{sz_w} = G \left[2n \left(\beta' + \frac{v_s'}{R} \right) + 2n \left(\frac{u_s' \beta}{R} \right) \right] \quad 4.95c$$

By using Eq. 4.95, the stress resultants associated with sectional deformation in Equation 4.94 can be expressed in terms of displacement.

$$M_{sv_f} = G K_{T_f} \left[\left(\beta' + \frac{v_s'}{R} - \alpha' \right) + \left(\frac{u_s' \beta}{R} - \frac{u_s' \alpha}{R} \right) \right] \quad 4.96a$$

$$M_{sv_w} = G K_{T_w} \left[\left(\beta' + \frac{v_s'}{R} \right) + \left(\frac{u_s' \beta}{R} \right) \right] \quad 4.96b$$

$$M_\alpha = E I_\alpha \alpha \quad 4.96c$$

Where:

$$K_{T_f} = 2 b \frac{t_f^3}{3} \quad 4.96d$$

$$K_{T_w} = d \frac{t_w^3}{3} \quad 4.96e$$

$$I_\alpha = \frac{t_w^3}{d} \quad 4.96c$$

b and d are the width and depth of the beam
t_f, and t_w are thickness of flange and web

By substituting the stress resultants in Equation 4.96 into Equation 4.94, the linear differential equations in terms of displacement are obtained:

$$E \left[-A \left(\tilde{w}_c'' - \frac{y_s}{R} \beta' \right) + \frac{I_y}{R} u_s''' + \frac{I_{xy}}{R} v_s''' + \frac{I_{x\omega}}{R} \beta_s''' \right] = f_z + \frac{m_y}{R} \quad 4.97a$$

$$E \left[I_y \tilde{u}_s^{iv} - \frac{I_{xy}}{R} \beta'' + I_{x\omega} \beta^{iv} - \left(\frac{y_s I_y}{R} - I_{xy} - \frac{I_{x\omega}}{R} \right) v_s^{iv} - \frac{A}{R} w_c' \right] = f_x - m_y' \quad 4.97b$$

$$E \left(y_s \frac{I_y}{R} + I_{xy} - \frac{I_{x\omega}}{R} \right) u_s^{iv} + E I_{xy} w_c''' + E \left(I_x + \frac{I_{y\omega}}{R} - \frac{I_{y\omega}}{R} \right) v_s^{iv} - \left(E \frac{I_x}{R} + G \frac{K_T}{R} \right) \beta'' \\ + E \left(I_{y\omega} + y_s \frac{I_{x\omega}}{R} + \frac{I_{y\omega}}{R} - \frac{I_\omega}{R} \right) \beta^{iv} + \frac{G K_{T_f}}{R} \alpha'' = f_y - m_x' - \frac{m_\omega'}{R} \quad 4.97c$$

$$E I_{x\omega} \tilde{u}_s^{iv} + \left(E I_{y\omega} - E y_s \frac{I_{x\omega}}{R} + E \frac{I_\omega}{R} \right) v_s^{iv} + (E I_\omega) \beta^{iv} - E \frac{I_{xy}}{R} u_s'' - \left(E \frac{I_x}{R} + G \frac{K_T}{R} \right) v_s'' \\ - \left(E \frac{I_{y\omega}}{R} + G K_T + E \frac{I_{y\omega}}{R} \right) \beta'' - E y_s \frac{A}{R} w_c' + G K_{T_f} \alpha'' = m_z - m_\omega' \quad 4.97d$$

$$G K_{T_f} \left(\beta'' + \frac{v_s''}{R} - \alpha'' \right) + E I_\alpha \alpha'' = 2 m_\alpha \quad 4.97e$$

Equations 4.97 apply to curved beams with a thin-walled cross section. If the orthogonal condition for doubly symmetric section is utilized, the linear equations Eqs. 4.97d and 4.97e can be simplified to the following equations:

$$E I_{\omega} \tilde{\beta}^{iv} - (G K_T) \tilde{\beta}'' + G K_{T_f} \alpha'' = -\frac{M_x^e}{R} + m_z - m_{\omega}' \quad 4.98$$

$$G K_{T_f} \tilde{\beta}'' - G K_{T_f} \alpha'' + E I_{\alpha} \alpha = 2 m_{\alpha} \quad 4.99$$

It is noted that M_x^e is the linear part of M_x , Eq. 4.95b, and is simplified from approximation a) and b) of Section 3.2.2. When only a concentrated external load, M_x is applied, Equation 4.99 can be further simplified as:

$$E I_{\omega} \alpha^{iv} + \left(\frac{E I_{\omega} E I_{\alpha} + G K_{T_f} G K_{T_w}}{G K_{T_f}} \right) \alpha'' - \frac{G K_T I_{\alpha}}{G K_{T_f}} \alpha = -\frac{M_x^e}{R} \quad 4.100$$

When the radius goes to infinity, the term M_x^e / R in Eq. 4.100 vanishes and Eq. 4.100 becomes differential equation of the straight beam. This equation is the same as that derived by Goodier and Barton (1944). This identity is a check of the adequacy of Eq. 4.97.

The homogeneous solution of Equation 4.100 is

$$\alpha(z) = C1 \sinh(k_1 z) + C2 \cosh(k_1 z) + C3 \sinh(k_2 z) + C4 \cosh(k_2 z) \quad 4.101a$$

Where:

$$k1 = \frac{1}{\sqrt{2}} \sqrt{-1 + \frac{G K_T}{E I_{\omega}} - \sqrt{\left(1 - \frac{G K_T}{E I_{\omega}}\right)^2 + \frac{4 K_T I_{\alpha}}{K_{T_f} I_{\omega}}}} \quad 4.101b$$

$$k2 = \frac{1}{\sqrt{2}} \sqrt{-1 + \frac{G K_T}{E I_{\omega}} + \sqrt{\left(1 - \frac{G K_T}{E I_{\omega}}\right)^2 - \frac{4 K_T I_{\alpha}}{K_{T_f} I_{\omega}}}} \quad 4.101c$$

The coefficients C1...C4 are determined by the boundary conditions of the web deformation angle α at the ends of the beam.

The exact solution for linear and nonlinear differential equation that including the effect of web deformation for an arbitrary boundary condition and loading condition is very difficult to obtain. Therefore, a numerical approximation procedure such as a finite element method or a finite strip method is recommended. In the present study, a finite line element that included the degree of freedom for sectional deformation will be developed in Chapter 5.

For sectional deformation associated with large rotation, the incremental analysis is necessary. This task can be done by deriving the incremental shear strains of Equation 4.90, and adding the incremental web deformation strain of ϵ_w . By the same procedure which is employed in Section 4.5.2, the incremental shear strains associated with web deformation and related strains can be derived as shown below.

The incremental strain from web-deformation is

$$\Delta \varepsilon_w = \Delta e_\alpha^0 = \Delta \alpha \left(12 \frac{y}{h^2} \right) x \quad 4.102$$

where Δe_α^0 is the component of linear incremental strain of web

The shear strains associated with large rotation are

$$\varepsilon_{zs_f} = 2n a \left(\beta' - \alpha' + \frac{v'_s}{R} \hat{c} + \frac{\tilde{u}'_s}{R} \hat{s} \right) \quad 4.103a$$

$$\varepsilon_{zs_w} = 2n a \left(\beta' + \frac{v'_s}{R} c + \frac{\tilde{u}'_s}{R} s \right) \quad 4.103b$$

Where \hat{s} , \hat{c} are $\cos(\beta-\alpha)$ and $\sin(\beta-\alpha)$

The linear incremental shear strains are

$$\Delta e_{zs_f}^0 = 2n \Delta e_{n_f}^0 \quad 4.104a$$

$$\Delta e_{zs_w}^0 = 2n \Delta e_{n_w}^0 \quad 4.104b$$

$$\Delta e_{n_f}^0 = a \left(\Delta \beta' - \Delta \alpha' + \frac{\Delta v'_s}{R} \hat{c} \right) \quad 4.104c$$

$$\Delta e_{n_w}^0 = a \left(\Delta \beta' + \frac{\Delta v'_s}{R} c \right) \quad 4.104d$$

where $\Delta e_{n_f}^0$ and $\Delta e_{n_w}^0$ are the component of linear incremental shear strain of the flange and the web. The incremental shear strains associated with initial displacement are

$$\Delta e_{zs_f}^i = 2n \Delta e_{n_f}^i \quad 4.105a$$

$$\Delta e_{zs_w}^i = 2n \Delta e_{n_w}^i \quad 4.105b$$

$$\Delta e_{n_f}^i = a \left(-\hat{s} \frac{v'_s}{R} (\Delta \beta - \Delta \alpha) + \hat{c} \frac{\tilde{u}'_s}{R} (\Delta \beta - \Delta \alpha) + \hat{s} \frac{\Delta \tilde{u}'_s}{R} \right) \quad 4.105c$$

$$\Delta e_{n_w}^i = a \left(-s \frac{v'_s}{R} \Delta \beta + c \frac{\tilde{u}'_s}{R} \Delta \beta + s \frac{\Delta \tilde{u}'_s}{R} \right) \quad 4.105d$$

The terms, $\Delta e_{n_f}^i$ and $\Delta e_{n_w}^i$, are the components of incremental shear strain of the flange and the web associated with initial displacement.

The quadric incremental shear strain associated with web deformation is

$$\Delta \eta_{zs_f} = 2n \Delta \eta_{n_f} \quad 4.106a$$

$$\Delta \eta_{zs_w} = 2n \Delta \eta_{n_w} \quad 4.106b$$

$$\Delta \eta_{n_f} = a \left(-\hat{s} (\Delta \beta - \Delta \alpha) \frac{\Delta v'_s}{R} + \hat{c} (\Delta \beta - \Delta \alpha) \frac{\Delta \tilde{u}'_s}{R} \right) \quad 4.106c$$

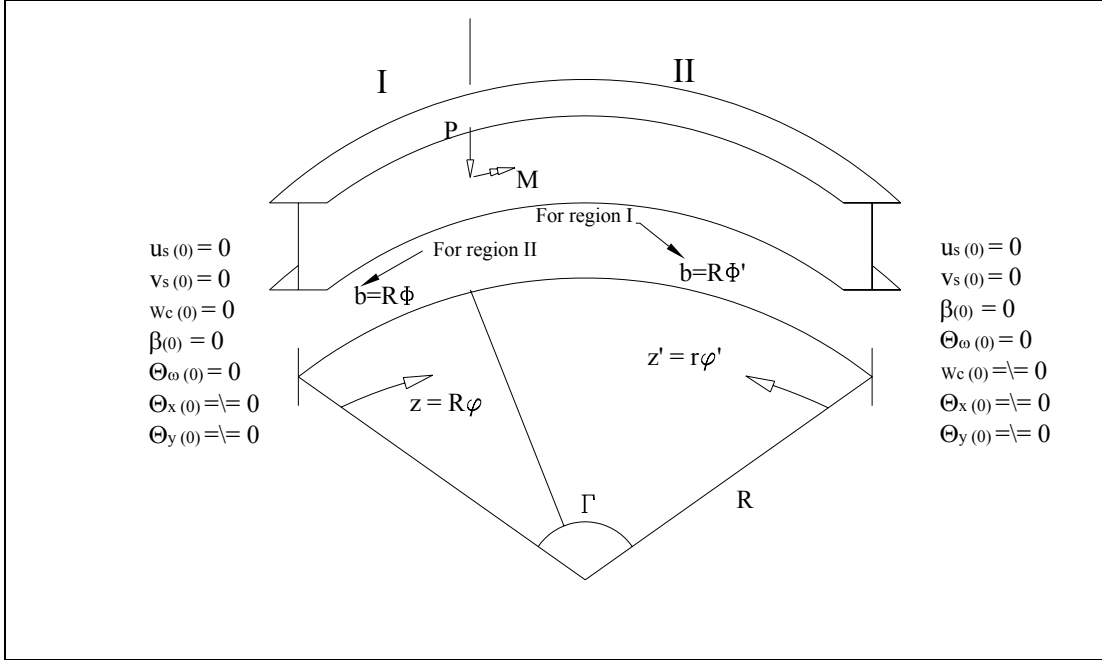
$$\Delta\eta_{n_w} = a \left(-s \frac{\Delta\beta \Delta v'_s}{R} + c \frac{\Delta\beta \Delta \tilde{u}'_s}{R} \right) \quad 4.106d$$

The terms, $\Delta\eta_{n_f}$ and $\Delta\eta_{n_w}$, are the components of quadric incremental shear strain of the flange and the web.

Precise load-deflection behavior of horizontally curved beam can be obtained when the nonlinear differential equations are solved. However, it is very difficult or impossible to derive exact solution for differential equations with sectional deformation, arbitrary loading and boundary condition. In order to overcome these difficulties, numerical approximate procedures such as finite element method is necessary.

In the next chapter, formulation of a finite line element will be derived based on the formulation in this chapter.

Table 4.1 Exact solutions for point load and end moment with fixed-warping boundary condition



M_x	I	$(PR - M) \frac{\sin(\beta')}{\sin(\Gamma)} \sin(\phi)$
	II	$(PR - M) \frac{\sin(\beta)}{\sin(\Gamma)} \sin(\phi')$
M_ω	I	$B_0 \cosh(kz) + T_0 \frac{\sinh(kz)}{k} + \frac{(PR - M)}{k} \eta \frac{\sin(\beta')}{\sin(\Gamma)} (\sinh(kz) - kR \sin(\phi))$
	II	$B_0 \cosh(kz') + T_0 \frac{\sinh(kz')}{k} + \frac{(PR - M)}{k} \eta \frac{\sin(\beta)}{\sin(\Gamma)} (\sinh(kz') - kR \sin(\phi'))$
T_0	$\frac{f_{12} f_{14} - f_{15} f_{11}}{f_{15} f_{13} - f_{12} f_{16}}$	
B_0	$\frac{f_{11} f_{16} - f_{13} f_{14}}{f_{15} f_{13} - f_{12} f_{16}}$	
$f_{11} = -M(kb - \sinh(kb)) + \frac{(PR - M)}{\sin(\Gamma)} \left(kR(\alpha \sin(\beta') - \beta' \sin(\Gamma)) - \eta(\sin(\beta') \sinh(kL) - \sin(\Gamma) \sinh(kb)) \right)$		
$f_{14} = \frac{(PR - M)}{\sin(\alpha)} \left((-\sin(\Gamma) + \sin(\beta') + \sin(\beta)) - \eta(-\sin(\Gamma) \cosh(kb) + \sin(\beta') \cosh(kL) + \sin(\beta)) \right) - M(1 - \cosh(kb))$		
$f_{12} = k(1 - \cosh(kL)) \quad f_{13} = kL - \sinh(kL) \quad f_{15} = -k \sinh(kL) \quad f_{16} = 1 - \cosh(kL)$		

Table 4.2 Exact solution solutions for point load and end moment with free and fixed boundary condition

$u_s(0) = 0$
 $v_s(0) = 0$
 $w_c(0) = 0$
 $\beta(0) = 0$
 $\Theta_{\omega}(0) = 0$
 $\Theta_x(0) = 0$
 $\Theta_y(0) = 0$

$u_s(0) = 0$
 $v_s(0) = 0$
 $\beta(0) = 0$
 $w_c(0) = 0$
 $\Theta_{\omega}(0) = 0$
 $\Theta_x(0) = 0$
 $\Theta_y(0) = 0$

M_x	I	$(PR - M) \frac{\sin(\beta')}{\sin(\Gamma)} \sin(\varphi)$
	II	$(PR - M) \frac{\sin(\beta)}{\sin(\Gamma)} \sin(\varphi')$
M_{ω}	I	$B_0 \cosh(kz) + T_0 \frac{\sinh(kz)}{k} + \frac{(PR - M)}{k} \eta \frac{\sin(\beta')}{\sin(\Gamma)} (\sinh(kz) - kR \sin(\varphi))$
	II	$B_0 \cosh(kz') + T_0 \frac{\sinh(kz')}{k} + \frac{(PR - M)}{k} \eta \frac{\sin(\beta)}{\sin(\Gamma)} (\sinh(kz') - kr \sin(\varphi'))$
T_0	$\frac{f_{22} f_{24} - f_{25} f_{21}}{f_{25} f_{23} - f_{22} f_{26}}$	
B_0	$\frac{f_{21} f_{26} - f_{23} f_{24}}{f_{12} f_{23} - f_{22} f_{26}}$	
$f_{21} = f_{11} \quad f_{22} = f_{12} \quad f_{23} = f_{13}$		
$f_{24} = \frac{(PR - M)}{\sin(\Gamma)} \eta (-\sin(\Gamma) \sinh(kb) + \sin(\beta') \sinh(kL)) - M \sinh(kb)$		
$f_{25} = k \cosh(kL) \quad f_{26} = \sinh(kL)$		

Table 4.3 Exact solution for distribute loading with fixed-fixed warping boundary condition

M _x	$\left(PR^2 - MR \right) \frac{\sin(\beta) + \sin(\beta')}{\sin(\Gamma)} - 1$
M _ω	$B_0 \cosh(kz) + T_0 \frac{\sinh(kz)}{k} - \frac{m}{k^2} (\cosh(kz) - 1) + \frac{(pR^2 - mR)}{k} \left\{ \eta \left[kr \left(\frac{\sin(\varphi) - \sin(\varphi')}{\sin(\Gamma)} + \cosh(kz) \right) + \frac{\sinh(kz)}{\sin(\Gamma)} (1 - \cos(\Gamma)) \right] + \frac{1 - \cosh(kz)}{kR} \right\}$
T ₀	$\frac{f_{32} f_{34} - f_{35} f_{31}}{f_{35} f_{33} - f_{32} f_{36}}$
B ₀	$\frac{f_{31} f_{36} - f_{33} f_{34}}{f_{35} f_{33} - f_{32} f_{36}}$
$f_{31} = -km \left(\frac{L^2}{2} - \frac{\cosh(kL) - 1}{k^2} \right) + (pR^2 - mR) \left[kR \left(\frac{\Gamma}{\sin(\Gamma)} - \frac{\Gamma}{\tan(\Gamma)} - \frac{\Gamma^2}{2} \right) + \frac{\eta}{\sin(\Gamma)} \left((\cos(\Gamma) - 1) \sinh(kL) + \frac{\sin(\Gamma)}{kR} (\cosh(kL) - 1) \right) \right]$ $f_{34} = -m \left(l - \frac{\sinh(kL)}{k} \right) + \frac{(pR^2 - mR)}{\sin(\Gamma)} \left[2(1 - \cos(\Gamma)) - \Gamma \sin(\Gamma) + \eta \left((\cos(\Gamma) - 1)(1 + \cosh(kL)) + \frac{\sin(\alpha) \sinh(kL)}{kR} \right) \right]$ $f_{32} = f_{12} \quad f_{33} = f_{13} \quad f_{35} = f_{15} \quad f_{36} = f_{16}$	

Table 4.4 Exact solution for distribute loading with free and fixed warping boundary condition

$ \begin{aligned} u_s(0) &= 0 \\ v_s(0) &= 0 \\ w_c(0) &= 0 \\ \beta(0) &= 0 \\ \Theta_x(0) &= 0 \\ \Theta_y(0) &= 0 \\ \Theta_\omega(0) &= 0 \end{aligned} $	$ \begin{aligned} u_s(0) &= 0 \\ v_s(0) &= 0 \\ w_c(0) &= 0 \\ \beta(0) &= 0 \\ \Theta_\omega(0) &= 0 \\ \Theta_x(0) &= 0 \\ \Theta_y(0) &= 0 \end{aligned} $
M_x	$(pR^2 - mR) \frac{\sin(\beta) + \sin(\beta')}{\sin(\Gamma)} - 1$
M_ω	$ \begin{aligned} & B_0 \cosh(kz) + T_0 \frac{\sinh(kz)}{k} - \frac{m}{k^2} (\cosh(kz) - 1) \\ & + \frac{(pR^2 - mR)}{k} \left\{ \eta \left[\left(kr \left(\frac{\sin(\varphi) - \sin(\varphi')}{\sin(\Gamma)} + \cosh(kz) \right) \right) \right. \right. \\ & \left. \left. + \frac{\sinh(kz)}{\sin(\Gamma)} (1 - \cos(\Gamma)) \right] + \frac{1 - \cosh(kz)}{kR} \right\} \end{aligned} $
T_0	$ \frac{f_{42} f_{44} - f_{45} f_{41}}{f_{43} f_{43} - f_{42} f_{46}} $
B_0	$ \frac{f_{41} f_{46} - f_{43} f_{44}}{f_{45} f_{43} - f_{42} f_{46}} $
$f_{41} = f_{31}$	
$ f_{44} = -m(\cosh(kL) - 1) - \frac{(pR^2 - mR)}{\sin(\Gamma)} \eta \left((\cos(\Gamma) - 1)(\sinh(kL)) + \frac{\sin(\alpha)(\cosh(kL) - 1)}{kR} \right) $	
$f_{42} = f_{12} \quad f_{43} = f_{13} \quad f_{45} = f_{25} \quad f_{46} = f_{26}$	

Table 4.5 Exact solution for one vertical end moment with fixed-fixed warping boundary condition

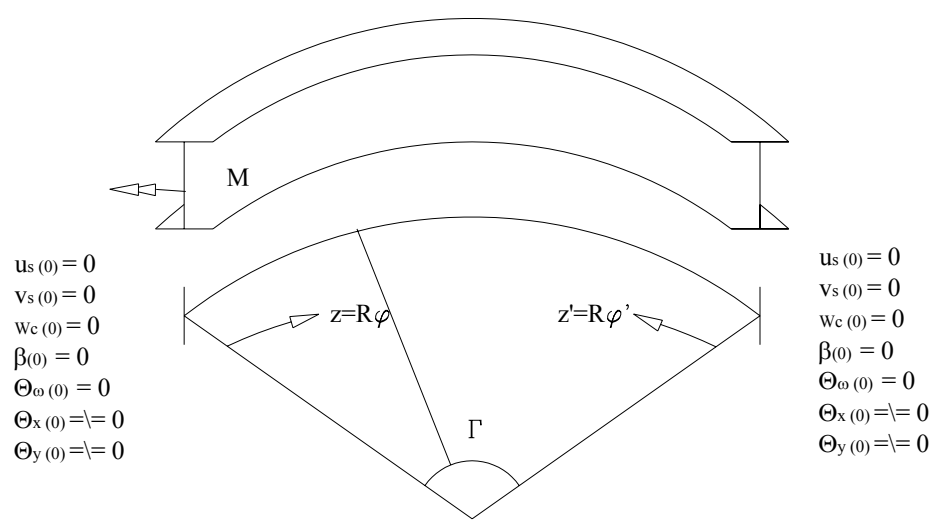
	
M_x	$M \frac{\sin(\varphi')}{\sin(\Gamma)}$
M_ω	$B_0 \cosh(kz) + T_0 \frac{\sinh(kz)}{k} + \frac{M}{\sin(\Gamma)} \eta \left(R(\sin(\Gamma) \cosh(kz) - \sin(\varphi')) - \frac{\cos(\Gamma) \sinh(kz)}{k} \right)$
T_0	$\frac{f_{52} f_{54} - f_{55} f_{51}}{f_{55} f_{53} - f_{52} f_{56}}$
B_0	$\frac{f_{51} f_{56} - f_{53} f_{54}}{f_{55} f_{53} - f_{52} f_{56}}$
$f_{51} = \frac{-M}{R \sin(\Gamma)} (kR(\alpha \cos(\Gamma) - \sin(\Gamma)) - \eta(\cos(\Gamma) \sinh(kL) - kR \sin(\Gamma) \cosh(kL)))$ $f_{54} = \frac{-M}{\sin(\Gamma)} (\cos(\Gamma) - \eta(-kR^2 - \cos(\Gamma) \cosh(kL) + kR \sin(\Gamma) \sinh(kL)))$ $f_{52} = f_{12} \quad f_{53} = f_{13} \quad f_{55} = f_{15} \quad f_{56} = f_{16}$	

Table 4.6 Exact solution for two different vertical end moments with fixed and free warping boundary condition

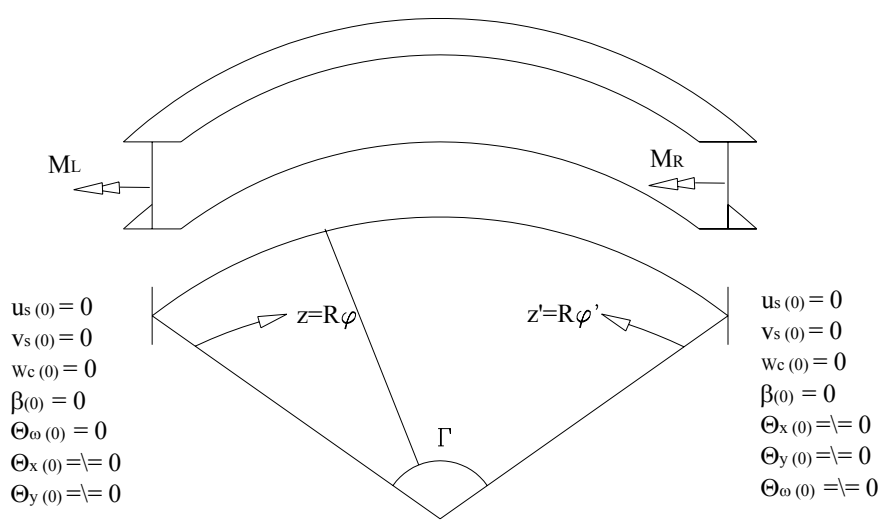
 <p> $u_s(0) = 0$ $v_s(0) = 0$ $w_c(0) = 0$ $\beta(0) = 0$ $\Theta_{\omega}(0) = 0$ $\Theta_x(0) = 0$ $\Theta_y(0) = 0$ </p> <p> $u_s(0) = 0$ $v_s(0) = 0$ $w_c(0) = 0$ $\beta(0) = 0$ $\Theta_x(0) = 0$ $\Theta_y(0) = 0$ $\Theta_{\omega}(0) = 0$ </p>	
M_x	$M_R \frac{\sin(\varphi)}{\sin(\Gamma)} + M_L \frac{\sin(\varphi')}{\sin(\Gamma)}$
M_{ω}	$B_0 \cosh(kz) + T_0 \frac{\sinh(kz)}{k} + \frac{\eta}{k} \left(M_R \left(-kR \frac{\sin(\varphi)}{\sin(\Gamma)} + \frac{\sinh(kz)}{\sin(\Gamma)} \right) + M_L \left(kR \left(\cosh(kz) - \frac{\sin(\varphi')}{\sin(\Gamma)} \right) - \frac{\sinh(kz)}{\tan(\Gamma)} \right) \right)$
T_0	$\frac{f_{62} f_{64} - f_{65} f_{61}}{f_{65} f_{63} - f_{62} f_{66}}$
B_0	$\frac{f_{61} f_{66} - f_{63} f_{64}}{f_{65} f_{63} - f_{62} f_{66}}$
	$f_{61} = - \left\{ \begin{aligned} &M_R \left(-kR \frac{\Gamma}{\sin(\Gamma)} + \eta \left(kR^3 + \frac{\sinh(kL)}{\sin(\Gamma)} \right) \right) \\ &+ M_L \left(kR \left(\frac{\Gamma}{\tan(\Gamma)} - 1 \right) + \eta \left(-\frac{\sinh(kL)}{\tan(\Gamma)} + kR \cosh(kL) \right) \right) \end{aligned} \right\}$ $f_{64} = \eta \left(M_R \left(-kR + \frac{\sinh(kL)}{\sin(\Gamma)} \right) + M_L \left(kR \cosh(kL) - \frac{\sinh(kL)}{\tan(\Gamma)} \right) \right)$ $f_{62} = f_{12} \quad f_{63} = f_{13} \quad f_{65} = f_{25} \quad f_{66} = f_{26}$

Table 4.7 Exact solution for one end bi-moment with fixed and free warping boundary condition

M_x	0
M_ω	$B_0 \cosh(kz) + T_0 \frac{\sinh(kz)}{k}$
T_0	$\frac{f_{72} f_{74} - f_{75} f_{71}}{f_{75} f_{73} - f_{72} f_{76}}$
B_0	$\frac{f_{71} f_{76} - f_{73} f_{74}}{f_{75} f_{73} - f_{72} f_{76}}$
$f_{71} = 0 \quad f_{74} = B_R k \quad f_{72} = f_{12} \quad f_{73} = f_{13} \quad f_{75} = f_{25} \quad f_{76} = f_{26}$	

Table 4.8 Comparison the results solution for point load (P=10) and end moment with fixed-warping boundary condition

	$z=0$	$z=L/2$	$z=L$
Exact Solution	94.6	-53.9	94.6
Approximation	104	-63.4	104

Table 4.9 Additional Incremental Strain Terms Associated with Non-Symmetric Section

Value	Additional terms
$\Delta e_{(0)}$	$-c a y_s \frac{\Delta\beta}{R}$
$\Delta e_{(x)}$	$c a \frac{y_s}{R} \Delta v_s''$

Table 4.10 Additional Incremental Terms Associated with Initial Displacement for Non-Symmetric Section

Value	Additional terms
$\Delta e^i_{(0)}$	$a \left(s x_s \frac{\Delta\beta}{R} \right) + a^2 \left(\begin{aligned} &+ (c y_s \Delta\beta' + s x_s \Delta\beta') (c y_s \beta' + s x_s \beta') \\ &+ (s y_s \Delta\beta' - c x_s \Delta\beta') (-c x_s \beta' + s y_s \beta') \\ &+ \frac{1}{R^2} (c \Delta\beta y_s + s \Delta\beta x_s) (s y_s + (1-c) x_s) \end{aligned} \right)$
$\Delta e^i_{(x)}$	$\begin{aligned} &-s \Delta\beta \left(a \frac{y_s}{R} (v_s'' - \tilde{u}_s' \beta') + a^2 \left(y_s \frac{\tilde{u}_s' v_s'}{R^2} + \frac{2x_s}{R^2} \right) \right) + c a \left(\frac{y_s}{R} (-\Delta \tilde{u}_s' \beta' - \tilde{u}_s' \Delta \beta') \right) \\ &+ c a^2 \left(y_s \frac{\Delta \tilde{u}_s' v_s' + \tilde{u}_s' \Delta v_s'}{R^2} \right) + s \left(-a \frac{y_s}{R} (\Delta \tilde{u}_s'' - \Delta v_s' \beta' - v_s' \Delta \beta') - 2a^2 \frac{y_s}{R^2} \tilde{u}_s' \Delta \tilde{u}_s' \right) \\ &+ c \Delta\beta \left(-a \frac{y_s}{R} (\tilde{u}_s'' - v_s' \beta') - a^2 \left(\frac{y_s}{R^2} \tilde{u}_s'^2 + \frac{y_s}{R^2} \right) \right) \\ &c^2 a^2 \left(-\frac{y_s}{R} (\Delta \beta' \tilde{u}_s' + \beta' \Delta \tilde{u}_s') + \frac{y_s^2}{R^2} (\Delta \beta' v_s' + \beta' \Delta v_s') - 2x_s \beta' \Delta \beta' \right) \\ &-s^2 a^2 x_s (\Delta \beta' \tilde{\beta}' + \beta' \Delta \tilde{\beta}') - s^2 a^2 x_s \frac{y_s}{R^2} (\Delta \tilde{u}_s' \beta' + \tilde{u}_s' \Delta \beta') - s c a^2 y_s (\Delta \beta' \tilde{\beta}' + \beta' \Delta \tilde{\beta}') \\ &-s c a^2 \frac{y_s^2}{R^2} (\Delta \tilde{u}_s' \beta' + \tilde{u}_s' \Delta \beta') + s c a^2 \frac{x_s y_s}{R} (\Delta \beta' v_s' + \beta' \Delta v_s') + 2y_s \beta' \Delta \beta' \end{aligned}$

$\Delta e^i_{(y)}$	$-c^2 a^2 y_s (\Delta \beta' \tilde{\beta}' + \beta' \Delta \tilde{\beta}') + s^2 a^2 \left(\frac{x_s}{R} (\Delta \tilde{u}'_s \beta' + \tilde{u}'_s \Delta \beta') - y_s 2 \beta' \Delta \beta' \right)$ $+ s c a^2 \left(-x_s (\Delta \beta' \tilde{\beta}' + \beta' \Delta \tilde{\beta}') + \frac{y_s}{R} (\Delta \tilde{u}'_s \beta' + \tilde{u}'_s \Delta \beta') + x_s 2 \beta' \Delta \beta' \right)$
$\Delta e^i_{(\omega)}$	$-c a^2 \frac{y_s}{R} 2 \beta' \Delta \beta' + s a^2 \Delta \beta \frac{y_s}{R} \beta'^2 - s a^2 \frac{x_s}{R} 2 \beta' \Delta \beta' - c a^2 \Delta \beta \frac{x_s}{R} \beta'^2$ $+ c^2 a^2 \left(-\frac{y_s}{R^2} (\Delta v'_s \beta' + v'_s \Delta \beta') \right) + s^2 a^2 \left(\frac{x_s}{R^2} (\Delta \tilde{u}'_s \beta' + \tilde{u}'_s \Delta \beta') \right)$ $+ c s \frac{a^2}{R^2} (y_s (\Delta \tilde{u}'_s \beta' + \tilde{u}'_s \Delta \beta') + x_s (\Delta v'_s \beta' + v'_s \Delta \beta'))$
$\Delta e^i_{(xx)}$	$+ c^2 a^2 \left(\frac{y_s^2}{R^4} v'_s \Delta v'_s + \Delta \beta' \beta' \right) + s^2 a^2 \frac{y_s^2}{R^4} \tilde{u}'_s \Delta \tilde{u}'_s - c s a^2 \frac{y_s^2}{R^4} (\Delta \tilde{u}'_s v'_s + \tilde{u}'_s \Delta v'_s)$
$\Delta e^i_{(xy)}$	$-c^2 a^2 \frac{y_s^2}{R^2} (v'_s \Delta \tilde{\beta}' + \tilde{\beta}' \Delta v'_s) - s^2 a^2 \frac{y_s^2}{R^3} (\Delta \tilde{u}'_s \tilde{u}'_s + \tilde{u}'_s \Delta \tilde{u}'_s)$ $+ c s a^2 \left(\frac{y_s}{R^2} (\Delta \tilde{\beta}' \tilde{u}'_s + \tilde{\beta}' \Delta \tilde{u}'_s) + \frac{y_s}{R^3} (\tilde{u}'_s \Delta v'_s + \Delta \tilde{u}'_s v'_s) \right)$
$\Delta e^i_{(x\omega)}$	$\Delta e^i_{(x\omega)} = -c \frac{y_s}{R} \frac{a^2}{R^2} (\Delta \beta' v'_s + \beta' \Delta v'_s) + s \frac{a^2}{R} \frac{y_s}{R^2} (\Delta \beta' \tilde{u}'_s + \beta' \Delta \tilde{u}'_s)$ $+ s \frac{a^2}{R^2} \frac{y_s}{R} (\beta' v'_s) \Delta \beta + c \frac{a^2}{R} \frac{y_s}{R^2} (\beta' \tilde{u}'_s) \Delta \beta - 2c^2 \frac{a^2}{R^3} \frac{y_s}{R} v'_s \Delta v'_s$ $- 2s^2 \frac{a^2}{R^2} \frac{y_s}{R^2} \tilde{u}'_s \Delta \tilde{u}'_s + 2c s \frac{a^2}{R^2} \frac{y_s}{R^2} (\Delta v'_s \tilde{u}'_s + v'_s \Delta \tilde{u}'_s)$

Table 4.11 Additional Incremental Terms Associated with Quadric Incremental Displacement for Non-Symmetric Section

Value	Additional Terms
$\Delta\eta_{(0)}$	$\frac{1}{2} a^2 \left(\begin{aligned} &(c y_s \Delta\beta' + s x_s \Delta\beta')(c y_s \Delta\beta' + s x_s \Delta\beta') \\ &+ (-c x_s \Delta\beta' + s y_s \Delta\beta')(-c x_s \Delta\beta' + s y_s \Delta\beta') \\ &+ \frac{1}{R^2} ((c\Delta\beta y_s + s\Delta\beta x_s)(c\Delta\beta y_s + s\Delta\beta x_s)) \end{aligned} \right)$
$\Delta\eta_{(x)}$	$\begin{aligned} &c a \left(-\frac{y_s}{R} (\Delta\tilde{u}'_s \Delta\beta') \right) + a^2 \left(y_s \frac{\Delta\tilde{u}'_s \Delta v'_s}{R^2} \right) - s a^2 \frac{y_s}{R^2} \Delta\tilde{u}'_s \Delta\tilde{u}'_s \\ &- s \Delta\beta \left(a \left(\frac{y_s}{R} (\Delta v'_s - \Delta\tilde{u}'_s \beta' - \tilde{u}'_s \Delta\beta') \right) + a^2 \left(y_s \frac{\Delta\tilde{u}'_s v'_s + \tilde{u}'_s \Delta v'_s}{R^2} \right) \right) \\ &c \Delta\beta \left(a \left(-\frac{y_s}{R} (\Delta\tilde{u}'_s - \Delta v'_s \beta' - v'_s \Delta\beta') \right) + a^2 \left(-2 \frac{y_s}{R^2} \tilde{u}'_s \Delta\tilde{u}'_s \right) \right) \\ &+ c^2 a^2 \left(-\frac{y_s}{R} \Delta\beta' \Delta\tilde{u}'_s + \frac{y_s^2}{R^2} \Delta\beta' \Delta v'_s - x_s \Delta\beta' \Delta\beta' \right) - s^2 a^2 x_s \frac{y_s}{R^2} \Delta\tilde{u}'_s \Delta\beta' \\ &- s c a^2 \left(y_s \Delta\beta' \Delta\tilde{\beta}' - \frac{y_s^2}{R^2} \Delta\tilde{u}'_s \Delta\beta' + \frac{x_s y_s}{R} \Delta\beta' \Delta v'_s + y_s \Delta\beta' \Delta\beta' \right) \end{aligned}$
$\Delta\eta_{(y)}$	$\begin{aligned} &c^2 a^2 (-y_s) (\Delta\beta' \Delta\tilde{\beta}') + s^2 a^2 \left(\frac{x_s}{R} \Delta\tilde{u}'_s \Delta\beta' - y_s \Delta\beta' \Delta\beta' \right) \\ &+ s c a^2 \left(-x_s \Delta\beta' \Delta\tilde{\beta}' + \frac{y_s}{R} \Delta\tilde{u}'_s \Delta\beta' + x_s \Delta\beta' \Delta\beta' \right) \end{aligned}$
$\Delta\eta_{(\omega)}$	$\begin{aligned} &(-s \Delta\beta) \left(a^2 \left(-\frac{y_s}{R} 2\beta' \Delta\beta' \right) \right) + c \left(a^2 \left(-\frac{y_s}{R} \Delta\beta' \Delta\beta' \right) \right) + (c \Delta\beta) \left(a^2 \left(-\frac{x_s}{R} 2\beta' \Delta\beta' \right) \right) \\ &+ s \left(a^2 \left(-\frac{x_s}{R} \Delta\beta' \Delta\beta' \right) \right) + c^2 \left(a^2 \left(-\frac{y_s}{R^2} \Delta v'_s \Delta\beta' \right) \right) + s^2 \left(a^2 \left(\frac{x_s}{R^2} \Delta\tilde{u}'_s \Delta\beta' \right) \right) \\ &+ (c s) \frac{a^2}{R^2} (y_s (\Delta\tilde{u}'_s \Delta\beta') + x_s (\Delta v'_s \Delta\beta')) \end{aligned}$
$\Delta\eta_{(xx)}$	$+ c^2 \frac{a^2}{2} \frac{y_s}{R^4} \Delta v_s'^2 + s^2 \frac{a^2}{2} \left(\frac{y_s}{R^2} \Delta\tilde{u}'_s \right) \left(\frac{y_s}{R^2} \Delta\tilde{u}'_s \right) + c s \frac{a^2}{R} \left(-\frac{y_s}{R^2} \Delta\tilde{u}'_s \right) \left(\frac{y_s}{R} \Delta v'_s \right)$

$\Delta\eta_{(xy)}$	$-c^2 \frac{a^2 y_s}{R^2} \Delta\tilde{\beta}' \Delta v'_s - \frac{s^2 a^2 y_s}{R^3} \Delta\tilde{u}'^2 + c s a^2 \left(\frac{y_s}{R^2} \Delta\tilde{\beta}' \Delta\tilde{u}'_s + \frac{y_s}{R^3} \Delta\tilde{u}'_s \Delta v'_s \right)$
$\Delta\eta_{(x\omega)}$	$\begin{aligned} & c \frac{a^2}{R^2} \left(-\frac{y_s}{R} \Delta\beta' \Delta v'_s \right) + s \frac{a^2}{R} \left(\frac{y_s}{R^2} \Delta\beta' \Delta\tilde{u}'_s \right) \left(-s \Delta\beta \right) \frac{a^2}{R^2} \left(-\frac{y_s}{R} (\Delta\beta' v'_s + \beta' \Delta v'_s) \right) \\ & + (c \Delta\beta) \frac{a^2}{R} \left(\frac{y_s}{R^2} (\Delta\beta' \tilde{u}'_s + \beta' \Delta\tilde{u}'_s) \right) + c^2 \frac{a^2}{R^3} \left(-\frac{y_s}{R} \Delta v'_s \Delta v'_s \right) \\ & + s^2 \frac{a^2}{R^2} \left(-\frac{y_s}{R^2} \Delta\tilde{u}'_s \Delta\tilde{u}'_s \right) + c s \left(\frac{a^2}{R^2} \left(\frac{y_s}{R^2} \Delta v'_s \Delta\tilde{u}'_s + \frac{y_s}{R^2} \Delta\tilde{u}'_s \Delta v'_s \right) \right) \end{aligned}$

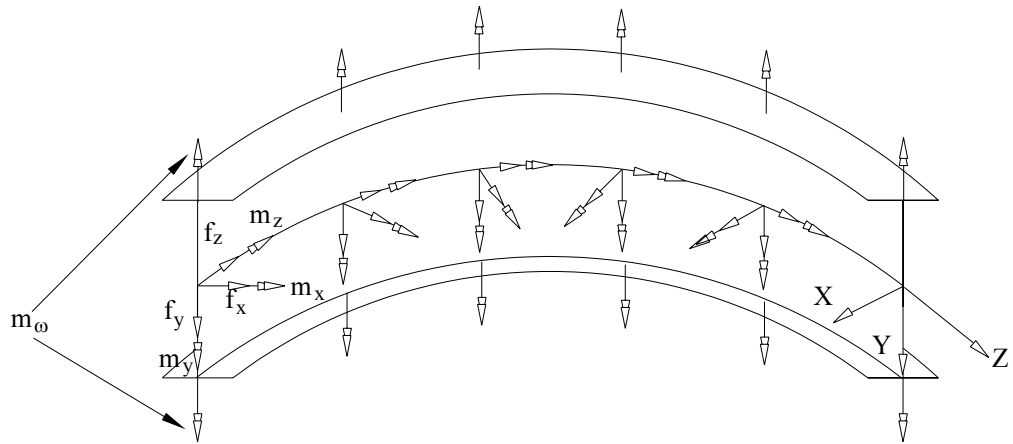


Figure 4.1 basic boundary and loading condition for shear force and moment.

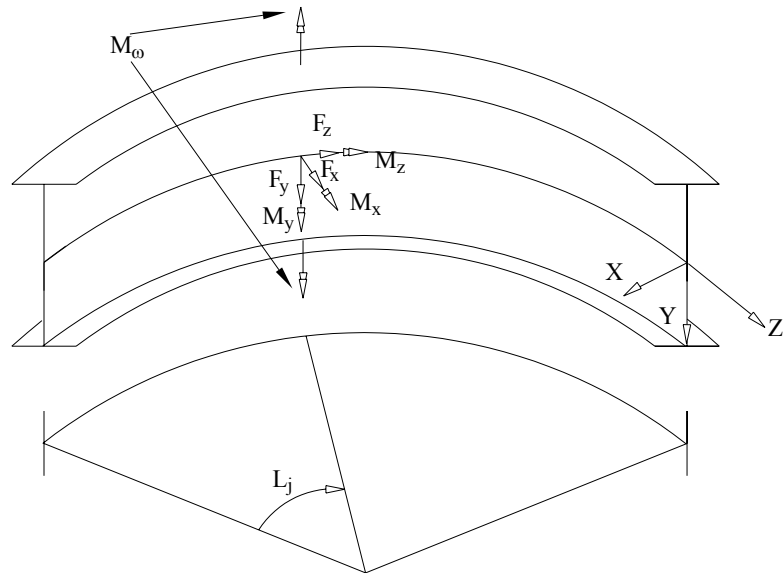
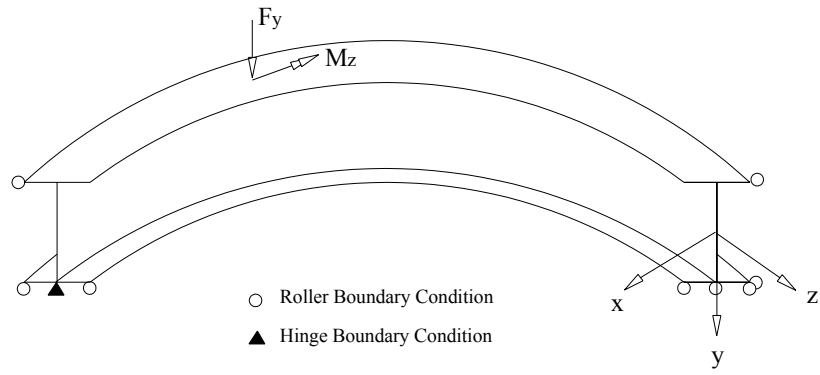
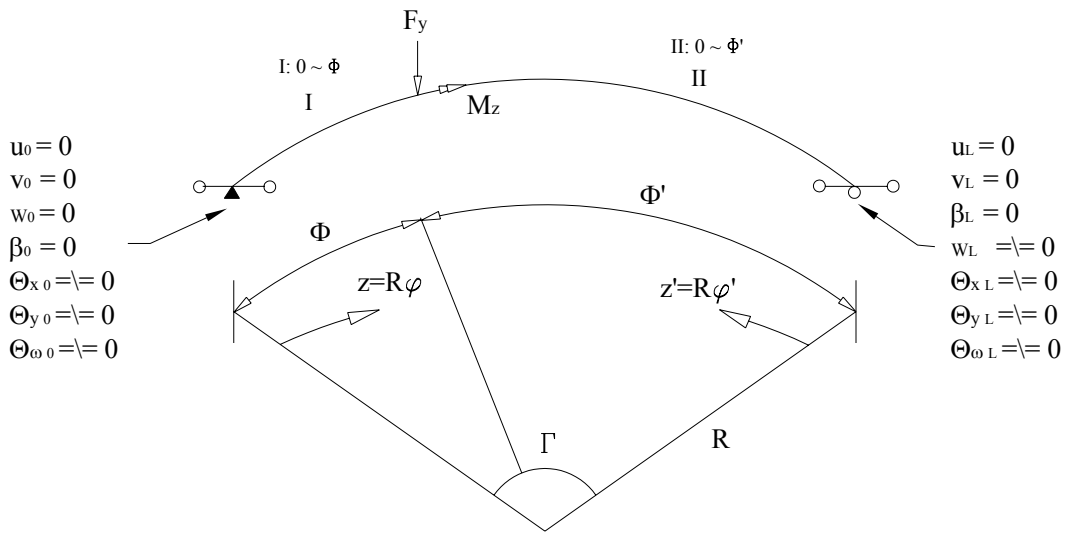


Figure 4.2 Shear forces and moments for load number j.

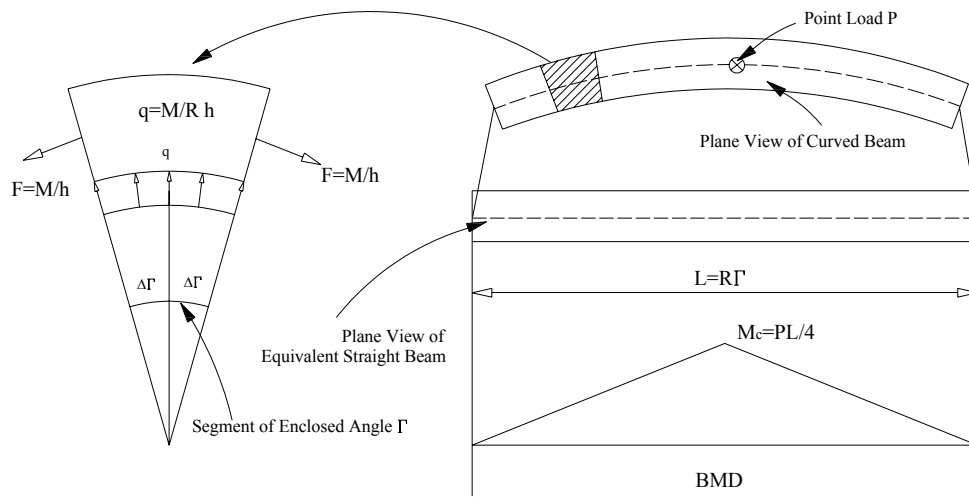


(a) 3-D Curved Beam Model

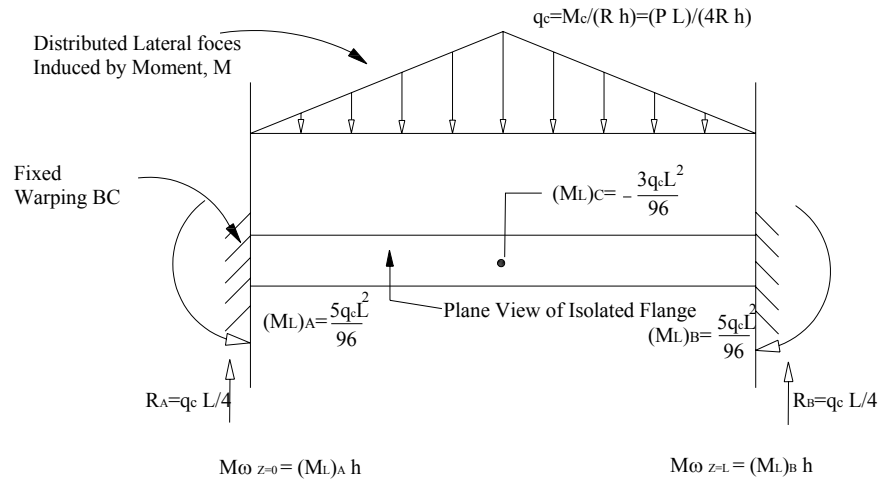


(b) 2-D Curved Beam Model

Figure 4.3 Curved Beam Models



(a)



(b)

Figure 4.4 (a) Small Segment of Curved Beam and Equivalent Straight Beam; (b) Procedure of Calculating Approximated Bi-moment

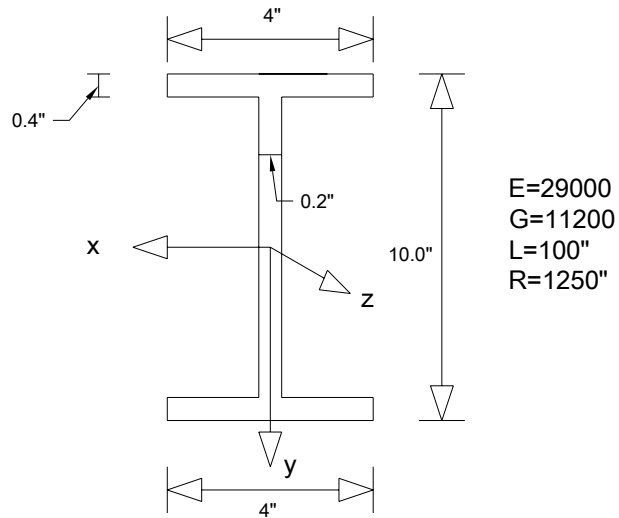


Figure 4.5 Cross section of curved beam for evaluation of exact solution

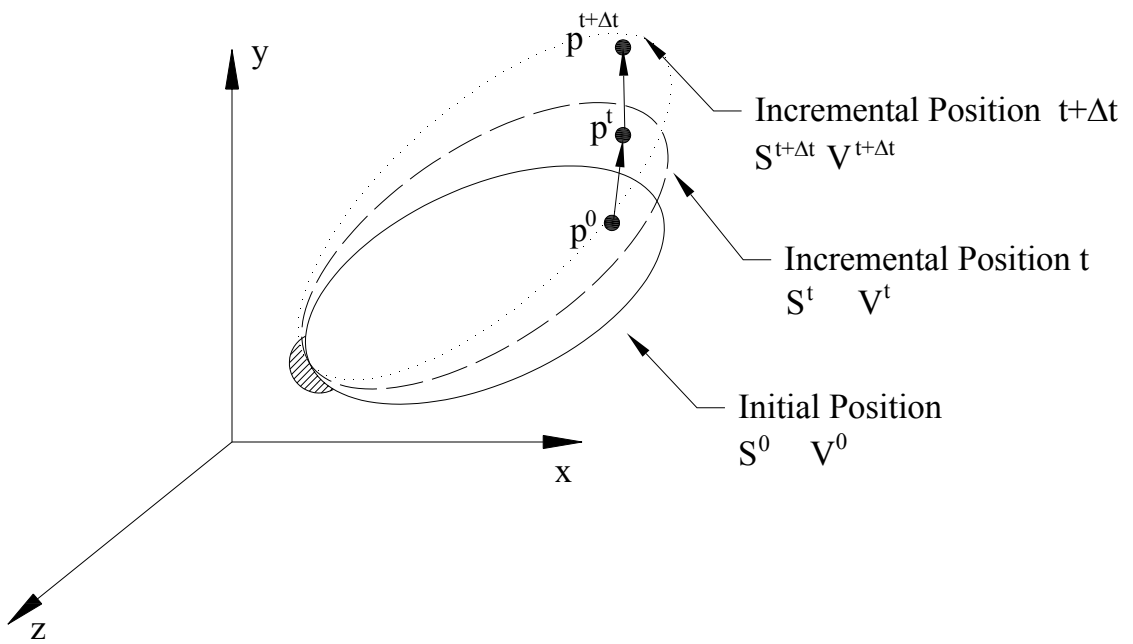


Figure 4.6 Elastic Body in Three Discrete Incremental Position

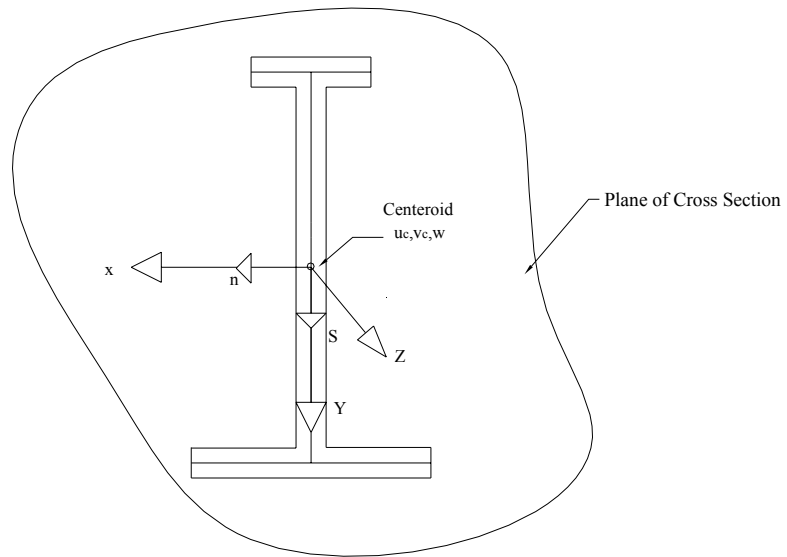


Figure 4.7 Section with Reference Line in Cross Section.

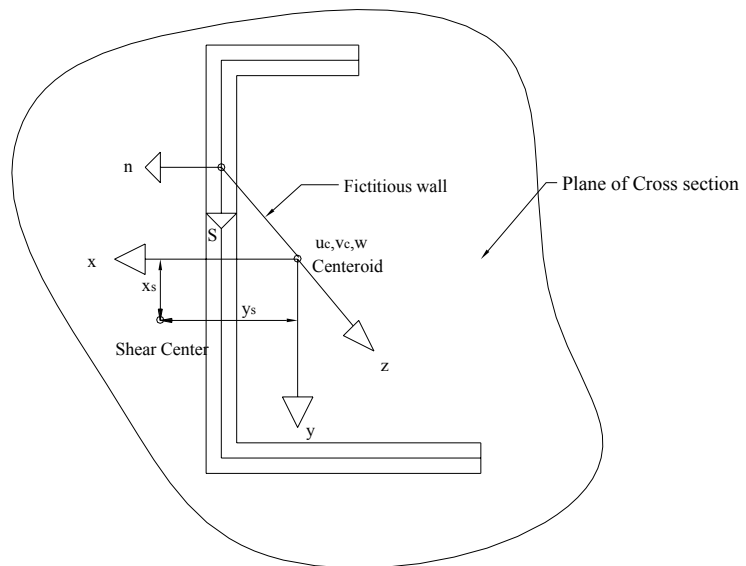


Figure 4.8 Section with Reference Line not in Cross Section.

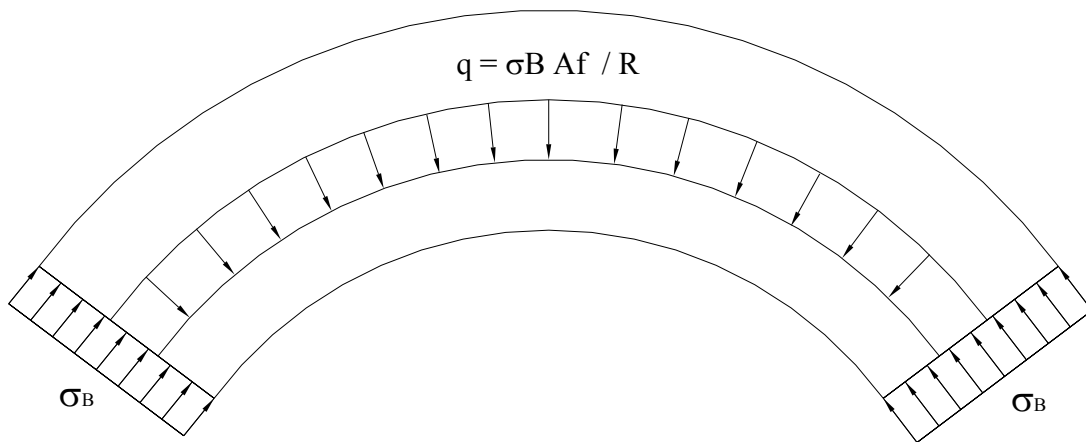


Figure 4.9 Radial Distributed Load on the Flange

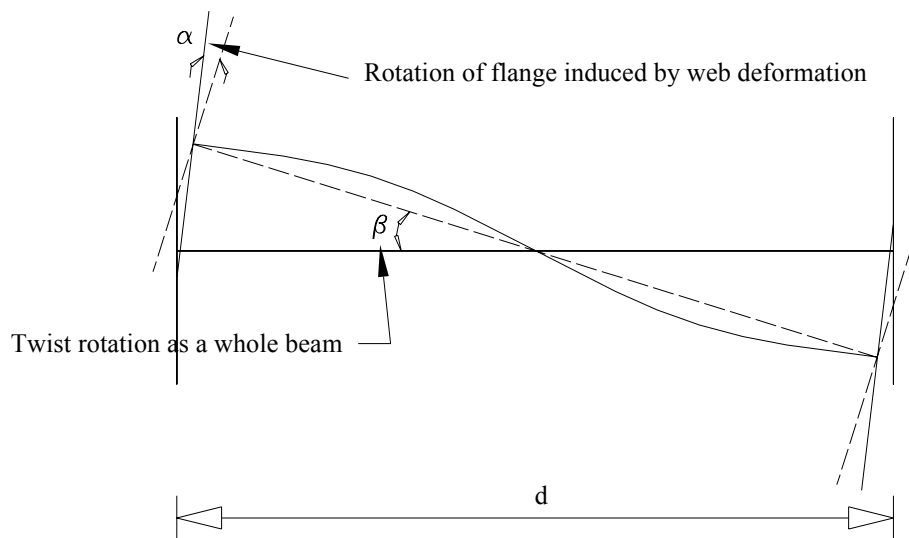


Figure 4.10 Rotation α Induced by the Sectional Deformation

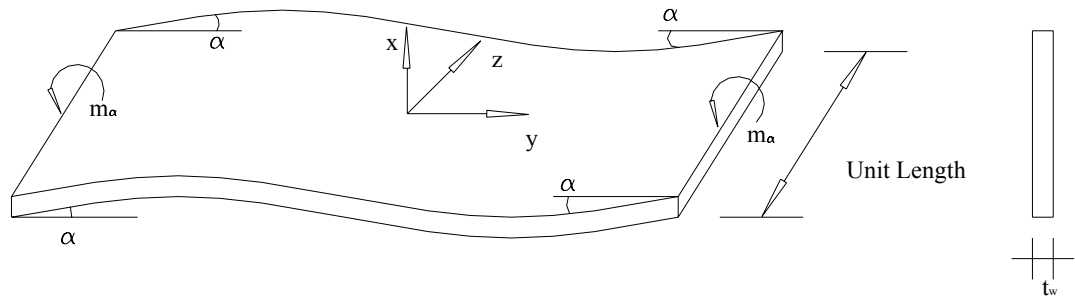


Figure 4.11 Web Deformation and Internal Moment m_α

5. Development of Line Element

5.1 Introduction

In last chapter, the differential equations of load-displacement relationships are developed for horizontally curved beams considering large displacements, rotations and deformations of the beam cross section. The makeup of terms of these equations is dependent upon loads and boundary conditions. The equations are too complex and are too complicated for closed-form solution. Even for individual cases of beam geometry and loading, exact solution is generally not possible and approximate solution by numerical procedure is difficult. Instead, most often the employed procedure for solution is the finite element method.

General purpose finite element packages with shell elements can be used for evaluation of behavior of individual curved beams, with satisfactory results. However, for examining the general behavior of curved beams, for evaluating the existing solutions of differential equation based on first order formulation and for the demanding task of developing stress equations for design of horizontally curved beams, utilization of a general purpose finite element program is a formidable undertaking.

In order to achieve the goals of this study, a finite line element for curved beams is developed in this chapter. The line element incorporates sectional deformation and warping of the beam cross section. The effects of different levels of simplification, as given in Chapter 3, can be compared by employing the line element. The P- Δ effect on curved beams will also be developed in this chapter.

The mathematical base of formulating the line element is essentially the same as that utilized in last chapter for the formulation of general equations.

5.2 Shape Function and Displacement Field

In a finite element analysis, a system is approximated by an assemblage of discrete line elements which are connected at the nodal points. The displacement field of the line element in the variation of minimum total potential energy, Equation 4.2, can be interpolated from nodal displacement by using shape functions.

$$\{u\} = [N]\bar{d} \quad \text{5.1a}$$

$$\{u\} = \{u_s \quad w_c \quad v_s \quad \beta \quad \alpha\}^T \quad \text{5.1b}$$

$$[N] = [N_1, N_2, N_3, N_4, N_5] \quad \text{5.1c}$$

where $\{u\}$ is displacement field vector

\bar{d} is nodal displacement vector

$[N]$ is the shape function or transformation matrix

Since five independent displacement variables are used in this study, five shape functions are needed. The other displacement variables shown in Eq. 4.39b can be expressed by the five independent variables. In the following section, the components

of the displacement vector and the shape function matrix for a curved beam element are presented.

5.2.1 Nodal Degree of Freedom

The line element for curved beam has two nodes. Each node has seven degrees of freedom (DOF) as shown in Figure 5.1: three translations and three rotations about x, y and z, and warping. Thus, fourteen degrees of freedom (DOF) are used for the nodal displacement vector of a line element. The nodal DOF can be expressed by the combination of displacements and twist rotation;

$$\bar{d} = \begin{Bmatrix} \bar{u}_0 \\ \bar{u}_L \end{Bmatrix} \quad 5.2a$$

$$\bar{u} = [B] \bar{u}^d \quad 5.2b$$

$$\bar{u}_0 = [B] \bar{u}_0^d \quad 5.2c$$

$$\bar{u}_L = [B] \bar{u}_L^d \quad 5.2d$$

Where:

$$\bar{u}_0 = \{u_{s0} \quad w_{c0} \quad \theta_{y0} \quad v_{s0} \quad \theta_{x0} \quad \beta_0 \quad \theta_{\omega0}\}^T \quad 5.2e$$

$$\bar{u}_L = \{u_{sL} \quad w_{cL} \quad \theta_{yL} \quad v_{sL} \quad \theta_{xL} \quad \beta_L \quad \theta_{\omega L}\}^T \quad 5.2f$$

$$\bar{u}^d = \{u_s \quad v_s \quad w_c \quad u'_s \quad v'_s \quad \beta \quad \beta'\}^T \quad 5.2g$$

$$\bar{u}_0^d = \{u_{s0} \quad v_{s0} \quad w_{c0} \quad u'_{s0} \quad v'_{s0} \quad \beta_0 \quad \beta'_0\}^T \quad 5.2h$$

$$\bar{u}_L^d = \{u_{sL} \quad v_{sL} \quad w_{cL} \quad u'_{sL} \quad v'_{sL} \quad \beta_L \quad \beta'_L\}^T \quad 5.2i$$

$$[B] = \begin{bmatrix} 1 & 0 & 0 & 0 & 0 & 0 & 0 \\ 0 & 1 & 0 & 0 & 0 & 0 & 0 \\ 0 & 0 & \frac{1}{R} & 1 & 0 & 0 & 0 \\ 0 & 1 & 0 & 0 & 0 & 0 & 0 \\ 0 & 0 & 0 & 0 & -1 & 0 & 0 \\ 0 & 0 & 0 & 0 & 0 & 1 & 0 \\ 0 & 0 & 0 & 0 & -\frac{1}{R} & 0 & -1 \end{bmatrix} \quad 5.2j$$

Where: u_{s0} , v_{s0} and w_{c0} are the displacement at nodal point ($z=0$)
 θ_{x0} , θ_{y0} and β_0 are rotational about x-, y- and z-axis ($z=0$)

$\theta_{\omega 0}$ is warping rotation at nodal point ($z=0$)
 u_{sL} , v_{sL} and w_{cL} are the displacement at nodal point ($z=L$)
 θ_{xL} , θ_{yL} and β_L are rotational about x-, y- and z-axis ($z=L$)
 $\theta_{\omega L}$ is warping rotation nodal point ($z=L$)

If sectional deformation is considered, another degree of freedom is needed. Since the sectional deformation degree of freedom is an independent variable, nodal displacement vector can be expressed in the following matrix form. For convenience, only the nodal DOF at $z=0$ are presented.

$${}^s \bar{d} = \begin{Bmatrix} {}^s \bar{u}_0 \\ {}^s \bar{u}_L \end{Bmatrix} \quad 5.3a$$

$${}^s \bar{u}_0 = [{}^s B] {}^s \bar{u}_0^d \quad 5.3b$$

Where

$${}^s \bar{u}^d = \{u_s \quad v_s \quad w_c \quad u'_s \quad v'_s \quad \beta \quad \beta' \quad \alpha\}^T \quad 5.3c$$

$${}^s \bar{u} = \{u_s \quad w_s \quad \theta_y \quad v_s \quad \theta_x \quad \beta \quad \theta_\omega \quad \theta_\alpha\}^T \quad 5.3d$$

$$[{}^s B] = \begin{bmatrix} 1 & 0 & 0 & 0 & 0 & 0 & 0 & 0 \\ 0 & 1 & 0 & 0 & 0 & 0 & 0 & 0 \\ 0 & 0 & \frac{1}{R} & 1 & 0 & 0 & 0 & 0 \\ 0 & 1 & 0 & 0 & 0 & 0 & 0 & 0 \\ 0 & 0 & 0 & 0 & -1 & 0 & 0 & 0 \\ 0 & 0 & 0 & 0 & 0 & 1 & 0 & 0 \\ 0 & 0 & 0 & 0 & -\frac{1}{R} & 0 & -1 & 0 \\ 0 & 0 & 0 & 0 & 0 & 0 & 0 & 1 \end{bmatrix} \quad 5.3e$$

${}^s \bar{u}_0^d$ and ${}^s \bar{u}_0$ are the vector ${}^s \bar{u}^d$ and ${}^s \bar{u}$ at $z=0$

The superscript “s” in Eq. 5.3 denotes sectional deformation. It is noted that two reference axes are used for the nodal displacement and rotation of Eq. 5.3. The longitudinal nodal displacement w_{c0} refers to the centroid; the lateral and vertical displacement u_{s0} and v_{s0} refers to the shear center. For the one-reference axis line element, all displacement and rotation refer to the centroid. Special care is needed to form nodal rotation, θ_x , θ_y and θ_w , from independent variables, u_c , v_c and β . This is presented in the following subsection.

5.2.2 Shape Functions

One of the issues of deriving a shape function is the problem of membrane locking. When a lower order independent interpolation function for displacement is used, the finite element model becomes too stiff resulting in displacement smaller than the exact value. Higher order interpolation functions are not efficient in terms of calculation time. In an effort to overcome the numerical difficulty and to have an efficient interpolation function, an approximate function based on the generalized linear strain is used. The generalized linear strain formulated on two reference line can be obtained from Eq. 3.7 and expressed as the following:

$$\begin{aligned}
 e_z = & \left\{ (w'_c - u_s / R) - \frac{y_s}{R} \sin \beta - \frac{x_s}{R} (1 - \cos \beta) \right\} \\
 & + x \left\{ \frac{1}{R} (1 - \cos \beta) - \cos \beta \left(u''_s + \frac{w_c}{R} \right) + \frac{x_s}{R} v''_s \cos \beta \right\} \\
 & + y \left\{ -v''_s \cos \beta + \frac{\sin \beta}{R} \right\} + \omega \left\{ -\beta'' - \cos \beta \frac{v''_s}{R} \right\}
 \end{aligned} \tag{5.4}$$

If the linear parts of strains are treated as independent variables, the strain terms inside of parentheses can be used for interpolation of element displacement. By assuming that strains associated with the flexural and torsional behavior of a curved beam line element can be approximated by linear functions and those strains associated with axial displacement can be approximated as constants, shape functions can be derived.

$$(w'_c - u_s / R) - \frac{y_s}{R} \sin \beta - \frac{x_s}{R} (1 - \cos \beta) = a_1 \frac{1}{R^2} \tag{5.5a}$$

$$\frac{1}{R} (1 - \cos \beta) - \cos \beta \left(u''_s + \frac{w_c}{R} \right) + \frac{x_s}{R} v''_s \cos \beta = \left(a_2 \frac{x}{R} + a_3 \right) \frac{1}{R^2} \tag{5.5b}$$

$$-v''_s \cos \beta + \frac{\sin \beta}{R} = \left(a_4 \frac{x}{R} + a_5 \right) \frac{1}{R^2} \tag{5.5c}$$

$$-\beta'' - \cos \beta \frac{v''_s}{R} = \left(a_6 \frac{x}{R} + a_7 \right) \frac{1}{R^2} \tag{5.5d}$$

Where: a1 to a7 are coefficients to be determined by nodal displacement.

The shape function of the sectional degree of freedom, α , is assumed as an independent variable and interpolated by a linear function.

$$\alpha' = \frac{a_8}{R^2} \tag{5.5e}$$

Equation 5.5 is solved to obtain the displacement components of the curved beam. The solutions are:

$$u_s = \sin\left(\frac{z}{R}\right)a_6 + \cos\left(\frac{z}{R}\right)a_s + a_2 - a_3 + a_1\left(\frac{z}{R}\right) + a_8\frac{y_s}{R} + a_7\frac{y_s}{R}\left(\frac{z}{R}\right) \quad 5.6a$$

$$w_c = -\cos\left(\frac{z}{R}\right)a_6 + \sin\left(\frac{z}{R}\right)a_s + a_2\left(\frac{z}{R}\right) + a_1\left(\frac{z}{R}\right)^2 - a_{14}y_s \cos\left(\frac{z}{R}\right) + a_{13}y_s \sin\left(\frac{z}{R}\right) + a_{10}y_s\left(\frac{z}{R}\right) + a_9\frac{y_s}{2}\left(\frac{z}{R}\right)^2 + a_4 \quad 5.6b$$

$$v_s = -a_{14}R \sin\left(\frac{z}{R}\right) - a_{13}R \cos\left(\frac{z}{R}\right) + a_{10}\frac{R}{2}\left(\frac{z}{R}\right)^2 + a_9\frac{z}{6}\left(\frac{z}{R}\right)^2 + a_{11}z + a_{12} \quad 5.6c$$

$$\beta = a_{14} \sin\left(\frac{z}{R}\right) + a_{13} \cos\left(\frac{z}{R}\right) + a_{10}\left(\frac{z}{R}\right)^2 + a_9\left(\frac{z}{R}\right) - \frac{a_8}{R} + a_7R\left(\frac{z}{R}\right) \quad 5.6d$$

$$\alpha = a_8 + a_{16}\left(\frac{z}{R}\right) \quad 5.6e$$

For convenience, only the shape functions for eight DOF which are associated with sectional deformation are presented. In matrix form, Equation 5.6 can be expressed as the following:

$$\{u\} = [{}^s\Phi] \bullet {}^s\bar{a} \quad 5.7a$$

where:

$${}^s\bar{a} = \{a_1 \dots a_{16}\}^T \quad 5.7b$$

$$\begin{aligned}
[{}^s\Phi] = [{}^s\bar{\Phi}_1 \quad {}^s\bar{\Phi}_2 \quad {}^s\bar{\Phi}_3 \quad {}^s\bar{\Phi}_4 \quad {}^s\bar{\Phi}_5] = & \begin{bmatrix}
\varphi & \varphi^2 & 0 & 0 & 0 \\
1 & \varphi & 0 & 0 & 0 \\
-1 & 0 & 0 & 0 & 0 \\
0 & 1 & 0 & 0 & 0 \\
c_z & s_z & 0 & 0 & 0 \\
\frac{-y_s}{R}\varphi & -c_z & 0 & 0 & 0 \\
\frac{y_s}{R} & 0 & 0 & R\varphi & 0 \\
0 & 0 & 0 & 0 & 1 \\
0 & 0 & 0 & -\frac{1}{R} & 0 \\
0 & \frac{y_s}{2}\varphi^2 & \frac{R}{6}\varphi^3 & \varphi & 0 \\
0 & y_s\varphi & \frac{2}{R}\varphi^2 & \varphi^2 & 0 \\
0 & 0 & R\varphi & 0 & 0 \\
0 & 0 & 1 & 0 & 0 \\
0 & s_z & -Rc_z & c_z & 0 \\
0 & y_sc_z & -Rs_z & s_z & 0 \\
0 & 0 & 0 & 0 & \varphi
\end{bmatrix} \\
& \mathbf{5.7c}
\end{aligned}$$

$$\varphi = \frac{z}{R}, \quad c_z = \cos\left(\frac{z}{R}\right) \text{ and } s_z = \sin\left(\frac{z}{R}\right)$$

The superscript “s” in Eq. 5.7 denotes the inclusion of sectional deformation. To link the displacement field, Eq. 5.6, with the nodal displacement, Eq. 5.3c, the following relationship is used.

$${}^s\bar{u}^d = [{}^s\Phi^d] \bullet {}^s\bar{a} \quad \mathbf{5.9a}$$

$$[{}^s\Phi^d] = [{}^s\bar{\Phi}_1 \quad {}^s\bar{\Phi}_3 \quad {}^s\bar{\Phi}_2 \quad {}^s\bar{\Phi}'_1 \quad {}^s\bar{\Phi}'_3 \quad {}^s\bar{\Phi}_4 \quad {}^s\bar{\Phi}'_4 \quad {}^s\bar{\Phi}_5] \quad \mathbf{5.9b}$$

The symbol prime denotes differentiation with respect to z. Since the nodal displacement is the displacement field at the ends of the curved beam element, the relationship between the integration constant or coefficient \bar{a} and nodal displacement ${}^s\bar{d} = \{ {}^s\bar{u}_0, {}^s\bar{u}_L \}^T$ can be established by combining Eq. 5.3a and Eq. 5.9a.

At z = 0;

$${}^s\bar{u}_0 = [{}^sB] \bullet ([{}^s\Phi_0^d] \bullet {}^s\bar{a}) \quad \mathbf{5.10a}$$

$$\left[{}^s\Phi_0^d \right] = \begin{bmatrix} 0 & 1 & -1 & 0 & 1 & 0 & \frac{y_s}{R} & 0 & 0 & 0 & 0 & 0 & 0 & 0 & 0 & 0 \\ 0 & 0 & 0 & 0 & 0 & 0 & 0 & 0 & 0 & 0 & 0 & 0 & 1 & -R & 0 & 0 \\ 0 & 0 & 0 & 1 & 0 & -1 & 0 & 0 & 0 & 0 & 0 & 0 & 0 & 0 & y_s & 0 \\ \frac{1}{R} & 0 & 0 & 0 & 0 & 0 & \frac{y_s}{R^2} & 0 & 0 & 0 & 0 & 0 & 0 & 0 & 0 & 0 \\ 0 & 0 & 0 & 0 & 0 & 0 & 0 & 0 & 0 & 0 & 0 & 1 & 0 & 0 & -1 & 0 \\ 0 & 0 & 0 & 0 & 0 & 0 & 0 & 0 & -\frac{1}{R} & 0 & 0 & 0 & 0 & 1 & 0 & 0 \\ 0 & 0 & 0 & 0 & 0 & 0 & 1 & 0 & 0 & \frac{1}{R} & 0 & 0 & 0 & 0 & \frac{1}{R} & 0 \\ 0 & 0 & 0 & 0 & 0 & 0 & 0 & 1 & 0 & 0 & 0 & 0 & 0 & 0 & 0 & 0 \end{bmatrix}^T \quad 5.10c$$

At $z = L$;

$${}^s\bar{u}_L = [{}^sB] \bullet \left([{}^s\Phi_L^d] \bullet {}^s\bar{a} \right) \quad 5.11a$$

$$\left[{}^s\Phi_L^d \right] = \begin{bmatrix} \varphi_L & 1 & -1 & 0 & c_L & \frac{y_s}{R}\varphi_L & \frac{y_s}{R} & 0 & 0 & 0 & 0 & 0 & 0 & 0 & 0 & 0 \\ 0 & 0 & 0 & 0 & 0 & 0 & 0 & 0 & \frac{R}{6}\varphi_L^3 & \frac{2}{R}\varphi_L^2 & R\varphi_L & 1 & -R c_L & -R s_L & 0 & 0 \\ \varphi_L^2 & \varphi_L & 0 & 1 & s_L & -c_L & 0 & 0 & 0 & \frac{y_s}{2}\varphi_L^2 & y_s\varphi_L & 0 & 0 & s & y_s c_L & 0 \\ \frac{1}{R} & 0 & 0 & 0 & \frac{s_L}{R} & \frac{y_s}{R^2} & 0 & 0 & 0 & 0 & 0 & 0 & 0 & 0 & 0 & 0 \\ 0 & 0 & 0 & 0 & 0 & 0 & 0 & 0 & \frac{\varphi_L^2}{2} & \frac{4}{R}\varphi_L & 1 & 0 & s_L & -c_L & 0 & 0 \\ 0 & 0 & 0 & 0 & 0 & 0 & R\varphi_L & 0 & -\frac{1}{R} & \varphi_L & \varphi_L^2 & 0 & 0 & c_L & s_L & 0 \\ 0 & 0 & 0 & 0 & 0 & 0 & 1 & 0 & 0 & \frac{1}{R} & \frac{2}{R}\varphi & 0 & 0 & -\frac{s_L}{R} & \frac{c_L}{R} & 0 \\ 0 & 0 & 0 & 0 & 0 & 0 & 0 & 1 & 0 & 0 & 0 & 0 & 0 & 0 & \varphi_L & 0 \end{bmatrix}^T \quad 5.11c$$

$$\text{Where: } \varphi_L = \frac{L}{R} \quad s_L = \sin\left(\frac{L}{R}\right) \quad c_L = \cos\left(\frac{L}{R}\right)$$

From Eqs. 5.3, 5.10 and 5.11, the integration constant ${}^s\bar{a}$ can be expressed by the following equation:

$${}^s \bar{a} = [{}^s \Psi] \bullet {}^s \bar{d} \quad 5.12a$$

$$[{}^s \Psi] = \begin{bmatrix} [{}^s \Phi_0^d] \\ [{}^s \Phi_L^d] \end{bmatrix} \quad 5.12b$$

By substituting Equation 5.12a into Equation 5.7a, the displacement field can be interpolated by the nodal displacement:

$$u_s = {}^s \bar{\Phi}_1^T \times [{}^s \Psi]^{-1} {}^s \bar{d} = {}^s \bar{N}_1 {}^s \bar{d} \quad 5.13a$$

$$w_c = {}^s \bar{\Phi}_2^T \times [{}^s \Psi]^{-1} {}^s \bar{d} = {}^s \bar{N}_2 {}^s \bar{d} \quad 5.13b$$

$$v_s = {}^s \bar{\Phi}_3^T \times [{}^s \Psi]^{-1} {}^s \bar{d} = {}^s \bar{N}_3 {}^s \bar{d} \quad 5.13c$$

$$\beta = {}^s \bar{\Phi}_4^T \times [{}^s \Psi]^{-1} {}^s \bar{d} = {}^s \bar{N}_4 {}^s \bar{d} \quad 5.13d$$

$$\alpha = {}^s \bar{\Phi}_5^T \times [{}^s \Psi]^{-1} {}^s \bar{d} = {}^s \bar{N}_5 {}^s \bar{d} \quad 5.13e$$

Where ${}^s \bar{N}_1 \dots {}^s \bar{N}_5$ are the shape function vector for u_s , w_c , v_s , β and α

The superscript “s” in ${}^s \bar{N}$ denotes the inclusion of sectional deformation. If it is not included in the analysis, the matrixes $[{}^s \Phi]$ and $[{}^s \Psi]$ in Eq. 5.13 have to be modified for the shape functions of the seven degrees of freedom (DOF) of the line element. The modified matrixes and the shape functions of the seven DOF are listed in Table 5.1 for later use in this study.

The shape functions ${}^s \bar{N}_1 \dots {}^s \bar{N}_5$ are developed from two reference lines. The procedure of developing the shape function from one reference line is the same as that for two reference lines except the terms x_s and y_s are replaced. However the definition of nodal rotation should be changed.

Since the rotation of arbitrary points which are not in a cross section is not affected by warping and is constant by the rigid body rotation of the cross section, only Saint-Venant torsion has to be considered for these points. The nodal rotation $\theta_y = u_c' + \frac{w_c}{R}$,

$\theta_x = v_c'$ and $\theta_\omega = \beta' + \frac{v_c'}{R}$ have two rotational components. The nodal displacement u_c and v_c in the expression of θ_x , θ_y and θ_ω can be expressed as $u_c = u_s + y_s \beta$ and $v_c = v_s - x_s \beta$. Thus, the nodal rotations are $\theta_y = u_s' + y_s \beta' + \frac{w_c}{R}$, $\theta_x = v_s' - x_s \beta'$ and

$\theta_\omega = \beta' + \frac{v_s' - x_s \beta'}{R}$. The terms $y_s \beta'$ and $x_s \beta'$ in the expression of nodal rotation are due to warping of the cross section. It implies that the rotation of the reference axis which

is located outside of the section includes warping deformation. However, warping deformation exists only in the section. Therefore, the rotation associated with warping deformation should be removed from the rotation of the reference axis outside of the cross section. Therefore, nodal rotations of one reference line are $\theta_y = (u_c - y_s \beta)' + \frac{w_c}{R}$,

$\theta_x = (v_c + x_s \beta)'$ and $\theta_\omega = \beta' + (v_c + x_s \beta)' / R$. The shape functions based on one reference line can be obtained by modifying the matrix $[\Phi]$, $[B]$ and $[\Psi]$ expressed in the Eq 5.7c, 5.3e and 5.12b. $[\Phi]$ can be modified as:

$$[\Phi_c] = \begin{bmatrix} \Phi_{c1} & \Phi_{c2} & \Phi_{c3} & \Phi_{c4} & \Phi_{c5} \end{bmatrix} = \begin{bmatrix} \varphi & 1 & -1 & 0 & c & 0 & 0 & 0 & 0 & 0 & 0 & 0 & 0 & 0 & 0 & 0 \\ \varphi^2 & \varphi & 0 & 1 & s & -c & 0 & 0 & 0 & 0 & 0 & 0 & 0 & s & 0 & 0 \\ 0 & 0 & 0 & 0 & 0 & 0 & 0 & 0 & 0 & \frac{R}{6}\varphi^3 & \frac{2}{R}\varphi^2 & R\varphi & 1 & -Rc & -Rs & 0 \\ 0 & 0 & 0 & 0 & 0 & 0 & R\varphi & 0 & -\frac{1}{R} & \varphi & \varphi^2 & 0 & 0 & c & s & 0 \\ 0 & 0 & 0 & 0 & 0 & 0 & 0 & 1 & 0 & 0 & 0 & 0 & 0 & 0 & 0 & \varphi \end{bmatrix}^T \quad 5.14$$

The superscript “s” and subscript “c” in $[\Phi_c]$ denote sectional deformation and centroid.

The nodal degree of freedom, ${}^s \bar{d}$, can be modified as;

$${}^s \bar{d}_c = \begin{Bmatrix} {}^s \bar{u}_{c0} \\ {}^s \bar{u}_{cL} \end{Bmatrix} \quad 5.15a$$

$${}^s \bar{u}_c = [{}^s B_c] {}^s \bar{u}_c^d \quad 5.15b$$

Where

$${}^s \bar{u}_c = \{u_c \quad w_c \quad \theta_y \quad v_c \quad \theta_x \quad \beta \quad \theta_\omega \quad \theta_\alpha\}^T \quad 5.15c$$

$${}^s \bar{u}_c^d = \{u_c \quad v_c \quad w_c \quad u'_c \quad v'_c \quad \beta \quad \beta' \quad \alpha\}^T \quad 5.15d$$

$$[{}^s B_c] = \begin{bmatrix} 1 & 0 & 0 & 0 & 0 & 0 & 0 & 0 \\ 0 & 1 & 0 & 0 & 0 & 0 & 0 & 0 \\ 0 & 0 & 0 & 0 & 1 & 0 & x_s & 0 \\ 0 & 1 & 0 & 0 & 0 & 0 & 0 & 0 \\ 0 & 0 & \frac{1}{R} & 1 & 0 & 0 & -y_s & 0 \\ 0 & 0 & 0 & 0 & 0 & 1 & 0 & 0 \\ 0 & 0 & 0 & 0 & -\frac{1}{R} & 0 & -1 & 0 \\ 0 & 0 & 0 & 0 & 0 & 0 & 0 & 1 \end{bmatrix} \quad 5.15e$$

The modified $[\Psi]$ are

$$[{}^s\Psi_c] = \begin{bmatrix} [{}^s\Phi_{c0}^d] \\ [{}^s\Phi_{cL}^d] \end{bmatrix} \quad 5.16a$$

$$[{}^s\Phi_{c0}^d] = \begin{bmatrix} 0 & 1 & -1 & 0 & 0 & 0 & 0 & 0 & 0 & 0 & 0 & 0 & 0 & 0 & 0 \\ 0 & 0 & 0 & 0 & 0 & 0 & 0 & 0 & 0 & 0 & 0 & 0 & 1 & -R & 0 & 0 \\ 0 & 0 & 0 & 1 & 0 & -1 & 0 & 0 & 0 & 0 & 0 & 0 & 0 & 0 & 0 & 0 \\ \frac{1}{R} & 0 & 0 & 0 & 0 & 0 & 0 & 0 & 0 & 0 & 0 & 0 & 0 & 0 & 0 & 0 \\ 0 & 0 & 0 & 0 & 0 & 0 & 0 & 0 & 0 & 0 & 0 & 1 & 0 & 0 & -1 & 0 \\ 0 & 0 & 0 & 0 & 0 & 0 & 0 & 0 & -\frac{1}{R} & 0 & 0 & 0 & 0 & 1 & 0 & 0 \\ 0 & 0 & 0 & 0 & 0 & 0 & 1 & 0 & 0 & \frac{1}{R} & 0 & 0 & 0 & 0 & \frac{1}{R} & 0 \\ 0 & 0 & 0 & 0 & 0 & 0 & 0 & 1 & 0 & 0 & 0 & 0 & 0 & 0 & 0 & 0 \end{bmatrix}^T$$

5.16b

$$[{}^s\Phi_{cL}^d] = \begin{bmatrix} \varphi_L & 0 & \varphi_L^2 & \frac{1}{R} & 0 & 0 & 0 & 0 \\ 1 & 0 & \varphi_L & 0 & 0 & 0 & 0 & 0 \\ -1 & 0 & 0 & 0 & 0 & 0 & 0 & 0 \\ 0 & 0 & 1 & 0 & 0 & 0 & 0 & 0 \\ c_L & 0 & s_L & \frac{s_L}{R} & 0 & 0 & 0 & 0 \\ 0 & 0 & -c_L & 0 & 0 & 0 & 0 & 0 \\ 0 & 0 & 0 & 0 & 0 & R\varphi_L & 1 & 0 \\ 0 & 0 & 0 & 0 & 0 & 0 & 0 & 1 \\ 0 & 0 & 0 & 0 & 0 & -\frac{1}{R} & 0 & 0 \\ 0 & \frac{R}{6}\varphi_L^3 & 0 & 0 & \frac{\varphi_L^2}{R} & \varphi_L & \frac{1}{R} & 0 \\ 0 & \frac{2}{R}\varphi_L^2 & 0 & 0 & \frac{4}{R}\varphi_L & \varphi_L^2 & \frac{2}{R}\varphi & 0 \\ 0 & R\varphi_L & 0 & 0 & 1 & 0 & 0 & 0 \\ 0 & 1 & 0 & 0 & 0 & 0 & 0 & 0 \\ 0 & -Rc_L & s & 0 & s_L & c_L & -\frac{s_L}{R} & 0 \\ 0 & -Rs_L & 0 & 0 & -c_L & s_L & \frac{c_L}{R} & 0 \\ 0 & 0 & 0 & 0 & 0 & 0 & 0 & \varphi_L \end{bmatrix}$$

5.16c

With the matrix $[{}^s\Phi_c]$, $[{}^sB_c]$ and $[{}^s\Psi_c]$, the displacement fields based on one reference line can be interpolated as the following equation.

$$u_c = {}^s \bar{\Phi}_{c1}^T \times [{}^s \Psi_c]^{-1} {}^s \bar{d} = {}^s \bar{N}_{c1} {}^s \bar{d} \quad 5.17a$$

$$w_c = {}^s \bar{\Phi}_{c2}^T \times [{}^s \Psi_c]^{-1} {}^s \bar{d} = {}^s \bar{N}_{c2} {}^s \bar{d} \quad 5.17b$$

$$v_s = {}^s \bar{\Phi}_{c3}^T \times [{}^s \Psi_c]^{-1} {}^s \bar{d} = {}^s \bar{N}_{c3} {}^s \bar{d} \quad 5.17c$$

$$\beta = {}^s \bar{\Phi}_{c4}^T \times [{}^s \Psi_c]^{-1} {}^s \bar{d} = {}^s \bar{N}_{c4} {}^s \bar{d} \quad 5.17d$$

$$\alpha = {}^s \bar{\Phi}_{c5}^T \times [{}^s \Psi_c]^{-1} {}^s \bar{d} = {}^s \bar{N}_{c5} {}^s \bar{d} \quad 5.17e$$

Where ${}^s \bar{N}_{c1} \dots {}^s \bar{N}_{c5}$ are the shape function vector based on one reference line (centroid) for u_c , w_c , v_c , β and α .

5.2.3 Nodal Load Vector

The nodal load vector can be derived from Eq 4.41. As mentioned before, body forces are not considered in this study. The nodal load vector is composed of two vectors, due to distributed and concentrated loads. By substituting the shape function of Eq. 5.13 into the first term (the integrand term) of Eq. 4.41, the distributed load can be transformed into an equivalent nodal load and expressed as the following equation:

$$\begin{aligned} \bar{f}^d \delta {}^s \bar{d} = & \\ = \int_0^L & \left[\begin{aligned} & \left(f_x - m_y' \right) {}^s \bar{N}_1 \delta \bar{d} + \left(f_y - m_x' - \frac{m_\omega'}{R} \right) {}^s \bar{N}_3 \delta \bar{d} \\ & + \left(f_z + \frac{m_y}{R} \right) {}^s \bar{N}_2 \delta \bar{d} + \left(m_z - m_\omega' \right) {}^s \bar{N}_4 \delta \bar{d} + (m_\alpha) {}^s \bar{N}_5 \delta \bar{d} \end{aligned} \right] dz \quad 5.18a \end{aligned}$$

$$\bar{f}^d = \begin{Bmatrix} \bar{f}_0 \\ \bar{f}_L \end{Bmatrix} \quad 5.18b$$

$$\bar{f}_0 = \left\{ f_{x0}^d \quad f_{y0}^d \quad f_{z0}^d \quad m_{x0}^d \quad m_{y0}^d \quad m_{z0}^d \quad m_{\omega 0}^d \quad m_{\alpha 0}^d \right\}^T \quad 5.18c$$

$$\bar{f}_L = \left\{ f_{xL}^d \quad f_{yL}^d \quad f_{zL}^d \quad m_{xL}^d \quad m_{yL}^d \quad m_{zL}^d \quad m_{\omega L}^d \quad m_{\alpha L}^d \right\}^T \quad 5.18d$$

Where \bar{f}^d is the equivalent nodal load vector due to distributed loads. The forces f_x^d , f_y^d , f_z^d , m_x^d , m_y^d , m_z^d , m_ω^d and m_α^d are equivalent nodal loads due to f_x , f_y , f_z , m_x , m_y , m_z , m_ω and m_α , respectively.

The nodal load vector due to concentrated forces can be derived from the last term of Eq 4.41. By limiting the location of concentrated load to the nodal points, the nodal force is:

$$\bar{F}^d = \begin{Bmatrix} \bar{F}_0 \\ \bar{F}_L \end{Bmatrix} \quad \mathbf{5.19a}$$

$$\bar{F}_0 = \{ F_{x0} \quad F_{y0} \quad F_{z0} \quad M_{x0} \quad M_{y0} \quad M_{z0} \quad M_{\omega0} \quad M_{\alpha0} \}^T \quad \mathbf{5.19b}$$

$$\bar{F}_L = \{ F_{xL} \quad F_{yL} \quad F_{zL} \quad M_{xL} \quad M_{yL} \quad M_{zL} \quad M_{\omega L} \quad M_{\alpha L} \}^T \quad \mathbf{5.19c}$$

Where \bar{F}^d is the nodal load vector due to concentrated external loads. The nodal load vectors are shown in Figure 5.1 for the single reference line formulation. In two reference line formulation, M_x, M_y, F_z are applied to the centroid of cross sections and F_x, F_y, M_z, M_ω are applied to the shear center.

For incremental analysis of large displacement and rotation, the variation of nodal displacements, distributed loads (Eq. 5.18) and concentrated loads (Eq. 5.19) are changed to incremental nodal displacements, distributed loads and concentrated loads.

$$\begin{aligned} \Delta \bar{f}^d \delta \Delta^s \bar{d} = & \\ = \int_0^L & \left[\begin{aligned} & \left(\Delta f_x - \Delta m_y' \right) {}^s \bar{N}_1 \delta \Delta^s \bar{d} + \left(\Delta f_y - \Delta m_x' - \frac{\Delta m_\omega'}{R} \right) {}^s \bar{N}_3 \delta \Delta^s \bar{d} \\ & + \left(\Delta f_z + \frac{\Delta m_y}{R} \right) {}^s \bar{N}_2 \delta \Delta^s \bar{d} + \left(\Delta m_z - \Delta m_\omega' \right) {}^s \bar{N}_4 \delta \Delta^s \bar{d} + \left(\Delta m_\alpha \right) {}^s \bar{N}_5 \delta \Delta^s \bar{d} \end{aligned} \right] dz \end{aligned} \quad \mathbf{5.20}$$

$$\Delta \bar{f}^d = \begin{Bmatrix} \Delta \bar{f}_0 \\ \Delta \bar{f}_L \end{Bmatrix} \quad \mathbf{5.21a}$$

$$\Delta \bar{f}_0 = \{ \Delta f_{x0}^d \quad \Delta f_{y0}^d \quad \Delta f_{z0}^d \quad \Delta m_{x0}^d \quad \Delta m_{y0}^d \quad \Delta m_{z0}^d \quad \Delta m_{\omega0}^d \quad \Delta m_{\alpha0}^d \}^T \quad \mathbf{5.21b}$$

$$\Delta \bar{f}_L = \{ \Delta f_{xL}^d \quad \Delta f_{yL}^d \quad \Delta f_{zL}^d \quad \Delta m_{xL}^d \quad \Delta m_{yL}^d \quad \Delta m_{zL}^d \quad \Delta m_{\omega L}^d \quad \Delta m_{\alpha L}^d \}^T \quad \mathbf{5.21c}$$

$$\Delta \bar{F}^d = \begin{Bmatrix} \Delta \bar{F}_0 \\ \Delta \bar{F}_L \end{Bmatrix} \quad \mathbf{5.21d}$$

$$\Delta \bar{F}_0 = \{ \Delta F_{x0} \quad \Delta F_{y0} \quad \Delta F_{z0} \quad \Delta M_{x0} \quad \Delta M_{y0} \quad \Delta M_{z0} \quad \Delta M_{\omega0} \quad \Delta M_{\alpha0} \}^T \quad \mathbf{5.21e}$$

$$\Delta \bar{F}_L = \{ \Delta F_{xL} \quad \Delta F_{yL} \quad \Delta F_{zL} \quad \Delta M_{xL} \quad \Delta M_{yL} \quad \Delta M_{zL} \quad \Delta M_{\omega L} \quad \Delta M_{\alpha L} \}^T \quad \mathbf{5.21f}$$

Because the line element is represented by reference lines and points, external concentrated loads have to be transformed to reference point loads. When concentrated loads are not on the reference point, it generates secondary forces corresponding to the displaced configuration of the beam. Figure 5.2 shows a concentrated load that is not

on the reference line. The load is coupled with the sectional rotation and displacement, and generates a secondary moment. By using the incremental form of potential energy due to applied loads, the secondary moment at the reference point can be derived with respect to the initial configuration. With the assumption of small rotation in each incremental step, secondary moment can be expressed by the following equation.

$$\Delta(\text{Potential Energy}) = (\text{Potential Energy})^{t+\Delta t} - (\text{Potential Energy})^t$$

$$\begin{aligned}\Delta M_z^{sm} &= \{(F_y + \Delta F_y)(\beta + \Delta\beta) - F_y \beta\} y_0 \\ &= \{F_y \Delta\beta + \Delta F_y \beta + \Delta F_y \Delta\beta\} y_0\end{aligned}\quad 5.22$$

Where, the superscript “sm” in Eq 5.22 denotes secondary moment. For large rotations with concentrated loads applied at arbitrary points of a cross section (y_0), secondary moment can be obtained using the following expressions.

$$\bar{M}^{sm} = ([\Delta T_1] + [\Delta T_2]) \bar{P} + ([T_1] + [T_2]) \Delta \bar{P} + ([\Delta T_1] + [\Delta T_2]) \Delta \bar{P} \quad 5.23a$$

Where:

$$\bar{M}^{sm} = \{M_x^{sm} \quad M_y^{sm} \quad M_z^{sm}\}^T \quad 5.23b$$

$$\Delta \bar{P} = \{\Delta F_x \quad \Delta F_y \quad \Delta F_z\}^T \quad 5.23c$$

$$\bar{P} = \{F_x \quad F_y \quad F_z\}^T \quad 5.23d$$

$$[T_1] = \begin{bmatrix} 0 & y_0 \sin(\theta_x) & y_0(2 - \cos(\beta) - \cos(\theta_x)) \\ -y_0 \sin(\theta_x) & 0 & y_0 \sin(\theta_z) \\ -y_0(2 - \cos(\theta_x) - \cos(\beta)) & y_0 \sin(\theta_z) & 0 \end{bmatrix} \quad 5.24a$$

$$[T_2] = \begin{bmatrix} 0 & x_0 \sin(\theta_y) & -x_0 \sin(\beta) \\ -x_0 \sin(\theta_y) & 0 & x_0(2 - \cos(\theta_y) - \cos(\beta)) \\ -x_0 \sin(\beta) & -x_0(2 - \cos(\theta_y) - \cos(\beta)) & 0 \end{bmatrix} \quad 5.24b$$

$$[\Delta T_1] = \begin{bmatrix} 0 & y_0(\Delta\theta_x) & 0 \\ -y_0(\Delta\theta_x) & 0 & y_0(\Delta\beta) \\ 0 & y_0(\Delta\beta) & 0 \end{bmatrix} \quad 5.24c$$

$$[\Delta T_2] = \begin{bmatrix} 0 & x_0(\Delta\theta_y) & -x_0(\Delta\beta) \\ -x_0(\Delta\theta_y) & 0 & 0 \\ -x_0(\Delta\beta) & 0 & 0 \end{bmatrix} \quad 5.24d$$

Where \bar{M}^{sm} is vector of the secondary moment

M_y^{sm} is the secondary moment about y-axis

M_x^{sm} is the secondary moment about x-axis

M_z^{sm} is the secondary moment about z-axis

x_0 and y_0 are the distances of point load from the reference point

$[T_1]$ are the transformation vector associated with y_0

$[T_2]$ are the transformation vector associated with x_0

5.2.4 Calculation of Stresses

With large displacements and rotations, curved beams may be subjected to relatively high stresses. It is necessary to calculate the maximum stress based on the large displacement and large rotation analysis, for checking against limit states.

The simplified longitudinal strain for an arbitrary cross section is obtained From Eq. 4.9a and expressed as the following.

$$\varepsilon_z = (e_0 + \eta_0) + x(e_x + \eta_x) + y(e_y + \eta_y) + \omega(e_\omega + \eta_\omega) \quad 5.25$$

In this equation, the terms associated with x^2 , y^2 , xy , $x\omega$ and $y\omega$ are not included. The components of the strain in Eq. 5.25 can be expressed in terms of sectional properties and stress resultants, M_x , M_y , M_z , Bi .

$$(e_0 + \eta_0) = \frac{F_z}{EA} \quad 5.26a$$

$$(e_x + \eta_x) = - \left(\frac{M_x (I_{xy} I_w - I_{xw} I_{yw}) + M_y (I_x I_w - I_{yw}^2) + Bi (I_x I_{xw} - I_{xy} I_{yw})}{E (I_x I_y I_w + 2 I_{xw} I_{xy} I_{yw} - I_y I_{yw}^2 - I_x I_{xw}^2 - I_{xy}^2)} \right) \quad 5.26b$$

$$(e_y + \eta_y) = \frac{M_x (I_y I_w - I_{xw}^2) + M_y (I_{xy} I_w - I_{xw} I_{yw}) + Bi (I_{xy} I_{xw} - I_y I_{yw})}{E (I_x I_y I_w + 2 I_{xw} I_{xy} I_{yw} - I_y I_{yw}^2 - I_x I_{xw}^2 - I_{xy}^2)} \quad 5.26c$$

$$(e_\omega + \eta_\omega) = \frac{M_x (I_{xy} I_{xw} - I_y I_{yw}) + M_y (I_{xw} I_x - I_{xy} I_{yw}) + Bi (I_x I_y - I_{xy}^2)}{E (I_x I_y I_w + 2 I_{xw} I_{xy} I_{yw} - I_y I_{yw}^2 - I_x I_{xw}^2 - I_{xy}^2)} \quad 5.26d$$

By substituting Equation 5.26 into Equation 5.25 and using the constitutive law, the following equation for calculating longitudinal normal stresses is obtained;

$$\sigma_z = \frac{F_z}{A} - x \left\{ \frac{M_x (I_{xy} I_w - I_{xw} I_{yw}) + M_y (I_x I_w - I_{yw}^2) + Bi (I_x I_{xw} - I_{xy} I_{yw})}{(I_x I_y I_w + 2 I_{xw} I_{xy} I_{yw} - I_y I_{yw}^2 - I_x I_{xw}^2 - I_{xy}^2)} \right\} \\ + y \left\{ \frac{M_x (I_y I_w - I_{xw}^2) + M_y (I_{xy} I_w - I_{xw} I_{yw}) + Bi (I_{xy} I_{xw} - I_y I_{yw})}{(I_x I_y I_w + 2 I_{xw} I_{xy} I_{yw} - I_y I_{yw}^2 - I_x I_{xw}^2 - I_{xy}^2)} \right\} \\ + \omega \left\{ \frac{M_x (I_{xy} I_{xw} - I_y I_{yw}) + M_y (I_{xw} I_x - I_{xy} I_{yw}) + Bi (I_x I_y - I_{xy}^2)}{(I_x I_y I_w + 2 I_{xw} I_{xy} I_{yw} - I_y I_{yw}^2 - I_x I_{xw}^2 - I_{xy}^2)} \right\} \quad 5.27$$

It should be noted that in Equation 5.27, approximation (b) in Section 3.2 is used and stress resultants K_{xx} , K_{yy} , K_{xy} and $K_{x\omega}$ associated with terms of x^2 , y^2 , xy and $x\omega$ are not included under the assumption that the contribution of these stress resultants are negligible. In order to use equation 5.27, the stress resultants, M_x , M_y , M_z and B_i have to be calculated first. Although the linear part of these stress resultants can be derived by solving linear differential equations or by free body diagrams, the complete stress resultants can only be obtained by solving higher order nonlinear differential equations. Furthermore, if the contributions of stress resultants, K_{xx} , K_{yy} , K_{xy} and $K_{x\omega}$ to the longitudinal stress are not negligible, obtaining stresses from Eq. 5.27 may generate inaccurate results.

In finite element analysis, on the other hand, stresses can be easily computed. In each incremental step, the displacement field is interpolated from the nodal displacements. By substituting the displacement field into Equation 4.9a and using the constitutive law, the longitudinal stresses can be calculated. With regard to the maximum longitudinal stress in the beam, an example equation for calculation including full nonlinear effects is developed in Chapter 8 by using this approach for curved beams subjected to end moments M_x .

5.3. Stiffness Matrix

5.3.1 Linear, Stress and Geometric Stiffness Matrixes

In order to solve the nonlinear equation in the variation of total potential energy, Eq. 4.2, linearization of the first term is necessary. Linearization can be done by ignoring the high order terms under the assumption that displacement and rotation are small and can be represented by the first term of Taylor's expansion. After linearization, first term of strain energy, Eq. 4.2 can be expressed as the following.

$$\int_V \bar{S}^T \delta \bar{\epsilon} dV = \int_V [\delta \bar{\epsilon}^T [C] \bar{\epsilon}] dV + \int_V [\bar{S}^T \delta \bar{\eta}] dV \quad 5.28$$

Where \bar{S} is the approximate stress vector and can be expressed as $\bar{S} = [C] \bar{\epsilon}$. The first term and the second term of the linearized variation of strain energy of Eq. 5.28 are defined as the linear stiffness matrix, $[K]$, and the stress stiffness matrix, $[K_s]$. Since there are two non-zero strains, longitudinal and shear strain, and only homogeneous material is considered, the linear stiffness matrix can be defined from the following equation:

$$\int_V [\delta \bar{\epsilon}^T [C] \bar{\epsilon}] dV = \int_V [E e_z \delta e_z] dV + \int_V [G e_{sz} \delta e_{sz}] dV \quad 5.29$$

By substituting the linear strains, Eq 4.9, into Eq 5.29, the following equations are obtained

$$\begin{aligned}
& \int_V [E e_z \delta e_z] dV = \\
& \int_V \left[E \left(\left(\tilde{w}'_c - \frac{\beta y_s}{R} \right) + x \left(-\tilde{u}''_s + \frac{y_s v''_s}{R} \right) + y \left(-v''_s + \frac{\beta}{R} \right) + \omega \left(-\beta'' - \frac{v''_s}{R} \right) \right) \right. \\
& \left. + \left(\left(\delta \tilde{w}'_c - \frac{\delta \beta y_s}{R} \right) + x \left(-\delta \tilde{u}''_s + \frac{y_s \delta v''_s}{R} \right) + y \left(-\delta v''_s + \frac{\delta \beta}{R} \right) + \omega \left(-\delta \beta'' - \frac{\delta v''_s}{R} \right) \right) \delta e_z \right] dV
\end{aligned} \tag{5.30a}$$

$$\int_V [G e_{sz} \delta e_{sz}] dV = \int_V \left[G \left(\beta' + \frac{v'_s}{R} \right) \left(\delta \beta' + \frac{\delta v'_s}{R} \right) \right] dV \tag{5.30b}$$

The displacement functions in equation 5.30 can be interpolated by the shape function in Table 5.1 and expressed as the following equation;

$$\int_V [E e_z \delta e_z] dV + \int_V [G e_{sz} \delta e_{sz}] dV = \bar{d}^T [K] \delta \bar{d} \tag{5.31a}$$

$$\begin{aligned}
[K] = \int_V & \left[E \begin{pmatrix} \left(\bar{N}'_2 - \frac{\bar{N}'_1}{R} - \frac{y_s \bar{N}'_4}{R} \right) + x \left(-\bar{N}''_1 - \frac{\bar{N}'_3}{R} + \frac{y_s \bar{N}''_3}{R} \right) \\ + y \left(-\bar{N}''_3 + \frac{\bar{N}'_4}{R} \right) + \omega \left(-\bar{N}''_4 - \frac{\bar{N}''_3}{R} \right) \end{pmatrix} \right]^T \\
& \times \begin{pmatrix} \left(\bar{N}'_2 - \frac{\bar{N}'_1}{R} - \frac{y_s \bar{N}'_4}{R} \right) + x \left(-\bar{N}''_1 - \frac{\bar{N}'_3}{R} + \frac{y_s \bar{N}''_3}{R} \right) \\ + y \left(-\bar{N}''_3 + \frac{\bar{N}'_4}{R} \right) + \omega \left(-\bar{N}''_4 - \frac{\bar{N}''_3}{R} \right) \end{pmatrix} \\
& + G 2n \left(\bar{N}'_4 + \frac{\bar{N}'_3}{R} \right)^T \times \left(\bar{N}'_4 + \frac{\bar{N}'_3}{R} \right) \Big] dV
\end{aligned} \tag{5.31b}$$

By using the sectional properties defined in Eq 4.60 to 4.65, the linear stiffness matrix in Eq 5.31 can be expressed as the following equation;

$$\begin{aligned}
[K] = E A \int & \left[\left(\bar{N}'_2 - \frac{\bar{N}'_1}{R} - \frac{y_s \bar{N}'_4}{R} \right)^T \times \left(\bar{N}'_2 - \frac{\bar{N}'_1}{R} - \frac{y_s \bar{N}'_4}{R} \right) \right] dz \\
& + EI_y \int \left[\left(-\bar{N}''_1 - \frac{\bar{N}'_3}{R} + \frac{y_s \bar{N}''_3}{R} \right)^T \times \left(-\bar{N}''_1 - \frac{\bar{N}'_3}{R} + \frac{y_s \bar{N}''_3}{R} \right) \right] dz \\
& + EI_x \int \left[\left(-\bar{N}''_3 + \frac{\bar{N}'_4}{R} \right)^T \times \left(-\bar{N}''_3 + \frac{\bar{N}'_4}{R} \right) \right] dz
\end{aligned}$$

$$\begin{aligned}
& + EI_{\omega} \int \left[\left(-\bar{N}_4'' - \frac{\bar{N}_3''}{R} \right)^T \times \left(-\bar{N}_4'' - \frac{\bar{N}_3''}{R} \right) \right] dz \\
& + EI_{xy} \int \left[\left(-\bar{N}_1'' - \frac{\bar{N}_3'}{R} + \frac{y_s \bar{N}_3''}{R} \right)^T \times \left(-\bar{N}_3'' + \frac{\bar{N}_4''}{R} \right) \right. \\
& \quad \left. + \left(-\bar{N}_3'' + \frac{\bar{N}_4''}{R} \right)^T \times \left(-\bar{N}_1'' - \frac{\bar{N}_3'}{R} + \frac{y_s \bar{N}_3''}{R} \right) \right] dz \\
& + EI_{x\omega} \int \left[\left(-\bar{N}_1'' - \frac{\bar{N}_3'}{R} + \frac{y_s \bar{N}_3''}{R} \right)^T \times \left(-\bar{N}_4'' - \frac{\bar{N}_3''}{R} \right) \right. \\
& \quad \left. + \left(-\bar{N}_4'' - \frac{\bar{N}_3''}{R} \right)^T \times \left(-\bar{N}_1'' - \frac{\bar{N}_3'}{R} + \frac{y_s \bar{N}_3''}{R} \right) \right] dz \\
& + EI_{y\omega} \int \left[\left(-\bar{N}_3'' + \frac{\bar{N}_4''}{R} \right)^T \times \left(-\bar{N}_4'' - \frac{\bar{N}_3''}{R} \right) \right. \\
& \quad \left. + \left(-\bar{N}_4'' - \frac{\bar{N}_3''}{R} \right)^T \times \left(-\bar{N}_3'' + \frac{\bar{N}_4''}{R} \right) \right] dz \\
& + GK_T \int \left[\left(\bar{N}_4' + \frac{\bar{N}_3'}{R} \right)^T \times \left(\bar{N}_4' + \frac{\bar{N}_3'}{R} \right) \right] dz
\end{aligned} \tag{5.32}$$

Similarly, the stress stiffness matrix, $[K_s]$, can be derived from the second term of Equation 5.28. By substituting the interpolation functions into the displacement field, the stress stiffness can be expressed by the nodal displacements and shape functions:

$$\begin{aligned}
& \int_V [\bar{S}^T \delta \bar{\eta}] dV = \bar{d}^T [K_s] \delta \bar{d} \tag{5.33a} \\
& [K_s] = \int_L F_z^a \left(\left(\bar{N}_1' + y_s \bar{N}_4' \right)^T \times \left(\bar{N}_1' + y_s \bar{N}_4' \right) + \left(\bar{N}_3' - x_s \bar{N}_4' \right)^T \times \left(\bar{N}_3' - x_s \bar{N}_4' \right) \right) \\
& \quad - M_y \left(\begin{array}{l} \frac{y_s}{R} \left(-\bar{N}_1'^T \times \bar{N}_4' - \bar{N}_4'^T \times \bar{N}_1' - \bar{N}_4'^T \times \bar{N}_1'' - \bar{N}_1''^T \times \bar{N}_4' \right) \\ -\bar{N}_3'^T \times \bar{N}_4' - \bar{N}_4'^T \times \bar{N}_3' - \bar{N}_4'^T \times \bar{N}_1'' - \bar{N}_1''^T \times \bar{N}_4' \end{array} \right) \\
& \quad - M_y^a \left(\begin{array}{l} -2 \frac{\bar{N}_1'^T \times \bar{N}_1'}{R} + \bar{N}_3'^T \times \bar{N}_4' + \bar{N}_4'^T \times \bar{N}_3' \\ -\frac{y_s}{R} \left(\bar{N}_4'^T \times \bar{N}_1' + \bar{N}_1'^T \times \bar{N}_4' \right) - 2x_s \bar{N}_4'^T \times \bar{N}_4' \end{array} \right)
\end{aligned}$$

$$\begin{aligned}
& + M_x \left(\widetilde{N}_1'^T \times \bar{N}_4' + \bar{N}_4'^T \times \widetilde{N}_1' + \bar{N}_4'^T \times \widetilde{N}_1'' + \widetilde{N}_1''^T \times \bar{N}_4' \right) \\
& + M_x^a \left(-\widetilde{N}_1'^T \times \widetilde{N}_4' + \widetilde{N}_4'^T \times \widetilde{N}_1' - y_s \left(\widetilde{N}_4'^T \times \bar{N}_4' + \bar{N}_4'^T \times \widetilde{N}_4' \right) \right) \\
& + M_\omega \left(\frac{\left(\bar{N}_4'^T \times \bar{N}_1' + \bar{N}_1'^T \times \bar{N}_4' \right)}{R} + \frac{\bar{N}_4'^T \times \bar{N}_1'' + \bar{N}_1''^T \times \bar{N}_4'}{R} \right) \\
& + M_\omega^a \left(-\frac{\left(\bar{N}_4'^T \times \bar{N}_1' + \bar{N}_1'^T \times \bar{N}_4' \right)}{R} - 2 \frac{y_s}{R} \bar{N}_4'^T \times \bar{N}_4' \right) \\
& + K_{xx}^a \left(\bar{N}_4'^T \times \bar{N}_4' \right) + K_{yy}^a \left(\bar{N}_4'^T \times \bar{N}_4' \right) + K_{xy}^a \left(\frac{\left(\bar{N}_4'^T \times \bar{N}_1' + \bar{N}_1'^T \times \bar{N}_4' \right)}{R} \right) \\
& + K_{y\omega}^a \left(\bar{N}_4'^T \times \bar{N}_4' \right) + M_{sv} \left(-\frac{\bar{N}_1'^T \times \bar{N}_4' + \bar{N}_4'^T \times \bar{N}_1'}{R} \right) \Big] dz \tag{5.33b}
\end{aligned}$$

$$\text{Where } \widetilde{N}_1' = \bar{N}_1' + \frac{\bar{N}_2}{R} \text{ and } \widetilde{N}_4' = \bar{N}_4' + \frac{\bar{N}_3}{R}$$

In Eq 5.33, the superscript “a” of stress resultants represents multiplying $\frac{R}{R-x}$ to the corresponding terms in the integration function of Eq 4.12, e.g., $F_z^a = \int_{A_0} \sigma \left(\frac{R}{R-x} \right) dA$.

The linear and stress stiffness matrix, Eq. 5.32 and Eq. 5.33 are developed under the assumption of small displacement and rotation. For large displacement and large rotation analysis, the incremental stiffness matrixes are needed. By using the incremental total Lagrange formulation derived in Section 4.5, the incremental stiffness matrixes can be developed. In this study, several different incremental stiffness matrixes are derived. The difference among them is in the approximation used in the simplification of incremental strains. These incremental stiffness matrixes will be used for analyzing the effect of simplification in large rotation stage.

The linear incremental stiffness matrix can be formulated from the first term of Equation 4.76. The incremental strain in $\Delta \bar{e}$ of Eq. 4.76 can be decomposed into two strains; the linear incremental strain and the initial incremental strain.

$$\Delta \bar{e} = \Delta \bar{e}^0 + \Delta \bar{e}^i \tag{5.34}$$

Where $\Delta \bar{e}^0$ is the linear incremental strain vector

$\Delta \bar{e}^i$ is the initial incremental strain associated with initial displacement

By using Eq. 5.34, Equation 4.76 is decomposed as

$$\int_{V_0} \delta(\Delta \bar{e}^0)^T [C] (\Delta \bar{e}^0) dV + \int_{V_0} \delta(\Delta \bar{e}^i)^T [C] (\Delta \bar{e}^i) dV + \int_{V_0} \bar{S}^T \delta(\Delta \bar{\eta}) dV = H^{\Delta} \quad 5.35$$

The first term and second term of the linearized variation of strain energy in Eq. 5.35 contain the incremental linear stiffness matrix, $[\Delta K]$, and the incremental geometric stiffness matrix, $[\Delta K_g]$. The third term contains the incremental stress stiffness matrix, $[\Delta K_s]$. Since there is only two non-zero incremental strain, longitudinal and shear strain, the first term of equation 5.35 can be written as the following equation;

$$\int_V \left[\delta \Delta \bar{e}^{0T} [C] \Delta \bar{e}^0 \right] dV = \int_V \left[E (\Delta e_z^0) \delta(\Delta e_z^0) \right] dV + \int_V \left[G (\Delta e_{sz}^0) \delta(\Delta e_{sz}^0) \right] dV \quad 5.36$$

By substituting the linear incremental strains, Eq. 4.81, into the first and second term of right hand side of Eq. 5.36, the linear incremental strain energy can be expressed in terms of the incremental displacement field:

$$\int_V \left[E (\Delta e_z^0) \delta(\Delta e_z^0) \right] dV = \int_V E a \left[\left(\left(\Delta \tilde{w}'_c - \frac{c \Delta \beta y_s}{R} \right) + x \left(c \left(-\Delta \tilde{u}''_s + \frac{y_s}{R} \Delta v''_s \right) \right) \right) \right. \\ \left. + y \left(-\Delta v''_s + \frac{\Delta \beta}{R} \right) + \omega \left(-\Delta \beta'' - \frac{\Delta v''_s}{R} \right) \right] \\ \left[\left(\left(\delta \Delta \tilde{w}'_c - \frac{\delta \Delta \beta y_s}{R} \right) + x \left(c \left(-\delta \Delta \tilde{u}''_s + \frac{y_s}{R} \delta \Delta v''_s \right) \right) \right) \right. \\ \left. + y \left(c \left(-\delta \Delta v''_s + \frac{\delta \Delta \beta}{R} \right) \right) + \omega \left(-\delta \Delta \beta'' - c \frac{\delta \Delta v''_s}{R} \right) \right] dV \quad 5.37a$$

$$\int_V \left[G (\Delta e_{sz}^0) \delta(\Delta e_{sz}^0) \right] dV = \int_V \left[G a \left(\Delta \beta' + c \frac{\Delta v'_s}{R} \right) \left(\delta \beta' + c \frac{\delta v'_s}{R} \right) \right] dV \quad 5.37b$$

By interpolating incremental displacement in equation 5.37 from the shape functions of Table 5.1, the incremental linear stiffness matrix can be obtained:

$$\int_V \left[E \Delta e_z^0 \delta \Delta e_z^0 \right] dV + \int_V \left[G \Delta e_{sz}^0 \delta \Delta e_{sz}^0 \right] dV = \Delta \bar{d}^T [\Delta K] \delta \Delta \bar{d} \quad 5.38a$$

$$\begin{aligned}
[\Delta K] = \int_V & \left[E a \left\{ \left(\left(\bar{N}'_2 - \frac{\bar{N}_1}{R} - \frac{c y_s \bar{N}_4}{R} \right) + x \left(c \left(-\bar{N}_1'' - \frac{\bar{N}_3'}{R} + \frac{y_s \bar{N}_3''}{R} \right) \right) \right) \right\}^T \right. \\
& \left. + y \left(c \left(-\bar{N}_3'' + \frac{\bar{N}_4}{R} \right) \right) + \omega \left(-\bar{N}_4'' - c \frac{\bar{N}_3''}{R} \right) \right. \\
& \left. \times \left\{ \left(\left(\bar{N}'_2 - \frac{\bar{N}_1}{R} - \frac{c y_s \bar{N}_4}{R} \right) + x \left(c \left(-\bar{N}_1'' - \frac{\bar{N}_3'}{R} + \frac{y_s \bar{N}_3''}{R} \right) \right) \right) \right\} \right. \\
& \left. + y \left(c \left(-\bar{N}_3'' + \frac{\bar{N}_4}{R} \right) \right) + \omega \left(-\bar{N}_4'' - c \frac{\bar{N}_3''}{R} \right) \right\} \right. \\
& \left. + G a (2n)^2 \left(\bar{N}_4' + c \frac{\bar{N}_3'}{R} \right)^T \times \left(\bar{N}_4' + c \frac{\bar{N}_3'}{R} \right) \right] dV \quad \mathbf{5.38b}
\end{aligned}$$

From orthogonal condition and the sectional properties defined in Eqs. 4.60 to 4.65, Eq. 5.38b is transformed to the following equation:

$$\begin{aligned}
[\Delta K] = \int_L & \left[E \left(\bar{N}'_2 - \frac{\bar{N}_1}{R} - \frac{y_s \bar{N}_4}{R} \right)^T \times \left\{ A^a \left(\bar{N}'_2 - \frac{\bar{N}_1}{R} - \frac{y_s \bar{N}_4}{R} \right) \right. \right. \\
& \left. + Q_y^a \left(c \left(-\bar{N}_1'' - \frac{\bar{N}_3'}{R} + \frac{y_s \bar{N}_3''}{R} \right) \right) + Q_x^a \left(c \left(-\bar{N}_3'' + \frac{\bar{N}_4}{R} \right) \right) + Q_\omega^a \left(-\bar{N}_4'' - c \frac{\bar{N}_3''}{R} \right) \right\} \\
& + E c \left(-\bar{N}_1'' - \frac{\bar{N}_3'}{R} + \frac{y_s \bar{N}_3''}{R} \right)^T \times \left\{ Q_y^a \left(\bar{N}'_2 - \frac{\bar{N}_1}{R} - \frac{y_s \bar{N}_4}{R} \right) \right. \\
& \left. + c I_y^a \left(-\bar{N}_1'' - \frac{\bar{N}_3'}{R} + \frac{y_s \bar{N}_3''}{R} \right) + c I_{xy}^a \left(-\bar{N}_3'' + \frac{\bar{N}_4}{R} \right) + I_{x\omega}^a \left(-\bar{N}_4'' - c \frac{\bar{N}_3''}{R} \right) \right\} \\
& + E c \left(-\bar{N}_3'' + \frac{\bar{N}_4}{R} \right)^T \times \left\{ Q_x^a \left(\bar{N}'_2 - \frac{\bar{N}_1}{R} - \frac{y_s \bar{N}_4}{R} \right) \right. \\
& \left. + c I_{xy}^a \left(-\bar{N}_1'' - \frac{\bar{N}_3'}{R} + \frac{y_s \bar{N}_3''}{R} \right) + c I_x^a \left(-\bar{N}_3'' + \frac{\bar{N}_4}{R} \right) + I_{y\omega}^a \left(-\bar{N}_4'' - c \frac{\bar{N}_3''}{R} \right) \right\} \\
& + E \left(-\bar{N}_4'' - c \frac{\bar{N}_3''}{R} \right)^T \times \left\{ Q_\omega^a \left(\bar{N}'_2 - \frac{\bar{N}_1}{R} - \frac{y_s \bar{N}_4}{R} \right) \right. \\
& \left. + c I_{x\omega}^a \left(-\bar{N}_1'' - \frac{\bar{N}_3'}{R} + \frac{y_s \bar{N}_3''}{R} \right) + c I_{y\omega}^a \left(-\bar{N}_3'' + \frac{\bar{N}_4}{R} \right) + I_\omega^a \left(-\bar{N}_4'' - c \frac{\bar{N}_3''}{R} \right) \right\}
\end{aligned}$$

$$+ GK_T^a \left(-\bar{N}'_4 + c \frac{\bar{N}'_3}{R} \right)^T \times \left(-\bar{N}'_4 + c \frac{\bar{N}'_3}{R} \right) dV \quad 5.39$$

The incremental geometric stiffness matrix $[\Delta K_g]$ can be derived from the second term of Equation 5.35. Several geometric stiffness matrixes are derived from the simplified longitudinal and shear strains in this study. For convenience, only the geometric stiffness matrix based on the complete incremental strain developed in Section 4.5.2, is expressed in Eq 5.41 and Eq. 5.42.

In $[\Delta K_g]$, two types of displacement are used, initial displacement and incremental displacement. Since at position $t+\Delta t$ of Figure 4.6, the initial displacement is known, the only unknown quantities are the components of the incremental displacement. Thus, the incremental geometric stiffness matrix can be obtained by interpolating the incremental displacement, resulting in the following equation.

$$\int_{V_0} \delta \Delta \bar{e}^i [C] (\Delta \bar{e}^i)^T dV = \Delta \bar{d}^T [\Delta K_g] \delta \Delta \bar{d} \quad 5.40$$

$$[\Delta K_g] =$$

$$\int_V \left[\begin{array}{l} E a \left({}^a \bar{D}_0 + {}^a \bar{D}_x x + {}^a \bar{D}_y y + {}^a \bar{D}_\omega \omega \right)^T \\ \times a \left(\begin{array}{l} \left({}^a \bar{D}_0^g + a {}^q \bar{D}_0^g + \left({}^a \bar{D}_x^g + a {}^q \bar{D}_x^g \right) x + \left({}^a \bar{D}_y^g + a {}^q \bar{D}_y^g \right) y + \left({}^a \bar{D}_\omega^g + a {}^q \bar{D}_\omega^g \right) \omega \right) \\ + a {}^q \bar{D}_{xx}^g x^2 + a {}^q \bar{D}_{yy}^g y^2 + a {}^q \bar{D}_{xy}^g xy + a {}^q \bar{D}_{x\omega}^g x\omega + a {}^q \bar{D}_{y\omega}^g y\omega \end{array} \right) \\ + G(2n)^2 \left(a {}^a \bar{D}_n \right)^T \times \left(a {}^a \bar{D}_n^g \right) \end{array} \right] dV$$

$$+ \int_V \left[\begin{array}{l} E a \left(\begin{array}{l} \left({}^a \bar{D}_0^g + a {}^q \bar{D}_0^g + \left({}^a \bar{D}_x^g + a {}^q \bar{D}_x^g \right) x + \left({}^a \bar{D}_y^g + a {}^q \bar{D}_y^g \right) y + \left({}^a \bar{D}_\omega^g + a {}^q \bar{D}_\omega^g \right) \omega \right)^T \\ + a {}^q \bar{D}_{xx}^g x^2 + a {}^q \bar{D}_{yy}^g y^2 + a {}^q \bar{D}_{xy}^g xy + a {}^q \bar{D}_{x\omega}^g x\omega + a {}^q \bar{D}_{y\omega}^g y\omega \end{array} \right) \\ \times a \left({}^a \bar{D}_0 + {}^a \bar{D}_x x + {}^a \bar{D}_y y + {}^a \bar{D}_\omega \omega \right) + G(2n)^2 \left(a {}^a \bar{D}_n^g \right)^T \times \left(a {}^a \bar{D}_n^g \right) \end{array} \right] dV$$

$$\begin{aligned}
& \left[\begin{aligned}
& E a \left(\begin{aligned}
& \left({}^a \bar{D}_0^g + a {}^q \bar{D}_0^g + \left({}^a \bar{D}_x^g + a {}^q \bar{D}_x^g \right) x + \left({}^a \bar{D}_y^g + a {}^q \bar{D}_y^g \right) y + \left({}^a \bar{D}_\omega^g + a {}^q \bar{D}_\omega^g \right) \omega \right)^T \\
& + a {}^q \bar{D}_{xx}^g x^2 + a {}^q \bar{D}_{yy}^g y^2 + a {}^q \bar{D}_{xy}^g xy + a {}^q \bar{D}_{x\omega}^g x\omega + a {}^q \bar{D}_{y\omega}^g y\omega
\end{aligned} \right) \\
& + \int_V \left(\begin{aligned}
& \left({}^a \bar{D}_0^g + a {}^q \bar{D}_0^g + \left({}^a \bar{D}_x^g + a {}^q \bar{D}_x^g \right) x + \left({}^a \bar{D}_y^g + a {}^q \bar{D}_y^g \right) y + \left({}^a \bar{D}_\omega^g + a {}^q \bar{D}_\omega^g \right) \omega \right) \\
& \times a \left(\begin{aligned}
& + a {}^q \bar{D}_{xx}^g x^2 + a {}^q \bar{D}_{yy}^g y^2 + a {}^q \bar{D}_{xy}^g xy + a {}^q \bar{D}_{x\omega}^g x\omega + a {}^q \bar{D}_{y\omega}^g y\omega
\end{aligned} \right)
\end{aligned} \right) dV \\
& + G(2n)^2 \left(a {}^a \bar{D}_n^g \right)^T \times \left(a {}^a \bar{D}_n^g \right)
\end{aligned} \right] \tag{5.41}
\end{aligned}$$

The strain vector terms \bar{D} in equation 5.41 are listed in Table 5.2. The superscript “g” of the symbols \bar{D}^g indicates that the strain vectors are associated with geometric stiffness matrix and are expressed with coupling between incremental and initial displacement. The superscript “a” and “q” in the symbol \bar{D}^g denote that strain terms are multiplied by the term $R/(R-x)$ and $R^2/(R-x)^2$.

In the total Lagrange formulation, the undeformed configuration is used as the reference for the subsequent positions. Thus, the initial displacement at each incremental position has to be updated by adding the incremental displacement from the last position to the initial displacement of that position. The nonlinear response in the load and deformation relationship is caused by the coupling between incremental and initial displacements as seen in Equation 5.41. This updating of the initial displacement and the coupling of terms make the geometric stiffness matrix very complicated. This is one of the disadvantages of the total Lagrange formulation.

The triple integration function of Equation 5.41 can be simplified to single integration by using orthogonal condition, the sectional properties and Eq 4.5. Because the complete expansion is quite lengthy, only the terms associated with A, Q_x , Q_y , Q_ω , I_x , I_y , I_ω and K_T are shown below in Eq. 5.42. The omitted terms are listed in Table 5.3. The complete geometric stiffness can be obtained by multiplying the sectional properties in the second column of Table 5.3 to the strain terms in the third column and adding to Eq 5.42.

$$\begin{aligned}
& [\Delta K_g] = \\
& E \int_L \left[A^a \left(\left({}^a \bar{D}_0^g \right)^T \times a \bar{D}_0^g \right) + A^q \left(\left({}^a \bar{D}_0^g \right)^T \times {}^q \bar{D}_0^g + \left({}^q \bar{D}_0^g \right)^T \times a \bar{D}_0^g \right) + A^r \left(\left({}^q \bar{D}_0^g \right)^T \times {}^q \bar{D}_0^g \right) \right] dz \\
& + E \int_L \left[Q_x^a \left(\left({}^a \bar{D}_0^g \right)^T \times a \bar{D}_x^g + \left({}^a \bar{D}_x^g \right)^T \times a \bar{D}_0^g \right) + Q_x^r \left(\left({}^q \bar{D}_0^g \right)^T \times {}^q \bar{D}_x^g + \left({}^q \bar{D}_x^g \right)^T \times {}^q \bar{D}_0^g \right) \right]
\end{aligned}$$

$$\begin{aligned}
& + Q_x^q \left(\left({}^a \bar{D}_0^g \right)^T \times^q \bar{D}_x^g + \left({}^q \bar{D}_0^g \right)^T \times^a \bar{D}_x^g \right) + \left(\left({}^a \bar{D}_{xi}^g \right)^T \times^q \bar{D}_0^g + \left({}^q \bar{D}_x^g \right)^T \times^a \bar{D}_0^g \right) \\
& + Q_y^q \left(\left({}^a \bar{D}_0^g \right)^T \times^q \bar{D}_y^g + \left({}^q \bar{D}_0^g \right)^T \times^a \bar{D}_y^g \right) + Q_y^r \left(\left({}^q \bar{D}_0^g \right)^T \times^q \bar{D}_y^g + \left({}^q \bar{D}_y^g \right)^T \times^q \bar{D}_0^g \right) \\
& + Q_y^q \left(\left({}^a \bar{D}_0^g \right)^T \times^q \bar{D}_y^g + \left({}^q \bar{D}_0^g \right)^T \times^a \bar{D}_y^g \right) + \left(\left({}^a \bar{D}_y^g \right)^T \times^q \bar{D}_0^g + \left({}^q \bar{D}_y^g \right)^T \times^a \bar{D}_0^g \right) \\
& + Q_\omega^q \left(\left({}^a \bar{D}_0^g \right)^T \times^q \bar{D}_\omega^g + \left({}^q \bar{D}_0^g \right)^T \times^a \bar{D}_\omega^g \right) + Q_\omega^r \left(\left({}^q \bar{D}_0^g \right)^T \times^q \bar{D}_\omega^g + \left({}^q \bar{D}_\omega^g \right)^T \times^q \bar{D}_0^g \right) \\
& + Q_\omega^q \left(\left({}^a \bar{D}_0^g \right)^T \times^q \bar{D}_\omega^g + \left({}^q \bar{D}_0^g \right)^T \times^a \bar{D}_\omega^g + \left({}^a \bar{D}_\omega^g \right)^T \times^q \bar{D}_0^g + \left({}^q \bar{D}_\omega^g \right)^T \times^a \bar{D}_0^g \right) dz \\
& + E \int_L \left[I_y^a \left(\left({}^a \bar{D}_x^g \right)^T \times^a \bar{D}_x^g \right) \right. \\
& + I_y^q \left(\left({}^a \bar{D}_x^g \right)^T \times^q \bar{D}_x^g + \left({}^q \bar{D}_x^g \right)^T \times^a \bar{D}_x^g + \left({}^a \bar{D}_0^g \right)^T \times^q \bar{D}_{xx}^g + \left({}^q \bar{D}_{xx}^g \right)^T \times^a \bar{D}_0^g \right) \\
& + I_y^r \left(\left({}^q \bar{D}_x^g \right)^T \times^q \bar{D}_x^g + \left({}^q \bar{D}_0^g \right)^T \times^q \bar{D}_{xx}^g + \left({}^q \bar{D}_{xx}^g \right)^T \times^q \bar{D}_0^g \right) + I_x^a \left(\left({}^a \bar{D}_y^g \right)^T \times^a \bar{D}_y^g \right) \\
& + I_x^q \left(\left({}^a \bar{D}_y^g \right)^T \times^q \bar{D}_y^g + \left({}^q \bar{D}_y^g \right)^T \times^a \bar{D}_y^g + \left(\bar{D}_0^g \right)^T \times^q \bar{D}_{yy}^g + \left({}^q \bar{D}_{yy}^g \right)^T \times^a \bar{D}_0^g \right) \\
& + I_x^r \left(\left({}^q \bar{D}_y^g \right)^T \times^q \bar{D}_y^g + \left({}^q \bar{D}_0^g \right)^T \times^q \bar{D}_{yy}^g + \left({}^q \bar{D}_{yy}^g \right)^T \times^q \bar{D}_0^g \right) \\
& + I_\omega^a \left(\left({}^a \bar{D}_\omega^g \right)^T \times^a \bar{D}_\omega^g \right) + I_\omega^q \left(\left({}^a \bar{D}_\omega^g \right)^T \times^q \bar{D}_\omega^g + \left({}^q \bar{D}_\omega^g \right)^T \times^a \bar{D}_\omega^g \right) + I_\omega^r \left(\left({}^q \bar{D}_\omega^g \right)^T \times^q \bar{D}_\omega^g \right) dz \\
& \left. + G \int_L \left[K_T^a \left(\left({}^a \bar{D}_n^g \right)^T \times^a \bar{D}_n^g \right) \right] dz \tag{5.42}
\end{aligned}$$

The incremental stress stiffness matrix $[\Delta K_s]$ can be derived from the third term of the variation of strain energy, Eq 5.35. Similar to the case of incremental geometric stiffness matrix, several stress stiffness matrices are derived from the simplified longitudinal and shear strains. Only the stiffness matrix based on the complete incremental strain developed in Section 4.5.2, is expressed in Eq 5.43 and 5.44.

$$\int_{V_0} \bar{S}^T \delta(\Delta \bar{\eta}) dV = \Delta \bar{d}^T [\Delta K_s] \delta \Delta \bar{d} \tag{5.43}$$

$$\begin{aligned}
[\Delta K_s] = \int_L & \left[\left({}^a F_z - \frac{{}^a M_y}{R} \right) \left[{}^q D_0^s \right] - M_y \left[{}^a D_x^s \right] - \left({}^a M_y - \frac{{}^a K_x}{R} \right) \left[{}^q D_x^s \right] + M_x \left[{}^a D_y^s \right] \right. \\
& + \left({}^a M_x + \frac{{}^a K_{xy}}{R} \right) \left[{}^q D_y^s \right] + M_\omega \left[{}^a D_\omega^s \right] + \left({}^a M_\omega + \frac{{}^a K_{x\omega}}{R} \right) \left[{}^q D_\omega^s \right] + {}^a K_x \left[{}^q D_{xx}^s \right] \\
& \left. + {}^a K_y \left[{}^q D_{yy}^s \right] + {}^a K_{xy} \left[{}^q D_{xy}^s \right] + {}^a K_{x\omega} \left[{}^q D_{x\omega}^s \right] + {}^a K_{x\omega} \left[{}^q D_{y\omega}^s \right] + M_{sv} \left[{}^a D_n^s \right] \right] dz \tag{5.44}
\end{aligned}$$

The matrix terms of incremental strains in Eq. 5.44, $[D_0^s]$ to $[D_n^s]$, are interpolated by the shape function in Table 5.1 and listed in Table 5.4. The superscripts ‘‘a’’ and ‘‘q’’ in

$[D^s]$ indicates that strain matrix terms are to be multiplied by $R/(R-x)$ and $R^2/(R-x)^2$, respectively

The incremental displacement and stress resultant are coupled in the stress stiffness matrix $[\Delta K_s]$, from which the nonlinear effect of initial stress resultants can be considered. In the total Lagrange formulation, stress resultants have to be updated at the end of each position and can be calculated by using Eq. 4.59.

The stiffness matrix, $[\Delta K]$, $[\Delta K_g]$ and $[\Delta K_s]$ in Eqs. 5.39, 5.42 and 5.44, are derived based on shape functions, $\bar{N}_1 \dots \bar{N}_4$ which do not consider sectional deformation and are listed in Table 5.1. When sectional deformation is considered, the stiffness matrix, $[\Delta K]$, $[\Delta K_g]$ and $[\Delta K_s]$ are changed to $[\Delta^s K]$, $[\Delta^s K_g]$ and $[\Delta^s K_s]$ which is linear, geometric and stress incremental stiffness matrix associated with sectional deformation. The superscript “s” denotes sectional deformation.

The linear incremental stiffness, $[\Delta K]$ Eq. 5.39, can be changed to $[\Delta^s K]$ by replacing $\bar{N}_1 \dots \bar{N}_4$ to ${}^s\bar{N}_1 \dots {}^s\bar{N}_4$ (Eq. 5.13) and modifying the last term of Eq. 5.38b, which is associated with shear strain and altered to the following equation.

$$\begin{aligned} & \int_{V_f} \left[G a (2n)^2 \left({}^s\bar{N}'_4 - {}^s\bar{N}'_5 + \frac{{}^s\bar{N}'_3}{R} \hat{c} \right)^T \times \left({}^s\bar{N}'_4 - {}^s\bar{N}'_5 + \frac{{}^s\bar{N}'_3}{R} \hat{c} \right) \right] dV \\ & + \int_{V_w} \left[G a (2n)^2 \left({}^s\bar{N}'_4 + \hat{c} \frac{{}^s\bar{N}'_3}{R} \right)^T \times \left({}^s\bar{N}'_4 + \hat{c} \frac{{}^s\bar{N}'_3}{R} \right) \right] dV \end{aligned} \quad 5.45$$

By using the sectional properties, Eq. 5.45 can be expressed as:

$$G \int_L \left[{}^a K_{T_f} \left(\bar{D}_{n_f} \right)^T \times \bar{D}_{n_f} \right] dz + G \int_L \left[{}^a K_{T_w} \left(\bar{D}_{n_w} \right)^T \times \bar{D}_{n_w} \right] dz \quad 5.46a$$

$$\bar{D}_{n_f} = {}^s\bar{N}'_4 - {}^s\bar{N}'_5 + \frac{{}^s\bar{N}'_3}{R} \hat{c} \quad 5.46b$$

$$\bar{D}_{n_w} = {}^s\bar{N}'_4 + \hat{c} \frac{{}^s\bar{N}'_3}{R} \quad 5.46c$$

Where K_{Tf} and K_{Tw} are Saint-Venant constant of flange and web respectively.

$${}^a K_{T_f} = \int_{A_f} (2n)^2 \left(\frac{R}{R-x} \right) dA \quad 5.47$$

$${}^a K_{T_w} = \int_{A_w} (2n)^2 \left(\frac{R}{R-x} \right) dA \quad 5.48$$

The geometric incremental stiffness, $[\Delta K_g]$ Eq. 5.42, can also be changed to $[\Delta^s K_g]$ by replacing $\bar{N}_1.. \bar{N}_4$ to ${}^s\bar{N}_1.. {}^s\bar{N}_4$ and modifying the last term of Eq. 5.42, which is associated with shear strain and altered to the following equation.

$$G \int_L \left[{}^a K_{T_f} \left({}^a \bar{D}_{n_f}^g \times {}^a \bar{D}_{n_f}^g \right) \right] dz + G \int_L \left[{}^a K_{T_w} \left({}^a \bar{D}_{n_w}^g \times {}^a \bar{D}_{n_w}^g \right) \right] dz \quad 5.49a$$

where:

$${}^a \bar{D}_{n_f}^g = \left(-\hat{s} \frac{v'}{R} ({}^s \bar{N}_4 - {}^s \bar{N}_5) - \hat{c} \frac{\tilde{u}'}{R} ({}^s \bar{N}_4 - {}^s \bar{N}_5) - \hat{s} \frac{{}^s \bar{N}_1'}{R} \right) \quad 5.49b$$

$${}^a \bar{D}_{n_w}^g = \left(-s \frac{v'}{R} ({}^s \bar{N}_4) - c \frac{\tilde{u}'}{R} ({}^s \bar{N}_4) - s \frac{{}^s \bar{N}_1'}{R} \right) \quad 5.49c$$

Similarly, the incremental stress stiffness, $[\Delta K_s]$ Eq. 5.44, is changed to $[\Delta^s K_s]$ by replacing $\bar{N}_1.. \bar{N}_4$ used in Table 5.4 to ${}^s\bar{N}_1.. {}^s\bar{N}_4$ and modifying the last term of Eq. 5.44 and is shown as below.

$$\int_L \left[M_{sv_f} \left[{}^a D_{n_f}^s \right] \right] dz + \int_L \left[M_{sv_w} \left[{}^a D_{n_w}^s \right] \right] dz \quad 5.50$$

Where:

$$\left[{}^a D_{n_f}^s \right] = \left(\begin{array}{l} \left(-\hat{s} ({}^s \bar{N}_4 - {}^s \bar{N}_5) \times \frac{({}^s \bar{N}_3')^T}{R} - \hat{c} ({}^s \bar{N}_4 - {}^s \bar{N}_5) \times \frac{({}^s \bar{N}_1')^T}{R} \right) \\ + \left(-\hat{s} ({}^s \bar{N}_4 - {}^s \bar{N}_5)^T \times \frac{{}^s \bar{N}_3'}{R} - \hat{c} ({}^s \bar{N}_4 - {}^s \bar{N}_5)^T \times \frac{{}^s \bar{N}_1'}{R} \right) \end{array} \right) \quad 5.51a$$

$$\left[{}^a D_{n_w}^s \right] = \left(-s \frac{{}^s \bar{N}_4^T \times {}^s \bar{N}_3'}{R} - c \frac{{}^s \bar{N}_4^T \times {}^s \bar{N}_1'}{R} - s \frac{{}^s \bar{N}_3'^T \times {}^s \bar{N}_4}{R} - c \frac{{}^s \bar{N}_1'^T \times {}^s \bar{N}_4}{R} \right) \quad 5.51b$$

$$M_{sv_f} = \int_{A_f} \left[\sigma_{sz_f} 2n \right] dA = G K_{T_f} \left(\beta' - \alpha_0 + \frac{v'}{R} \hat{c} - \frac{\tilde{u}'}{R} \hat{s} \right) \quad 5.51c$$

$$M_{sv_w} = \int_{A_w} \left[\sigma_{sz_w} 2n \right] dA = G K_{T_w} \left(\beta_0' + \frac{v'}{R} c - \frac{\tilde{u}'}{R} s \right) \quad 5.51d$$

Additional incremental stiffness matrixes associated with the web deformation are needed. With the web-deformation strain and the incremental shear strain expressed in Eq. 4.102 and 4.103, the additional linear stiffness matrix associated with web

deformation can be derived. The following equation shows the additional stiffness matrix:

$$\int_V \sigma_w \delta \varepsilon_w dV = \int_V E \Delta e_\alpha^0 \delta \Delta e_\alpha^0 dV = \Delta \bar{d}^T [\Delta K]_{sw} \delta \Delta \bar{d} \quad 5.52a$$

$$[\Delta K]_{sw} = E I_{sw} \int_L [{}^s \bar{N}'_5]^T \times [{}^s \bar{N}'_5] dz \quad 5.52b$$

Where:

$$I_{sw} = \int_A \left[\left(12 \frac{y}{d^2} x \right)^2 \right] dA \quad 5.52c$$

$[\Delta K]_{sw}$ is the additional linear stiffness matrix

Δe_α^0 is the component of linear incremental strain of the web, Eq. 4.102

It is noted that the shape function with superscript “s” and subscript “5” in Eq. 5.45 to Eq. 5.52 indicates sectional deformation and shape function of sectional deformation.

So far, incremental stiffness matrixes for seven and eight DOF are developed. The total incremental stiffness matrix is the sum of linear, geometric and stress incremental stiffness matrixes and can be expressed as the following.

- For a seven DOF element

$$[\Delta K_{Total}] = [\Delta K] + [\Delta K_g] + [\Delta K_s]$$

Where

$[\Delta K_{Total}]$ is the total incremental stiffness matrix

$[\Delta K]$ is the incremental linear stiffness matrix, Eq. 5.39

$[\Delta K_g]$ is the incremental geometric stiffness matrix, Eq. 5.42

$[\Delta K_s]$ is the incremental stress stiffness matrix, Eq. 5.44

- For a eight DOF element

$$[\Delta^s K_{Total}] = [\Delta^s K] + [\Delta^s K_g] + [\Delta^s K_s] + [\Delta K]_{sw}$$

Where

$[\Delta^s K_{Total}]$ is the total incremental stiffness matrix for eight DOF element

$[\Delta^s K]$ is the incremental linear stiffness matrix for eight DOF element

$[\Delta^s K_g]$ is the incremental geometric stiffness matrix for eight DOF element

$[\Delta^s K_s]$ is the incremental stress stiffness matrix for eight DOF element

$[\Delta K]_{sw}$ is the additional incremental stiffness matrix, Eq. 5.52b

5.3.2 Unbalanced Matrix

Because of the approximation used in linearization, the solution may have an error. The magnitude of error can be checked by evaluating the unbalanced forces based on Equation 4.81. The unbalanced forces can be adjusted to within tolerance by updating the incremental displacement through iteration. The detailed procedure of iteration is presented in Section 5.4.

In Section 4.5.1, the error in virtual work by external load was expressed by Eq. 4.77. The first term of the equation is a known value. In the second term, the variation of total strain at position $t+\Delta t$, $\delta \bar{\epsilon}^{(t+\Delta t)k}$, is equivalent to $\delta \bar{\epsilon}^{(\Delta t)k}$ because at position t equilibrium is already satisfied and there is no variation of strain. Therefore the equation can be expressed as the following.

$$error = \bar{H}^{(t+\Delta t)k} - \int_{V_0} (\delta \bar{\epsilon}^k)^T \bar{S}^{(t+\Delta t)k} dV \quad 5.53$$

where k is iteration number

By using the incremental strain, the second term of equation 5.53 can be written as:

$$\int_{V_0} (\delta \bar{\epsilon}^k)^T \bar{S}^{(t+\Delta t)k} dV = \int_{V_0} \left((\delta \bar{\epsilon}^0)^k + (\delta \bar{\epsilon}^i)^k \right)^T \bar{S}^{(t+\Delta t)k} dV \quad 5.54$$

By using the shape functions of Table 5.1, Eq. 5.54 can be interpolated as:

$$\int_{V_0} \left((\delta \bar{\epsilon}^0)^k + (\delta \bar{\epsilon}^i)^k \right)^T \bar{S}^{(t+\Delta t)k} dV = \bar{g} \delta \Delta d \quad 5.55$$

$$\begin{aligned} \bar{g} = \int_L & \left[F_z \left({}^a \bar{D}_0 + {}^a \bar{D}_0^g \right) - M_y \left({}^a \bar{D}_x + {}^a \bar{D}_x^g \right) + M_x \left({}^a \bar{D}_y + {}^a \bar{D}_y^g \right) + M_\omega \left({}^a \bar{D}_\omega + {}^a \bar{D}_\omega^g \right) \right. \\ & + \left({}^a F_z - \frac{{}^a M_y}{R} \right) {}^q \bar{D}_0^g - \left({}^a M_y - \frac{{}^a K_x}{R} \right) {}^q \bar{D}_x^g \\ & + \left({}^a M_x + \frac{{}^a K_{xy}}{R} \right) {}^q \bar{D}_y^g + \left({}^a M_\omega + \frac{{}^a K_{x\omega}}{R} \right) {}^q \bar{D}_\omega^g \\ & \left. + {}^a K_x {}^q \bar{D}_{xx}^g + {}^a K_y {}^q \bar{D}_{yy}^g + {}^a K_{xy} {}^q \bar{D}_{xy}^g + {}^a K_{x\omega} {}^q \bar{D}_{x\omega}^g + {}^a K_{\omega y} {}^q \bar{D}_{y\omega}^g + M_{sv} {}^a \bar{D}_n^g \right] dz \quad 5.56 \end{aligned}$$

Where:

$${}^a \bar{D}_0 = \left(\tilde{N}'_2 - \frac{c y_s}{R} N_4 \right) \quad 5.57a$$

$${}^a \bar{D}_x = \left(c \left(-\tilde{N}''_1 + \frac{y_s}{R} N_3 \right) + \frac{(c-1)}{R^2} N_1 \right) \quad 5.57b$$

$${}^a\bar{D}_y = \left(-c N_3'' + c \frac{N_4}{R} \right) \quad 5.57c$$

$${}^a\bar{D}_\omega = \left(-N_4'' - c \frac{N_3''}{R} \right) \quad 5.57d$$

$${}^a\bar{D}_{sz} = \left(N_4' + c \frac{N_3'}{R} \right) \quad 5.57e$$

When sectional deformation is considered, shape functions, $\bar{N}_1 \dots \bar{N}_4$ in Eq. 5.57 have to be replaced by ${}^s\bar{N}_1 \dots {}^s\bar{N}_4$ and the last term of equation 5.56 need to be modified as the following;

$$\int_L \left[M_{sv_f} {}^a\bar{D}_{n_f}^g \right] dz + \int_L \left[M_{sv_w} {}^a\bar{D}_{n_w}^g \right] dz \quad 5.57$$

An additional term associated with the sectional deformation moment has to be included in Eq. 5.56.

$$\int_L \left[M_\alpha \alpha \right] dz \quad 5.58$$

The stress resultant M_α is defined in Eq. 4.96c.

5.4 Numerical Solution Technique for Incremental Analysis

Several numerical solution schemes for solving nonlinear problems have been developed. The characteristics of numerical solution is represented in terms of stability, accuracy and efficient for convergence. Originally, incremental analysis starts with the “pure” incremental method. The loading is divided into small steps. Within each step, structural behavior is considered linear. In this method, no iteration for reducing the unbalance forces from linearization is performed. The accuracy of the pure incremental method depends on the size of steps. In Newton-Raphson method, constant load steps are used with iteration for reducing the unbalance forces and error. The limitation of this method is that when the structural member becomes “unstable”, i.e. singularity in stiffness matrix when the load-deflection curve reaches the maximum point and starts to unload, convergence problem occurs. As long as the structural member has a positive stiffness matrix, this method is relatively simple and efficient. In this study, this method is adopted as a checking tool.

In order to circumvent the singularity problem, the displacement control method and the arc-length method have been developed. In the displacement control method, constant displacement steps instead of constant loading steps are used. When the structural response changes sharply, e.g. a snap-through behavior of an arch type structure, the displacement control method may have difficulty in convergence. A snap-through behavior can be handled by considering the variation of nonlinearity in each incremental step. The arc-length method adopts variable loading and displacement steps based on the response of the previous incremental step. And orthogonal condition is applied for the convergence. The arc-length method is chosen for the current study.

The nonlinear equation for incremental analysis of a structure can be expressed as the following:

$$\left[K^{(t+\Delta t)k} \right] \Delta \bar{u}^{(t+\Delta t)k} = \bar{H}^{(t+\Delta t)k} - \bar{F}^{(t+\Delta t)k-1} \quad 5.59$$

Where $\Delta \bar{u}^{(t+\Delta t)k}$ is the incremental displacement of the k^{th} iteration in incremental position $t+\Delta t$, $\bar{F}^{(t+\Delta t)k-1}$ is the internal stress resultant forces of the k^{th} iteration in incremental position $t+\Delta t$, and $\bar{H}^{(t+\Delta t)k}$ is the external nodal load applied on the structure.

The initial conditions of equation 5.59 are

$$\left[K^{(t+\Delta t)0} \right] = \left[K^{(t)} \right] \quad 5.60a$$

$$\Delta \bar{u}^{(t+\Delta t)0} = \Delta \bar{u}^{(t)} \quad 5.60b$$

$$\bar{F}^{(t+\Delta t)0} = \bar{F}^{(t)} \quad 5.60c$$

The external load $\bar{H}^{(t+\Delta t)k}$ is composed of two components;

$$\bar{H}^{(t+\Delta t)k} = \bar{H}^{(t+\Delta t)k-1} + \Delta \lambda^{(t+\Delta t)k} \bar{\bar{H}} \quad 5.61$$

Where $\Delta \lambda^{(t+\Delta t)k}$ is the load increment factor for the k^{th} iteration in incremental position $t+\Delta t$ and $\bar{\bar{H}}$ is the reference external load that should be decided in the beginning of the incremental step. After the k^{th} iteration, the total displacement can be calculated by

$$\bar{u}^{(t+\Delta t)k} = \bar{u}^{(t+\Delta t)k-1} + \Delta \bar{u}^{(t+\Delta t)k} \quad 5.62$$

Another expression for the incremental displacement $\Delta \bar{u}^{(t+\Delta t)k}$ is the summation of the reference displacement and the unbalance displacement;

$$\left[K^{(t+\Delta t)k-1} \right] \Delta \bar{\bar{u}}^k = \bar{\bar{H}} \quad 5.63$$

$$\left[K^{(t+\Delta t)k-1} \right] \Delta \bar{\bar{\bar{u}}}^k = \bar{H}^{(t+\Delta t)k-1} - \bar{F}^{(t+\Delta t)k-1} = \bar{\bar{\bar{F}}}^{(t+\Delta t)k-1} \quad 5.64$$

Where $\Delta \bar{\bar{u}}^k$ is the reference displacement, $\Delta \bar{\bar{\bar{u}}}^k$ is the unbalance displacement and $\bar{\bar{\bar{F}}}^{(t+\Delta t)k-1}$ is the unbalance force at the $(k-1)^{\text{th}}$ iteration in incremental position $t+\Delta t$. With the reference and unbalance displacement, the incremental displacement can be expressed by the following equation;

$$\Delta \bar{u}^{(t+\Delta t)k} = \Delta \lambda^{(t+\Delta t)k} \Delta \bar{\bar{u}}^k + \Delta \bar{\bar{\bar{u}}}^k \quad 5.65$$

A numerical solution technique is characterized by the procedure of calculating the incremental load factors. In the following, the procedures of calculating the load factors by Newton-Raphson method and by the arc-length method are shown.

- **Newton-Raphson Method**

In the Newton-Raphson method, the incremental load factor is set for a constant value. Equation 5.65 in Newton-Raphson method can be written as the following equation;

$$\Delta \bar{u}^{(t+\Delta t)k} = \Delta \lambda^{(t+\Delta t)k} \Delta \bar{\bar{u}}^k + \Delta \bar{\bar{\bar{u}}}^k \quad 5.66$$

Figure 5-3 illustrates the process of solution by Newton-Raphson method.

- **Arc-Length Method**

The arc length method considers the constraint condition for determining the first load increments in each step and makes the solution converge to equilibrium by using the orthogonal condition. This is illustrated in figure 5-4. The following constraint condition is used for determining the load incremental factor and for performing iterations;

$$\left(\Delta\bar{u}^{(t+\Delta t)1}\right)^T \Delta\bar{u}^{(t+\Delta t)k} + \Delta\lambda^{(t+\Delta t)1} \Delta\lambda^{(t+\Delta t)k} = \Delta s^2 \quad 5.67$$

Where $\Delta\bar{u}^{(t+\Delta t)1}$ and $\Delta\bar{u}^{(t+\Delta t)k}$ are the incremental displacement at the first and the k^{th} iteration at incremental position $t+\Delta t$, and Δs is the prescribed arc length. In the beginning of each step, the arc length can be calculated from the following equation;

$$\Delta s^{(t+\Delta t)1} = \Delta s^{(1)1} \sqrt{\frac{I^L}{I^{(t)}}} \quad 5.68$$

Where I^L and $I^{(t)}$ is the limitation of number of iteration and the number of iteration on the preceding incremental step, and $\Delta s^{(1)1}$ is the prescribed arc length at the first incremental step. $\Delta s^{(1)1}$ can be calculated from Equation 5.69 with the unit incremental load factor.

$$\Delta s^{(1)1} = \sqrt{\left(\Delta\bar{u}^{(1)1}\right)^T \Delta\bar{u}^{(1)1} + 1} \quad 5.69$$

At the first step of position $t+\Delta t$, i.e., $k=1$, the incremental displacement, $\Delta\bar{u}^{(t+\Delta t)1}$ can be calculated from Equation 5.66 with no unbalanced forces ($\Delta\bar{u}^{\bar{\bar{1}}} = 0$);

$$\Delta\bar{u}^{(t+\Delta t)1} = \Delta\lambda^{(t+\Delta t)1} \Delta\bar{u}^{\bar{\bar{(t+\Delta t)1}}} \quad 5.70$$

By substituting Equation 5.70 into Equation 5.67, the load parameter $\Delta\lambda^{(t+\Delta t)1}$ can be calculated;

$$\Delta\lambda^{(t+\Delta t)1} = \frac{\Delta s^{(t+\Delta t)1}}{\sqrt{\left(\Delta\bar{u}^{\bar{\bar{(t+\Delta t)1}}}\right)^T \Delta\bar{u}^{\bar{\bar{(t+\Delta t)1}}} + 1}} \quad 5.71$$

After the first iteration, the iteration path follows the normal vector, N_r , as shown in Figure 5.4. This task can be done by letting $\Delta s^{(1)k} = 0$ for $k > 1$.

By substituting Equation 5.65 into Equation 5.67 and using $\Delta s^{(1)k} = 0$, the load factor can be calculated;

$$\Delta\lambda^{(t+\Delta t)k} = \frac{\left(\Delta\bar{u}^{(t+\Delta t)1}\right)^T \Delta\bar{u}^{\bar{\bar{(t+\Delta t)1}}}}{\left(\Delta\bar{u}^{(t+\Delta t)1}\right)^T \Delta\bar{u}^{\bar{\bar{(t+\Delta t)1}}} + \lambda^{(t+\Delta t)1}} \quad 5.72$$

With the load factor, the incremental displacement for the k^{th} iteration in position $t+\Delta t$ can be calculated from Equation 5.65.

With the establishment of the displacement field, nodal forces and stiffness matrixes, a finite line element for curved beam is developed. Different from conventional beam element, the curved beam line element incorporates large rotation, large displacement, cross sectional deformation and P- Δ effect. Different levels of simplification of strain can be incorporated into the line element. The evaluation of the line element will be conducted next.

Table 5.1 Nodal Displacement and Shape Function Vector for Seven DOF

\bar{u}	$\{u_s \ w_c \ \theta_y \ v_s \ \theta_x \ \beta \ \theta_\omega\}^T$
\bar{d}	$\begin{Bmatrix} \bar{u}_0 \\ \bar{u}_L \end{Bmatrix} = \begin{Bmatrix} [B] \bar{u}_0^d \\ [B] \bar{u}_L^d \end{Bmatrix}$
\bar{u}_0^d	$\{u_{s0} \ v_{s0} \ w_{c0} \ u'_{s0} \ v'_{s0} \ \beta_0 \ \beta'_0\}^T$
\bar{u}_L^d	$\{u_{sL} \ v_{sL} \ w_{cL} \ u'_{sL} \ v'_{sL} \ \beta_L \ \beta'_L\}^T$
$[B]$	$\begin{bmatrix} 1 & 0 & 0 & 0 & 0 & 0 & 0 \\ 0 & 1 & 0 & 0 & 0 & 0 & 0 \\ 0 & 0 & \frac{1}{R} & 1 & 0 & 0 & 0 \\ 0 & 1 & 0 & 0 & 0 & 0 & 0 \\ 0 & 0 & 0 & 0 & -1 & 0 & 0 \\ 0 & 0 & 0 & 0 & 0 & 1 & 0 \\ 0 & 0 & 0 & 0 & -\frac{1}{R} & 0 & -1 \end{bmatrix}$
$[\Phi]$	$\begin{aligned} & [\bar{\Phi}_1 \ \bar{\Phi}_2 \ \bar{\Phi}_3 \ \bar{\Phi}_4] = \\ & \begin{bmatrix} \varphi & 1 & -1 & 0 & c_z & \frac{-y_s}{R} \varphi & \frac{y_s}{R} & 0 & 0 & 0 & 0 & 0 & 0 & 0 \\ \varphi^2 & \varphi & 0 & 1 & s_z & -c_z & 0 & 0 & \frac{y_s}{2} \varphi^2 & y_s \varphi & 0 & 0 & s_z & y_s c_z \\ 0 & 0 & 0 & 0 & 0 & 0 & 0 & 0 & \frac{R}{6} \varphi^3 & \frac{2}{R} \varphi^2 & 1 & -R c_z & -R s_z & 0 \\ 0 & 0 & 0 & 0 & 0 & 0 & R \varphi & -\frac{1}{R} & \varphi & \varphi^2 & 0 & 0 & c_z & s_z \end{bmatrix}^T \end{aligned}$
$[\Phi_0^d]$	$\begin{bmatrix} 0 & 1 & -1 & 0 & 1 & 0 & \frac{y_s}{R} & 0 & 0 & 0 & 0 & 0 & 0 & 0 \\ 0 & 0 & 0 & 0 & 0 & 0 & 0 & 0 & 0 & 0 & 0 & 1 & -R & 0 \\ 0 & 0 & 0 & 1 & 0 & -1 & 0 & 0 & 0 & 0 & 0 & 0 & 0 & y_s \\ \frac{1}{R} & 0 & 0 & 0 & 0 & \frac{y_s}{R^2} & 0 & 0 & 0 & 0 & 0 & 0 & 0 & 0 \\ 0 & 0 & 0 & 0 & 0 & 0 & 0 & 0 & 0 & 0 & 1 & 0 & 0 & -1 \\ 0 & 0 & 0 & 0 & 0 & 0 & 0 & -\frac{1}{R} & 0 & 0 & 0 & 0 & 1 & 0 \\ 0 & 0 & 0 & 0 & 0 & 0 & 0 & 0 & \frac{1}{R} & 0 & 0 & 0 & 0 & \frac{1}{R} \end{bmatrix}^T$

$[\Phi_L^d]$	$\begin{bmatrix} \varphi_L & 0 & \varphi_L^2 & \frac{1}{R} & 0 & 0 & 0 \\ 1 & 0 & \varphi_L & 0 & 0 & 0 & 0 \\ -1 & 0 & 0 & 0 & 0 & 0 & 0 \\ 0 & 0 & 1 & 0 & 0 & 0 & 0 \\ c_L & 0 & s_L & \frac{s_L}{R} & 0 & 0 & 0 \\ \frac{y_s}{R}\varphi_L & 0 & -c_L & \frac{y_s}{R^2} & 0 & 0 & 0 \\ \frac{y_s}{R} & 0 & 0 & 0 & 0 & R\varphi_L & 1 \\ 0 & 0 & 0 & 0 & 0 & -\frac{1}{R} & 0 \\ 0 & \frac{R}{6}\varphi_L^3 & \frac{y_s}{2}\varphi_L^2 & 0 & \frac{\varphi_L^2}{2} & \varphi_L & \frac{1}{R} \\ 0 & \frac{2}{R}\varphi_L^2 & y_s\varphi_L & 0 & \frac{4}{R}\varphi_L & \varphi_L^2 & \frac{2}{R}\varphi \\ 0 & R\varphi_L & 0 & 0 & 1 & 0 & 0 \\ 0 & 1 & 0 & 0 & 0 & 0 & 0 \\ 0 & -Rc_L & s & 0 & s_L & c_L & -\frac{s_L}{R} \\ 0 & -Rs_L & y_sc_L & 0 & -c_L & s_L & \frac{c_L}{R} \end{bmatrix}$
$[\Psi]$	$\begin{bmatrix} [\Phi_0^d] \\ [\Phi_L^d] \end{bmatrix}$
$[N]$	$[\bar{N}_1, \bar{N}_2, \bar{N}_3, \bar{N}_4] = \left[\{\bar{\Phi}_1^T \times [\Psi]^{-1}\}, \{\bar{\Phi}_2^T \times [\Psi]^{-1}\}, \{\bar{\Phi}_3^T \times [\Psi]^{-1}\}, \{\bar{\Phi}_4^T \times [\Psi]^{-1}\} \right]$

Table 5.2 The strain terms in the equation 5.41

	Equation
${}^a\bar{D}_0^g$	$s x_s \frac{\bar{N}_4}{R}$
${}^q\bar{D}_0^g$	$\begin{aligned} & \left(\bar{N}'_1 + c y_s \bar{N}'_4 + s x_s \bar{N}'_4 \right) (\tilde{u}'_s + c y_s \beta' + s x_s \beta') \\ & + \left(\bar{N}'_3 - c x_s \bar{N}'_4 + s y_s \bar{N}'_4 \right) (v' - c x_s \beta' + s y_s \beta') \\ & + \frac{1}{R^2} \left(\bar{N}'_1 + c y_s \bar{N}'_4 + s x_s \bar{N}'_4 \right) (u_s + s y_s + (1-c)x_s) \end{aligned}$
${}^a\bar{D}_x^g$	$\begin{aligned} & \left(-s \left(-\tilde{u}''_s - \frac{1}{R} + \frac{y_s}{R} (v''_s - \tilde{u}'_s \beta') - v'_s \beta' \right) + c \left(-v''_s - \frac{y_s}{R} (\tilde{u}''_s - v'_s \beta') + \tilde{u}'_s \beta' \right) \right) \bar{N}_4 \\ & + c \left(\frac{y_s}{R} \left(-\beta' \bar{N}'_1 - \tilde{u}'_s \bar{N}'_4 \right) - \beta' \bar{N}'_3 - v' \bar{N}'_4 \right) + s \left(\bar{N}'_4 \tilde{u}'_s + \beta' \bar{N}'_1 - \bar{N}''_3 \right) \end{aligned}$
${}^q\bar{D}_x^g$	$\begin{aligned} & \left(c \left(\tilde{u}'_s \tilde{\beta}' - \frac{y_s}{R^2} \tilde{u}_s'^2 - \frac{y_s}{R^2} \right) - s \left(\frac{\tilde{u}_s'^2}{R} - \frac{y_s}{R^2} \tilde{u}'_s v'_s + \frac{(u_s + 2x_s)}{R^2} + v'_s \beta' \right) \right) \bar{N}_4 \\ & + c \left(-\frac{2\tilde{u}'_s \bar{N}'_1}{R} + y_s \frac{v'_s \bar{N}'_1 + \tilde{u}'_s \bar{N}'_3}{R^2} + \bar{N}'_3 \beta' + v'_s \bar{N}'_4 \right) \\ & + s \left(-\tilde{\beta}' \bar{N}'_1 - \tilde{u}'_s \bar{N}'_4 - 2 \frac{y_s}{R^2} \tilde{u}'_s \bar{N}'_1 \right) \\ & + c^2 \left(-\frac{y_s}{R} \left(\tilde{u}'_s \bar{N}'_4 + \beta' \bar{N}'_1 \right) + \frac{y_s^2}{R^2} (v'_s \bar{N}'_4 + \beta' \bar{N}'_3) - 2x_s \beta' \bar{N}'_4 \right) \\ & + s^2 x_s \left(-\left(\tilde{\beta}' \bar{N}'_4 + \beta' \bar{N}'_4 \right) - \frac{y_s}{R^2} \left(\beta' \bar{N}'_1 + \tilde{u}'_s \bar{N}'_4 \right) \right) \\ & + s c \left(-y_s \left(\tilde{\beta}' \bar{N}'_4 + \beta' \bar{N}'_4 \right) - \frac{y_s^2 + R x_s}{R^2} \left(\beta' \bar{N}'_1 + \tilde{u}'_s \bar{N}'_4 \right) \right. \\ & \left. + \frac{x_s y_s}{R} (v'_s \bar{N}'_4 + \beta' \bar{N}'_3) + 2y_s \beta' \bar{N}'_4 \right) \end{aligned}$
${}^a\bar{D}_y^g$	$c \left(\beta' \bar{N}'_1 + \tilde{u}'_s \bar{N}'_4 \right) + (s (v''_s + \tilde{u}'_s \beta') + c (\tilde{u}''_s + v'_s \beta')) \bar{N}_4 + s \left(\bar{N}''_1 + \bar{N}'_3 \beta' + v'_s \bar{N}'_4 \right)$
${}^q\bar{D}_y^g$	$\begin{aligned} & -c \left(\bar{N}'_1 \tilde{\beta}' + \tilde{u}'_s \bar{N}'_4 \right) + s \left(\frac{2\bar{N}'_1 \tilde{u}'_s}{R} - \frac{\bar{N}'_1}{R^2} - (N'_3 \beta' + v'_s N'_4) \right) \\ & + \left(c \left(\frac{\tilde{u}_s'^2}{R} - \frac{u_s}{R^2} - \beta' v'_s \right) + s (\tilde{u}'_s \beta') \right) \bar{N}_4 \end{aligned}$

	$+ c^2 y_s \left(\bar{N}'_4 \tilde{\beta}' + \beta' \bar{N}'_4 \right) + s^2 \left(\frac{x_s}{R} \left(\bar{N}'_1 \beta' + \tilde{u}'_s \bar{N}'_4 \right) - y_s 2\beta' \bar{N}'_4 \right)$ $+ s c \left(-x_s \left(\bar{N}'_4 \tilde{\beta}' + \beta' \bar{N}'_4 \right) + \frac{y_s}{R} \left(\bar{N}'_1 \beta' + \tilde{u}'_s \bar{N}'_4 \right) + x_s 2\beta' \bar{N}'_4 \right)$
${}^a \bar{D}_\omega^g$	$c \left(\frac{\bar{N}'_1 \beta' + \tilde{u}'_s \bar{N}'_4}{R} \right) + s \left(\frac{\bar{N}'_1 + \bar{N}'_3 \beta' + v'_s \bar{N}'_4}{R} \right) + \left(c \left(\frac{\tilde{u}''_s}{R} + \frac{v'_s \beta'}{R} \right) - s \left(-\frac{v''_s}{R} + \frac{\tilde{u}'_s \beta'}{R} \right) \right) \bar{N}'_4$
${}^q \bar{D}_\omega^g$	$c \left(-\frac{\bar{N}'_1 v'_s + \tilde{u}'_s \bar{N}'_3}{R^2} - \frac{y_s}{R} 2\beta' \bar{N}'_4 \right) - \frac{\bar{N}'_1 \beta' + \tilde{u}'_s \bar{N}'_4}{R} + s \left(\frac{2\tilde{u}'_s \bar{N}'_1}{R^2} - \frac{x_s}{R} 2\beta' \bar{N}'_4 \right)$ $- c^2 \frac{y_s}{R^2} (\bar{N}'_3 \beta' + v'_s \bar{N}'_4) + s^2 \frac{x_s}{R^2} (\bar{N}'_1 \beta' + \tilde{u}'_s \bar{N}'_4) + \left(c \left(\frac{\tilde{u}'_s{}^2}{R^2} - \frac{x_s}{R} \beta'^2 \right) + s \left(\frac{\tilde{u}'_s v'_s}{R^2} + \frac{y_s}{R} \beta'^2 \right) \right) \bar{N}'_4$ $+ \frac{c s}{R^2} \left(y_s \left(\beta' \bar{N}'_1 + \tilde{u}'_s \bar{N}'_4 \right) + x_s \left(\beta' \bar{N}'_3 + v'_s \bar{N}'_4 \right) \right)$
${}^q \bar{D}_{xx}^g$	$+ c^2 \left(\left(-\frac{\tilde{u}'_s}{R} + \frac{y_s}{R^2} v'_s \right) \left(-\frac{\bar{N}'_1}{R} + \frac{y_s}{R^2} \bar{N}'_3 \right) + \bar{N}'_4 \beta' \right) + s^2 \left(-\tilde{\beta}' - \frac{y_s}{R^2} \tilde{u}'_s \right) \left(-\bar{N}'_4 - \frac{y_s}{R^2} \bar{N}'_1 \right)$ $+ \frac{c s}{R} \left(\left(-\bar{N}'_4 - \frac{y_s}{R^2} \bar{N}'_1 \right) \left(-\tilde{u}'_s + \frac{y_s}{R} v'_s \right) + \left(-\tilde{\beta}' - \frac{y_s}{R^2} \tilde{u}'_s \right) \left(-\bar{N}'_1 + \frac{y_s}{R} \bar{N}'_3 \right) \right)$
${}^q \bar{D}_{yy}^g$	$\left(c^2 \bar{N}'_4 \tilde{\beta}' + s^2 \left(\frac{\tilde{u}'_s \bar{N}'_1}{R^2} + \bar{N}'_4 \tilde{\beta}' \right) + c s \left(-\frac{\tilde{u}'_s \bar{N}'_4 + \bar{N}'_1 \tilde{\beta}'}{R} \right) \right)$
${}^q \bar{D}_{xy}^g$	$\frac{c^2}{R} \left(\bar{N}'_4 \left(\tilde{u}'_s - \frac{y_s}{R} v'_s \right) + \tilde{\beta}' \left(\bar{N}'_1 - \frac{y_s}{R} \bar{N}'_3 \right) \right)$ $+ \frac{s^2}{R} \left(\bar{N}'_1 \left(-\tilde{\beta}' - \frac{y_s}{R^2} \tilde{u}'_s \right) + \tilde{u}'_s \left(-\bar{N}'_4 - \frac{y_s}{R^2} \bar{N}'_1 \right) \right)$ $+ c s \left(2\tilde{\beta}' \bar{N}'_4 + \frac{y_s}{R^2} \left(\bar{N}'_4 \tilde{u}'_s + \tilde{\beta}' \bar{N}'_1 \right) - \frac{2\tilde{u}'_s \bar{N}'_1}{R^2} + \frac{y_s}{R^3} \left(\tilde{u}'_s \bar{N}'_3 + \bar{N}'_1 v'_s \right) - 2\beta' \bar{N}'_4 \right)$
${}^q \bar{D}_{x\omega}^g$	$\frac{c}{R^2} \left(\bar{N}'_4 \tilde{u}'_s + \beta' \bar{N}'_1 - \frac{y_s}{R} \left(\bar{N}'_4 v'_s + \beta' \bar{N}'_3 \right) \right) + \frac{s}{R} \left(\bar{N}'_4 \tilde{\beta}' + \beta' \bar{N}'_4 + \frac{y_s}{R^2} \left(\bar{N}'_4 \tilde{u}'_s + \beta' \bar{N}'_1 \right) \right)$ $\left(-\frac{s}{R^2} \left(\beta' \tilde{u}'_s - \frac{y_s}{R} v'_s \beta' \right) + \frac{c}{R} \left(\tilde{\beta}' \beta' + \frac{y_s}{R^2} \tilde{u}'_s \beta' \right) \right) \bar{N}'_4$ $+ \frac{c^2}{R^3} \left(\bar{N}'_3 \tilde{u}'_s + v'_s \bar{N}'_1 - 2 \frac{y_s}{R} v'_s \bar{N}'_3 \right) + \frac{s^2}{R^2} \left(-\bar{N}'_1 \tilde{\beta}' - \tilde{u}'_s \bar{N}'_4 - 2 \frac{y_s}{R^2} \tilde{u}'_s \bar{N}'_1 \right)$ $+ \frac{c s}{R^2} \left(\bar{N}'_3 \tilde{\beta}' + v'_s \bar{N}'_4 + \frac{y_s}{R^2} \left(\bar{N}'_3 \tilde{u}'_s + v'_s \bar{N}'_1 \right) - \frac{2\tilde{u}'_s \bar{N}'_1}{R} + \frac{y_s}{R^2} \left(\bar{N}'_1 v'_s + \tilde{u}'_s \bar{N}'_3 \right) \right)$

${}^q\bar{D}_{y\omega}^g$	$\frac{c}{R}(\bar{N}'_4\tilde{\beta}' + \beta'\bar{N}'_4) + \frac{s}{R^2}(-\bar{N}'_4\tilde{u}'_s - \beta'\bar{N}'_1) + \left(-\frac{s}{R}(\tilde{\beta}'\beta') + \frac{c}{R^2}(-\tilde{u}'_s\beta')\right)\bar{N}_4$ $+ \frac{c^2}{R^2}(\nu'_s\bar{N}'_4 + \bar{N}'_3\tilde{\beta}') + \frac{s^2}{R^3}(2\tilde{u}'_s\bar{N}'_1) + c s \left(-\frac{\bar{N}'_3\tilde{u}'_s + \nu'_s\bar{N}'_1}{R^3} - \frac{\bar{N}'_1\tilde{\beta}' + \tilde{u}'_s\bar{N}'_4}{R^2}\right)$
${}^a\bar{D}_n^g$	$-\left(s\frac{\nu'_s}{R}\bar{N}_4\right) - \left(c\frac{\tilde{u}'_s}{R}\bar{N}_4\right) - \left(s\frac{\bar{N}'_1}{R}\right)$

Table 5.3 Additional term of geometric stiffness matrix in equation 5.42

	Sect	Equation
I_{xy}	I_{xy}^a	$({}^a\bar{D}_x^g)^T \times {}^a\bar{D}_y^g + ({}^a\bar{D}_y^g)^T \times {}^a\bar{D}_x^g$
	I_{xy}^r	$({}^q\bar{D}_x^g)^T \times {}^q\bar{D}_y^g + ({}^q\bar{D}_y^g)^T \times {}^q\bar{D}_x^g + ({}^q\bar{D}_0^g)^T \times {}^a\bar{D}_{xy}^g + ({}^a\bar{D}_{xy}^g)^T \times {}^q\bar{D}_0^g$
	I_{xy}^q	$({}^a\bar{D}_x^g)^T \times {}^q\bar{D}_y^g + ({}^q\bar{D}_x^g)^T \times {}^a\bar{D}_y^g + ({}^a\bar{D}_y^g)^T \times {}^q\bar{D}_x^g + ({}^q\bar{D}_y^g)^T \times {}^a\bar{D}_x^g$ $+ ({}^a\bar{D}_0^g)^T \times {}^a\bar{D}_{xy}^g + ({}^a\bar{D}_{xy}^g)^T \times {}^a\bar{D}_0^g$
$I_{x\omega}$	$I_{x\omega}^a$	$({}^a\bar{D}_x^g)^T \times {}^a\bar{D}_\omega^g + ({}^a\bar{D}_\omega^g)^T \times {}^a\bar{D}_x^g$
	$I_{x\omega}^r$	$({}^q\bar{D}_x^g)^T \times {}^q\bar{D}_\omega^g + ({}^q\bar{D}_\omega^g)^T \times {}^q\bar{D}_x^g + ({}^q\bar{D}_0^g)^T \times {}^a\bar{D}_{x\omega}^g + ({}^a\bar{D}_{x\omega}^g)^T \times {}^q\bar{D}_0^g$
	$I_{x\omega}^q$	$({}^a\bar{D}_x^g)^T \times {}^q\bar{D}_\omega^g + ({}^q\bar{D}_x^g)^T \times {}^a\bar{D}_\omega^g + ({}^a\bar{D}_\omega^g)^T \times {}^q\bar{D}_x^g + ({}^q\bar{D}_\omega^g)^T \times {}^a\bar{D}_x^g$ $+ ({}^a\bar{D}_0^g)^T \times {}^a\bar{D}_{x\omega}^g + ({}^a\bar{D}_{x\omega}^g)^T \times {}^a\bar{D}_0^g$
$I_{y\omega}$	$I_{y\omega}^a$	$({}^a\bar{D}_y^g)^T \times {}^a\bar{D}_\omega^g + ({}^a\bar{D}_{\omega i}^g)^T \times {}^a\bar{D}_y^g$
	$I_{y\omega}^r$	$({}^q\bar{D}_y^g)^T \times {}^q\bar{D}_\omega^g + ({}^q\bar{D}_\omega^g)^T \times {}^q\bar{D}_y^g + ({}^q\bar{D}_0^g)^T \times {}^a\bar{D}_{y\omega}^g + ({}^a\bar{D}_{y\omega}^g)^T \times {}^q\bar{D}_0^g$
	$I_{y\omega}^q$	$({}^a\bar{D}_y^g)^T \times {}^q\bar{D}_\omega^g + ({}^q\bar{D}_y^g)^T \times {}^a\bar{D}_\omega^g + ({}^a\bar{D}_{\omega i}^g)^T \times {}^q\bar{D}_y^g + ({}^q\bar{D}_{\omega}^g)^T \times {}^a\bar{D}_y^g$ $+ ({}^a\bar{D}_0^g)^T \times {}^a\bar{D}_{y\omega}^g + ({}^a\bar{D}_{y\omega}^g)^T \times {}^a\bar{D}_0^g$
I_{xxx}	I_{xxx}^q	$({}^a\bar{D}_x^g)^T \times {}^q\bar{D}_{xx}^g + ({}^q\bar{D}_{xx}^g)^T \times {}^a\bar{D}_x^g$
	I_{xxx}^r	$({}^q\bar{D}_x^g)^T \times {}^q\bar{D}_{xx}^g + ({}^q\bar{D}_{xx}^g)^T \times {}^q\bar{D}_x^g$
I_{yyy}	I_{yyy}^q	$({}^a\bar{D}_y^g)^T \times {}^q\bar{D}_{yy}^g + ({}^q\bar{D}_{yy}^g)^T \times {}^a\bar{D}_y^g$
	I_{yyy}^r	$({}^q\bar{D}_y^g)^T \times {}^q\bar{D}_{yy}^g + ({}^q\bar{D}_{yy}^g)^T \times {}^q\bar{D}_y^g$

I_{xyy}	Γ_{xyy}^q	$({}^a\bar{D}_x^g)^T \times {}^q\bar{D}_{yy}^g + ({}^q\bar{D}_{yy}^g)^T \times {}^a\bar{D}_x^g + ({}^a\bar{D}_y^g)^T \times {}^q\bar{D}_{xy}^g + ({}^q\bar{D}_{xy}^g)^T \times {}^a\bar{D}_y^g$
	Γ_{xyy}^r	$({}^q\bar{D}_x^g)^T \times {}^q\bar{D}_{yy}^g + ({}^q\bar{D}_{yy}^g)^T \times {}^q\bar{D}_x^g + ({}^q\bar{D}_y^g)^T \times {}^q\bar{D}_{xy}^g + ({}^q\bar{D}_{xy}^g)^T \times {}^q\bar{D}_y^g$
I_{xxy}	Γ_{xxy}^q	$({}^a\bar{D}_x^g)^T \times {}^q\bar{D}_{xy}^g + ({}^q\bar{D}_{xy}^g)^T \times {}^a\bar{D}_x^g + ({}^a\bar{D}_y^g)^T \times {}^q\bar{D}_{xx}^g + ({}^q\bar{D}_{xx}^g)^T \times {}^a\bar{D}_y^g$
	Γ_{xxy}^r	$({}^q\bar{D}_x^g)^T \times {}^q\bar{D}_{xy}^g + ({}^q\bar{D}_{xy}^g)^T \times {}^q\bar{D}_x^g + ({}^q\bar{D}_y^g)^T \times {}^q\bar{D}_{xx}^g + ({}^q\bar{D}_{xx}^g)^T \times {}^q\bar{D}_y^g$
$I_{xx\omega}$	$\Gamma_{xx\omega}^q$	$({}^a\bar{D}_x^g)^T \times {}^q\bar{D}_{x\omega}^g + ({}^q\bar{D}_{x\omega}^g)^T \times {}^a\bar{D}_x^g + ({}^a\bar{D}_\omega^g)^T \times {}^q\bar{D}_{xx}^g + ({}^q\bar{D}_{xx}^g)^T \times {}^a\bar{D}_\omega^g$
	$\Gamma_{xx\omega}^r$	$({}^q\bar{D}_x^g)^T \times {}^q\bar{D}_{x\omega}^g + ({}^q\bar{D}_{x\omega}^g)^T \times {}^q\bar{D}_x^g + ({}^q\bar{D}_\omega^g)^T \times {}^q\bar{D}_{xx}^g + ({}^q\bar{D}_{xx}^g)^T \times {}^q\bar{D}_\omega^g$
$I_{yy\omega}$	$\Gamma_{yy\omega}^q$	$({}^a\bar{D}_y^g)^T \times {}^q\bar{D}_{y\omega}^g + ({}^q\bar{D}_{y\omega}^g)^T \times {}^a\bar{D}_y^g + ({}^a\bar{D}_\omega^g)^T \times {}^q\bar{D}_{yy}^g + ({}^q\bar{D}_{yy}^g)^T \times {}^a\bar{D}_\omega^g$
	$\Gamma_{yy\omega}^r$	$({}^q\bar{D}_y^g)^T \times {}^q\bar{D}_{y\omega}^g + ({}^q\bar{D}_{y\omega}^g)^T \times {}^q\bar{D}_y^g + ({}^q\bar{D}_\omega^g)^T \times {}^q\bar{D}_{yy}^g + ({}^q\bar{D}_{yy}^g)^T \times {}^q\bar{D}_\omega^g$
$I_{x\omega\omega}$	$\Gamma_{x\omega\omega}^q$	$({}^a\bar{D}_\omega^g)^T \times {}^q\bar{D}_{x\omega}^g + ({}^q\bar{D}_{x\omega}^g)^T \times {}^a\bar{D}_\omega^g + ({}^a\bar{D}_\omega^g)^T \times {}^q\bar{D}_{y\omega}^g + ({}^q\bar{D}_{y\omega}^g)^T \times {}^a\bar{D}_\omega^g$
	$\Gamma_{x\omega\omega}^r$	$({}^q\bar{D}_\omega^g)^T \times {}^q\bar{D}_{x\omega}^g + ({}^q\bar{D}_{x\omega}^g)^T \times {}^q\bar{D}_\omega^g + ({}^q\bar{D}_\omega^g)^T \times {}^q\bar{D}_{y\omega}^g + ({}^q\bar{D}_{y\omega}^g)^T \times {}^q\bar{D}_\omega^g$
$I_{xy\omega}$	$\Gamma_{xy\omega}^q$	$({}^a\bar{D}_x^g)^T \times {}^q\bar{D}_{y\omega}^g + ({}^q\bar{D}_{y\omega}^g)^T \times {}^a\bar{D}_x^g + ({}^a\bar{D}_y^g)^T \times {}^q\bar{D}_{x\omega}^g + ({}^q\bar{D}_{x\omega}^g)^T \times {}^a\bar{D}_y^g$ $+ ({}^a\bar{D}_\omega^g)^T \times {}^q\bar{D}_{xy}^g + ({}^q\bar{D}_{xy}^g)^T \times {}^a\bar{D}_\omega^g$
	$\Gamma_{xy\omega}^r$	$({}^q\bar{D}_x^g)^T \times {}^q\bar{D}_{y\omega}^g + ({}^q\bar{D}_{y\omega}^g)^T \times {}^q\bar{D}_x^g + ({}^q\bar{D}_y^g)^T \times {}^q\bar{D}_{x\omega}^g + ({}^q\bar{D}_{x\omega}^g)^T \times {}^q\bar{D}_y^g$ $+ ({}^q\bar{D}_\omega^g)^T \times {}^q\bar{D}_{xy}^g + ({}^q\bar{D}_{xy}^g)^T \times {}^q\bar{D}_\omega^g$
I_{xxxx}	Γ_{xxxx}^r	$({}^q\bar{D}_{xx}^g)^T \times {}^q\bar{D}_{xx}^g$
I_{yyyy}	Γ_{yyyy}^r	$({}^q\bar{D}_{yy}^g)^T \times {}^q\bar{D}_{yy}^g$
$I_{yy\omega\omega}$	$\Gamma_{yy\omega\omega}^r$	$({}^q\bar{D}_{y\omega}^g)^T \times {}^q\bar{D}_{y\omega}^g$
$I_{xx\omega\omega}$	$\Gamma_{xx\omega\omega}^r$	$({}^q\bar{D}_{x\omega}^g)^T \times {}^q\bar{D}_{x\omega}^g$
I_{xxyy}	Γ_{xxyy}^r	$({}^q\bar{D}_{xy}^g)^T \times {}^q\bar{D}_{xy}^g + ({}^q\bar{D}_{xx}^g)^T \times {}^q\bar{D}_{yy}^g + ({}^q\bar{D}_{yy}^g)^T \times {}^q\bar{D}_{xx}^g$
$I_{xxy\omega}$	$\Gamma_{xxy\omega}^r$	$({}^q\bar{D}_{xx}^g)^T \times {}^q\bar{D}_{y\omega}^g + ({}^q\bar{D}_{y\omega}^g)^T \times {}^q\bar{D}_{xx}^g + ({}^q\bar{D}_{xy}^g)^T \times {}^q\bar{D}_{x\omega}^g + ({}^q\bar{D}_{x\omega}^g)^T \times {}^q\bar{D}_{xy}^g$
$I_{xyy\omega}$	$\Gamma_{xyy\omega}^r$	$({}^q\bar{D}_{yy}^g)^T \times {}^q\bar{D}_{x\omega}^g + ({}^q\bar{D}_{x\omega}^g)^T \times {}^q\bar{D}_{yy}^g + ({}^q\bar{D}_{xy}^g)^T \times {}^q\bar{D}_{y\omega}^g + ({}^q\bar{D}_{y\omega}^g)^T \times {}^q\bar{D}_{xy}^g$
$I_{xxx\omega}$	$\Gamma_{xxx\omega}^r$	$({}^q\bar{D}_{xx}^g)^T \times {}^q\bar{D}_{x\omega}^g + ({}^q\bar{D}_{x\omega}^g)^T \times {}^q\bar{D}_{xx}^g$
$I_{x\omega\omega\omega}$	$\Gamma_{x\omega\omega\omega}^r$	$({}^q\bar{D}_{x\omega}^g)^T \times {}^q\bar{D}_{x\omega}^g + ({}^q\bar{D}_{\omega\omega}^g)^T \times {}^q\bar{D}_{x\omega}^g$
I_{xyyy}	Γ_{xyyy}^r	$({}^q\bar{D}_{yy}^g)^T \times {}^q\bar{D}_{xy}^g + ({}^q\bar{D}_{xy}^g)^T \times {}^q\bar{D}_{yy}^g$
$I_{yyy\omega}$	$\Gamma_{yyy\omega}^r$	$({}^q\bar{D}_{yy}^g)^T \times {}^q\bar{D}_{y\omega}^g + ({}^q\bar{D}_{y\omega}^g)^T \times {}^q\bar{D}_{yy}^g$
$I_{xy\omega\omega}$	$\Gamma_{xy\omega\omega}^r$	$({}^q\bar{D}_{x\omega}^g)^T \times {}^q\bar{D}_{y\omega}^g + ({}^q\bar{D}_{y\omega}^g)^T \times {}^q\bar{D}_{x\omega}^g$

Table 5.4 the notation of D^s in the equation 5.44

	Equation
$[{}^q D_0^s]$	$\begin{aligned} & \left(\bar{N}'_1 + (c y_s + s x_s) \bar{N}'_4 \right)^T \times \left(\bar{N}'_1 + (c y_s + s x_s) \bar{N}'_4 \right) \\ & + \left(\bar{N}'_3 - (c x_s - s y_s) \bar{N}'_4 \right)^T \times \left(\bar{N}'_3 - (c x_s - s y_s) \bar{N}'_4 \right) \\ & + \frac{1}{R^2} \left(\bar{N}'_1 + (c y_s + s x_s) \bar{N}'_4 \right)^T \times \left(\bar{N}'_1 + (c y_s + s x_s) \bar{N}'_4 \right) \end{aligned}$
$[{}^a D_x^s]$	$\begin{aligned} & c \left(-y_s \frac{\bar{N}'_1{}^T \times \bar{N}'_4}{R} - \bar{N}'_3{}^T \times \bar{N}'_4 \right) - s \bar{N}'_4{}^T \times \left(-\bar{N}''_1 + \frac{y_s}{R} \bar{N}''_3 \right) \\ & + s \left(\bar{N}'_4{}^T \times \bar{N}'_1 - \frac{y_s}{R} \bar{N}'_3{}^T \times \bar{N}'_4 \right) - c \left(\bar{N}'_4{}^T \times \bar{N}'_3 + \frac{y_s}{R} \bar{N}'_4{}^T \times \bar{N}''_1 \right) \\ & - s \bar{N}'_4{}^T \times \left(-\bar{N}''_1 + \frac{y_s}{R} \left(\bar{N}''_3 - \beta' \bar{N}'_1 - \tilde{u}'_s \bar{N}'_4 \right) - \beta' \bar{N}'_3 - v'_s \bar{N}'_4 \right) \\ & + c \bar{N}'_4{}^T \times \left(\tilde{u}'_s \bar{N}'_4 + \beta' \bar{N}'_1 - \bar{N}''_3 - \frac{y_s}{R} \left(\bar{N}''_1 - \beta' \bar{N}'_3 - v'_s \bar{N}'_4 \right) \right) \\ & + c \left(-y_s \frac{\bar{N}'_4{}^T \times \bar{N}'_1}{R} - \bar{N}'_4{}^T \times \bar{N}'_3 \right) - \left(-\bar{N}''_1 + \frac{y_s}{R} \bar{N}''_3 \right)^T \times s \bar{N}'_4 \\ & + s \left(\bar{N}'_1{}^T \times \bar{N}'_4 - \frac{y_s}{R} \bar{N}'_4{}^T \times \bar{N}'_3 \right) - c \left(\bar{N}'_3{}^T \times \bar{N}'_4 + \frac{y_s}{R} \bar{N}'_1{}^T \times \bar{N}'_4 \right) \\ & - s \left(-\bar{N}''_1 + \frac{y_s}{R} \left(\bar{N}''_3 - \beta' \bar{N}'_1 - \tilde{u}'_s \bar{N}'_4 \right) - \beta' \bar{N}'_3 - v'_s \bar{N}'_4 \right)^T \times \bar{N}'_4 \\ & + c \left(\tilde{u}'_s \bar{N}'_4 + \beta' \bar{N}'_1 - \bar{N}''_3 - \frac{y_s}{R} \left(\bar{N}''_1 - \beta' \bar{N}'_3 - v'_s \bar{N}'_4 \right) \right)^T \times \bar{N}'_4 \end{aligned}$
$[{}^q D_x^s]$	$\begin{aligned} & c \left(\frac{\bar{N}'_1{}^T \times \bar{N}'_1}{R} + y_s \frac{\bar{N}'_1{}^T \times \bar{N}'_3}{R^2} + \bar{N}'_3{}^T \times \bar{N}'_4 \right) + s \left(-\bar{N}'_1{}^T \times \bar{N}'_4 - \frac{y_s}{R^2} \bar{N}'_1{}^T \times \bar{N}'_1 \right) \\ & - s \bar{N}'_4{}^T \times \left(-2 \frac{\tilde{u}'_s \bar{N}'_1}{R} + \frac{y_s}{R^2} \left(v'_s \bar{N}'_1 + \tilde{u}'_s \bar{N}'_3 \right) + \frac{\bar{N}'_1}{R^2} + \beta' \bar{N}'_3 + v'_s \bar{N}'_4 \right) \\ & + c \bar{N}'_4{}^T \times \left(-\tilde{\beta}' \bar{N}'_1 - \tilde{u}' \bar{N}'_4 - 2 \frac{y_s}{R^2} \tilde{u}' \bar{N}'_1 \right) + s^2 x_s \left(-\bar{N}'_4{}^T \times \bar{N}'_4 - \frac{y_s}{R^2} \bar{N}'_1{}^T \times \bar{N}'_4 \right) \\ & + c^2 \left(-\frac{y_s}{R} \bar{N}'_4{}^T \times \bar{N}'_1 + \frac{y_s^2}{R^2} \bar{N}'_4{}^T \times \bar{N}'_3 - x_s \bar{N}'_4{}^T \times \bar{N}'_4 \right) \\ & + s c \left(-y_s \bar{N}'_4{}^T \times \bar{N}'_4 - \frac{y_s^2 - R x_s}{R^2} \bar{N}'_1{}^T \times \bar{N}'_4 + \frac{x_s y_s}{R} \bar{N}'_4{}^T \times \bar{N}'_3 + y_s \bar{N}'_4{}^T \times \bar{N}'_4 \right) \end{aligned}$

	$ \begin{aligned} & +c\left(\frac{\tilde{N}'^T \times \tilde{N}'_1}{R} + y_s \frac{N_3'^T \times \tilde{N}'_1}{R^2} + N_4'^T \times N_3'\right) + s\left(-\tilde{N}'_4'^T \times \tilde{N}'_1 - \frac{y_s}{R^2} \tilde{N}'_1'^T \times \tilde{N}'_1\right) \\ & -s\left(-2\frac{\tilde{u}'_s \tilde{N}'_1}{R} + \frac{y_s}{R^2} (v'_s \tilde{N}'_1 + \tilde{u}'_s \tilde{N}'_3) + \frac{\bar{N}'_1}{R^2} + \beta' \bar{N}'_3 + v'_s \bar{N}'_4\right)^T \times \bar{N}'_4 \\ & +c\left(-\tilde{\beta}' \tilde{N}'_1 - \tilde{u}'_s \tilde{N}'_4 - 2\frac{y_s}{R^2} \tilde{u}'_s \tilde{N}'_1\right)^T \times \bar{N}'_4 + s^2 x_s \left(-\tilde{N}'_4'^T \times \bar{N}'_4 - \frac{y_s}{R^2} \bar{N}'_4'^T \times \tilde{N}'_1\right) \\ & +c^2 \left(-\frac{y_s}{R} \tilde{N}'_1'^T \times \bar{N}'_4 + \frac{y_s^2}{R^2} \bar{N}'_3'^T \times \bar{N}'_4 - x_s \bar{N}'_4'^T \times \bar{N}'_4\right) \\ & +sc\left(-y_s \tilde{N}'_4'^T \times \bar{N}'_4 - \frac{y_s^2 - Rx}{R^2} \bar{N}'_4'^T \times \tilde{N}'_1 + \frac{x_s y_s}{R} \bar{N}'_3'^T \times \bar{N}'_4 + y_s \bar{N}'_4'^T \times \bar{N}'_4\right) \end{aligned} $
$[{}^a D_y^s]$	$ \begin{aligned} & c \tilde{N}'_1'^T \times \bar{N}'_4 + s \bar{N}'_3'^T \times \bar{N}'_4 + c \bar{N}'_4'^T \times \tilde{N}'_1 + s \bar{N}'_4'^T \times \bar{N}'_3 \\ & + s \bar{N}'_4'^T \times (\bar{N}'_3 + \beta' \tilde{N}'_1 + \tilde{u}'_s \tilde{N}'_4) + c \bar{N}'_4'^T \times (\tilde{N}'_1 + \beta' \bar{N}'_3 + v'_s \bar{N}'_4) \\ & + s (\bar{N}'_3 + \beta' \tilde{N}'_1 + \tilde{u}'_s \tilde{N}'_4)^T \times \bar{N}'_4 + c (\tilde{N}'_1 + \beta' \bar{N}'_3 + v'_s \bar{N}'_4)^T \times \bar{N}'_4 \end{aligned} $
$[{}^q D_y^s]$	$ \begin{aligned} & -c(\tilde{N}'_1'^T \times \tilde{N}'_4) + s\left(\frac{\tilde{N}'_1'^T \times \tilde{N}'_1}{R} - \bar{N}'_4'^T \times \bar{N}'_3\right) \\ & -c(\tilde{N}'_4'^T \times \tilde{N}'_1) + s\left(\frac{\tilde{N}'_1'^T \times \tilde{N}'_1}{R} - \bar{N}'_3'^T \times \bar{N}'_4\right) \\ & -s \bar{N}'_4'^T \times (-\tilde{\beta}' \tilde{N}'_1 - \tilde{u}'_s \tilde{N}'_4) + c \bar{N}'_4'^T \times \left(\frac{2\tilde{u}'_s \tilde{N}'_1}{R} - \frac{N_1}{R^2} - \beta' \bar{N}'_3 - v'_s \bar{N}'_4\right) \\ & +c^2 y_s (\bar{N}'_4'^T \times \tilde{N}'_4) + s^2 \left(\frac{x_s}{R} \tilde{N}'_1'^T \times \bar{N}'_4 - y_s \bar{N}'_4'^T \times \bar{N}'_4\right) \\ & +sc\left(-x_s \bar{N}'_4'^T \times \tilde{N}'_4 + \frac{y_s}{R} \tilde{N}'_1'^T \times \bar{N}'_4 + x_s \bar{N}'_4'^T \times \bar{N}'_4\right) \\ & -s(-\tilde{\beta}' \tilde{N}'_1 - \tilde{u}'_s \tilde{N}'_4)^T \times \bar{N}'_4 + c\left(\frac{2\tilde{u}'_s \tilde{N}'_1}{R} - \frac{N_1}{R^2} - \beta' \bar{N}'_3 - v'_s \bar{N}'_4\right)^T \times \bar{N}'_4 \\ & +c^2 y_s (\tilde{N}'_4'^T \times \bar{N}'_4) + s^2 \left(\frac{x_s}{R} \bar{N}'_4'^T \times \tilde{N}'_1 - y_s \bar{N}'_4'^T \times \bar{N}'_4\right) \\ & +sc\left(-x_s \tilde{N}'_4'^T \times \bar{N}'_4 + \frac{y_s}{R} \bar{N}'_4'^T \times \tilde{N}'_1 + x_s \bar{N}'_4'^T \times \bar{N}'_4\right) \end{aligned} $

$[{}^a D_\omega^s]$	$c \frac{(\widetilde{N}'_1)^T \times \overline{N}'_4{}^T}{R} + s \frac{\overline{N}'_3{}^T \times \overline{N}'_4}{R} + c \frac{\overline{N}'_4{}^T \times \widetilde{N}'_1}{R} + s \frac{\overline{N}'_4{}^T \times \overline{N}'_3}{R}$ $- s \overline{N}'_4{}^T \times \left(-\frac{\overline{N}''_3}{R} + \frac{\beta' \widetilde{N}'_1 + \widetilde{u}'_s \overline{N}'_4}{R} \right) + c \overline{N}'_4{}^T \times \left(\frac{\widetilde{N}''_1}{R} + \frac{\beta' \overline{N}'_3 + \nu'_s \overline{N}'_4}{R} \right)$ $- s \left(-\frac{\overline{N}''_3}{R} + \frac{\beta' \widetilde{N}'_1 + \widetilde{u}'_s \overline{N}'_4}{R} \right)^T \times \overline{N}'_4 + c \left(\frac{\widetilde{N}''_1}{R} + \frac{\beta' \overline{N}'_3 + \nu'_s \overline{N}'_4}{R} \right)^T \times \overline{N}'_4$
$[{}^q D_\omega^s]$	$c \left(-\frac{\widetilde{N}'_1{}^T \times \overline{N}'_3}{R^2} - \frac{y_s \overline{N}'_4{}^T \times \overline{N}'_4}{R} \right) + s \left(\frac{\widetilde{N}'_1{}^T \times \widetilde{N}'_1}{R^2} - \frac{x_s \overline{N}'_4{}^T \times \overline{N}'_4}{R} \right)$ $- s \overline{N}'_4{}^T \times \left(-\frac{\nu'_s \widetilde{N}'_1 + \widetilde{u}'_s \overline{N}'_3}{R} - \frac{2y_s \beta' \overline{N}'_4}{R} \right) + c \overline{N}'_4{}^T \times \left(\frac{2\widetilde{u}'_s \widetilde{N}'_1}{R^2} - \frac{x_s \beta' \overline{N}'_4}{R} \right)$ $+ c^2 \left(-\frac{y_s \overline{N}'_3{}^T \times \overline{N}'_4}{R^2} \right) + s^2 \left(\frac{x_s \overline{N}'_4{}^T \times \overline{N}'_4}{R^2} \right) + \frac{c s}{R^2} \left(y_s (\widetilde{N}'_1{}^T \times \overline{N}'_4) + x_s (\overline{N}'_3{}^T \times \overline{N}'_4) \right)$ $+ c \left(-\frac{\overline{N}'_3{}^T \times \widetilde{N}'_1}{R^2} - \frac{y_s \overline{N}'_4{}^T \times \overline{N}'_4}{R} \right) + s \left(\frac{\widetilde{N}'_1{}^T \times \widetilde{N}'_1}{R^2} - \frac{x_s \overline{N}'_4{}^T \times \overline{N}'_4}{R} \right)$ $- s \left(-\frac{\nu'_s \widetilde{N}'_1 + \widetilde{u}'_s \overline{N}'_3}{R} - \frac{2y_s \beta' \overline{N}'_4}{R} \right)^T \times \overline{N}'_4 + c \left(\frac{2\widetilde{u}'_s \widetilde{N}'_1}{R^2} - \frac{x_s \beta' \overline{N}'_4}{R} \right)^T \times \overline{N}'_4$ $+ c^2 \left(-\frac{y_s \overline{N}'_4{}^T \times \overline{N}'_3}{R^2} \right) + s^2 \left(\frac{x_s \overline{N}'_4{}^T \times \widetilde{N}'_1}{R^2} \right) + \frac{c s}{R^2} \left(y_s (\overline{N}'_4{}^T \times \widetilde{N}'_1) + x_s (\overline{N}'_4{}^T \times \overline{N}'_3) \right)$
$[{}^q D_{xx}^s]$	$\frac{c^2}{2} \left(\left(-\frac{\widetilde{N}'_1}{R} + \frac{y_s \overline{N}'_3}{R^2} \right)^T \times \left(-\frac{\widetilde{N}'_1}{R} + \frac{y_s \overline{N}'_3}{R^2} \right) + \overline{N}'_4{}^T \times \overline{N}'_4 \right)$ $+ \frac{c^2}{2} \left(\left(-\frac{\widetilde{N}'_1}{R} + \frac{y_s \overline{N}'_3}{R^2} \right)^T \times \left(-\frac{\widetilde{N}'_1}{R} + \frac{y_s \overline{N}'_3}{R^2} \right) + \overline{N}'_4{}^T \times \overline{N}'_4 \right)$ $+ \frac{s^2}{2} \left(-\widetilde{N}'_4 - \frac{y_s \widetilde{N}'_1}{R^2} \right)^T \times \left(-\widetilde{N}'_4 - \frac{y_s \widetilde{N}'_1}{R^2} \right) + \frac{c s}{R} \left(-\widetilde{N}'_4 - \frac{y_s \widetilde{N}'_1}{R^2} \right)^T \times \left(-\widetilde{N}'_1 + \frac{y_s}{R} \right)$ $+ \frac{s^2}{2} \left(-\widetilde{N}'_4 - \frac{y_s \widetilde{N}'_1}{R^2} \right)^T \times \left(-\widetilde{N}'_4 - \frac{y_s \widetilde{N}'_1}{R^2} \right) + \frac{c s}{R} \left(-\widetilde{N}'_1 + \frac{y_s \overline{N}'_3}{R} \right)^T \times \left(-\widetilde{N}'_4 - \frac{y_s}{R^2} \right)$

$[{}^q D_{yy}^s]$	$\frac{c^2}{2}(\widetilde{N}_4'^T \times \widetilde{N}_4') + \frac{s^2}{2} \left(\frac{\widetilde{N}_1'^T \times \widetilde{N}_1'}{R^2} + \widetilde{N}_4'^T \times \widetilde{N}_4' \right) + cs \left(-\frac{\widetilde{N}_1'^T \times \widetilde{N}_4'}{R} \right)$ $+ \frac{c^2}{2}(\widetilde{N}_4'^T \times \widetilde{N}_4') + \frac{s^2}{2} \left(\frac{\widetilde{N}_1'^T \times \widetilde{N}_1'}{R^2} + \widetilde{N}_4'^T \times \widetilde{N}_4' \right) + cs \left(-\frac{\widetilde{N}_4'^T \times \widetilde{N}_1'}{R} \right)$
$[{}^q D_{xy}^s]$	$\frac{c^2}{R} \left(\widetilde{N}_4'^T \times \left(\widetilde{N}_1' - \frac{y_s}{R} \widetilde{N}_3' \right) \right) + \frac{s^2}{R} \left(\widetilde{N}_1'^T \times \left(-\widetilde{N}_4' - \frac{y_s}{R^2} \widetilde{N}_1' \right) \right)$ $+ cs \left(\widetilde{N}_4'^T \times \widetilde{N}_4' + \frac{y_s}{R^2} \widetilde{N}_4'^T \times \widetilde{N}_1' - \frac{\widetilde{N}_1'^T \times \widetilde{N}_1'}{R^2} + \frac{y_s}{R^3} \widetilde{N}_1'^T \times \widetilde{N}_3' - \widetilde{N}_4'^T \times \widetilde{N}_4' \right)$ $+ \frac{c^2}{R} \left(\left(\widetilde{N}_1' - \frac{y_s}{R} \widetilde{N}_3' \right)^T \times \widetilde{N}_4' \right) + \frac{s^2}{R} \left(\left(-\widetilde{N}_4' - \frac{y_s}{R^2} \widetilde{N}_1' \right)^T \times \widetilde{N}_1' \right)$ $+ cs \left(\widetilde{N}_4'^T \times \widetilde{N}_4' + \frac{y_s}{R^2} \widetilde{N}_1'^T \times \widetilde{N}_4' - \frac{\widetilde{N}_1'^T \times \widetilde{N}_1'}{R^2} + \frac{y_s}{R^3} \widetilde{N}_3'^T \times \widetilde{N}_1' - \widetilde{N}_4'^T \times \widetilde{N}_4' \right)$
$[{}^a D_{x\omega}^s]$	$\frac{c}{R^2} \left(\widetilde{N}_4'^T \times \widetilde{N}_1' - \frac{y_s}{R} \widetilde{N}_4'^T \times \widetilde{N}_3' \right) + \frac{s}{R} \left(\widetilde{N}_4'^T \times \widetilde{N}_4' + \frac{y_s}{R^2} \widetilde{N}_4'^T \times \widetilde{N}_1' \right)$ $- (N_4)^T \times \frac{s}{R^2} \left(\widetilde{u}'_s N_4' + \beta' \widetilde{N}_1' - \frac{y_s}{R} (v'_s N_4' + \beta' N_3') \right)$ $+ (N_4)^T \times \frac{c}{R} \left(\widetilde{\beta}' N_4' + \beta' \widetilde{N}_4' + \frac{y_s}{R^2} (\widetilde{u}'_s N_4' + \beta' \widetilde{N}_1') \right)$ $+ \frac{c^2}{R^3} \left(N_3'^T \times \widetilde{N}_1' - \frac{y_s}{R} N_3'^T \times N_3' \right) + \frac{s^2}{R^2} \left(-\widetilde{N}_1'^T \times \widetilde{N}_4' - \frac{y_s}{R^2} \widetilde{N}_1'^T \times \widetilde{N}_1' \right)$ $+ \frac{cs}{R^2} \left(N_3'^T \times \widetilde{N}_4' + \frac{y_s}{R^2} N_3'^T \times \widetilde{N}_1' - \frac{\widetilde{N}_1'^T \times \widetilde{N}_1'}{R} + \frac{y_s}{R^2} \widetilde{N}_1'^T \times N_3' \right)$ $+ \frac{c}{R^2} \left(\widetilde{N}_1'^T \times N_4' \times -\frac{y_s}{R} N_3'^T \times N_4' \right) + \frac{s}{R} \left(\widetilde{N}_4'^T \times N_4' + \frac{y_s}{R^2} \widetilde{N}_1'^T \times N_4' \right)$ $- \frac{s}{R^2} \left(\widetilde{u}'_s N_4' + \beta' \widetilde{N}_1' - \frac{y_s}{R} (v'_s N_4' + \beta' N_3') \right)^T \times N_4$ $+ \frac{c}{R} \left(\widetilde{\beta}' N_4' + \beta' \widetilde{N}_4' + \frac{y_s}{R^2} (\widetilde{u}'_s N_4' + \beta' \widetilde{N}_1') \right)^T \times N_4$ $+ \frac{c^2}{R^3} \left(\widetilde{N}_1'^T \times N_3' - \frac{y_s}{R} N_3'^T \times N_3' \right) + \frac{s^2}{R^2} \left(-\widetilde{N}_4'^T \times \widetilde{N}_1' - \frac{y_s}{R^2} \widetilde{N}_1'^T \times \widetilde{N}_1' \right)$ $+ \frac{cs}{R^2} \left(\widetilde{N}_4'^T \times N_3' + \frac{y_s}{R^2} \widetilde{N}_1'^T \times N_3' - \frac{\widetilde{N}_1'^T \times \widetilde{N}_1'}{R} + \frac{y_s}{R^2} N_3'^T \times \widetilde{N}_1' \right)$

$[{}^q D_{y\omega}^s]$	$\begin{aligned} & \frac{c}{R}(N_4'^T \times \tilde{N}_4') + \frac{s}{R^2}(-N_4'^T \times \tilde{N}_1') + \frac{c}{R}(\tilde{N}_4'^T \times N_4') + \frac{s}{R^2}(-\tilde{N}_1'^T \times N_4') \\ & - (N_4)^T \times \frac{s}{R}(N_4' \tilde{\beta}' + \beta' \tilde{N}_4') + (N_4)^T \times \frac{c}{R^2}(-N_4' \tilde{u}'_s - \beta' \tilde{N}_1') \\ & + \frac{c^2}{R^2}(N_3'^T \times \tilde{N}_4') + \frac{s^2}{R^3}(\tilde{N}_1'^T \times \tilde{N}_1') + c s \left(-\frac{N_3'^T \times \tilde{N}_1'}{R^3} - \frac{\tilde{N}_1'^T \times \tilde{N}_4'}{R^2} \right) \\ & - \frac{s}{R}(N_4' \tilde{\beta}' + \beta' \tilde{N}_4')^T \times N_4 + \frac{c}{R^2}(-N_4' \tilde{u}'_s - \beta' \tilde{N}_1')^T \times N_4 \\ & + \frac{c^2}{R^2}(\tilde{N}_4'^T \times N_3') + \frac{s^2}{R^3}(\tilde{N}_1'^T \times \tilde{N}_1') + c s \left(-\frac{\tilde{N}_1'^T \times N_3'}{R^3} - \frac{\tilde{N}_4'^T \times \tilde{N}_1'}{R^2} \right) \end{aligned}$
$[D_n^s]$	$-s \frac{N_4'^T \times N_3'}{R} - c \frac{N_4'^T \times \tilde{N}_1'}{R} - s \frac{N_3'^T \times N_4}{R} - c \frac{\tilde{N}_1'^T \times N_4}{R}$

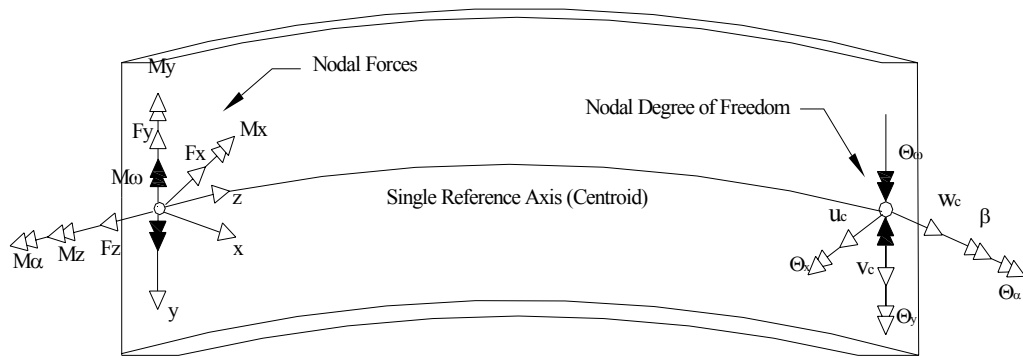


Figure 5.1 Nodal Degrees of Freedom and Nodal Loads

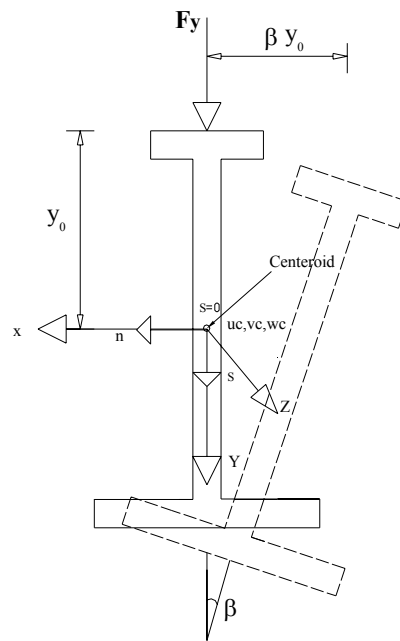


Figure 5.2 Concentrated Load on Top Flange

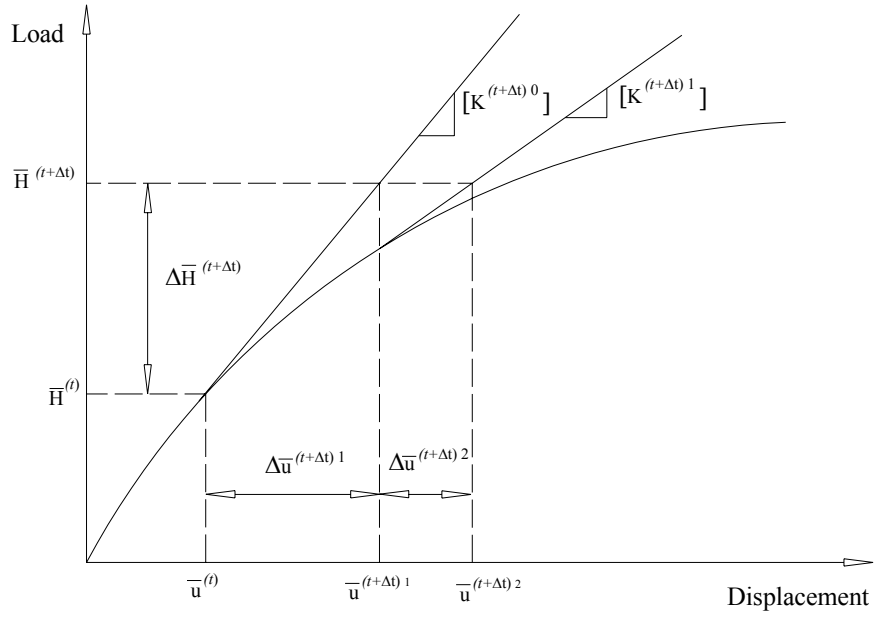


Figure 5.3 Newton-Raphson Method.

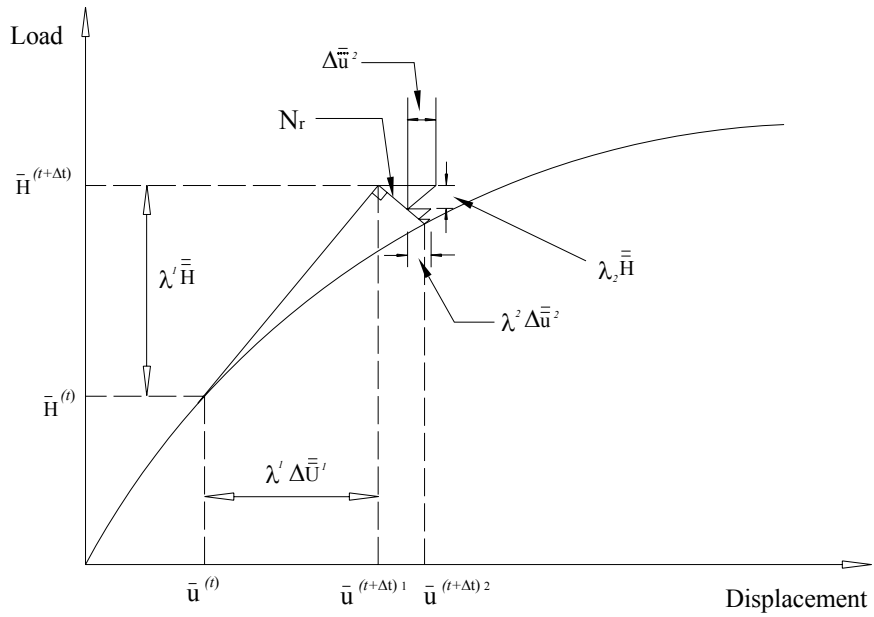


Figure 5.4 Arch Length Method

6. Load and Deflection Curves

6.1 Introduction

In the previous chapters, the derivation of equations for analyzing nonlinear response of horizontally curved beams has been presented. In Chapter 3, simplified strains based on different degrees of approximation that have been used in curved beam studies are derived. In Chapter 4, comprehensive nonlinear differential equations incorporating large displacement and rotation, simplified strains, P-delta effect and sectional deformation are developed. In Chapter 5, a numerical solution tool, the finite line element (FLE), for solving those complicated nonlinear differential equations is developed. In this chapter evaluation of the derived equations and the finite line element is presented.

The evaluation is conducted through analyzing a number of beams which were studied and reported in the literature. Unfortunately, the variations of beam cross sections, boundary conditions and loading cases of previous studies are limited. Most studies are on doubly symmetric cross sections. The study of singly symmetric and non-symmetric cross sections with different combination of loading and boundary conditions is very rare. On experimental study, only a few symmetric cross sections under pure flexural moment or point loading have been investigated. These very limited experimental and analytical data are insufficient for the evaluation of the derived equations and the finite line element. To overcome this situation, a three-dimensional finite element model is developed using the readily available program ABAQUS to generate load-deflection curves for comparison. The results of three dimensional finite element analyses (3DFEA) are calibrated against existing experimental data.

For the comparison of results from 3DFEA and from the finite line element analysis (FLEA), two set of boundary conditions are introduced for transforming the boundary conditions of the line element to three-dimensional boundary conditions. The evaluation is conducted by comparing load-deflection curves generated by 3DFEA, FLEA and experiments. Stress distributions in beam cross sections are also compared. Various cross sections and loading conditions are used for this numerical study.

6.2 3D Finite Element Analysis (3DFEA)

6.2.1 Finite Element Model

The general purpose finite element analysis program ABAQUS is used. The choice of mesh size and element type relies on the balance of accuracy of results and the required computational time. Because a curved beam member is composed of thin plates, shell element is the best fit for the constant or linear stress distribution through the plate thickness. The shell element, S4R, a four node shell element capable of handling large strains and material and geometrical nonlinearity is chosen in this study. Also S4R element is “shear deformable” element, by which transverse shear deformation is allowed. Conventionally, the significance of shear deformation of a beam depends on the ratio of cross sectional dimensions and span length. It is

necessary to find out the limitation of ignoring shear deformation of horizontally curved beam, as it is assumed in the development of the finite line element.

The Riks' method is used for performing incremental nonlinear analysis in the finite element program. Increment of load and displacement is controlled simultaneously within the specified error criteria in this method. Because only homogeneous elastic material is considered in this study, linear stress and strain constitutive law is used for modeling curved beam.

A horizontally curved beam modeled by S4R shell element is shown in Fig 6.1. The same mesh size is used throughout the span. The curved beam is simply supported with the boundary condition of $u = v = w = \beta = 0$, $\theta_w \neq 0$ at one end and $u = v = \beta = 0$, $w \neq 0$, $\theta_w \neq 0$ at the other end, where u , v , β and θ_w are the lateral and vertical displacement, rotation about the longitudinal axis and warping with respect to reference line. The cross section of the curved beam is shown in Figure 6.2. For a convergence test, two models with 943 and 2371 elements are used. Several loading cases are considered including bi-moment, moment about x-axis and about z-axis. Results indicate that the model with 943 shell elements is sufficiently accurate. In Figure 6.1, the displacement shape of the 943 element model generated by the moment about x-axis M_x , is shown.

6.2.2. Boundary Conditions

In order to compare the results from the three-dimensional model of 3DFEA with those from the line element model of FLEA, the boundary conditions of the line element have to be translated into those of the three dimensional model. In this study, a basic boundary condition of a horizontally curved beam is defined. The basic boundary system can undergo the most flexible stable nonlinear response of the curved beam system. The basic boundary condition has the displacement u , v , w and β restrained at one end section and u , v and β are restrained at the other end section. Warping of cross section, θ_w , is not restrained at the ends.

The above assumption in three dimensional boundary constraints of two dimensional curved beams and the simulating line element is difficulty to interpret for three dimensional models. The interpretation of the assumption that plane cross sections of beams retain their original shape but can warp in the longitudinal direction is that only rigid movement in the transverse and longitudinal direction is allowed of the boundary or end cross sections. When external and nodal loads are applied, there may be slight or severe local deformation of cross section at the ends of three dimensional models. In order to make the assumptions consistent for the line element model and the three dimensional finite element models, rigid beams are introduced to the end cross sections of the three-dimensional finite element model. The three rigid beams are attached into the components of the boundary cross sections, as shown in Fig. 6.3. The connections between the flanges and the web are accomplished by a hinge to allow for rotational movement of the flanges about the y-axis only for warping distortion.

Because the reference points of doubly and singly symmetric I-shaped cross section of curved beams are in the cross section, external forces and boundary condition can be directly applied to the centroid and shear center in the 3DFEA model. For non-

symmetric cross section as seen in Figure 6.3, the centroid and shear center are not located in the cross section. Because there is coupling between displacement and nodal forces at the end cross sections, direct transferring of centroidal boundary condition of finite line element analysis (FLEA) into 3DFEA of beams with un-symmetric cross section is difficult. Further more, when large rotation is considered, transferring of rotation may not be done by merely considering rigid body rotation. It may need matrix formulation of large rotation (Argyris 1982). In order to overcome this difficult, an additional rigid beam is introduced to connect the centroid with a point of the cross section, as indicated in Fig. 4.8.

For comparison purpose, a boundary cross section without the rigid beams is introduced, Fig. 6.4 so that the cross section is free to warp and deform. When the centroid and the shear center are not in the cross section, transferring of the FLEA centroidal restrain into 3DFEA cross sectional restrain is needed. But with coupling between the translation and large rotation and the condition of free warping and deformation at end cross sections, a method of transfer has not been developed. Therefore the free-to-deform boundary condition is limited to cases where the beam is fixed against rotation about the z-axis. The rigid boundary condition is defined as the upper bound and the free to deform condition is the lower bound in this study

6.2.3 Comparison with Experimental Results

The purpose of the comparison is not to reproduce analytically by 3DFEA the results of the experiments but to investigate the influence of the significant factors affecting the behavior of curved beams. However it is very difficult to obtain detail information of the experiments from literature. The behavior of the bearings and lateral bracing system is often not reported. Such information is essential for the appropriate analysis of beam behavior. Two set of experimental results are compared: test results of Culver and Mozer (1971) and by Fukumoto and Nakai (1981).

6.2.3.1 Comparison with Results of Beams Tested as a Pair

Table 6.1 contains the sectional and geometrical properties of a pair of horizontally curved and simply supported beams, L1A and L2A, tested by Culver and McManus. The beams were hybrid, consisting of two different grades of steel. The flanges and loading stiffeners were made of ASTM-A36 steel. The web and transverse stiffeners were fabricated from ASTM-A570 Grade B steel with a minimum yield stress of 30 ksi. The Loading and bearing stiffeners were attached to both sides of a web and the intermediate stiffeners were on one side only. Specimen L1A had full depth transverse stiffeners, whereas L2A had cut short stiffeners. Figure 6.5 shows the boundary and loading condition. There were a transverse diaphragm at each end and a bracing system at each loading point. The vertical, concentrated loads at the third points of the beam span generated a constant strong-axis flexural moment between the loads. The end diaphragms provided torsional restraint to stabilize the specimen under its own weight and under the external loads during testing. The Full depth loading stiffeners are considered to be able to restrain warping in the analysis. The lateral bracing system, placed symmetrically about mid-span, provided restraint to twist rotation. Because the sectional properties, material properties and boundary condition of the bracing system

are not known, different schemes are developed to simulate, including one as a beam and another one as a direct restraint at the upper and bottom flange. The materials of the beams are assumed elastic perfectly plastic in stress-strain relationship. Residual stresses and initial imperfection are not included in this analysis.

The load-deflection curved for specimens L1A and L2A are plotted in Figures 6.6 and 6.7. Five analyses were conducted to examine the effects of different schemes of bracing simulation. These are pin-pin ends (B1) and fixed-roller ends (B2) for the rigid bracing beams, direct restraint of nodes at loading point (B3), and sectional properties of $EA/L=1667$ k/in (S1) and 3750 k/in (S2) for the bracing beams. Another curve labeled as “Elastic & Geo-nonlinear” in the load-deflection plots is for the case in which only the geometrical nonlinearity is considered.

Figures 6.6a and 6.6b compare the vertical deflection at mid-span. At loads below the first yield, the beam behavior is basically linear. The experimental results show a “softer” behavior than that from analyses. This response is attributed to the residual stresses and boundary settlement and rotation. Near and beyond the ultimate load, the load-deflection curves corresponding to the five lateral bracing conditions differ slightly. The computed ultimate strength by 3DFEA agrees well with the experiment result.

The load and rotation responses at the end sections of the beams are not computed for comparison with the experimental results. Without detailed information of material and sectional properties of floor beams and end diaphragms at the end sections and loading points, computation can only provide rough estimates. In this part of study, only the comparisons of finite element analysis results with different assumed bracing condition are examined.

In Figures 6.7a and 6.7b, the rotation at the mid-span is compared. The computed results of the five cases of lateral bracing are somewhat different and are much less than the experimental results. Two possible contributions to this large difference exist. First, rotation at the mid-span is the sum of all rotations including the twist rotation at the end sections. Second, the end diaphragm and bearing system are assumed as rigid against rotation and warping in the finite element modeling. This condition strongly indicates the short coming of attempting to estimate accurately the magnitude of rotation of curved beams.

It is interesting to find out the degree of warping constraint at bracing points. The middle third of L1A was subjected to constant bending moment with the same warping restraint at the bracing points. Table 6.2 lists the computed warping moment from the finite line element analysis using the fixed-fixed and free-free conditions of warping restraint at the bracing points. The warping moment introduced by the lateral bracing, as evaluated from the experiment is much closer to that of fixed-fixed than of the free-free condition of constraint.

6.2.3.2 Comparison with Results of Beams Tested Individually

Fukumoto and Nakai tested four beams individually (1981). Figure 6.8 shows the loading and boundary condition. The beams were simply supported at the ends where rotation was restrained but warping was free. A concentrated load at mid-span generated large rotation and it coupled with loading. Therefore, the P- Δ effect should

be considered. The evaluation of P-Δ effect is presented in Chapter 5 for the incremental analysis:

$$Mz = (P \Delta u + \Delta P u + \Delta P \Delta u) y_0 \quad \mathbf{6.1a}$$

The torsional moment, Mz , is automatically incorporated in the three dimensional finite element analysis (3DFEA). This torsional moment is used as an external load in the finite line element analysis (FLEA). The comparison between the measured rotation and the results of 3DFEA is presented in Figures 6.9 to 6.12. Two boundary conditions are used for analysis; one is free-to-warp and the other one is rigid against warping. For both conditions, analyses are conducted considering geometric nonlinearity in the elastic range. In the inelastic range, elastic-perfectly-plastic material properties are used with the geometric nonlinearity (ABQ free ML in the figures). All rotations presented in Figs. 6.9 to 6.12 are at the mid-span. The magnitudes of rotation are much higher than those of beams in Fig. 6.6 and 6.7. Among the four beams of this group, specimen AR1 had an L/b ratio almost half that of the other three and above first yielding the computed rotation based on geometric nonlinearity only is quite different from those generated by considering both material and geometric nonlinearities. The BR series specimens, on the other hand, undergo large rotation and displacement before yielding. The specimens exhibit nonlinear behavior from the very beginning of loading. From the fact that the BR series beams are within the range of dimensional specifications, it is quite evident that nonlinear analysis based on large rotations and large displacements is necessary for the evaluation of behavior of curved beams.

Overall, the computed rotations agree well with the experimental results. The three dimensional finite element model is to be used for evaluating the results of the finite line element procedure.

6.3 Effects of Simplification of Strains

In Chapter 3, several simplified strains are developed based on the following approximations; a) the nonlinear term divided by quantities R^2 and higher can be ignored, b) $(R-x)/R$ can be simplified as unity, c) the nonlinear term divided by R can be ignored, d) with small rotation, $\cos(\beta)$ and $\sin(\beta)$ can be simplified as their first term of Taylor expansion and e) the inextensible conditions; $\frac{\partial w}{\partial z} - \frac{u}{R} \cong 0$ and

$\frac{\partial w}{\partial z} \cong 0$. Each simplified strain is used in formulating the finite line element in Chapter 5. In this section, the effects of approximation a) to c) are examined using a numerical study. As mentioned in Chapter 3, approximation e) vanishes by the adoption of approximation a). The effect of approximation d) will be examined in Chapter 7.

The numerical study is accomplished by comparing the results from analyzing a beam by the finite line element based on approximations a) to c).

The dimensions and sectional properties of the beam are shown in Fig. 6.13. The sectional properties $L/b=25$, $L/R=0.1$, $b_f/t_f=20$, $d/t_w=165$, $d/b_f=2$, $t_f/t_w=3$ and $A_f/A_w=1.3$ are near or at the current limits of AASHTO Specifications. High effects of nonlinear response are expected. The basic boundary condition is used that the ends are constrained against rotation but are allowed to warp. For the external load, equal moments about the x-axis, M_x , applied at the end section.

The effects of approximation a) that the nonlinear term divided by quantities R^2 and higher can be ignored are shown in Figures 6.14 to 6.16. Figure 6.14 shows the lateral displacement at the mid-span. Two curves are plotted; one is from the analysis in which all the nonlinear terms are included and the other is associated with approximation a). The two curves are essentially identical. In a similar way, the vertical displacement and rotation curves plotted in Figures 6.15 and 6.16 are also nearly identical. The effects of approximation a) are trivial.

The effects of approximations a) and b), in which $(R-x)/R$ are simplified as unity, is shown in Figures 6.17 to 6.19. The figures show that for the lateral, vertical and rotational response of the curved beam, the difference between the results of no simplification and of adopting approximations a) plus b) is very small. Practically no difference is founded.

With the approximations a), b) and c), in which nonlinear terms divided by R are ignored, the effects of simplification are detectable in Figures 6.20 to Figure 6.22. Approximation c) implies that only first order terms coupling with trigonometric functions are considered. It is observed that the lateral displacement and rotation are slightly higher with the approximations whereas the vertical displacement is slightly less. The maximum difference is about 4%, and the effects of approximations can still be ignored.

The results of this case study imply that the benefit of simplification overcomes the loss of accuracy. Therefore, from the practical point of view, the usage of simplified form of strains based on the approximation a), b) plus c) is justifiable. In the following section, simplification using the approximations a), b) plus c) will be used for numerical studies of horizontally curved beams.

6.4 Comparison of Deflections by 3DFEA and FLEA

In previous sections, the three dimensional finite element analysis model is calibrated with experimental results and the simplification for the finite line element is determined. In this section, the developed finite line element will be evaluated by comparing the results from its use with the results from using the three dimensional model. Four different shapes of cross section are examined, i.e., doubly symmetric, singly symmetric about x-axis (C-shape), singly symmetric about y-axis (I-shape) and un-symmetric cross sections. For each cross section, four different external loads are used, i.e., M_x , M_y , M_z and Bi-Moment. Two different boundary conditions are used in the 3DFEA model: free-to-deform and rigid boundary condition. For the line element analysis, twelve line elements incorporating large displacement, large rotation and cross sectional deformation are used. The number of twelve elements is decided by a

convergency test. The numerical studies for evaluating the line element are conducted within the elastic range of material properties.

6.4.1 Doubly Symmetric Cross Section

6.4.1.1 Load and Deflection Response

For the geometry and material properties of the doubly symmetric cross section, the beam studied by Fukumoto and Nishida (1981) is used. This cross section is shown in Figure 6.23. The material properties are $E=29,000$ ksi and $G=12,000$ ksi. The beam is restrained by the basic boundary condition. The ratio of sectional dimensions are $b/t_f \approx 12$, $d/b \approx 2.5$, $d/t_w \approx 50$, $L/R = 0.008$, $L/b=27$. Among the ratios, the sectional property of L/b is significant for the load-deflection behavior of curved beams. With a L/b ratio of 27, being slightly higher than the AASHTO limit of 25, relatively severe flexural response is expected.

Moment about the x-axis, M_x

The vertical end moment, M_x , in the three dimensional finite element model is generated from the point loads as shown in Figure 6.24. Because of the boundary condition of the model, the point loads may not generate the exact amount of vertical moment. In order to check this, it is necessary to calculate the stress resultants at the loading section. The resultant forces can be calculated from the stresses obtained from the finite element model and the definition of fundamental stress resultants.

$$F_z = \int \sigma_z dA, \quad M_x = \int \sigma_z y dA, \quad M_y = \int \sigma_z x dA, \quad B_i = \int \sigma_z \omega dA \quad 6.1$$

This approach is used in calculating all nodal forces for the line elements at the bracing points of curved beams, especially for calculating bi-moments. For a continuous curved beam braced by lateral bracing, the segment between the bracing points is modeled as a single span with external load. Different from the other six nodal forces of line elements, the bi-moment can not be calculated statically. Table 6.4 shows the externally applied and resultant forces, which agree well.

The load-deflection curves at the centroid at mid-span are shown in Figures 6.25 to 6.27. In all cases, the line element results agree well with the three dimensional finite element results. The curves also show that the rigid and free-to-deform boundary condition act as the upper and lower bound of deflection response.

Torsion at Mid-span (M_z)

The point loads for generating moment M_z at mid-span in the ABAQUS model are depicted in Figure 6.28a. The deformation of the beam under the torsional moment is shown in figure 6.28b.

Figures 6.29 to 6.31 show that the displacements of the centroid at the midspan as generated by the finite line element analysis (FLEA) are in between those by the three-dimensional finite element analysis (3DFEA) with the rigid and free-to-deform boundary condition.

Bi-Moment

The point loading system and the corresponding deformation are shown in Figure 6.32a and Figure 6.32b. The lateral deflection, vertical deflection and rotation of the centroid at the mid-span are shown in Figures 6.33 to 6.35.

Again, the results of line element analysis are in between those from the upper bound and lower bound boundary conditions of 3DFEA. A notable phenomenon is the relatively wide range between the results of the upper and lower bound boundary conditions.

Moment about the y-axis, M_y

The point loading system in the three-dimensional finite element model for generating M_y and the corresponding deformation shape are shown in Figure 6.36a and Figure 6.36b. Different from other loading condition, lateral bending moment is “in-plane” loading for the curved beam. Therefore, there is no coupling of rotation and vertical displacement. Only lateral displacement is developed as plotted in Figure 6.37. With this loading condition, the horizontally curved beam is transformed into an arch. Figure 6.37 shows that the results of finite line element analysis (FELA) agree well with that of three dimensional finite element analysis (3DFEA).

6.4.1.2 Stress Distribution

Two sets of stress calculations are conducted: by linear analysis and nonlinear analysis. Calculation of stresses by linear analysis is done by calculating the linear stress resultants and plugging into the corresponding parts of Eq. 5.27. The linear part of stress resultants, F_z , M_x , M_y , at mid-span can be obtained from statics. The linear part of bi-moment can be calculated by solving the linear differential equation Eq. 4.65 or using Table 4.1 to 4.7 for different set of warping boundary condition. Stresses based on the nonlinear analysis can be also calculated by using Eq 5.27. In order to use Eq 5.27 in nonlinear analysis, the linear and nonlinear parts of stress resultants, i.e., Eq 4.59, have to be calculated. Calculation of the nonlinear part of stress resultants requires solving nonlinear differential equation. This task may not be easily accomplished. Furthermore, in Eq 5.27, the stress resultants associated with x^2 , y^2 , xy and $x\omega$ are not included. In this study, the stresses from nonlinear analysis are obtained by substituting total displacement of each incremental step into Eq. 4.9a and using the constitutive law.

The stress distributions in the cross section at mid-span due to two equal end moments, M_x , are shown in Figures 6.38 to 6.43 for two different loading stages, $M_x=100$ k-in and 250 k-in, ($\sigma_{\max} = 0.3\sigma_y$ and $0.9\sigma_y$). The cross section in Figure 6.23 and the basic boundary condition are used for calculating the stresses. The stresses calculated by the three-dimensional finite element model with rigid and free to deform ends (ABQ Rigid and ABQ Free) and by the line element model with linear analysis and nonlinear analysis (Linea Anal and Line Ele) are compared. Figure 6.38 to Figure 6.40 show the stress distribution along the top flange, web and bottom flange when $M_x=100$ kips-in ($\sigma_{\max} = 0.3\sigma_y$). Figure 6.41 to Figure 6.43 show the stress distribution when $M_x=250$ kips-in ($\sigma_{\max} = 0.9\sigma_y$). As seen in Figures 6.38, 6.40, 6.41 and 6.43 for stress

distribution in the flanges, the results of the nonlinear analysis from the three dimensional finite element model and from the line element model agree quite well. On the other hand, even at $M_x=100$ k-in ($\sigma_{\max} = 0.3\sigma_y = 15$ ksi), there are relatively large differences between the results from the non-linear analysis and the linear analysis. At $M_x=250$ kip-in ($\sigma_{\max} = 0.9\sigma_y$), the stress at the tip of the top flange calculated by the linear analysis is about one third lower and at the tip of the bottom flange, about one third higher. Since the contribution of stress resultants, M_y , on longitudinal stresses is not anymore secondary and can not be generated from linear analysis, these differences occur. Also the stress resultants, K_{xx} , K_{yy} , K_{xw} , K_{yw} , can not be generated from linear analysis and cause more difference in relatively high loading stages. This condition suggests that linear analysis is not adequate for the computation of flange stresses of horizontally curved beams.

6.4.2 Singly Symmetric Cross Section (I-Shape)

The cross sectional shape and dimensions are given in Figure 6.44. The length and radius of the curved beam are $L=107$ (in) and $R=1338$ (in). The elastic and shear modulus are $E=29,000$ ksi and $G=12,000$ ksi. The beam has simple boundary condition with respect to bending and torsion at ends, where axial rotation is prevented. The beam is subjected separately to a vertical moment (M_x), a lateral moment (M_y), a torsional moment (M_z) and a bi-moment (Bi). Both axes of vertical and lateral moment pass through the centroid of the cross section. Torsional moment and bi-moment are applied through the shear-center.

In the analysis, both the procedures of one-reference line and two-reference lines are evaluated. Twelve line elements are used for the line element analysis. For the three dimensional finite element model, 943 shell elements are used. External point loads similar to those for the doubly symmetric cross section of the last example are used for generating M_x , M_y , M_z and Bi-moment in the three dimensional finite element model.

Moment about the x-axis (M_x)

For the applied vertical bending moment (M_x) at the end sections, a set of point loads similar to that of Figure 6.24 is used. The lateral, vertical and rotational displacements are plotted in Figure 6.45 to Figure 6.47. For all displacement, the results of using one-reference line and two-reference lines are the same. It confirms the fact that if sectional properties of any I-shaped cross section are properly introduced, the strain equations for the development of partial differential equation of doubly symmetric cross sections can be used for non-symmetric I-sections.

Similar to the case of doubly symmetric cross sections, the results of displacement from the line element analysis are closer to the upper bound results from 3DFEA. The stress distribution in the unsymmetric I-section is also similar to that of a doubly symmetric cross section. The stress distribution at two loading stages are plotted in Figures 6.48 to 6.53 for $M_x = 100$ kips-in ($\sigma_{\max} = 0.35\sigma_y$) and $M_x = 220$ kips-in ($\sigma_{\max} = \sigma_y$). For both the top and bottom flanges at both loads, the stresses calculated by the line element model and the three-dimensional finite element model are in good agreement. The stress distributions calculated from considering only the linear part of stress resultants do not provide accurate results. At $M_x = 100$ kip-in, the maximum

stress calculated by the linear analysis is about 25% lower and at $M_x=220$ kips-in, about 40% lower than that from the nonlinear analysis. Further more, surprisingly at $M_x=220$ kips-in, the trend of stress distribution in the bottom flange is opposite between the linear and the nonlinear analysis. This situation strongly indicates the necessity of nonlinear analysis.

Moment about z axis (M_z)

A point load system similar to that of Figure 6.28 for the doubly symmetric cross section is applied at the mid-span of the singly symmetric I-section to generate torsional moment in the span. The load and deflection curves for the lateral displacement, the vertical displacement and the rotation at the mid-span are presented in Figures 6.54 to 6.56. These results are quantitatively identical to the corresponding ones in Figures 6.29 to 6.31 for doubly symmetric I-beams. The results from the line element analyses are between the lower and upper bound results from the three-dimensional finite element analysis.

Bi-Moment

Under an applied bi-moment similar to that of Figure 6.32 for a doubly symmetric cross sections, the load-deflection behaviors are also similar. The deflection curves are plotted in Figure 6.57 to Figure 6.59. The results of the line element analysis are in between those from the upper bound and lower bound boundary condition of 3DFEA. Similar to the case of doubly symmetric cross section, the difference between the curves of upper bound and lower bound conditions is relatively big when the beam is subjected to bi-moment.

M_y and Bi-moment

Because the beam cross section is only symmetric about the y-axis, “in-plane” loading as shown in Figure 6.32 generates not only M_y but also a bi-moment. The bi-moment can be easily calculated from the sectorial area of the cross section. For the given cross section, the magnitude of the bi-moment is $3.5 \cdot M_y$. The load and deflection curve from the line element analysis of the combination of these two loads is shown in Figure 6.60. The results agree well with those by 3DFEA. The magnitudes of the vertical displacement and rotation are quite small in comparison to that of the lateral displacement, and are not presented.

6.4.3 Singly Symmetric Cross Section about x-axis (Channel Section)

The axes of centroid and shear center of singly symmetric channel section are out side of the cross section. When a reference line is not in the cross section, special care is needed to interpret the warping displacement, as presented in Section 4.6.

The cross section of the simply supported beam for analysis is shown in Figure 6.61. The length of the channel section is $L=107$ in. The L/R ratio is 0.008. The beam is restrained by the basic boundary condition. Two different loads are applied; a vertical moment, M_x , and a bi-moment, B_i . For the line element analysis, twelve line elements are used.

For comparison, a three-dimensional finite element model is again used with equivalent external point loads. The boundary conditions as shown in Figure 6.62 are used for generating Upper bound and lower bound of load and deflection curves.

It is noted that for cross sections singly symmetric about x-axis, point loads at beam ends usually generate two or more stress resultants. The point loads in Figure 6.62 generates not only M_x but also B_i . By using the stress distribution from the three-dimensional finite element analysis, stress resultants can be calculated. The stress resultants can be used for checking the external loads calculated by statics. The stress distribution along the flanges and the web at the end of the beam are plotted in Figures 6.63 to 6.65. It is interesting that the stress distribution along the web is not linear. Since a fictitious wall is used to link the centroidal reference point to the middle point of the cross section in 3DFEA as shown in Figure 6.3, local deformation at the junction point is inevitable and may cause nonlinear stress distribution in the web. The stress resultants calculated from these stresses and Eq 6.1 are listed in Table 6.5. The external loads and stress resultants are in good agreement.

The lateral, vertical and rotational deflection curves from the line element analysis and those from 3DFEA with upper bound and lower bound boundary conditions are compared in Figures 6.66 to 6.68. All load-deflection curves are in good agreement, with the line element results fall in between the upper and lower bound curves of the three dimensional finite element analysis. The results generated from using two-reference lines and using one-reference line produce almost identical results.

Figures 6.69 to 6.74 show the stress distribution along the top flange, web and bottom flange when $M_x=1145$ kips-in ($\sigma_{\max} = 0.35\sigma_y$) and 3000 kips-in ($\sigma_{\max} = \sigma_y$). Similar to the conclusion from the singly symmetric I section, the linear analysis does not provide adequate results especially in the flange at relatively high magnitude of stresses.

6.4.4 Unsymmetrical Cross Section

6.4.4.1 Deflections

To evaluate the application of the line element to general thin-walled open cross sections, the cross section in Figure 6.75 is selected. The span length, L/R ratio, material properties and boundary condition are the same as those used for the singly symmetric I-shaped and channel cross sections. From the point loads shown in Figure 6.75 for a vertical bending moment M_x , a bi-moment B_i is generated. The magnitude of the balancing bi-moment is $B_i=0.1 M_x$. The results of the line element analysis and the 3D finite element analysis are shown in Figures 6.76 to 6.78

As shown in these figures, the lateral deflection and the rotation curves for the centroid as produced by the line element analysis agree well with those by the 3D finite element analysis. The load versus vertical displacement curve is quite different from the other curves. The vertical displacement decreases sharply as the magnitude of M_x increases beyond 3000(k-in). The reasons are the coupling of M_x and bi-moment and the relatively rapid increase of rotation under load. The more flexible free-to-warp boundary condition permits more rotation than the rigid boundary condition, and leads to more reduction of the vertical displacement at centroid. Although general

unsymmetrical cross sections are not normally used for structural members, the unused behavior warrants more study, particularly in conjunction with material nonlinearity.

6.4.4.2 Stress distribution

The stress distributions developed from the line element analysis are compared with those from the three-dimensional finite element analysis (3DFEA) and from a linear analysis. The stresses along the mid thickness of the section at the mid span of the beam are plotted in Figures 6.79 to 6.84 for end moments of $M_x=870$ kips-in ($\sigma_{\max} = 0.41\sigma_y$) and $M_x=1742$ kips-in ($\sigma_{\max} = 0.9\sigma_y$).

Similar to the cases of the doubly and singly symmetric cross sections, all results agree well at relatively lower loads. In the top flange, the stress distribution by the linear analysis deviates from those by 3DFEA and FLEA at moderately high loads.

6.4.5 Comparison of Results from FLEA and Tests

Until now, evaluation of the finite line element analysis (FLEA) has been done by comparison of its results with the results of the three dimensional finite element analysis (3DFEA). Direct comparison with test data is needed. The experimental results of Fukumoto and Nakai (1981) are used.

Their experimental results of four test beams have been shown in Figures 6.9 to 6.12. These results are compared here with the results of their elastic analysis considering geometric nonlinearity and with the results of the line element analysis of this study. The load-deflection curves are plotted in Figures 6.85 to 6.88. The analytical results from the line element analysis are in good agreement with the test results except for beam BR3. With a small curvature, the contribution of geometrical nonlinearity on deflections is relatively small for this beam. The computed rotation from the line element analysis (Fig. 6.88) and from 3DFEA (Fig. 6.12) are less than those from the test. On the other hand, for the other three beams with large curvature, AR1, BR1, BR2, the geometric nonlinearity initiate at an early stage of loading, the line element analysis provides very good agreement with the test results. Since all sectional properties of test specimen are within the practical range of horizontally cured beams, it is evident from the comparison that geometric nonlinearity should be included in the design and analysis of horizontally curved beams.

6.5 Evaluation of Exact Solution of Some Cases

In Chapter 4, exact solutions for seven loading and boundary conditions based on small displacement and rotation are given. These solutions differ from those approximate solutions as is shown in Table 4.8. With the development of the line element, direct comparison can be made. Because the differential equations from which an exact solution is derived are base on small displacement and rotation, a line element formulated with approximations a), b), c) and d) is used. The beam cross sectional and material properties of Figure 4.5 are used for evaluation.

Table 6.6 to 6.12 list the bi-moments at the ends and mid-span for warping boundary and loading condition listed in the table 4.1 to 4.7. The bi-moments calculated from the expression of exact solution agree quite well with those computed from the line

element analysis with the corresponding simplification, confirming the adequacy of both the exact solution and the line element.

However, it must be emphasized again that linear analysis under estimates displacement and stresses, and considering geometrical nonlinearity in the analysis of horizontally curved beams is essential.

Table 6.1 Sectional and Geometrical Properties of Beams, Culver and McManus

Specimen	d_w (in)	b (in)	t_w (in)	t_f (in)	L (in)	R (in)
L1A	17.87	5.94	0.12	0.39	180	595
L2A	17.93	6.0	0.119	0.39	180	606.7

Table 6.2 Warping Moment at Bracing Points, L1A

Applied Constant Moment(k-in)	Bi Moment Fixed-Fixed		Bi Moment Free-Free		Bi Moment L1A	
665	332	332	0	0	269	269
1255	628	628	0	0	550	550

Table 6.3 Dimensions and Sectional Properties of Beams Tested by Fukumoto and Nakai

Specimen	d (in)	b (in)	t_w (in)	t_f (in)	L (in)	R (in)	L/R
AR1	9.91	4	0.220	0.331	66.93	911.9	0.07
BR1	9.85	3.96	0.217	0.331	110.24	1336	0.08
BR2	9.91	3.96	0.224	0.327	110.24	2838	0.04
BR3	9.86	3.86	0.220	0.327	110.24	19002	0.006

Table 6.4 Applied Vertical Bending Moment and Resultant Forces

	F_z	M_x	M_y	B_i
Stress Resultant	0	69.4	0.03	0
External load	0	70.0	0	0

Table 6.5 Stress Resultants at End Sections, Channel Shape

	M_x	M_y	B_i
Stress Resultant	101.08	-0.00075	67.33
External load	100	0	66.7

Table 6.6 Comparison the results solution for point load ($P=10$) and end moment with fixed-warping boundary condition

	$z=0$	$z=L/2$	$z=L$
Exact Solution	94.6	-53.9	94.6
Line Element	94.0	-53	94

Table 6.7 Comparison the results solution for point load ($P=10$) and end moment with fixed and free warping boundary condition

	$z=0$	$z=L/2$	$z=L$
Exact Solution	131.6	-70	0
Line Element	131	-69.8	0

Table 6.8 Comparison the results solution for distribute loading ($p=0.1$) with fixed-warping boundary condition

	$z=0$	$z=L/2$	$z=L$
Exact Solution	60.84	-32.2	60.84
Line Element	60	-31.4	60.84

Table 6.9 Comparison the results solution for distribute loading ($p=0.1$) with fixed and free warping boundary condition

	$z=0$	$z=L/2$	$z=L$
Exact Solution	84.5	-42.5	84.5
Line Element	83.6	-41.8	83.6

Table 6.10 Comparison the results solution for one vertical end moment ($M_x=100$) with fixed warping boundary condition

	$z=0$	$z=L/2$	$z=L$
Exact Solution	36.97	-14.27	24.1
Line Element	36.4	-14	23.9

Table 6.11 Comparison the results solution for two different vertical end moments ($M_x=100, M_y=200$) with fixed and free warping boundary condition

	$z=0$	$z=L/2$	$z=L$
Exact Solution	131	-57.3	0
Line Element	12.9	-56.8	0

Table 6.12 Comparison the results solution for one end bi-moment ($Bi=100$) with fixed and free warping boundary condition

	$z=0$	$z=L/2$	$z=L$
Exact Solution	-39	16.93	100
Line Element	-38	16.1	100

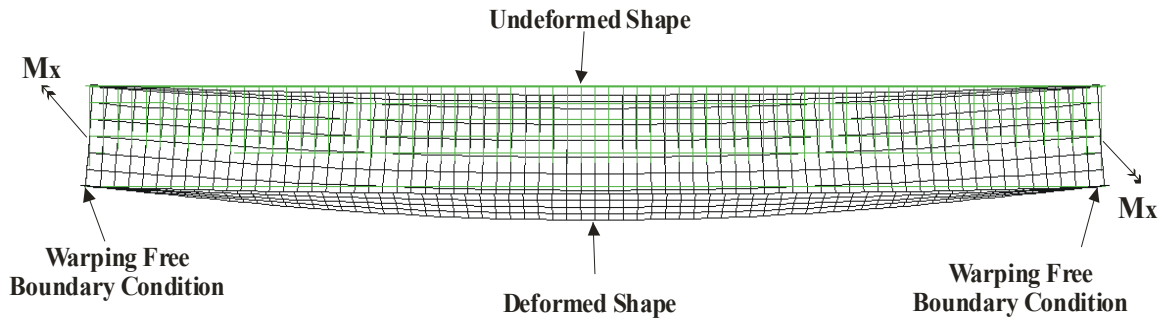


Figure 6.1 Finite Element model of Horizontally Curved Beams

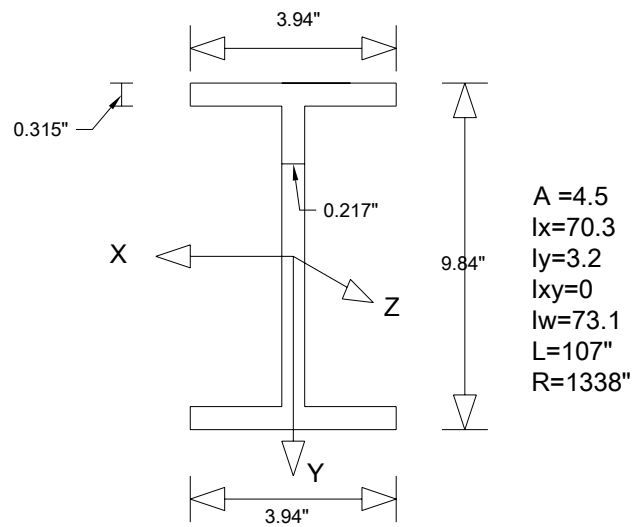


Figure 6.2 Cross section of beam for convergence test

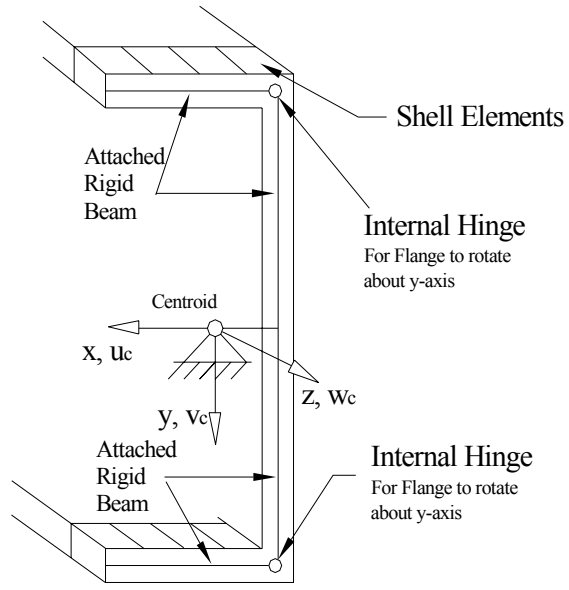


Figure 6.3 Rigid Boundary Modeled with Rigid Beams

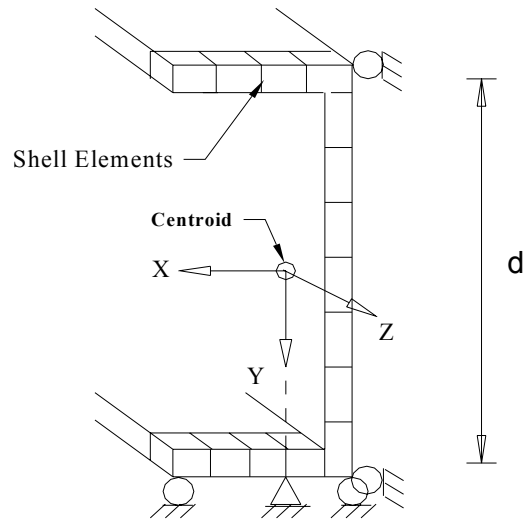


Figure 6.4 Free-to-deform Boundary Condition

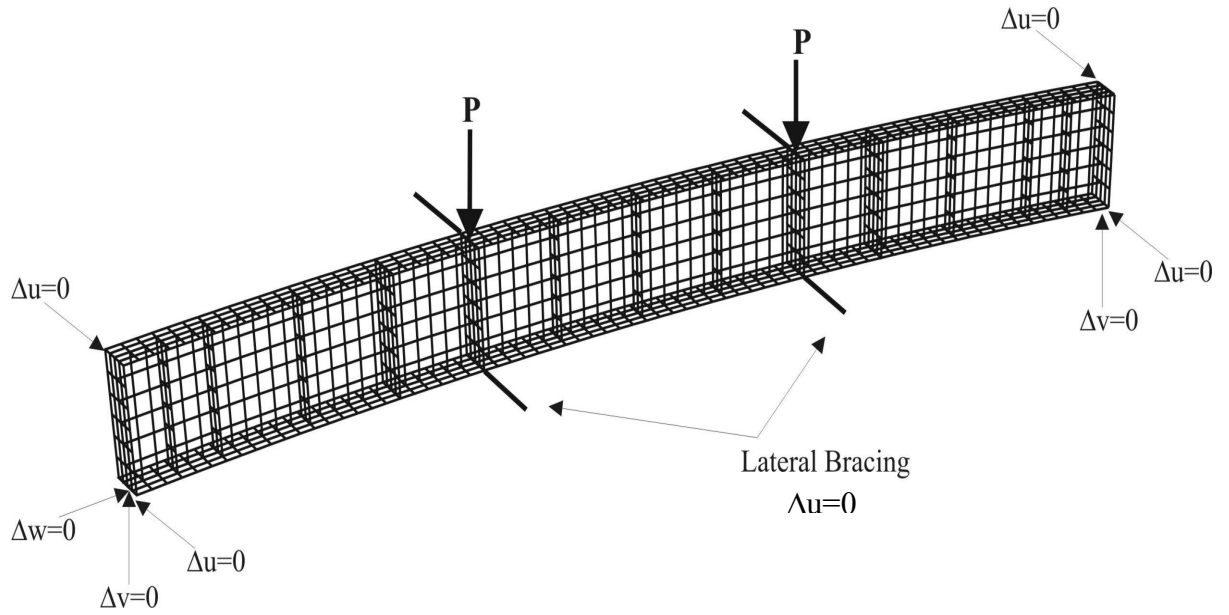


Figure 6.5 Specimen L1A

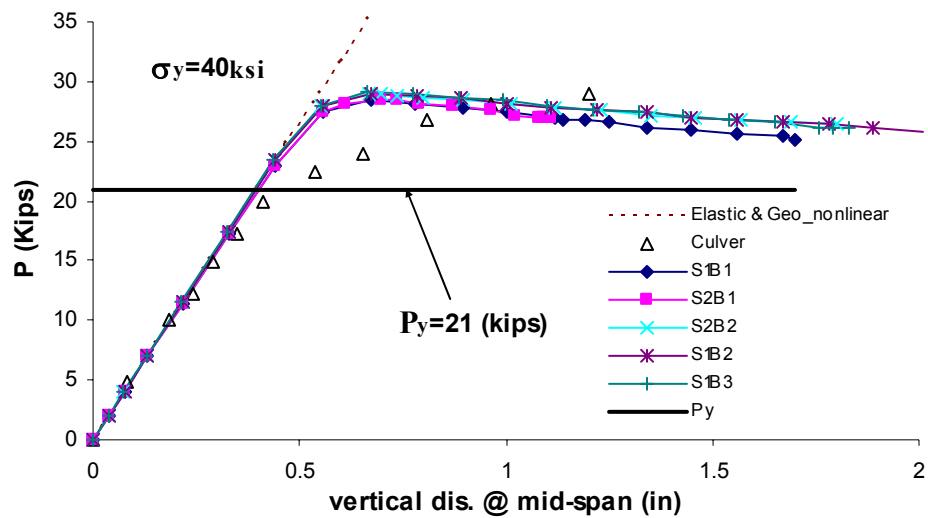


Figure 6.6a Load and vertical deflection of Specimen L1A

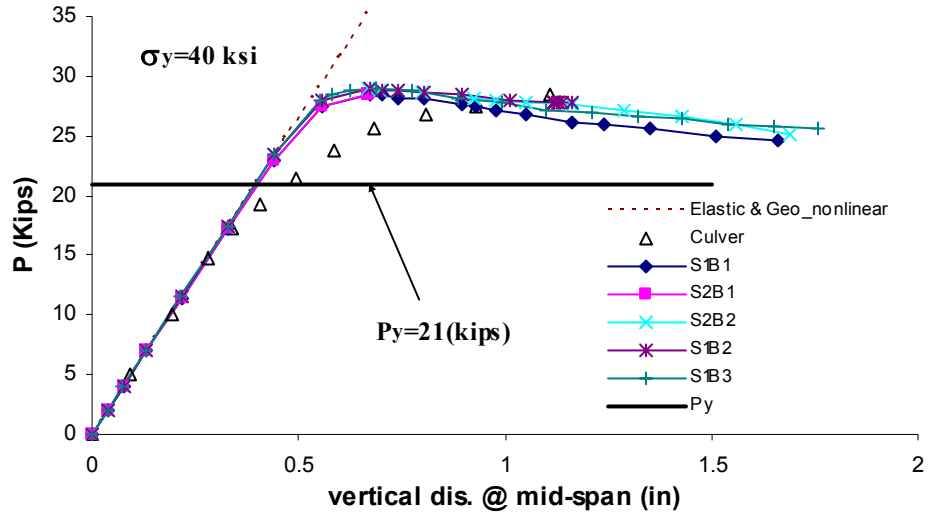


Figure 6.6b Load and vertical deflection of Specimen L2A

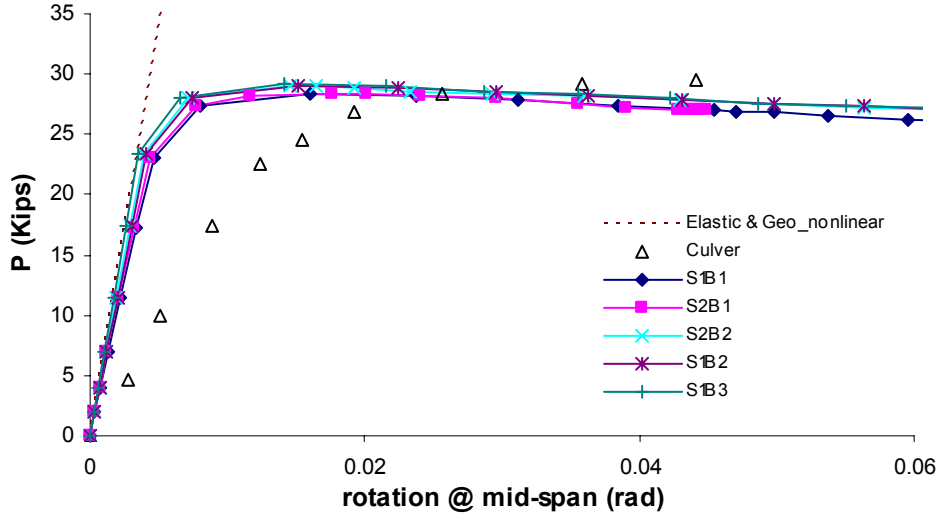


Figure 6.7a Load and rotation of specimen L1A

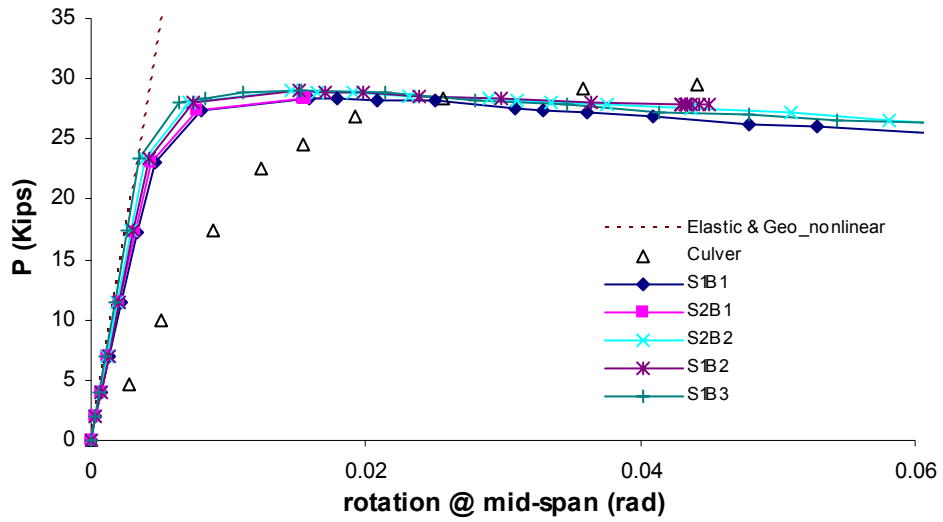


Figure 6.7b Load and rotation of specimen L2A

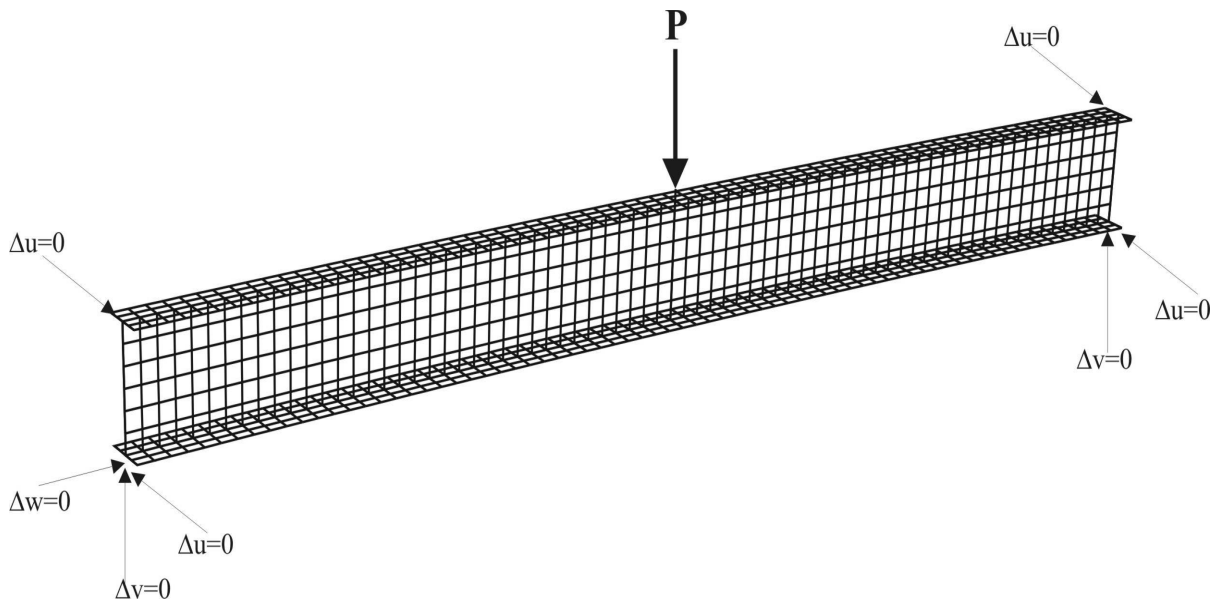


Figure 6.8 Boundary and Loading Condition of Beams Tested by Fukumoto and Nakai

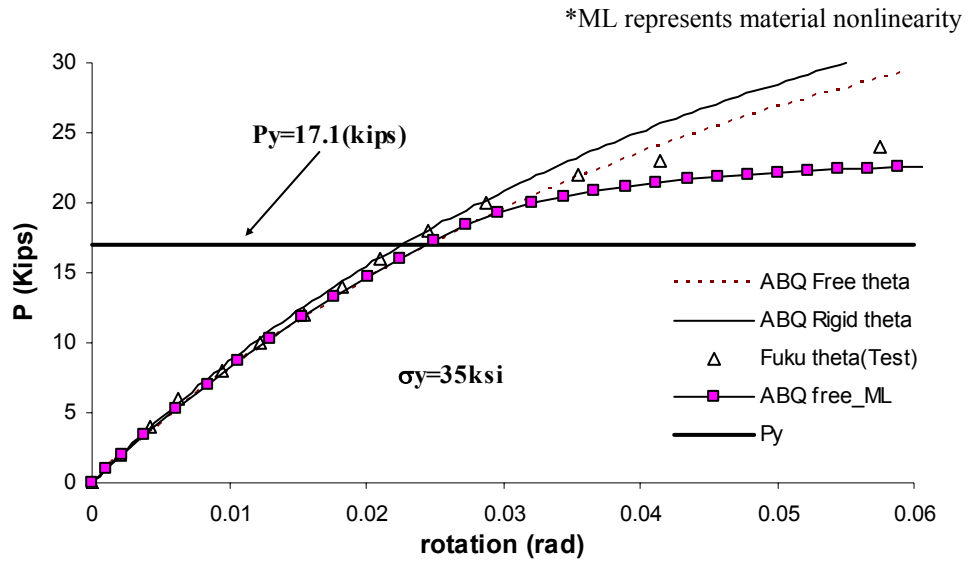


Figure 6.9 Load and rotation of Specimen AR1

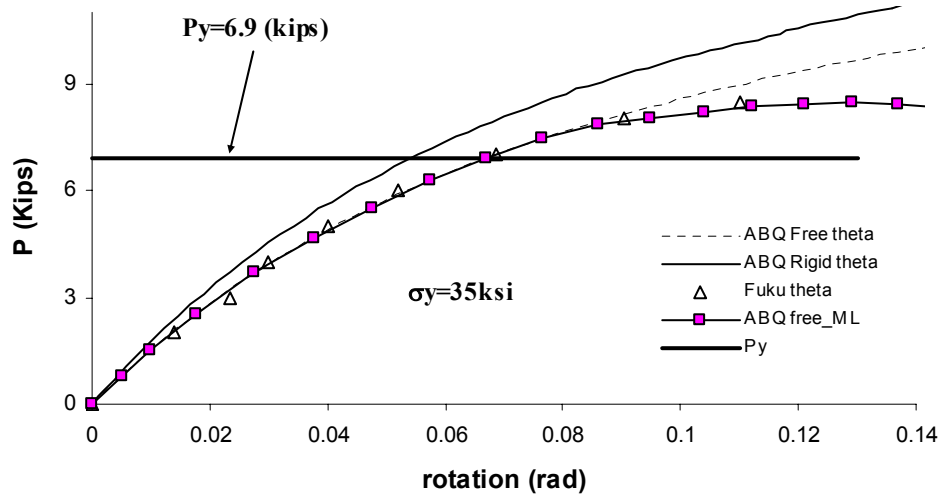


Figure 6.10 Load and rotation of Specimen BR1

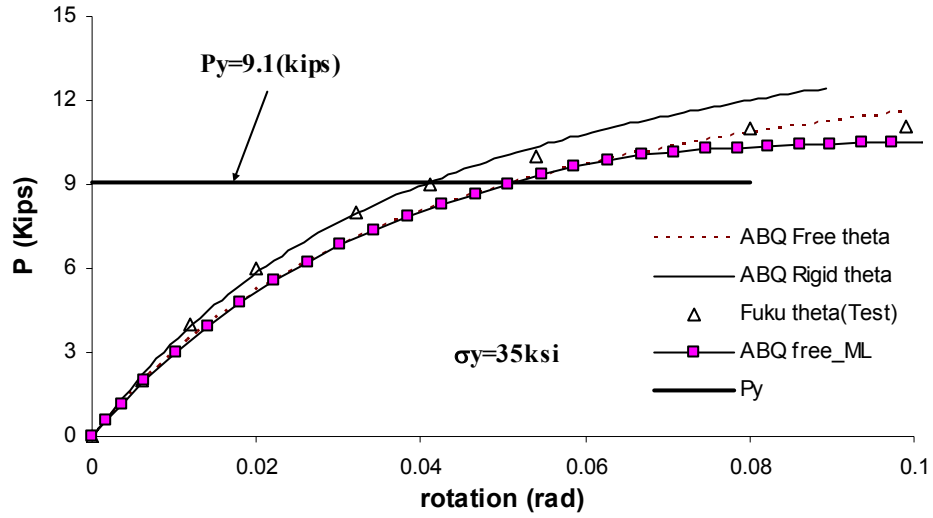


Figure 6.11 Load and rotation of Specimen BR2

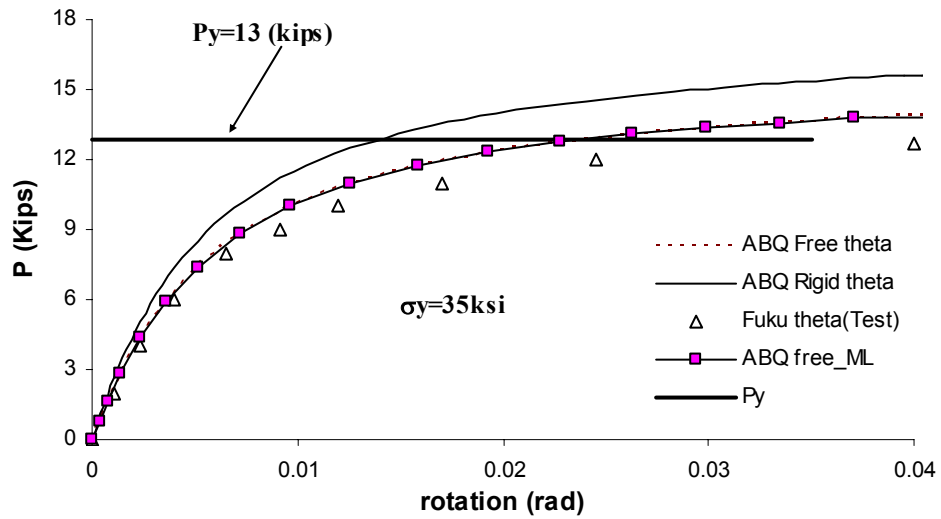


Figure 6.12 Load and rotation of Specimen BR3

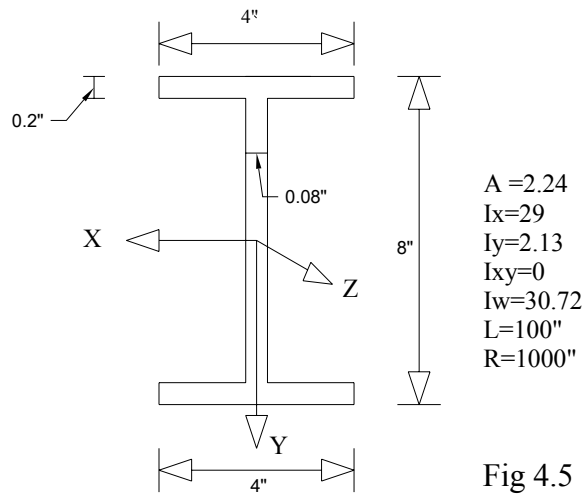


Fig 4.5

Figure 6.13 Dimension and Properties of Beam

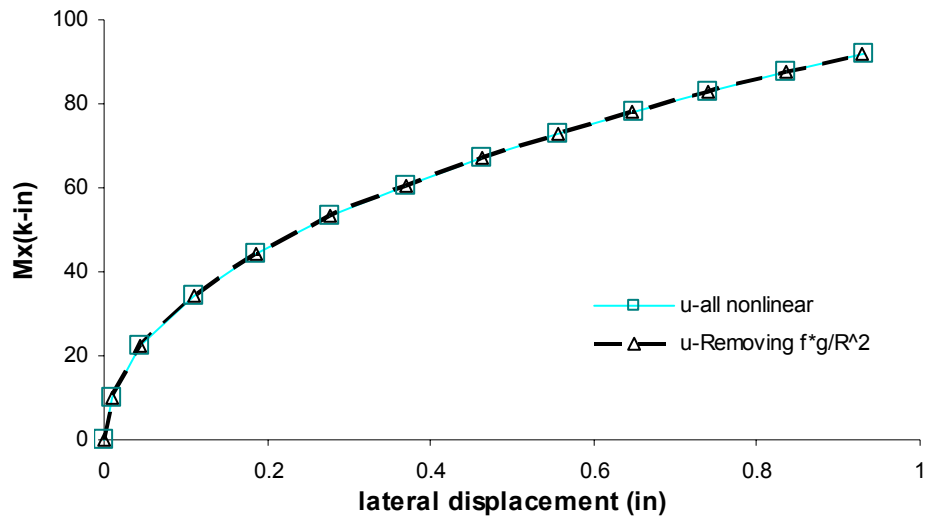


Figure 6.14 Load and Lateral Displacement for Approximation a)

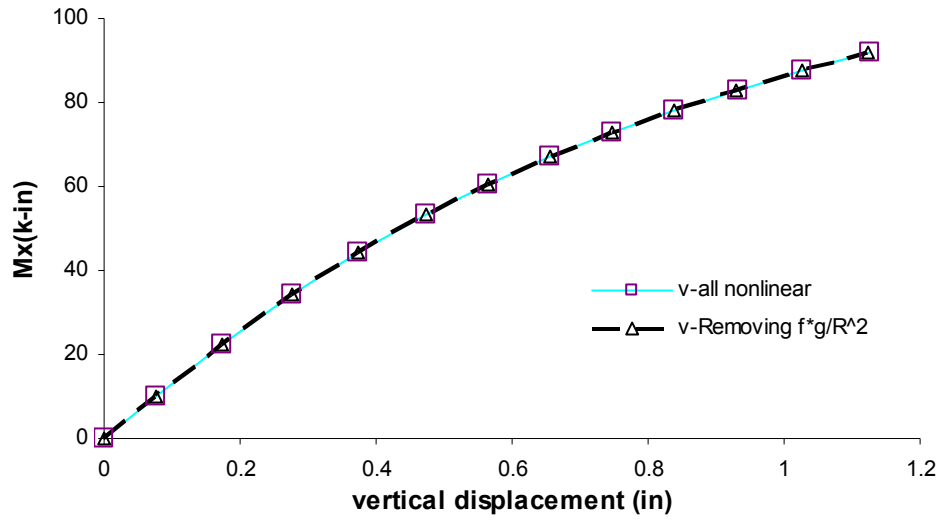


Figure 6.15 Load and Vertical Displacement for Approximation a)

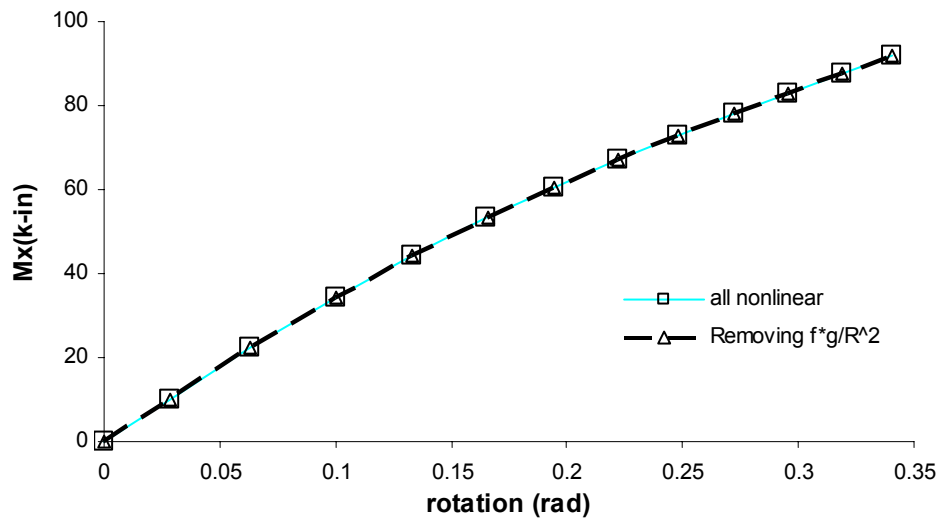


Figure 6.16 Load and Rotation for Approximation a)

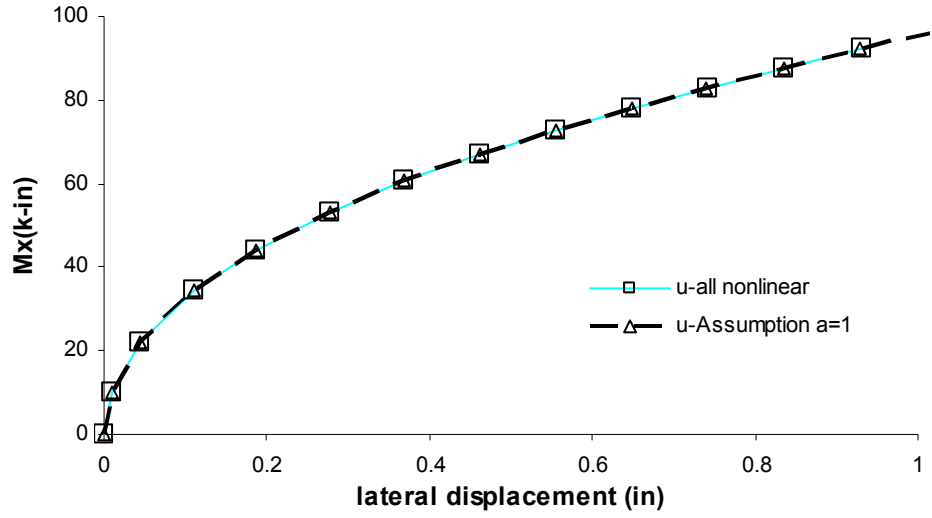


Figure 6.17 Load and lateral displacement for Approximations a) + b)

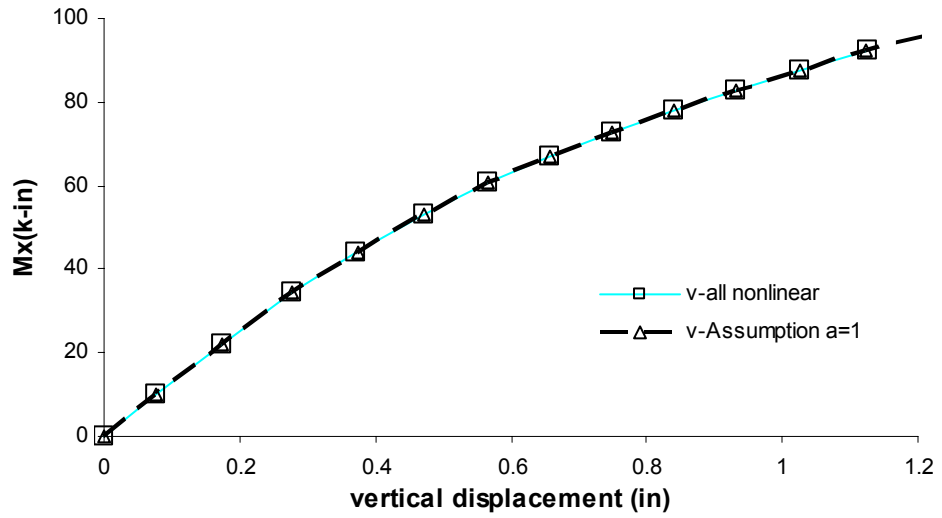


Figure 6.18 Load and vertical displacement for Approximations a) + b)

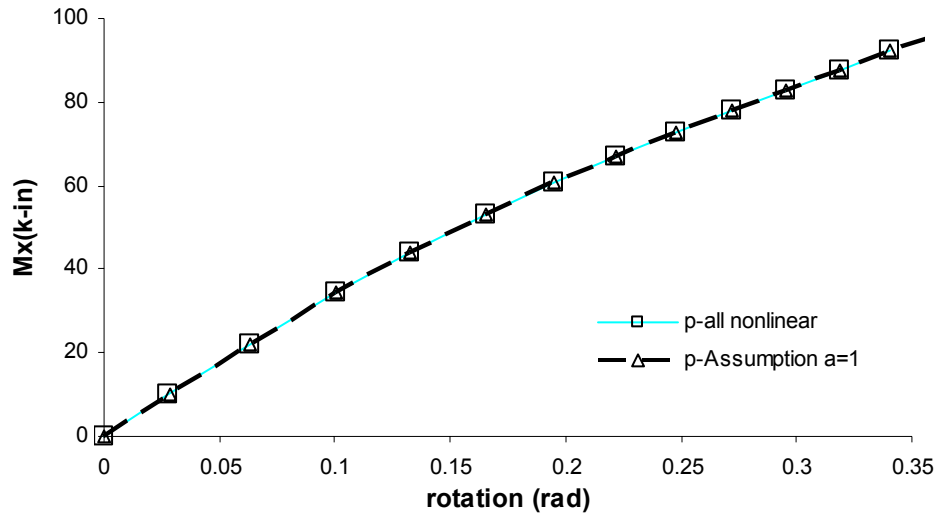


Figure 6.19 Load and rotation for Approximations a) + b)

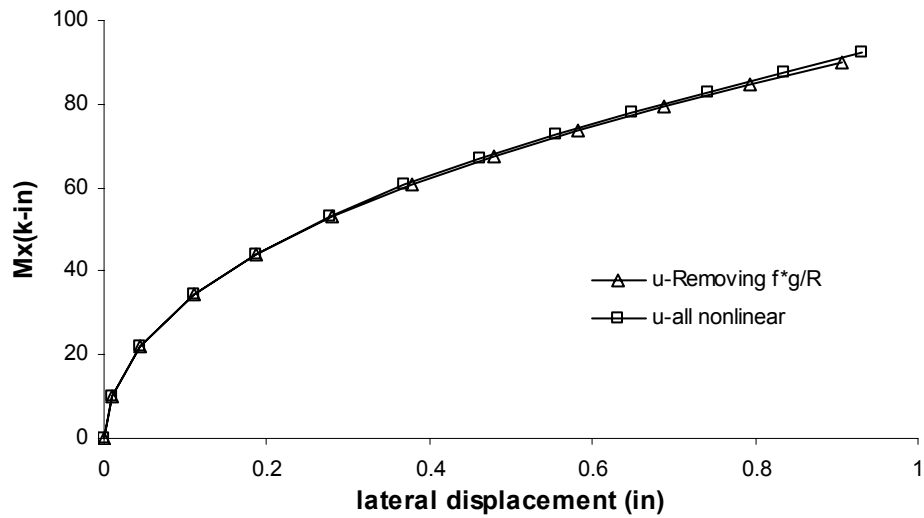


Figure 6.20 Load and lateral displacement for Approximations a) + b) + c)

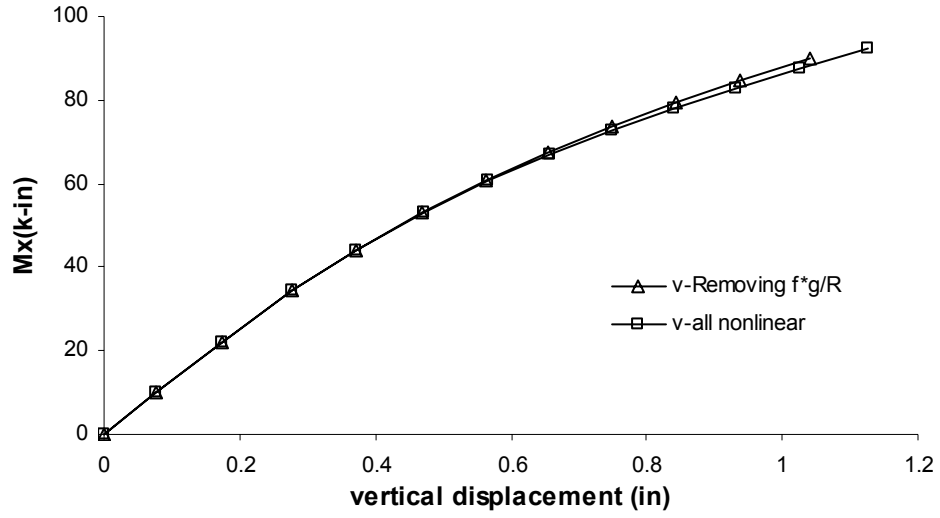


Figure 6.21 Load and vertical displacement for Approximations a) + b) + c)

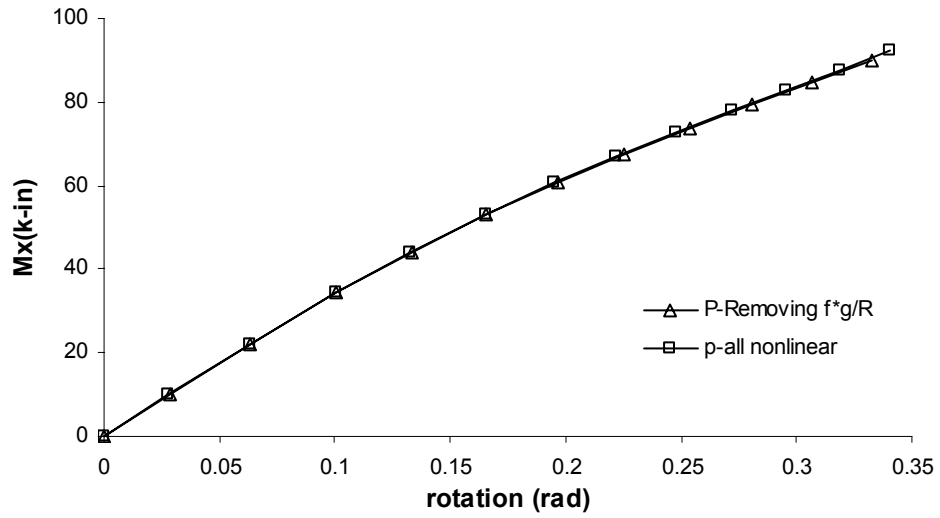


Figure 6.22 Load and rotation for Approximations a) + b) + c)

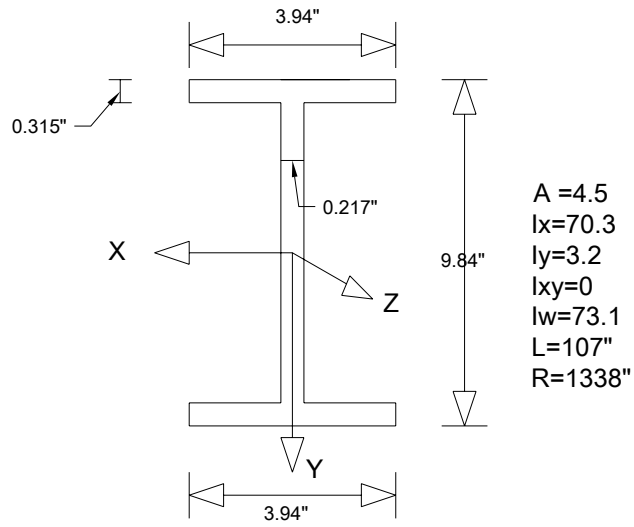


Figure 6.23 Doubly Symmetric Cross Section for Numerical Studies

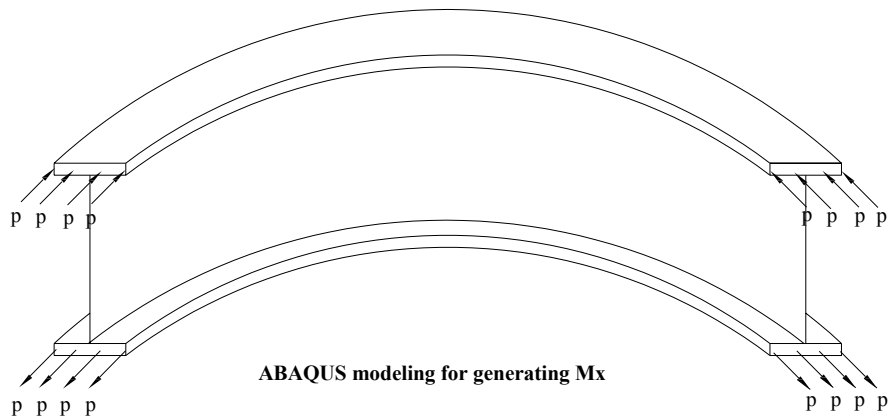


Figure 6.24a Model for M_x

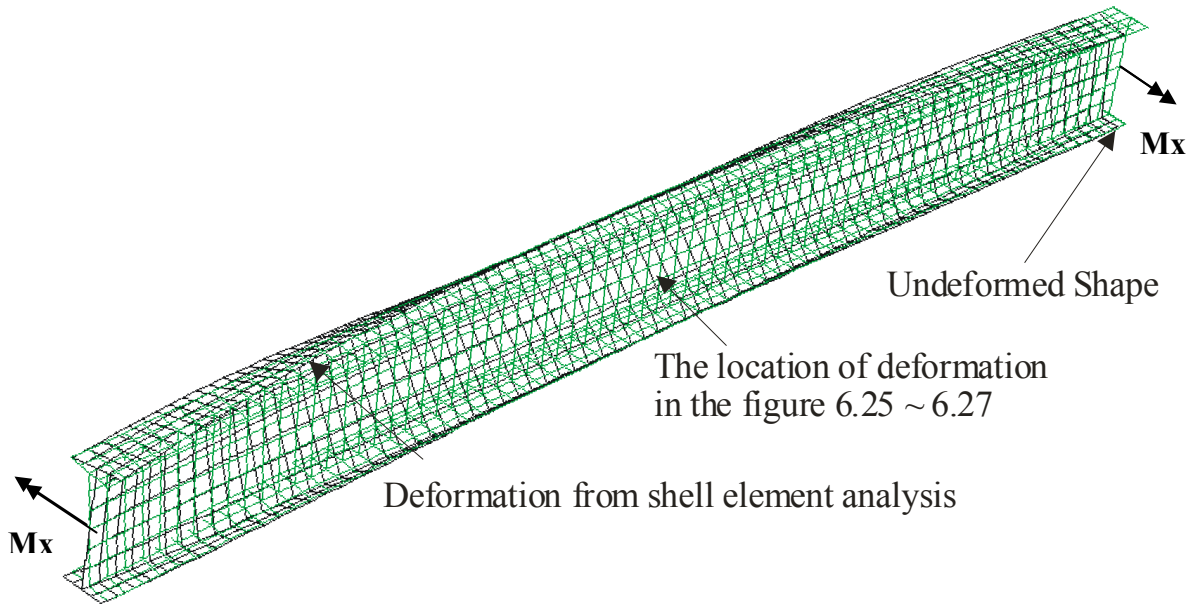


Figure 6.24b Vertical Bending Moment and Deformed Shapes

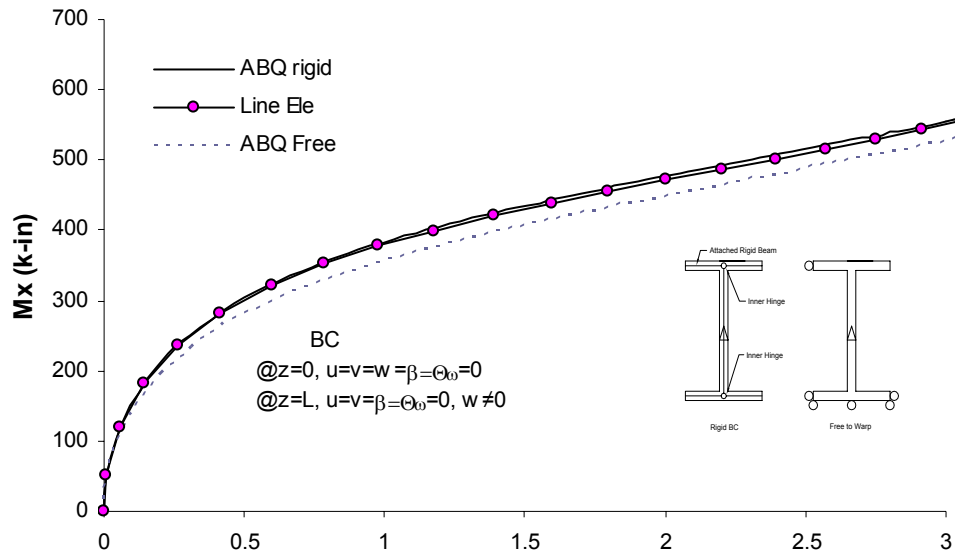


Figure 6.25 Lateral Displacement Due to Vertical bending moment

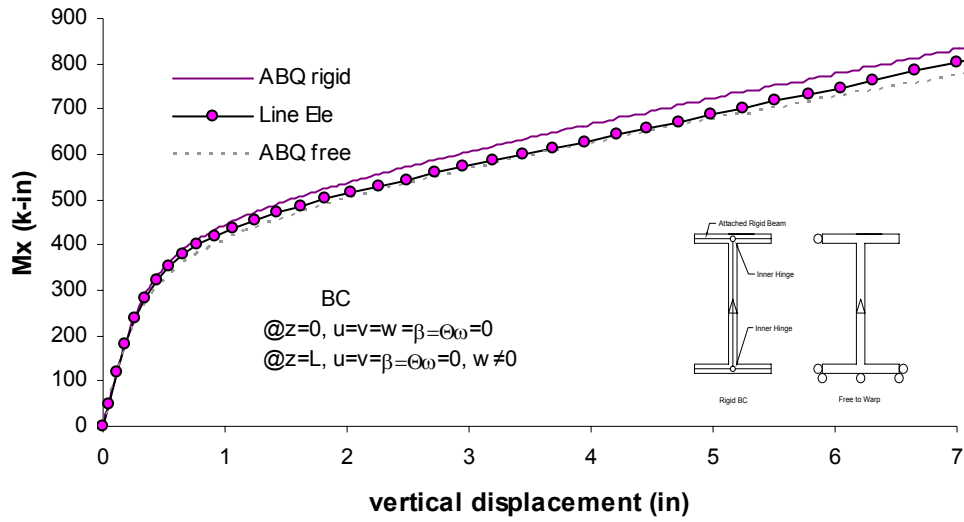


Figure 6.26 Vertical Displacement Due to Vertical bending moment

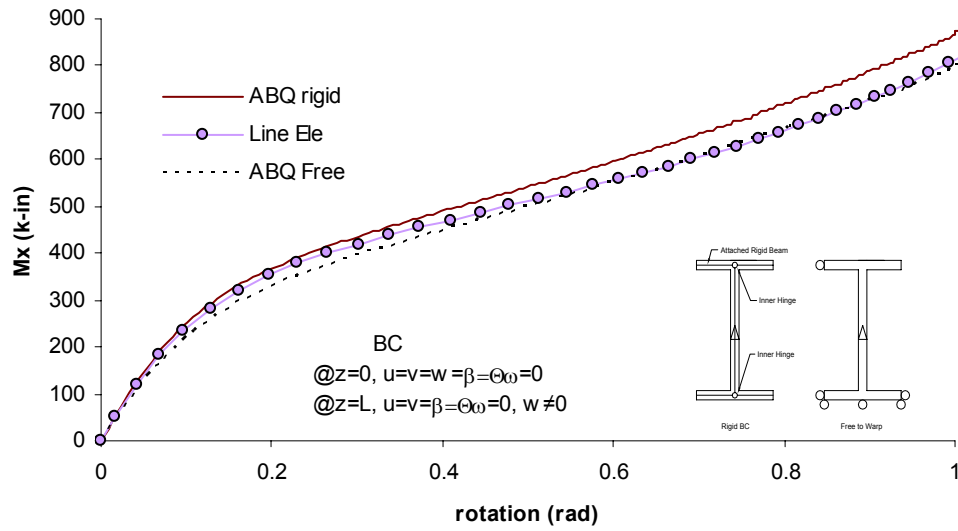


Figure 6.27 Rotation Due to Vertical bending moment

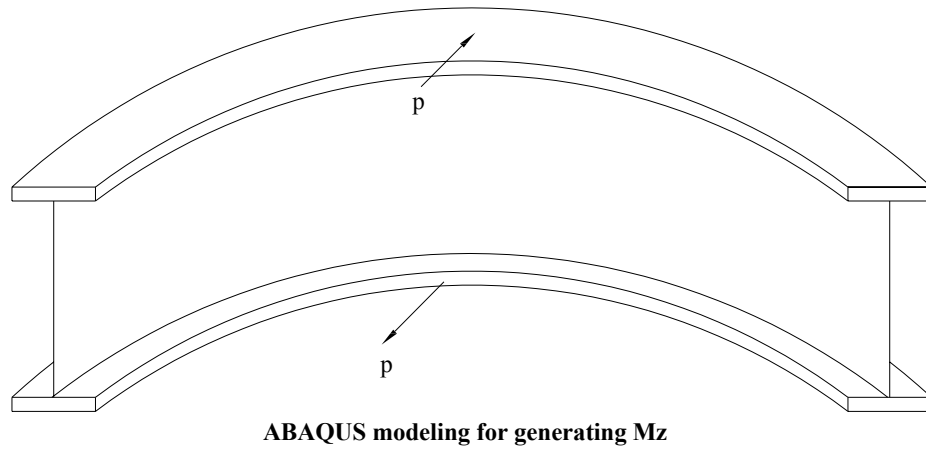


Figure 6.28a Point Loads for Torsional Moment M_z

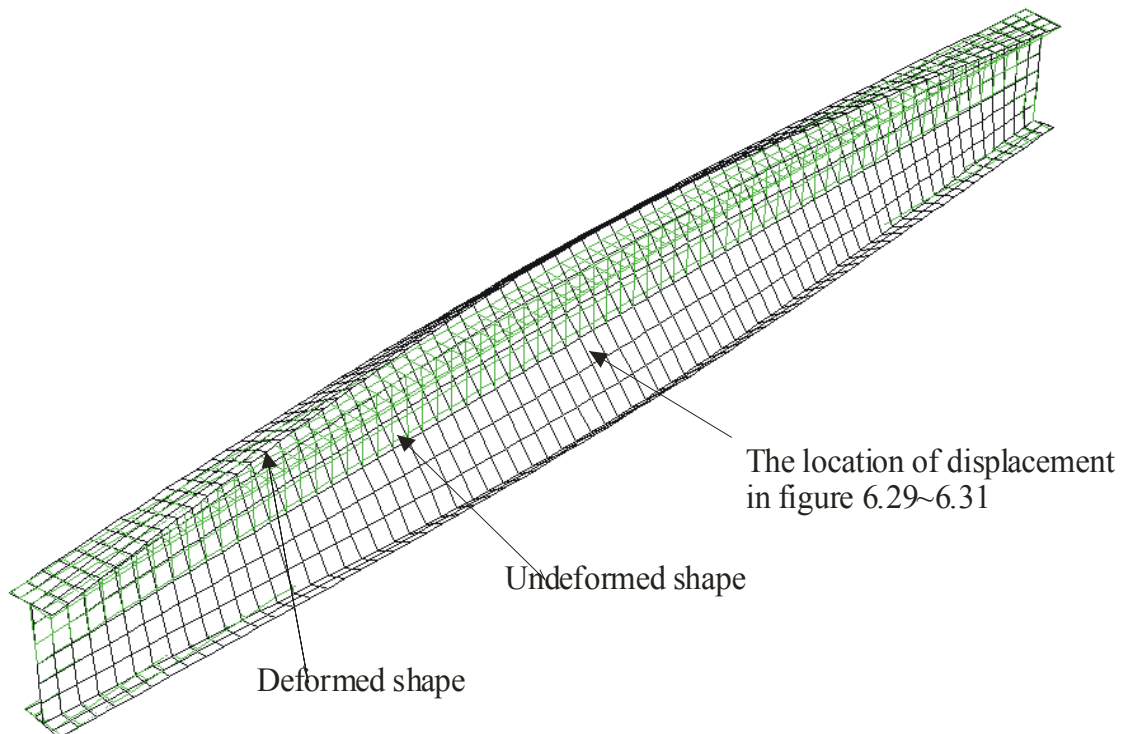


Figure 6.28b Deformation of Curved Beam Due to M_z

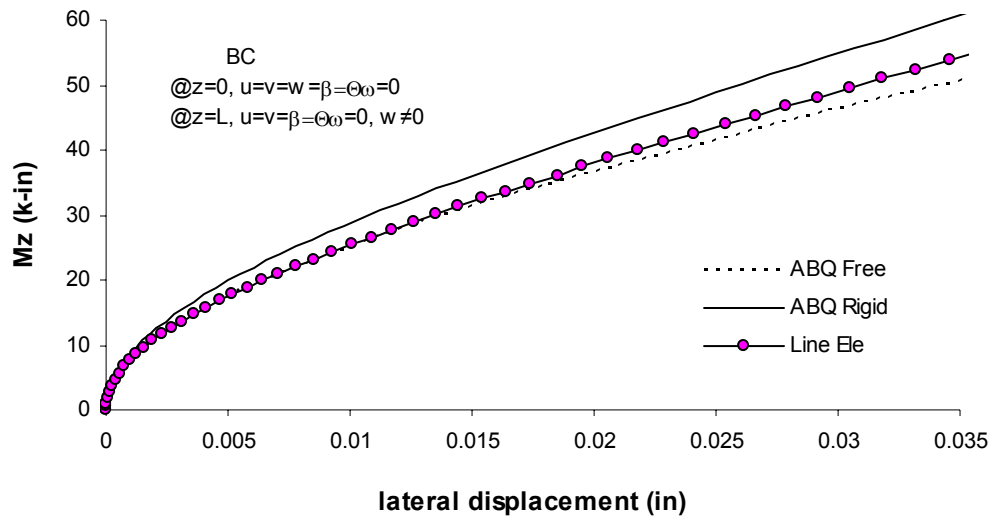


Figure 6.29 Lateral Displacement Due To Mz

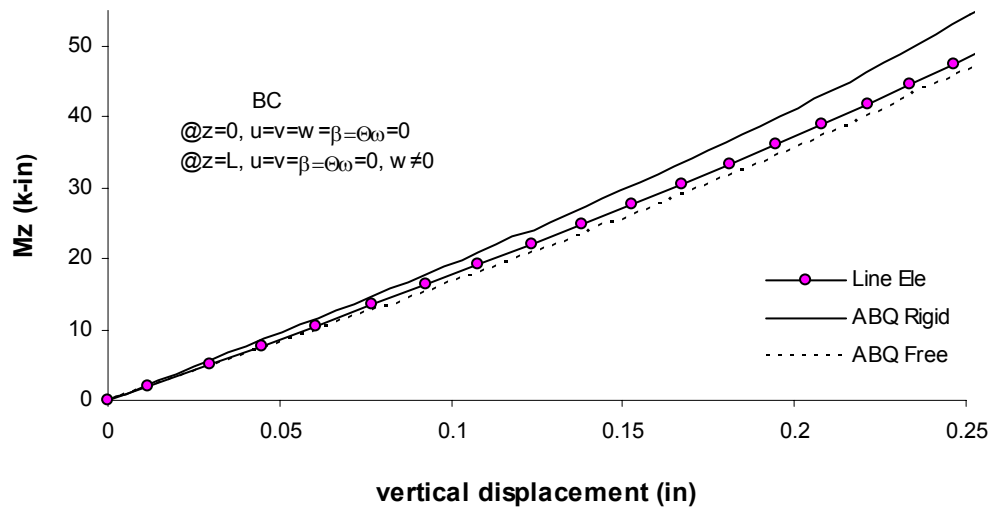


Figure 6.30 Load and vertical displacement generated from torsional moment

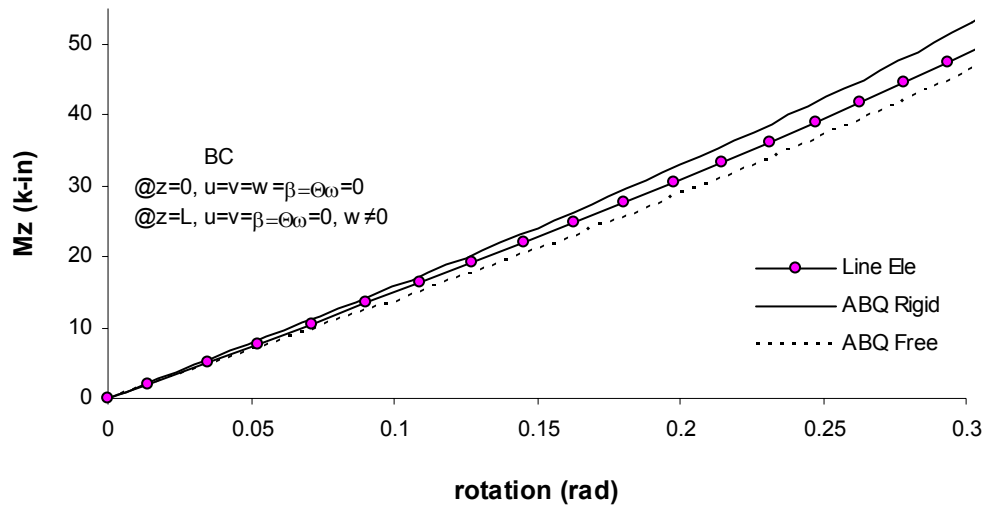


Figure 6.31 Rotation Due To Mz

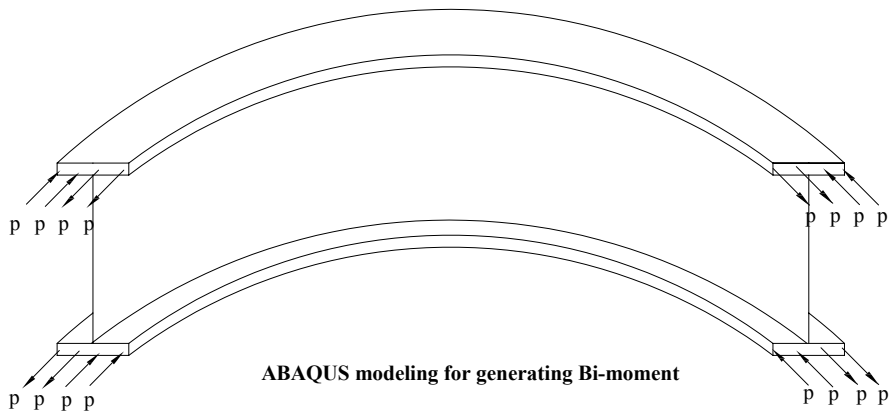


Figure 6.32a The Point Loads for Bi-moment

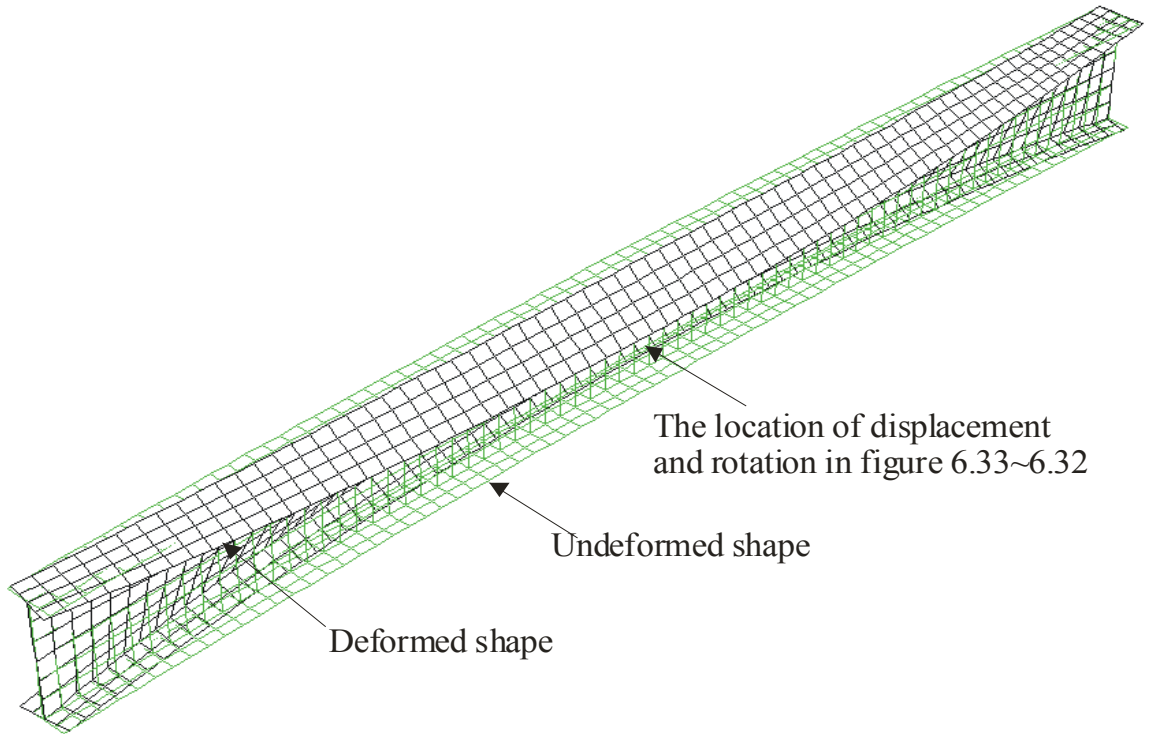


Figure 6.32b Deformation Shape by Bi-Moment

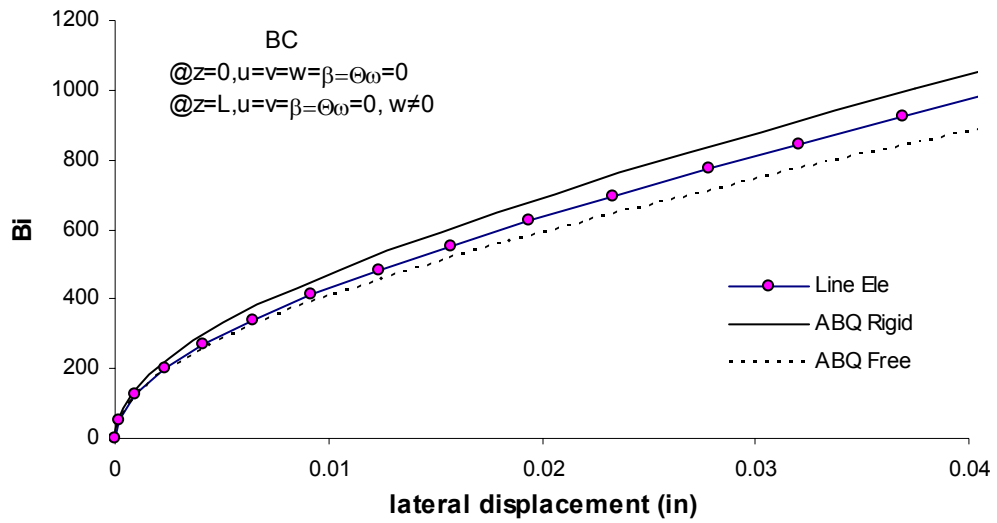


Figure 6.33 Lateral Displacement Due to bi-moment

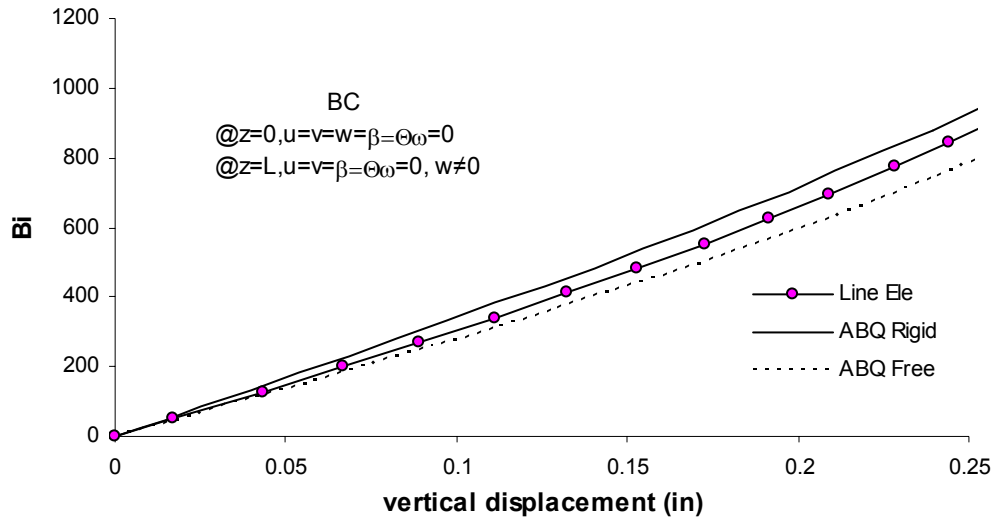


Figure 6.34 Vertical Displacement due to Bi-Moment

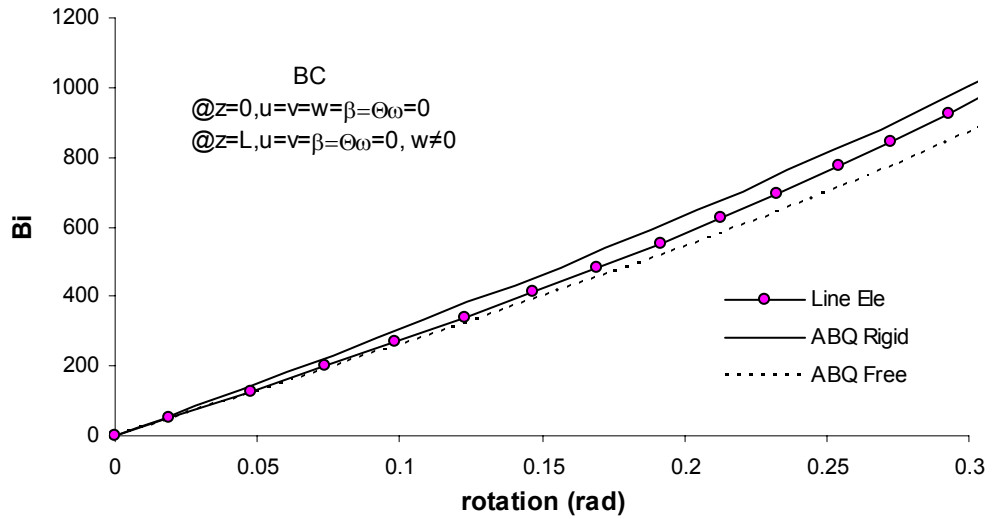


Figure 6.35 Rotation due to Bi-Moment

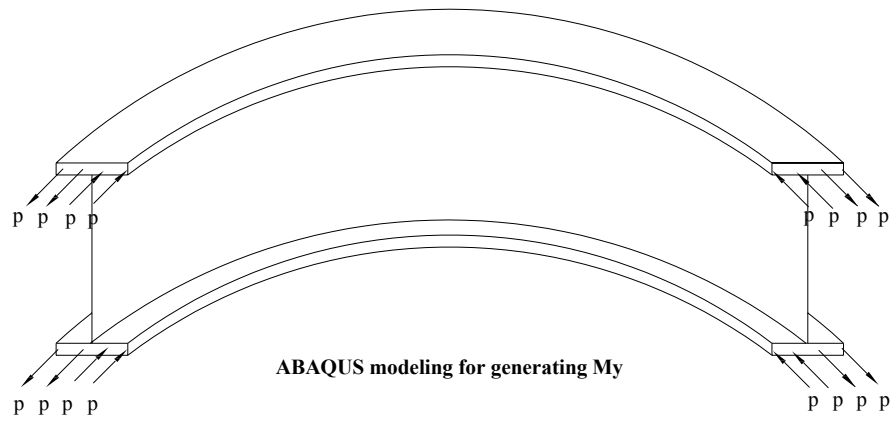


Figure 6.36a Point Loading System for Lateral Bending Moment, M_y

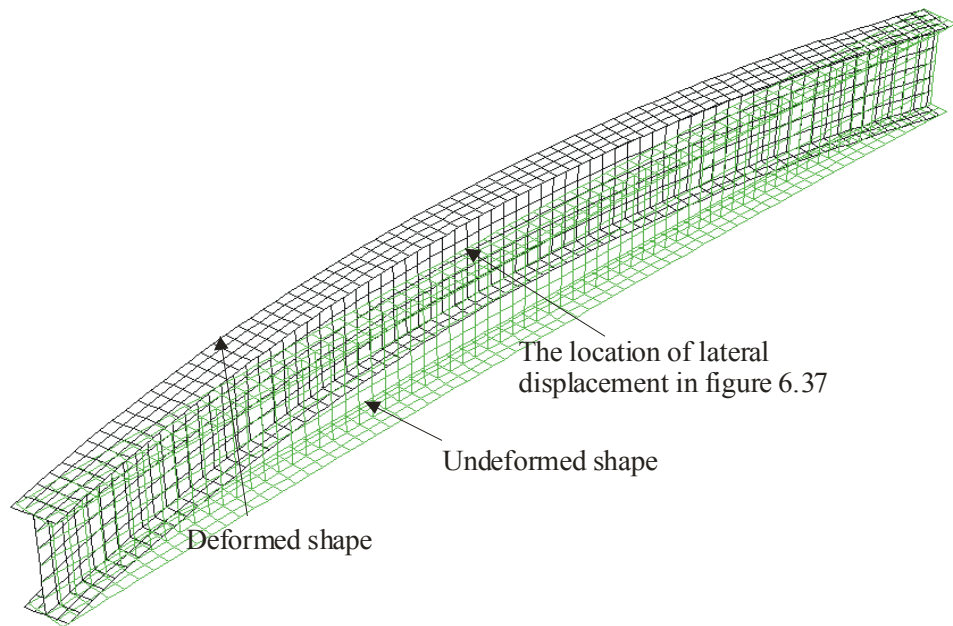


Figure 6.36b Deformation Shape by the Lateral Bending Moment

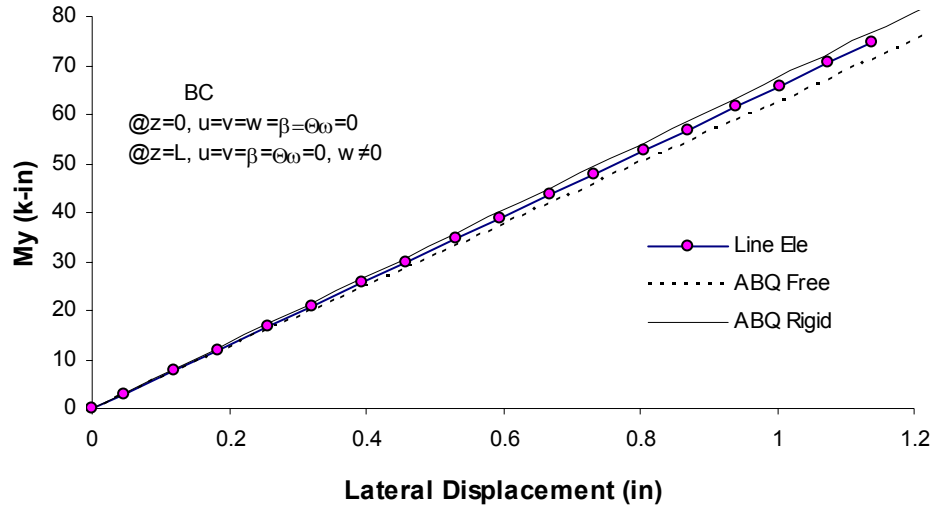


Figure 6.37 Lateral Displacement due to lateral bending moment, My

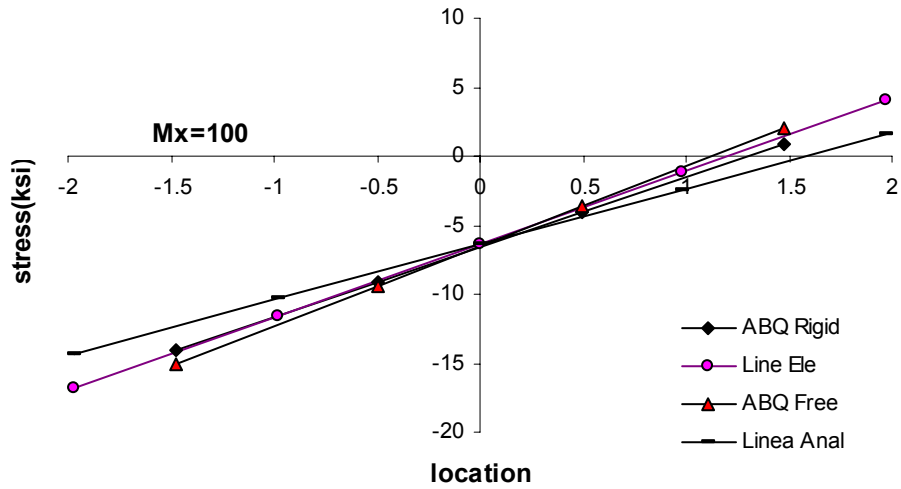


Figure 6.38 Stress Distribution of Top Flange at Mx= (100 k-in)

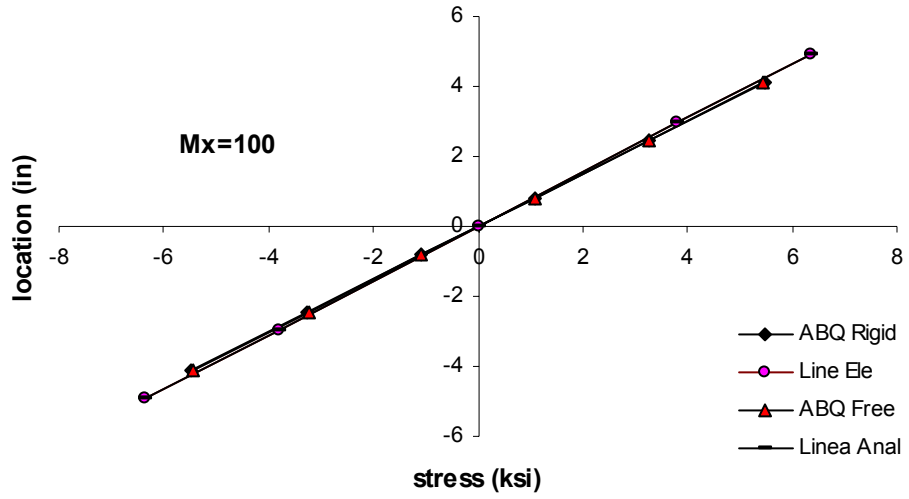


Figure 6.39 Stress Distribution of Web at Mx= (100 k-in)

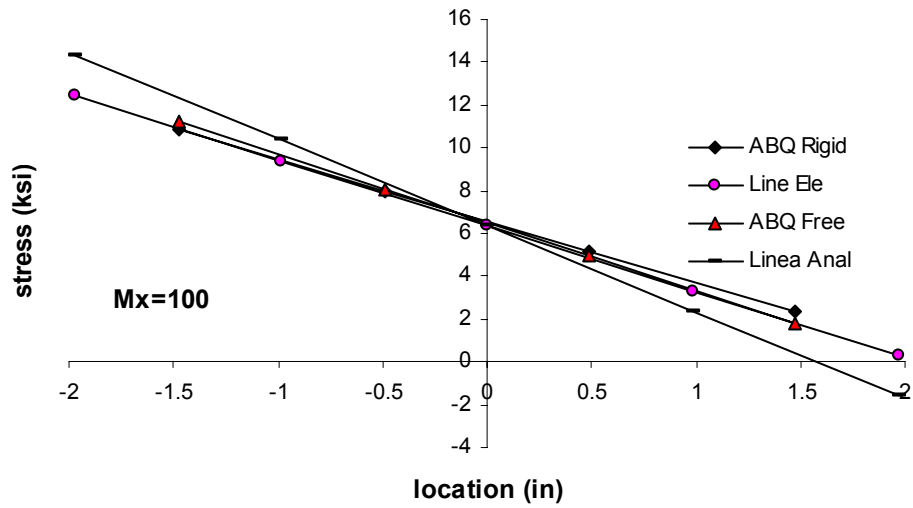


Figure 6.40 Stress Distribution of Bottom Flange at Mx= (100 k-in)

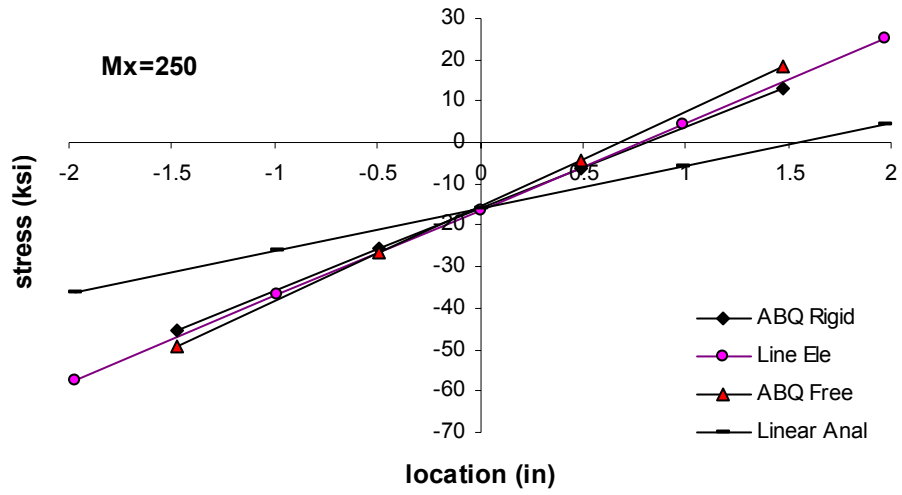


Figure 6.41 Stress Distribution of Top Flange at Mx= (250 k-in)

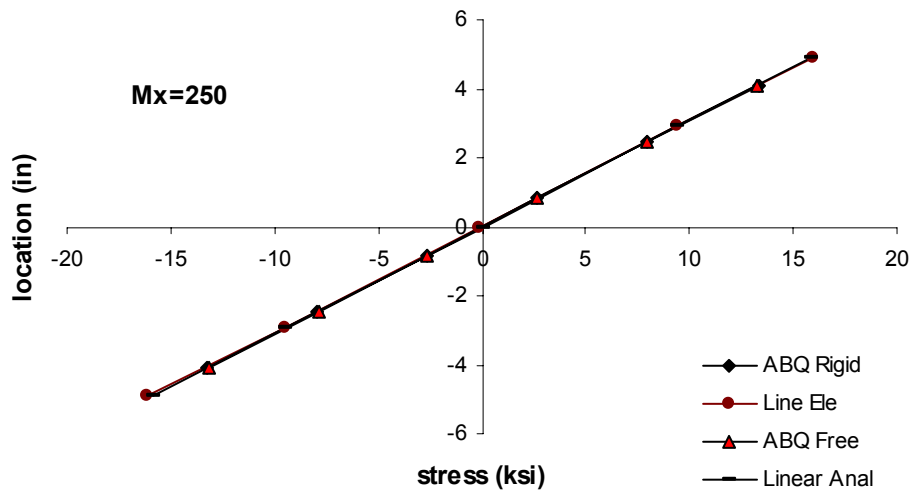


Figure 6.42 Stress Distribution of Web at Mx= (250 k-in)

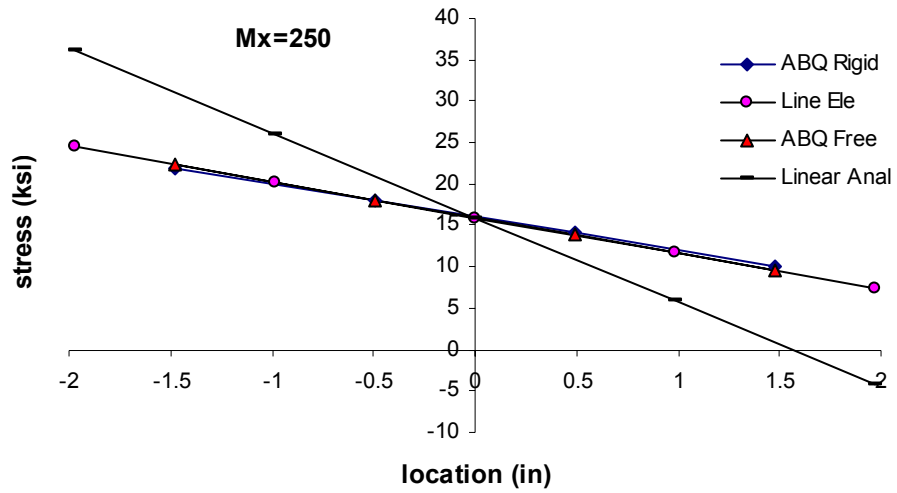


Figure 6.43 Stress Distribution of Bottom Flange at $M_x = (250 \text{ k-in})$

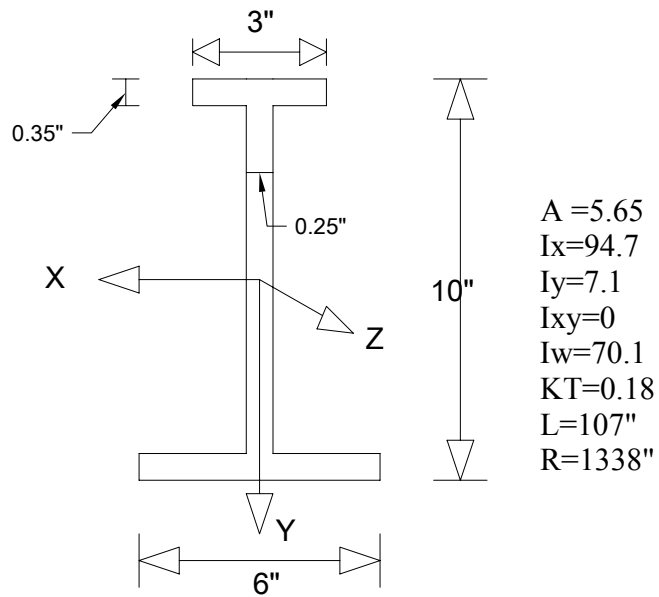


Figure 6.44 Singly Symmetric Cross Section and Sectional Properties

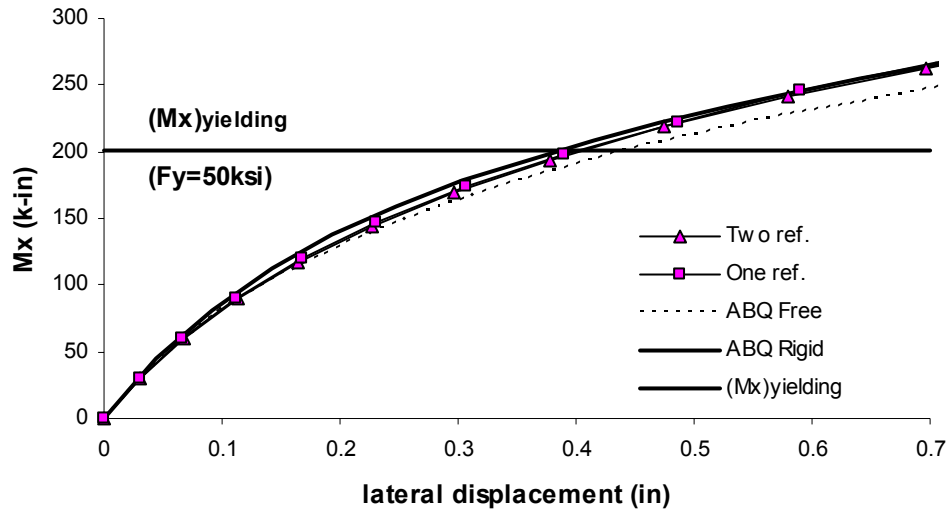


Figure 6.45 Lateral Displacement due to Vertical Bending Moment, Singly Symmetric I-Shape

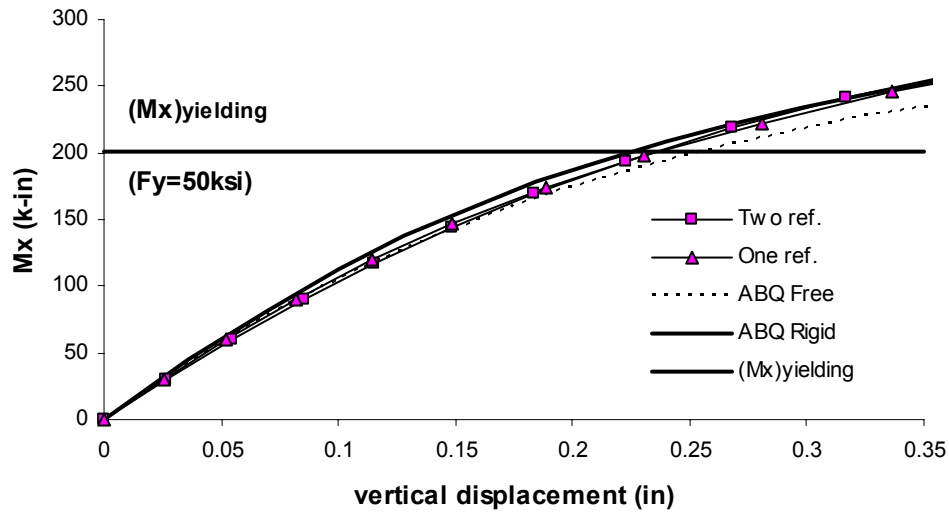


Figure 6.46 Vertical Displacements due to Vertical Bending Moment, Singly Symmetric I-Shape

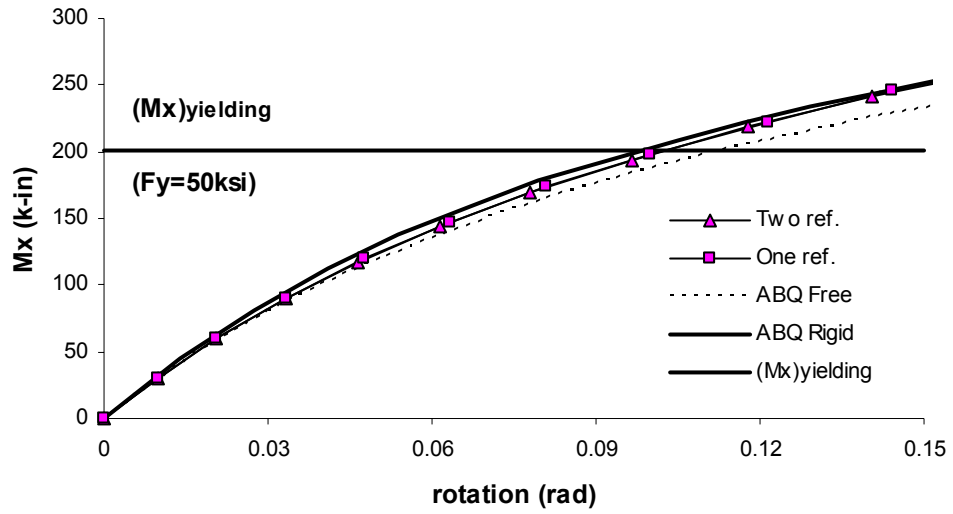


Figure 6.47 Rotations from Vertical Bending Moment, Singly Symmetric I-Shape

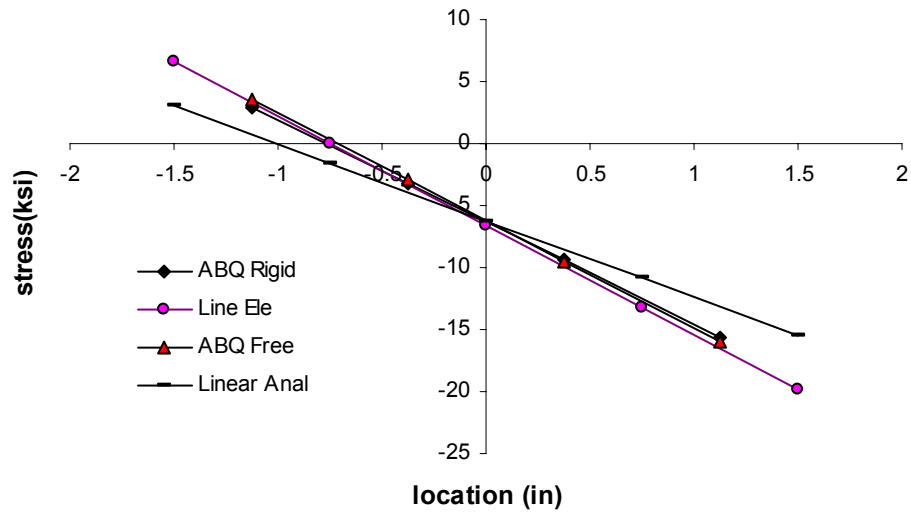


Figure 6.48 Stress Distribution of Top Flange at $M_x = (100 \text{ k-in})$, Singly Symmetric I-Shape

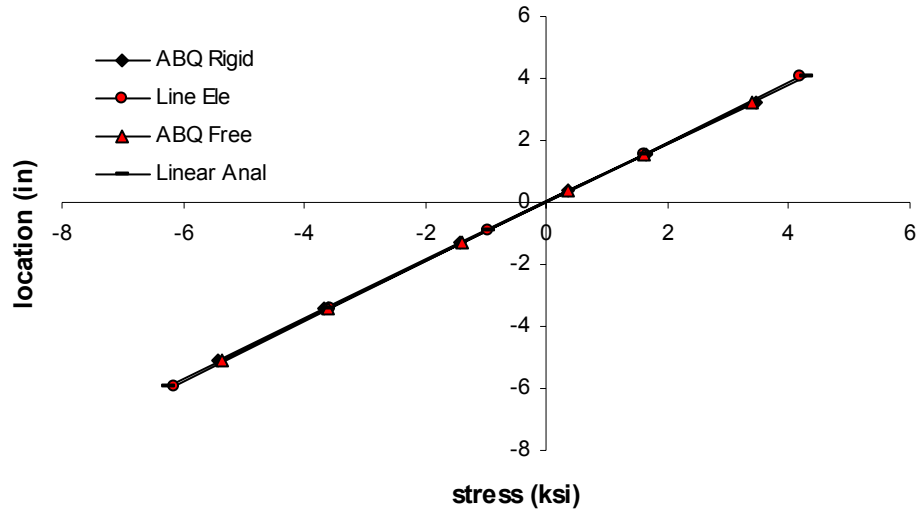


Figure 6.49 Stress Distribution of Web at $M_x = (100 \text{ k-in})$, Singly Symmetric I-Shape

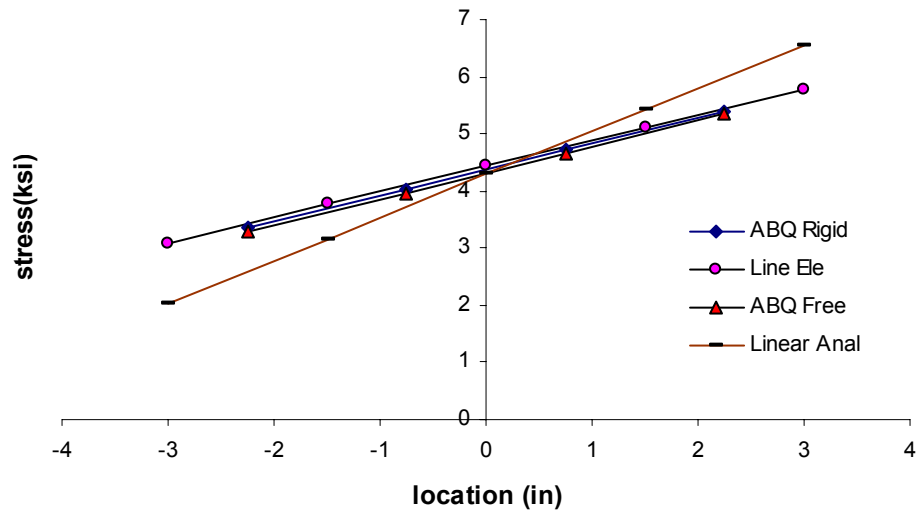


Figure 6.50 Stress Distribution of Bottom Flange at $M_x = (100 \text{ k-in})$, Singly Symmetric I-Shape

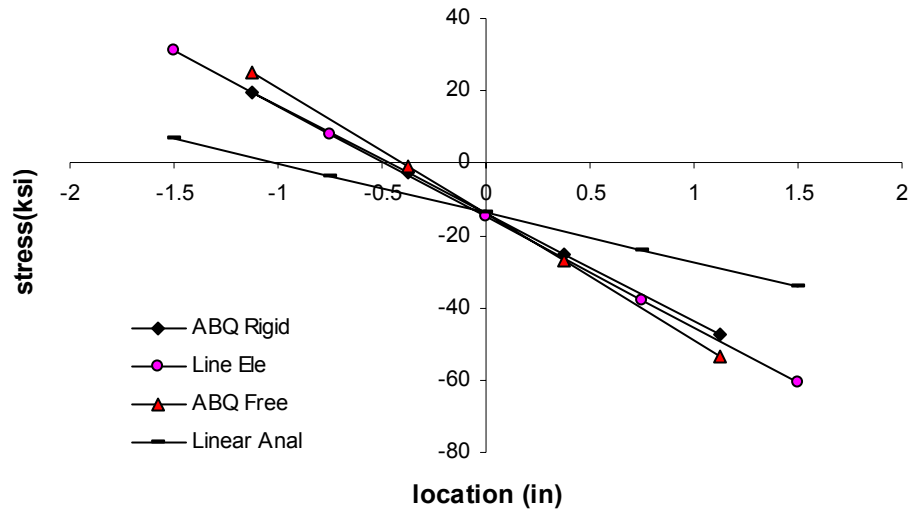


Figure 6.51 Stress Distribution of Top Flange at $M_x = (220 \text{ k-in})$, Singly Symmetric I-Shape

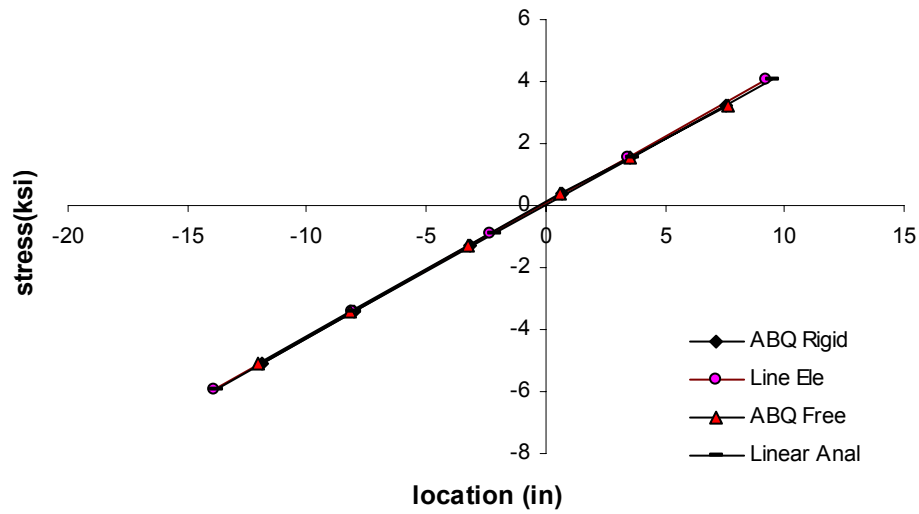


Figure 6.52 Stress Distribution of Web at $M_x = (220 \text{ k-in})$, Singly Symmetric I-Shape

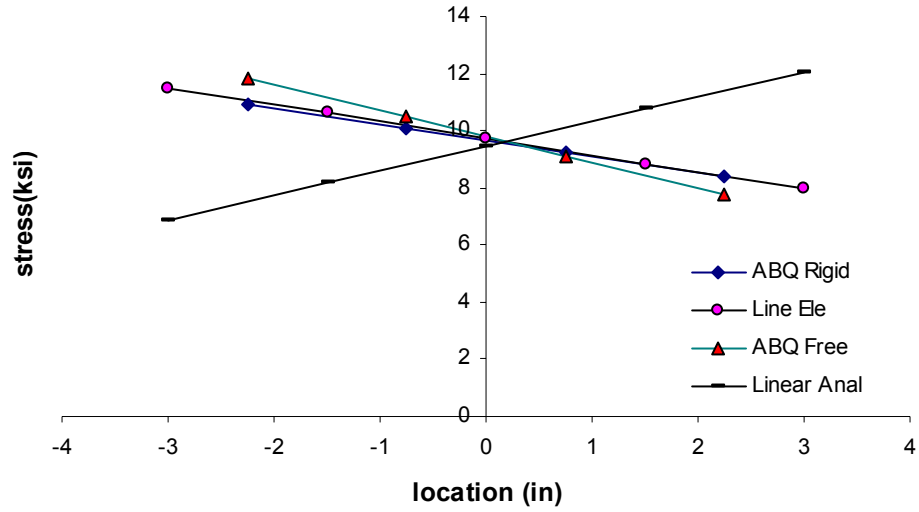


Figure 6.53 Stress Distribution of Bottom Flange at $M_x = (220 \text{ k-in})$, Singly Symmetric I-Shape

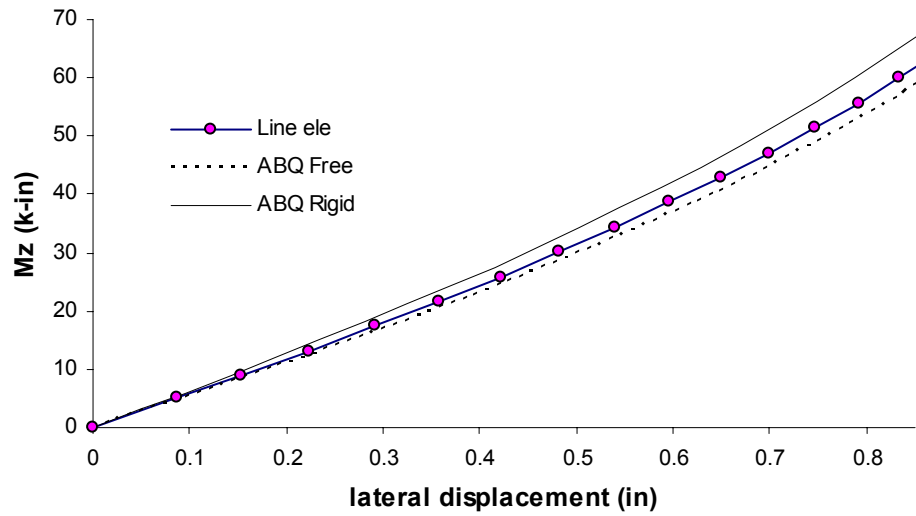


Figure 6.54 Lateral Displacement by Torsional Moment, Singly Symmetric I-Shape

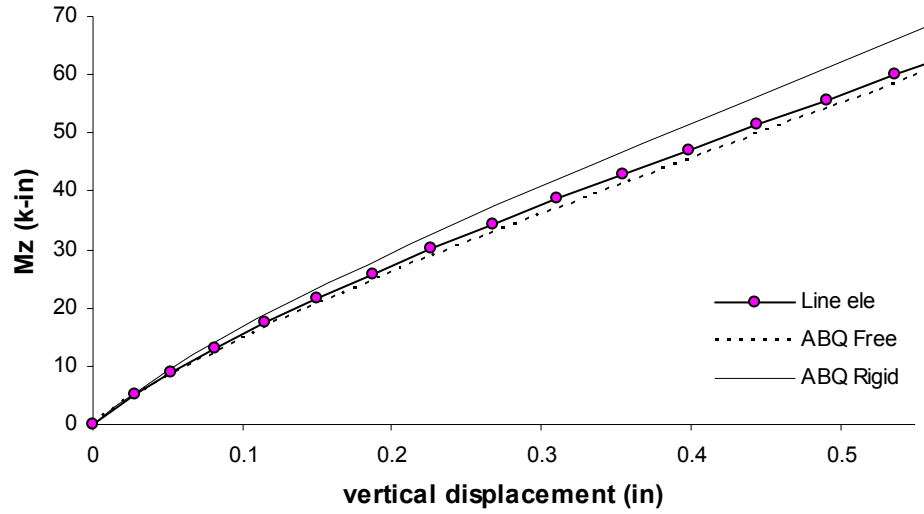


Figure 6.55 Vertical Displacements by Torsional Moment, Singly Symmetric I-Shape

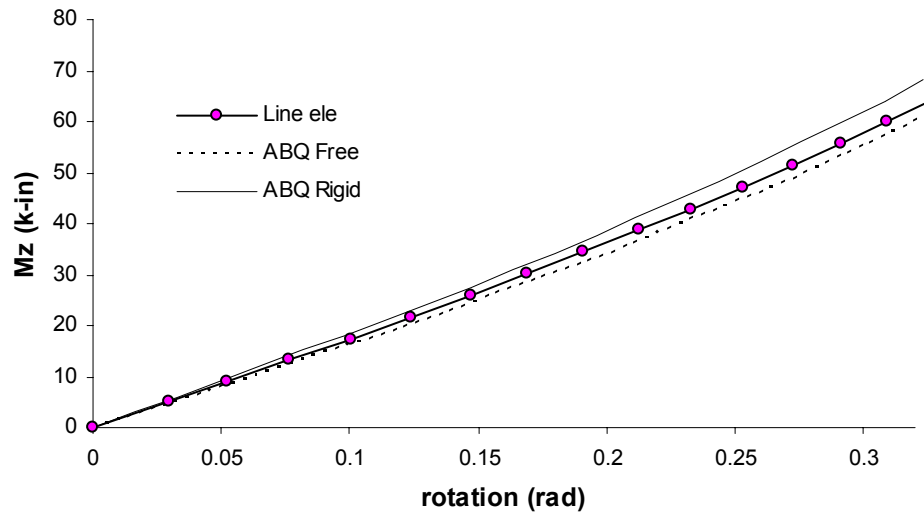


Figure 6.56 Rotation by Torsional Moment, Singly Symmetric I-Shape

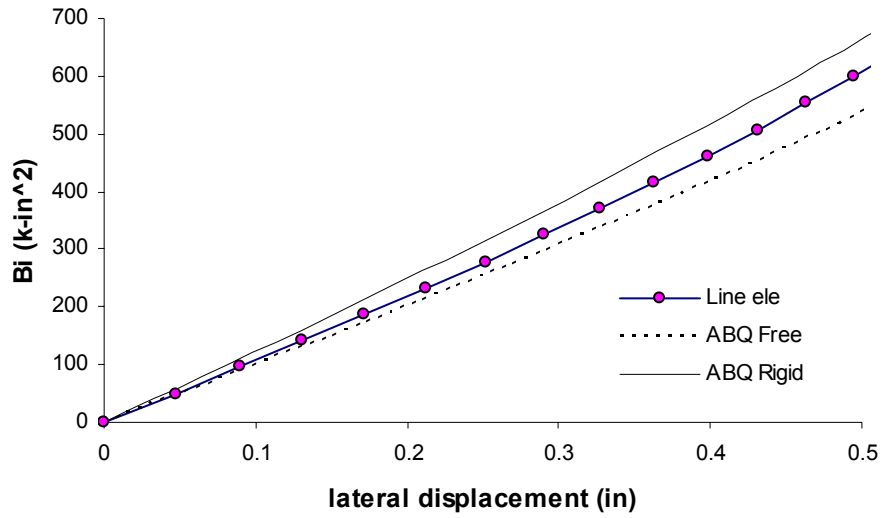


Figure 6.57 Lateral Displacements by Bi-Moment, Singly Symmetric I-Shape

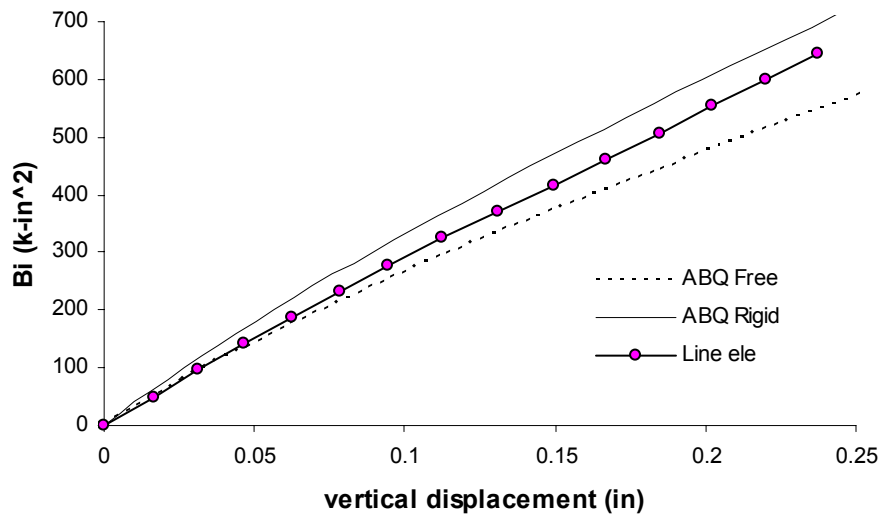


Figure 6.58 Vertical Displacement by Bi-Moment, Singly Symmetric I-Shape

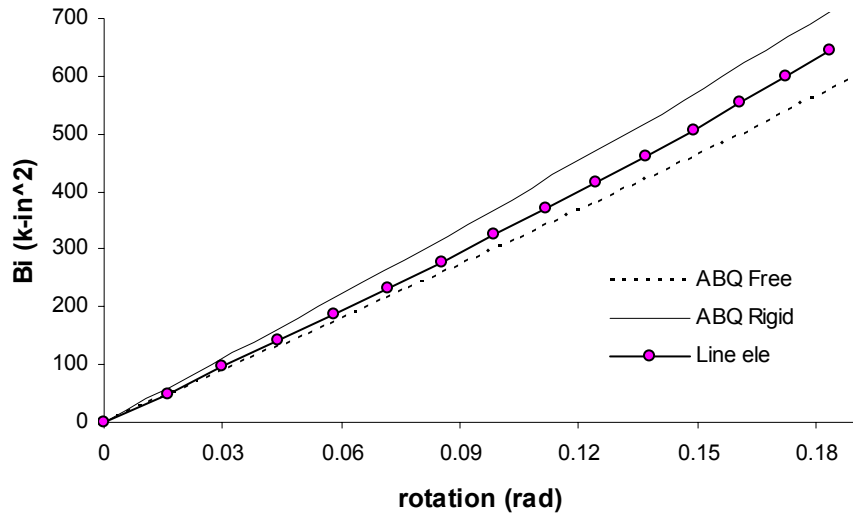


Figure 6.59 Rotations by Bi-Moment, Singly Symmetric I-Shape

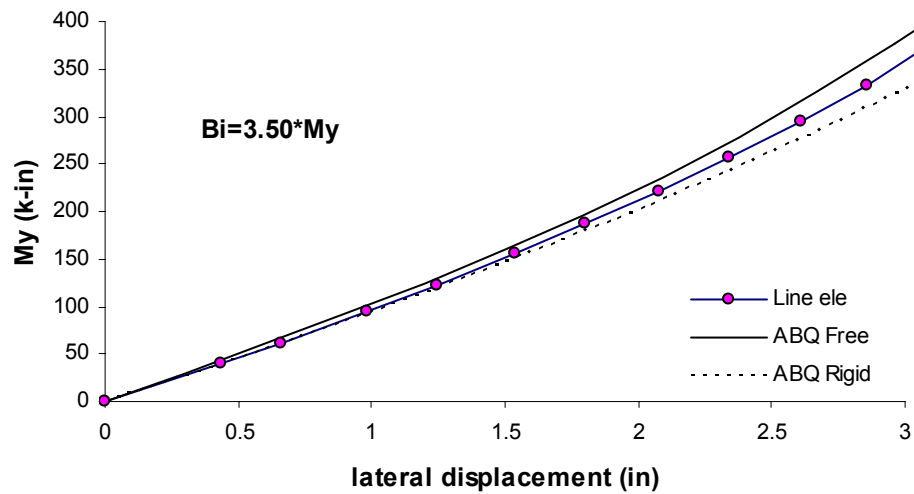


Figure 6.60 Lateral Displacement by Combined Load My and Bi-moment, Singly Symmetric I-Shape

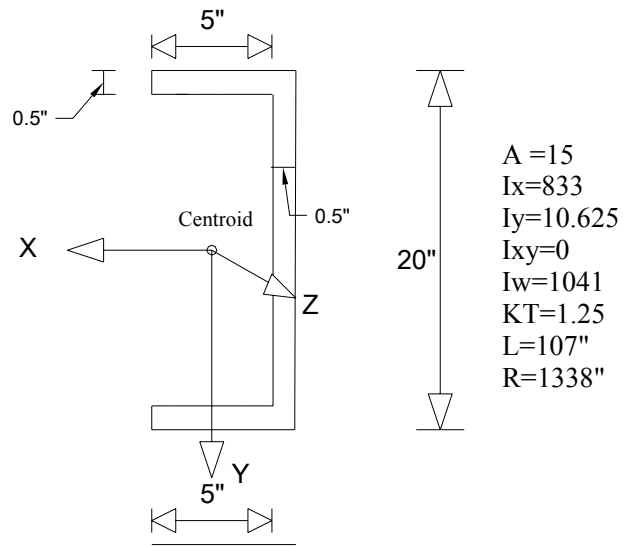


Figure 6.61 Singly Symmetric Channel Section

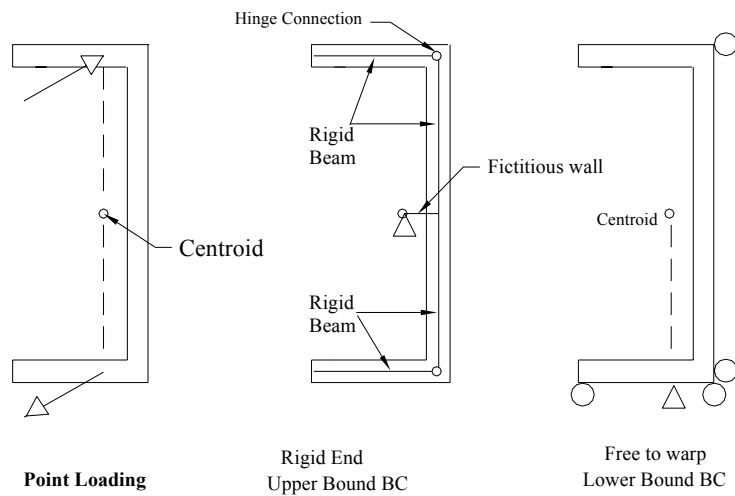


Figure 6.62 Point loads and Boundary Conditions of Symmetric Channel Section

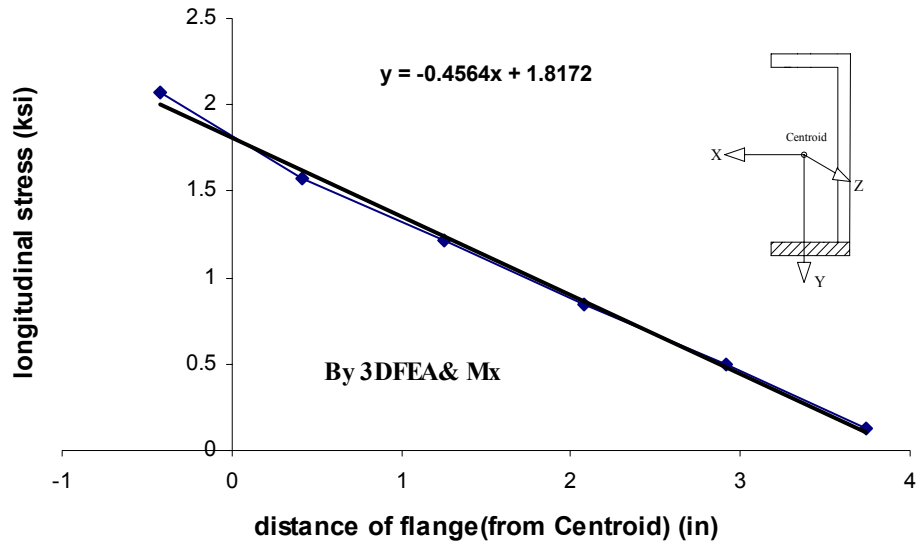


Figure 6.63 Stress Distributions along Bottom Flange by Vertical Bending Moment

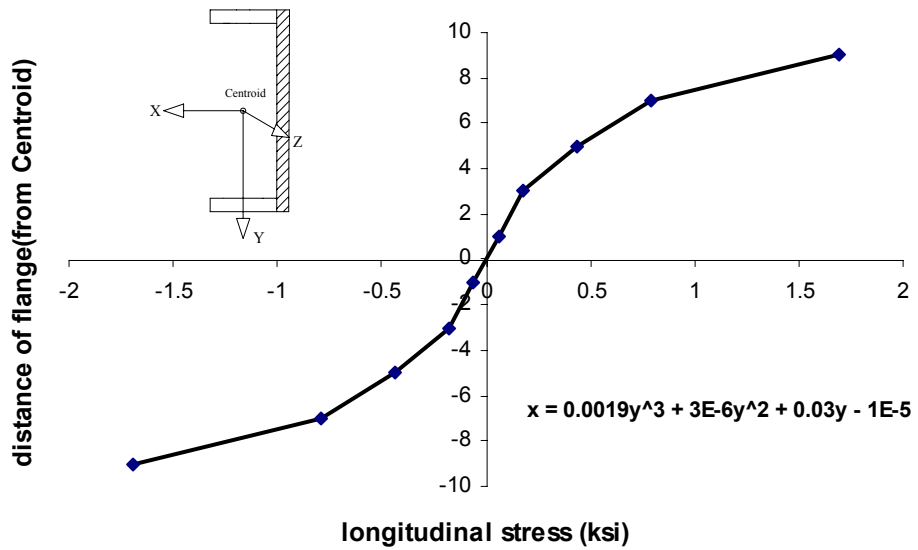


Figure 6.64 Stress Distributions along Web by Vertical Bending Moment

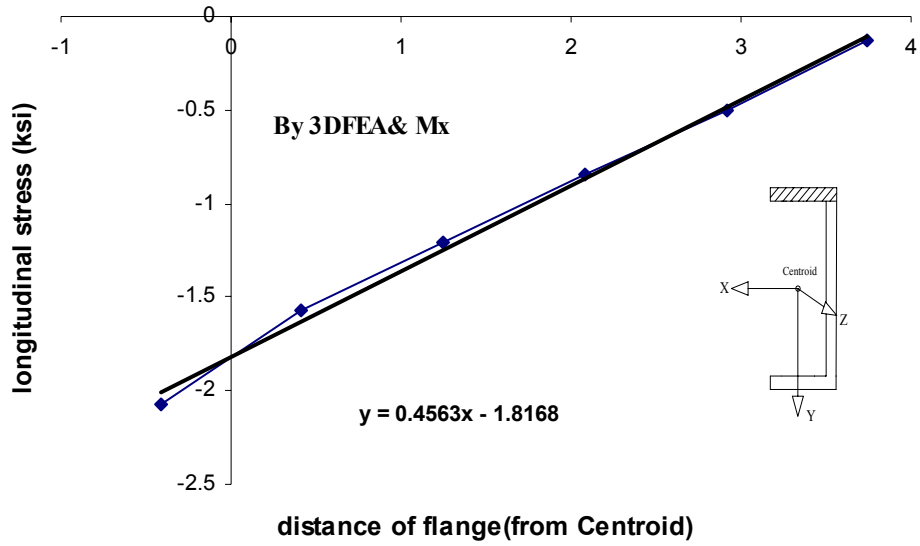


Figure 6.65 Stress Distribution along Top Flange by Vertical Bending Moment

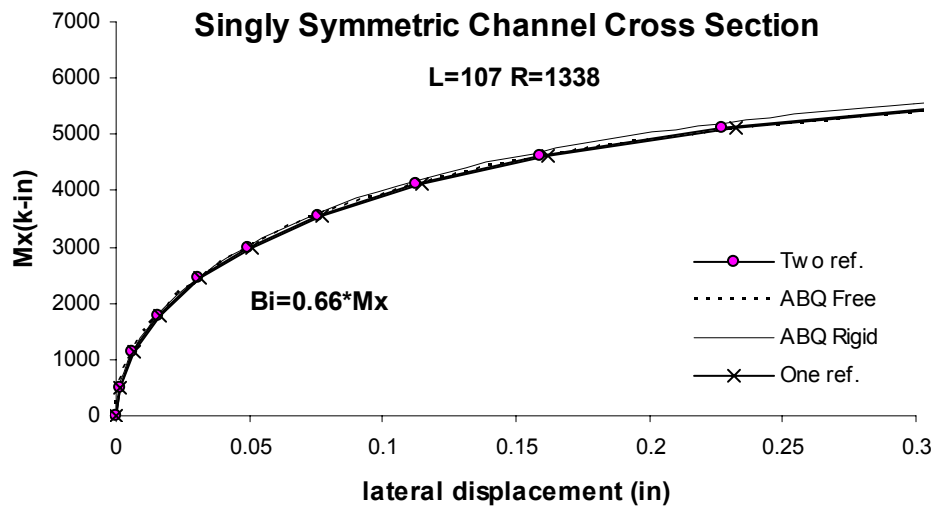


Figure 6.66 Lateral Displacement by Mx and Bi-Moment

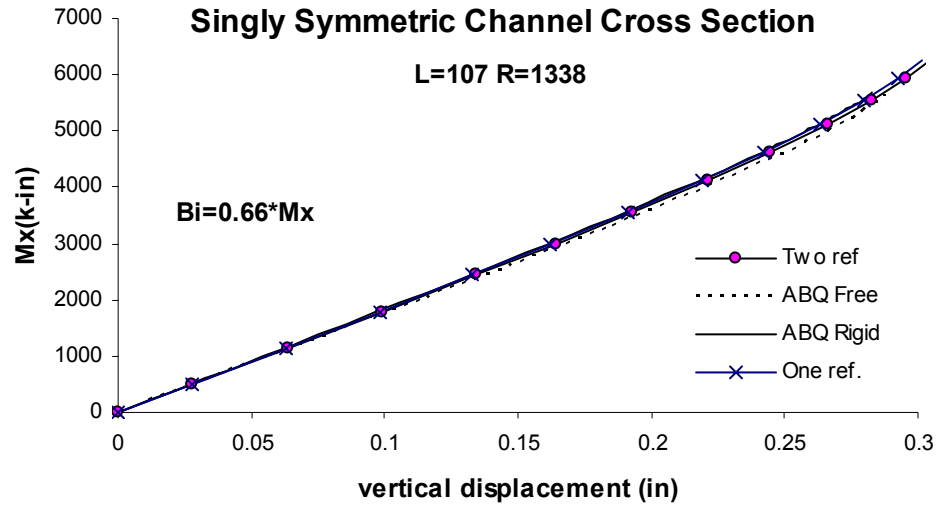


Figure 6.67 Vertical Displacement by Mx and Bi-Moment

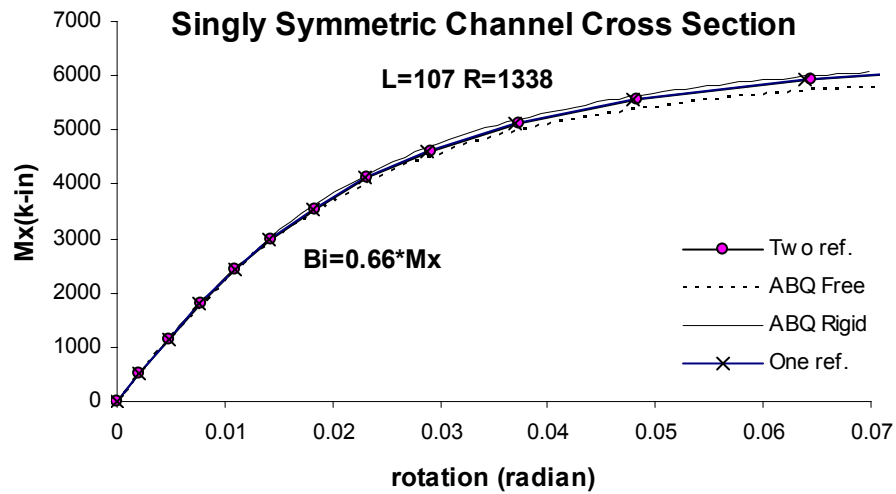


Figure 6.68 Rotation Induced by Mx and Bi-Moment

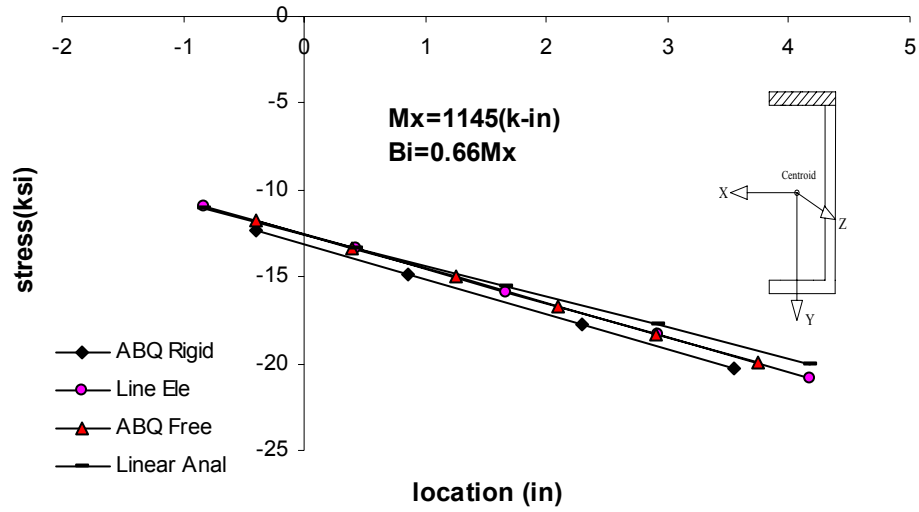


Figure 6.69 Stress Distribution along Top Flange, by $M_x=1145$ and B_i

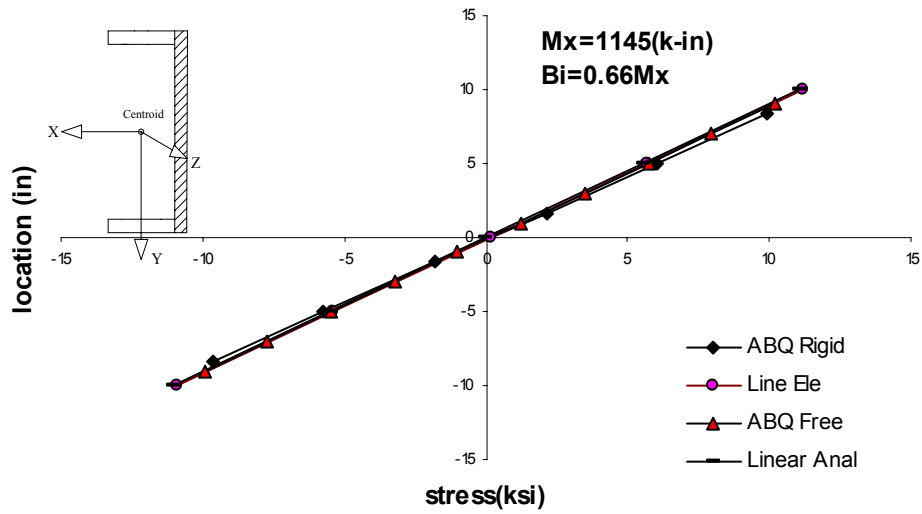


Figure 6.70 Stress Distribution along Web Induced, by $M_x=1145$ and B_i -moment

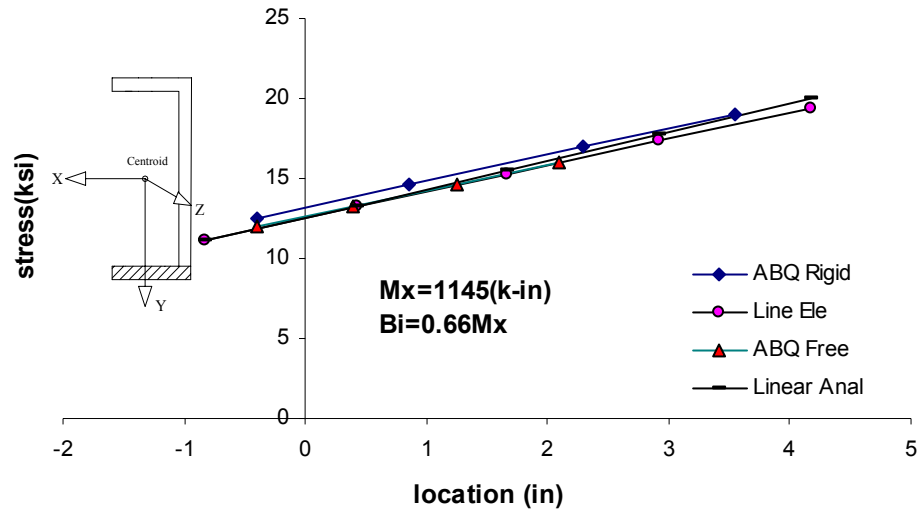


Figure 6.71 Stress Distribution along Bottom Flange, by $M_x=1145$ and Bi-moment

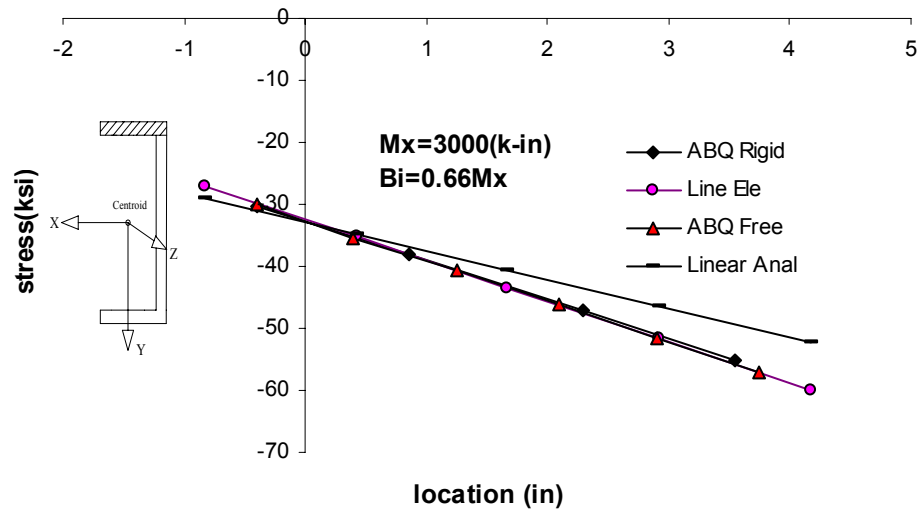


Figure 6.72 Stress Distribution along Top Flange, by $M_x=3000$ and Bi-moment

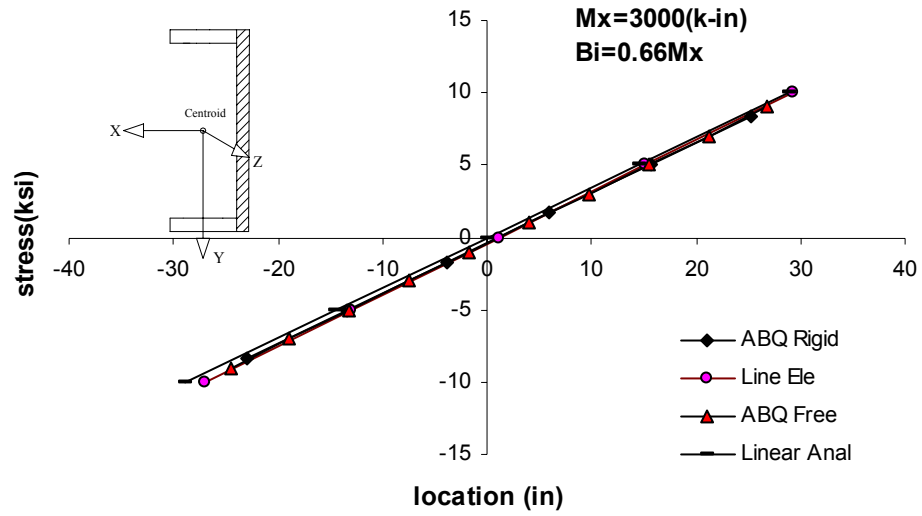


Figure 6.73 Stress Distribution along Web induced, by $M_x=3000$ and Bi-moment

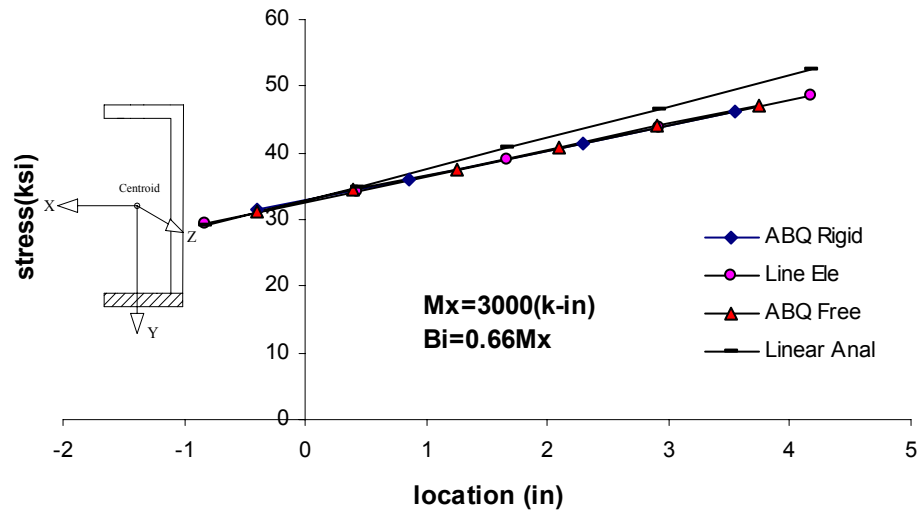


Figure 6.74 Stress Distribution along Bottom Flange, by $M_x=3000$ and Bi-moment

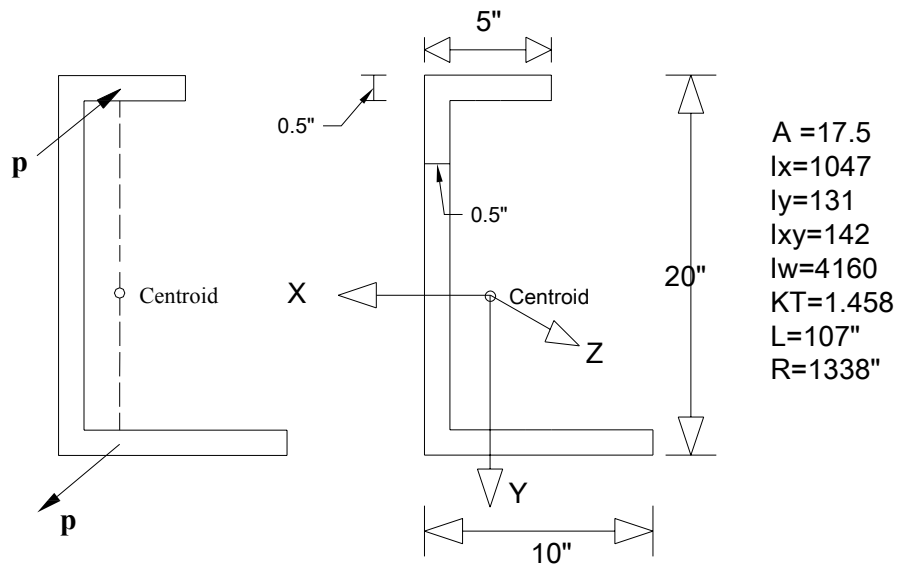


Figure 6.75 Point Loads and Unsymmetric Sectional Properties

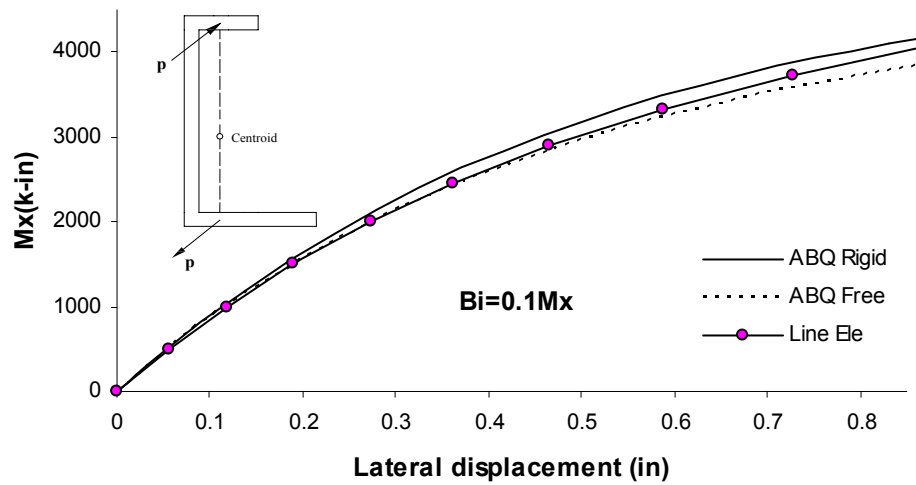


Figure 6.76 Lateral Displacement by Coupled Loads M_x and Bi-moment (Unsymmetric Cross Section)

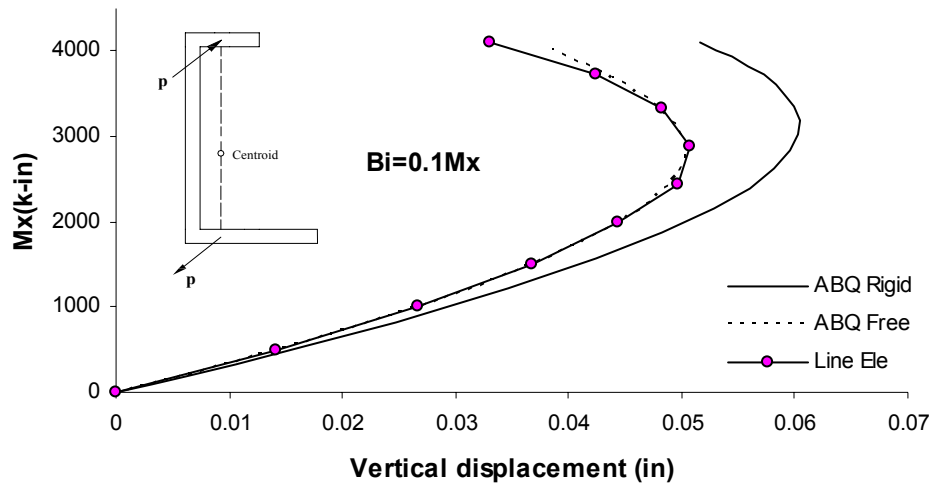


Figure 6.77 Vertical Displacement by Coupled Loads M_x and Bi-moment (Unsymmetric Cross Section)

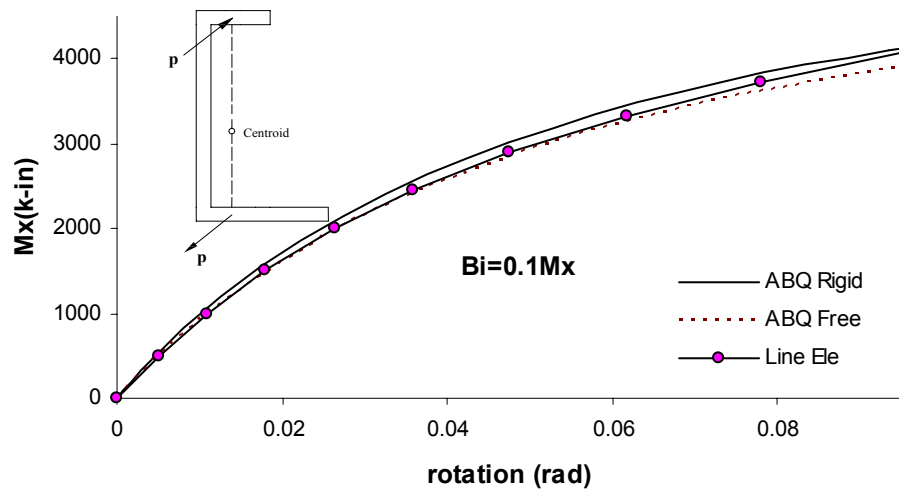


Figure 6.78 Rotation by Coupled Loads M_x and Bi-moment (Unsymmetric Cross Section)

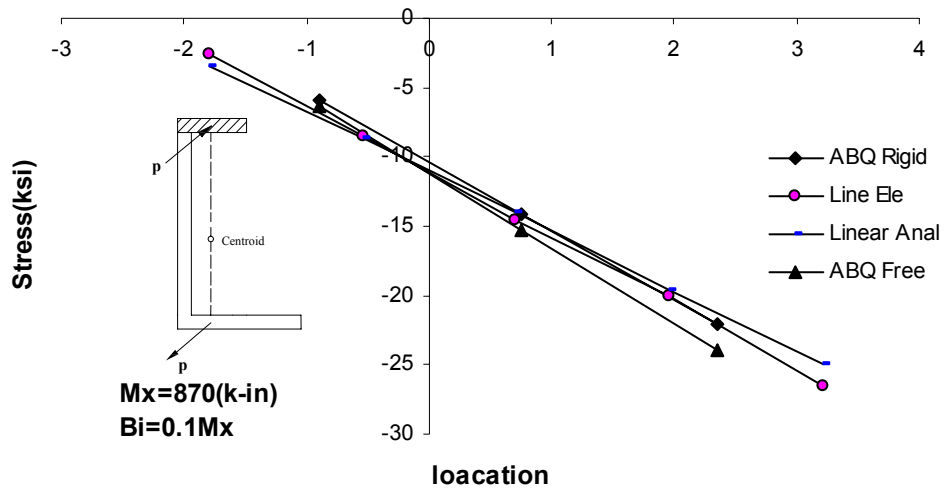


Figure 6.79 Stress Distribution along Top Flange, $M_x=870(\text{k-in})$

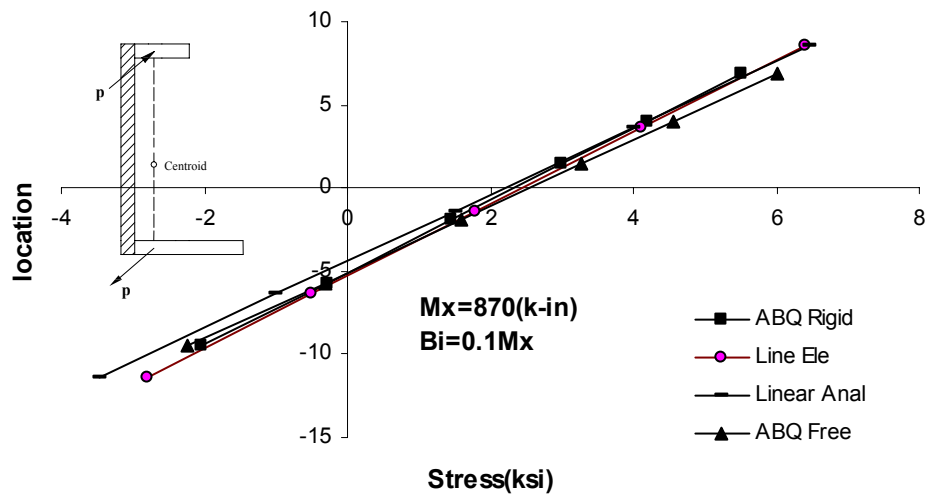


Figure 6.80 Stress Distribution along Web, $M_x=870(\text{k-in})$

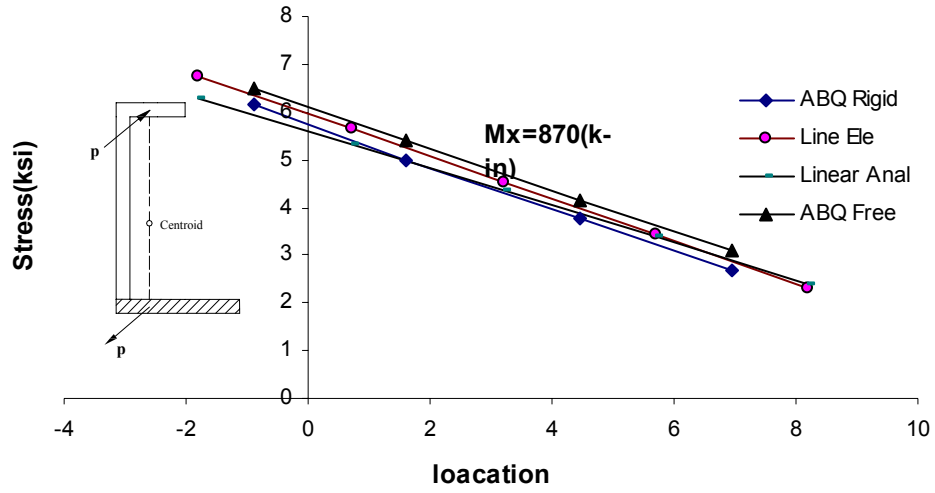


Figure 6.81 Stress Distribution along Bottom Flange, $M_x=870$ (k-in)

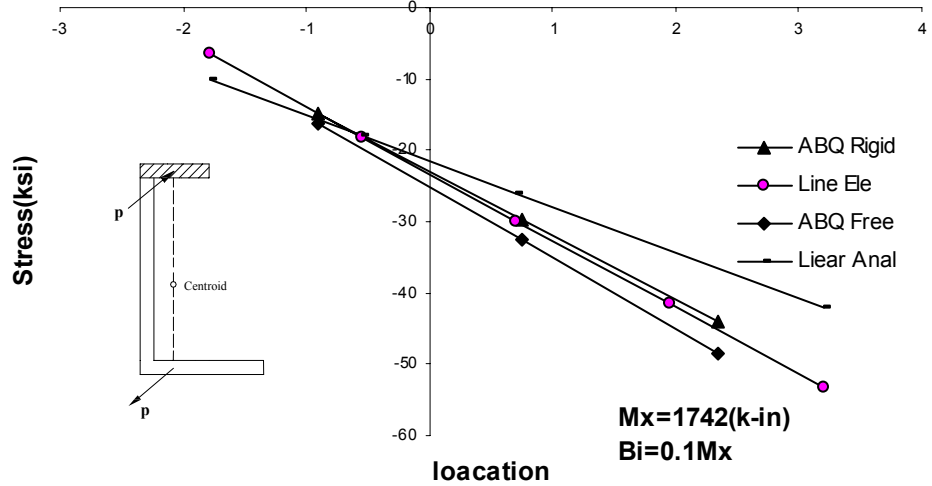


Figure 6.82 Stress Distribution along Top Flange, $M_x=1742$ (k-in)

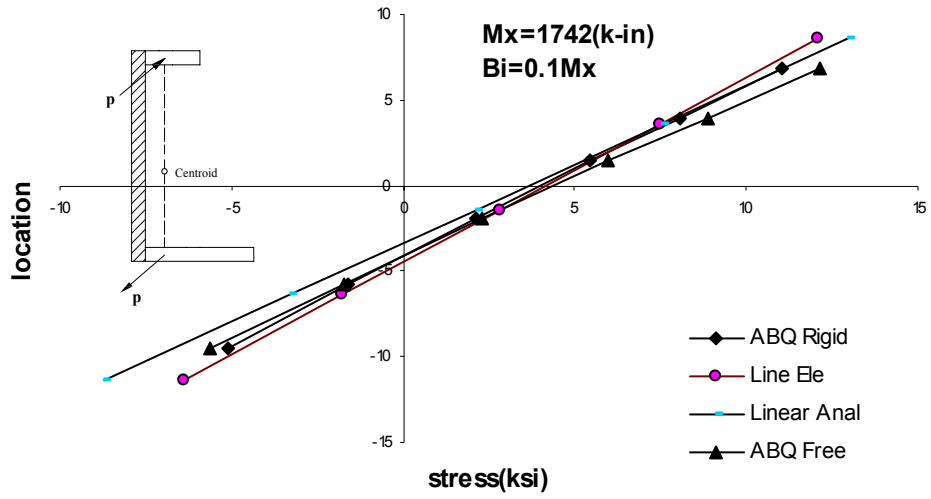


Figure 6.83 Stress Distribution along Web, $M_x=1742(k-in)$

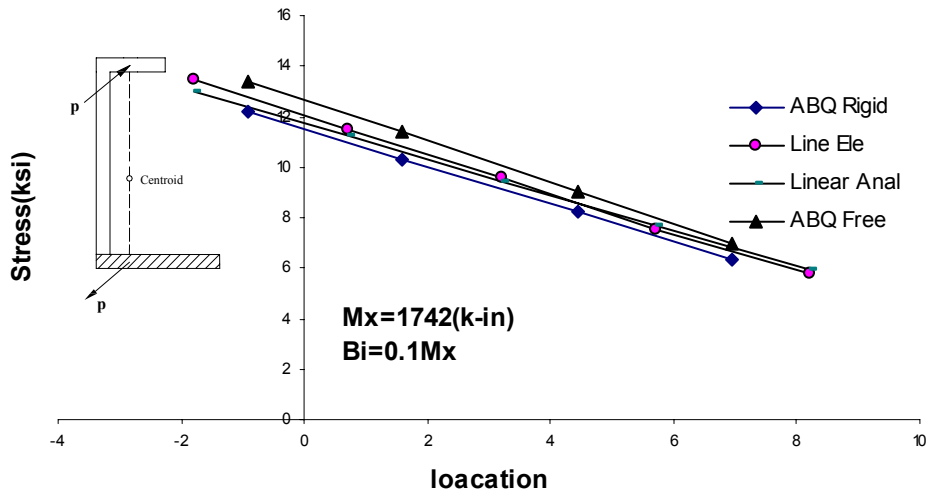


Figure 6.84 Stress Distribution along Bottom Flange, $M_x=1742(k-in)$

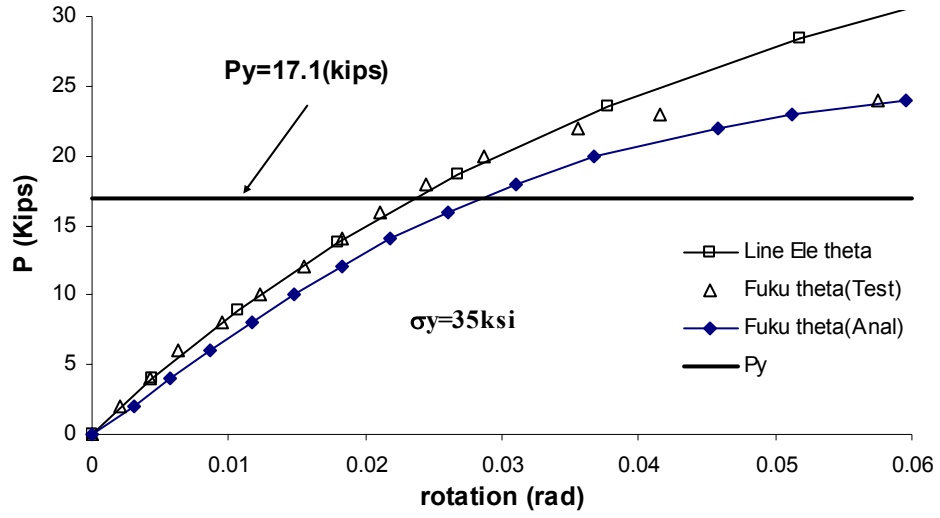


Figure 6.85 Load and rotation of Specimen AR1

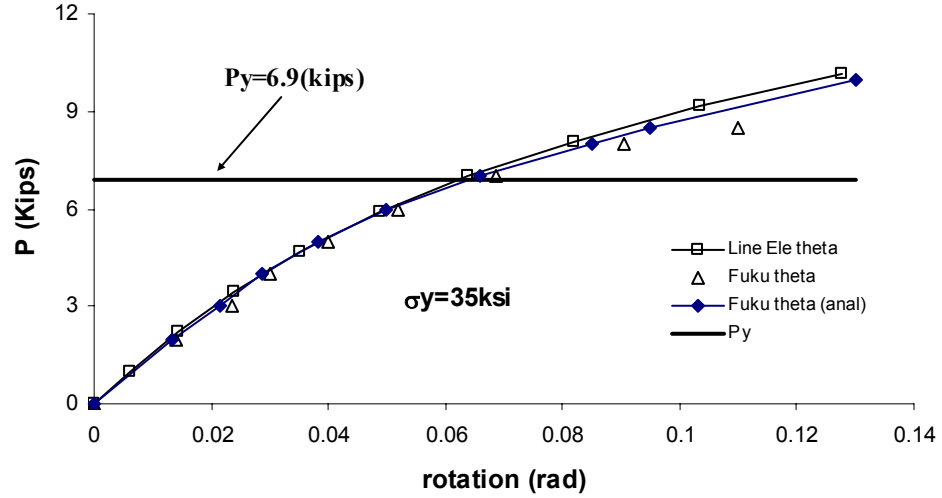


Figure 6.86 Load and rotation of Specimen BR1

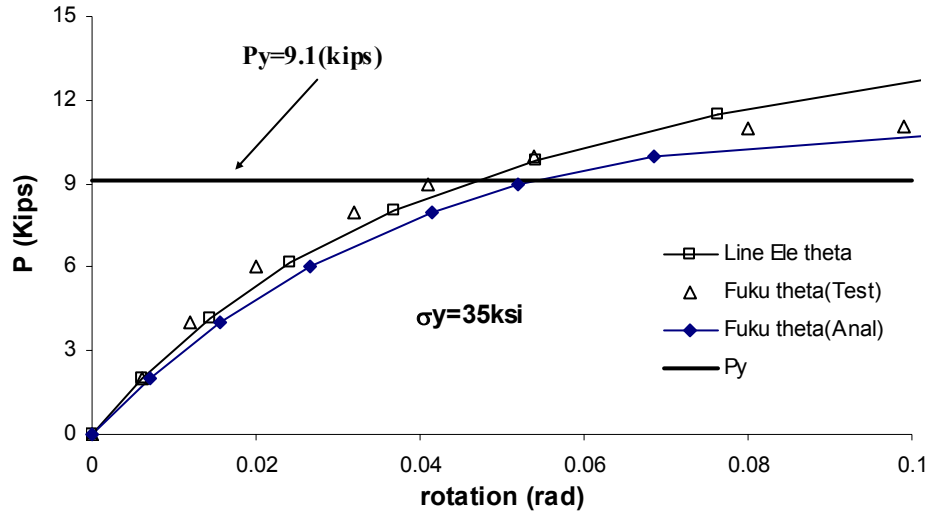


Figure 6.87 Load and rotation of Specimen BR2

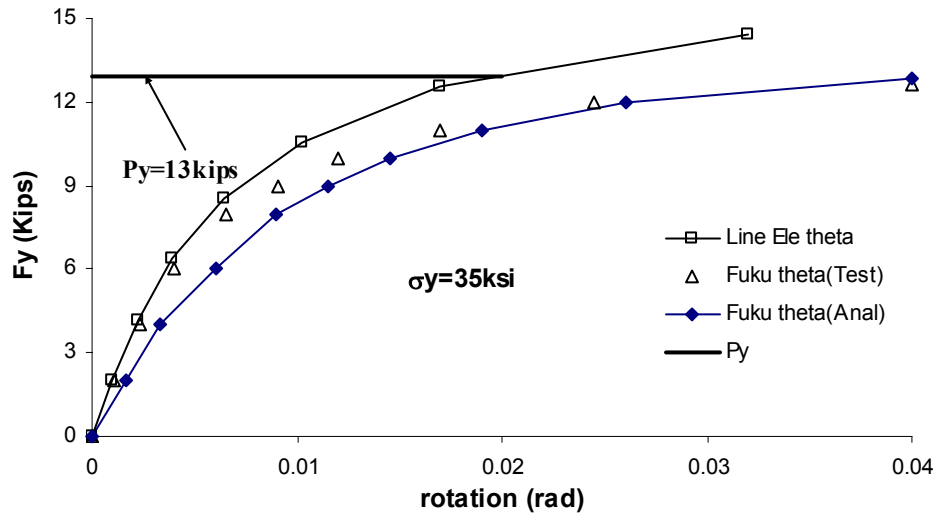


Figure 6.88 Load and rotation of Specimen BR3

7. The Sources of Nonlinearity

7.1 Introduction

In Chapters 4 and 5 differential equations and a finite line element for curved beams were developed including the strains of large deflection, large rotation, P-delta action and cross sectional deformation. These are the sources of large nonlinearity in the load-displacement relationship of curved beams.

In Section 6.3, it is shown that the commonly adopted approximations, a) ignoring $1/R^2$ terms, b) adopting $[(R-x)/R]=1$ and c) ignoring $1/R$ terms in Section 3.2, do not have significant effects on the deflection and rotation of the beams. Consequently, the major contributors to the high magnitude of displacement most likely are the approximation d) that $\cos \beta = 1$ and $\sin \beta = \beta$, the P-delta action and the cross sectional deformation. Numerical analyses to examine these contributions are made in this chapter.

7.2 Large Rotation

With the adoption of the approximation d) (in Section 3.2) in addition to approximations a), b) and c), the condition is that of assuming small rotation in an analysis. To examine that, the cross section of Figure 6.2 is used with the boundary condition of a simply supported beam with rotational restraint at the end sections. A constant vertical Moment, M_x , is applied at the end sections as the external load. Figure 7.1 shows the load-deflection curves obtained from the linear analysis, a large displacement with small rotation analysis (approximations a), b), c) and d)), a large displacement with large rotation analysis (approximation a), b) and c)) and the three-dimensional finite element analysis using ABAQUS. The material strength of $\sigma_y=36\text{ksi}$, is used as a reference. All except the linear analysis give almost the same lateral displacement when the applied M_x is fairly low. At higher loads, the analysis considering large displacement with small rotation underestimates the deflection. The analyses by McManus (1971), Yang (1987) and Kang (1992) are in this group. Only the analysis considering both large displacement and large rotation can predict the load-deflection behavior of the horizontally curved beam adequately. From Figure 7.1, it is evident that if the yield point is higher than 36 ksi, the magnitude of underestimation by the assumption of small rotation can be quite high even in the elastic range of material strength.

7.3 P-Delta Effect.

When a applied load is not on the centroid or the reference point of a cross section of a horizontally curved beam, the load couples with the twist rotation and generates a secondary moment by the p-delta effect. Figure 7.2 show the situation. The magnitude of the computed secondary moment and its contribution to the estimated load-deflection behavior of a beam depend on the procedure of analysis. For example there is no consideration of coupling between loads and displacement in the linear analysis, and secondary moment is not generated. In this section, by using the expressions in Eq. 5.22 to 5.24 for P-delta effect, it can be investigated.

For a numerical analysis, two beams of different cross section are selected: one has a flexible cross section and the other is stocky. Figure 7.3 shows the sectional and material properties of the cross sections. The sectional properties of both cross sections are within the ranges of AASHTO Guide Specification (2003). The basic boundary condition is used for the beams. A point load is applied on the top flange at the mid-span. Figures 7.4 to 7.6 and Figures 7.7 to 7.9 show the load-displacement curves of the beams with and without including the P-delta effects. For the beam with the flexible cross section, the effect is so significant that the difference of load-displacement curve starts at the onset of loading. For the stocky cross section, the effects of P-delta occur at relatively high magnitude of load. Once started, the p-delta effect increases rapidly with the increasing load. Thus, secondary moments generated by the p-delta effect must be considered for horizontally curved beams.

7.4 Sectional Deformation

The sectional deformation caused by the deformation of the web is derived in Chapter 4 and Chapter 5. To evaluate the effects of web deformation, the results of analysis using the line elements with and without the additional degree of freedom for sectional deformation are compared with the results of a three dimensional finite element analysis.

Two different cross sections are selected for this comparison. One is a cross section for which the ratio of warping constant I_ω and Saint Venant constant K_T (I_ω/K_T) is high and the other one has a low ratio of I_ω/K_T . The sectional dimensions of the cross sections are shown in Figure 7.10. The ratios $b/t_f=6$ and $d/t_w=24$ are selected for the low I_ω/K_T ratio cross section and $b/t_f=10$ and $d/t_w=180$ are selected for high I_ω/K_T ratio cross section. For the boundary condition of the beams, warping and rotation about y-axis at both ends are restrained. Figure 7.11 shows a beam and its boundary conditions. In the formulation of equations for sectional deformation, it is assumed that the web deforms with a double curvature. This assumption is confirmed by the shape in Figure 7.12 that is generated by the three dimensional finite element analysis.

The effects of sectional deformation for the cross section with a low and high I_ω/K_T ratio are shown in Figures 7.13 to 7.15 and Figures 7.16 to 7.18, respectively. From the figures, it is recognized that overall the effect of sectional deformation is not very significant, particularly for the cross section with high I_ω/K_T ratio. Since only the shear strain is changed by the sectional deformation, as seen in Equation 4.97, only Saint-Venant torsional resistance is reduced by the web deformation. For cross section with relatively low I_ω/K_T ratio, the twisting moment is mostly resisted by Saint Venant action. The reduction of Saint-Venant torsional resistance directly affects the total torsional moment resistance. This fact can be seen in the figure 7.15 in which a relatively larger difference exist between the rotation curves with and without considering web deformation. For the cross section with a high I_ω/K_T ratio, torsional moment is mostly resisted by the warping torsion. The reduction of Saint Venant torsional resistance does not affect much the behavior of the deflection curves of Figure 7.18.

It should be noted that in the H type of beams with the horizontal web in the plane of curvature, the web deformation affects warping resistance also. The web-deformation of H-beam changes not only the shear strains but also the longitudinal strains, both the resistance of warping torsion and Saint-Venant torsion are changed corresponding to the web deformation.

From the examination of the sources of nonlinearity, it is evident that the contributions of large rotation, p-delta effect and deformation of cross section need to be considered in the analysis of horizontally curved beams.

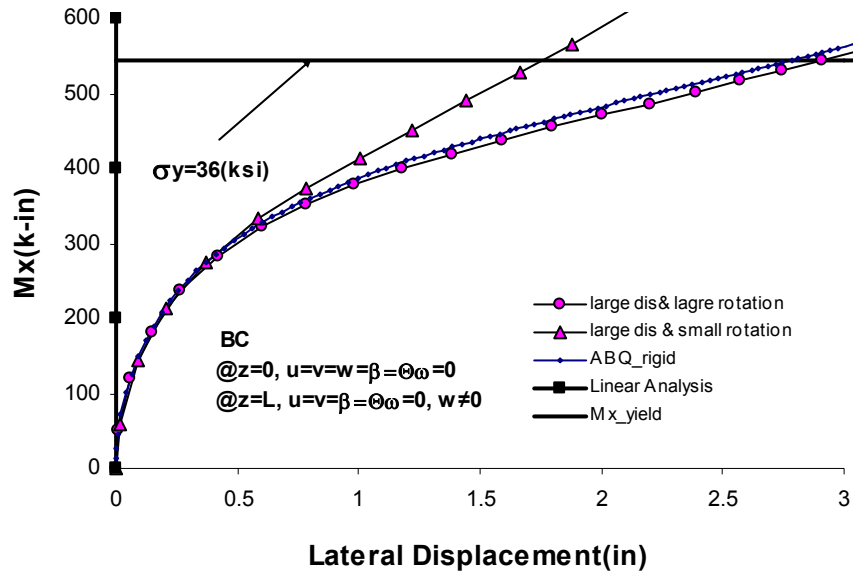


Figure 7.1 Lateral Displacement by Different Approximation

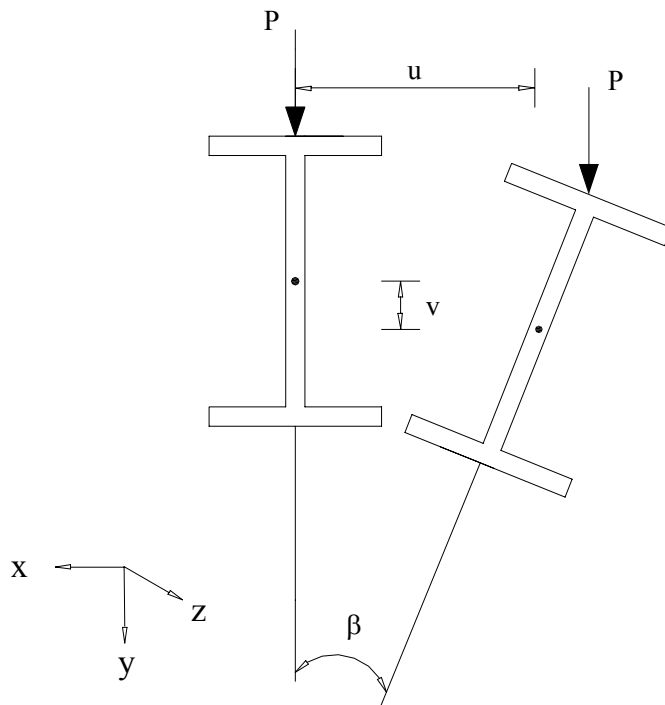


Figure 7.2 P-Delta Effect

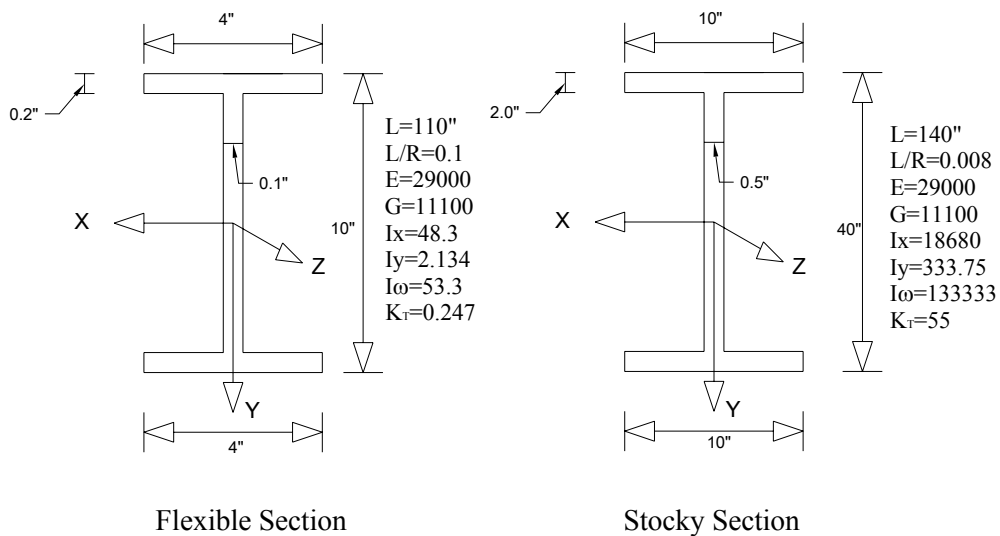


Figure 7.3 Sectional and Material properties of Cross Sections for P-Delta Effects

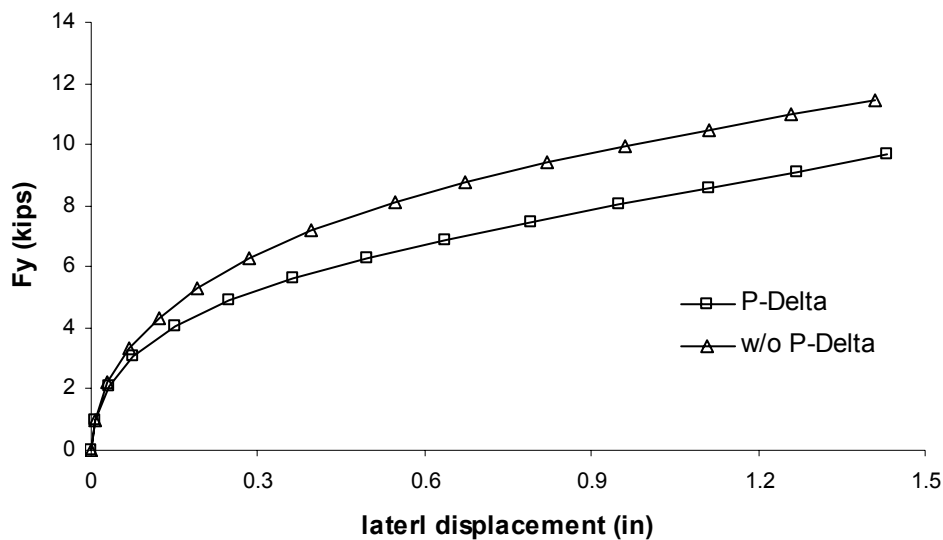


Figure 7.4 Lateral Displacement by Point Load, Flexible Cross Section

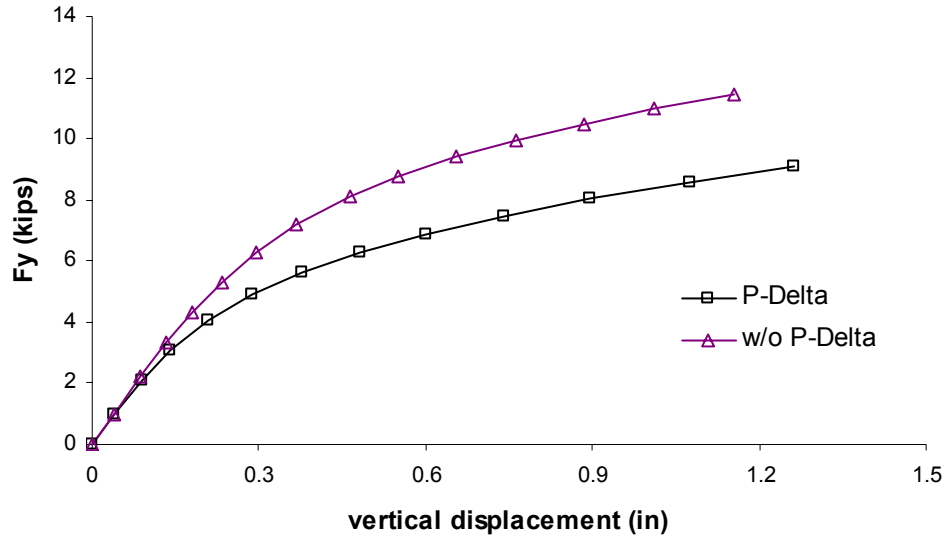


Figure 7.5 Vertical Displacement by Point Load, Flexible Cross Section

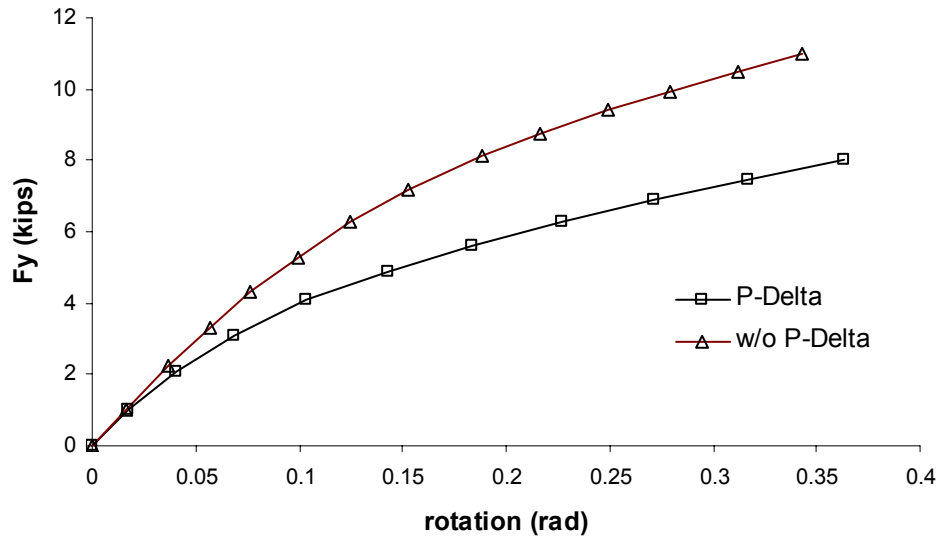
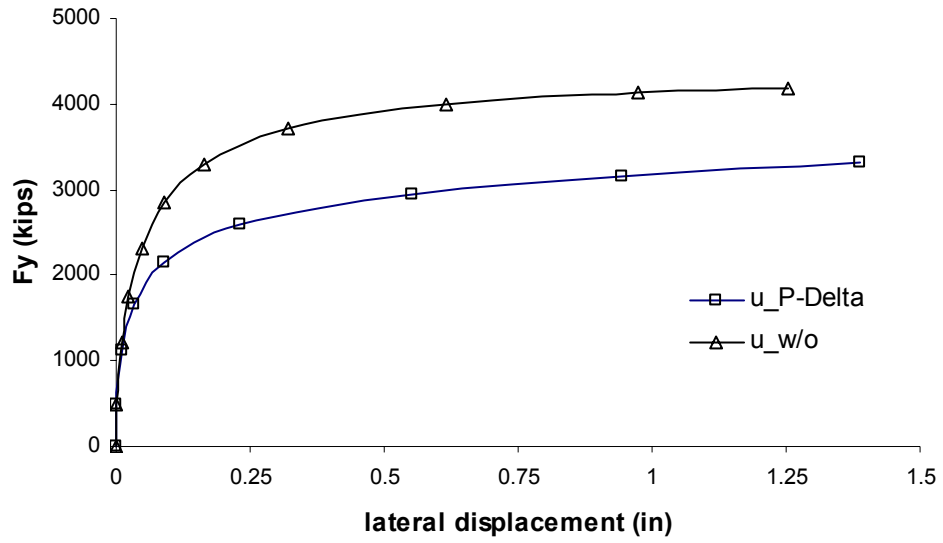
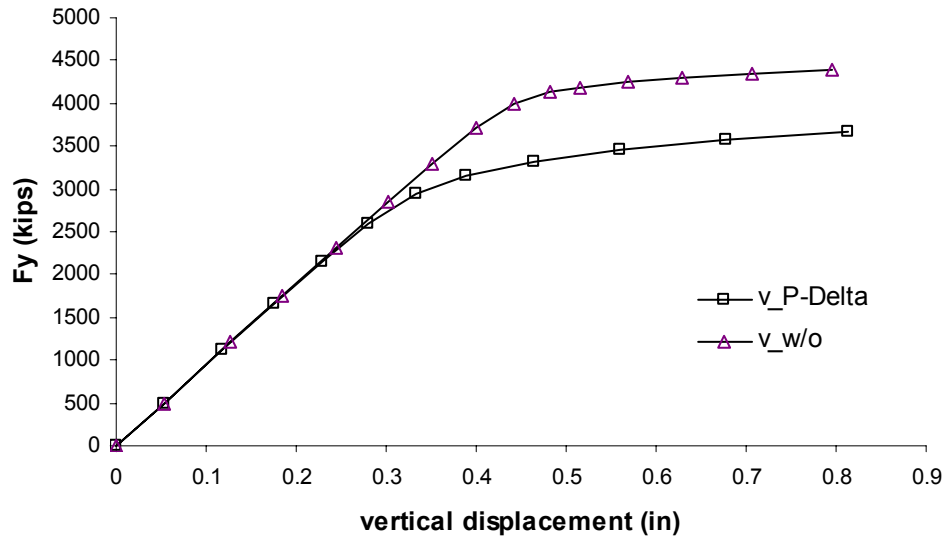


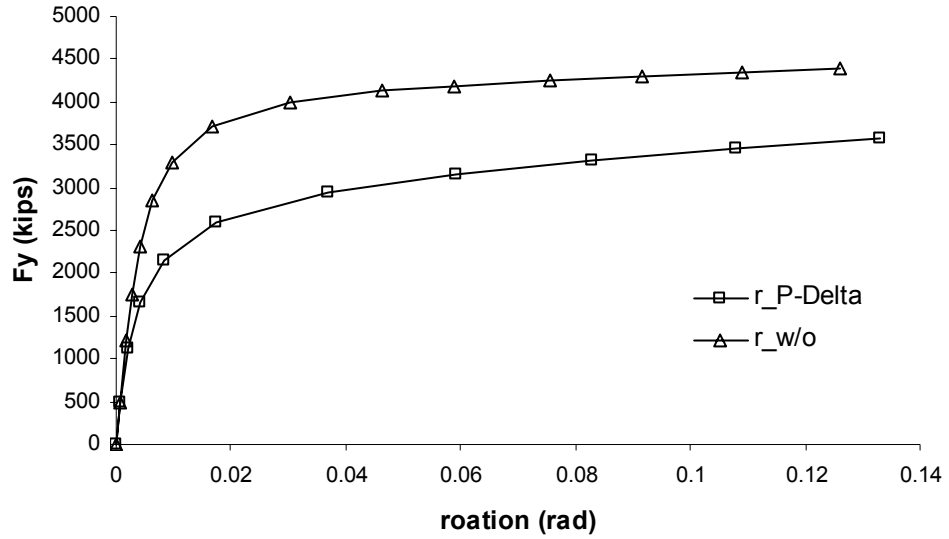
Figure 7.6 Rotation by Point Load, Flexible Cross Section



Figurer 7.7 Lateral Displacement by Point Load, Stocky Cross Section



Figurer 7.8 Vertical Displacement by Point Load, Stocky Cross Section



Figurer 7.9 Rotation by Point Load, Stocky Cross Section

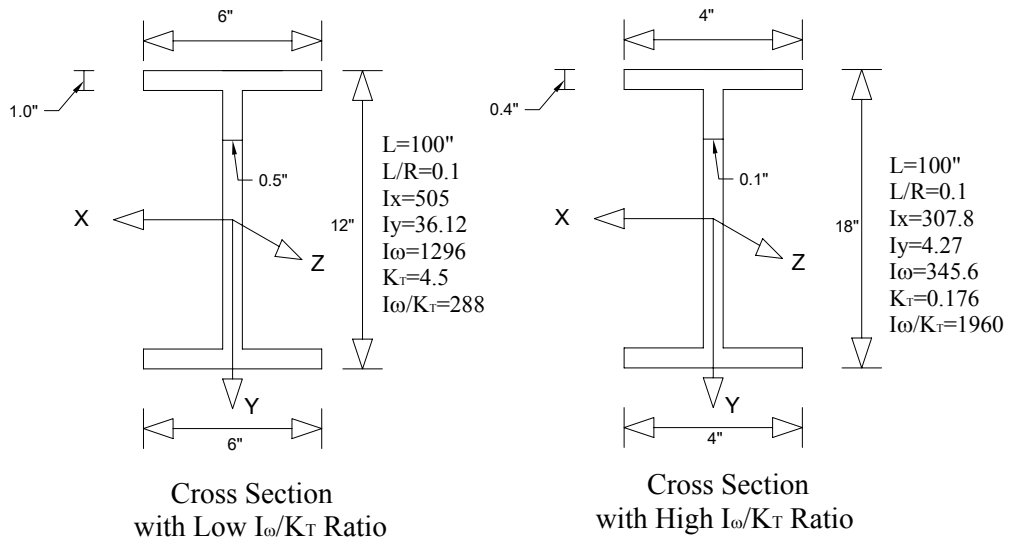


Figure 7.10 Cross Sections with Low and High I_{ω}/K_T Ratio

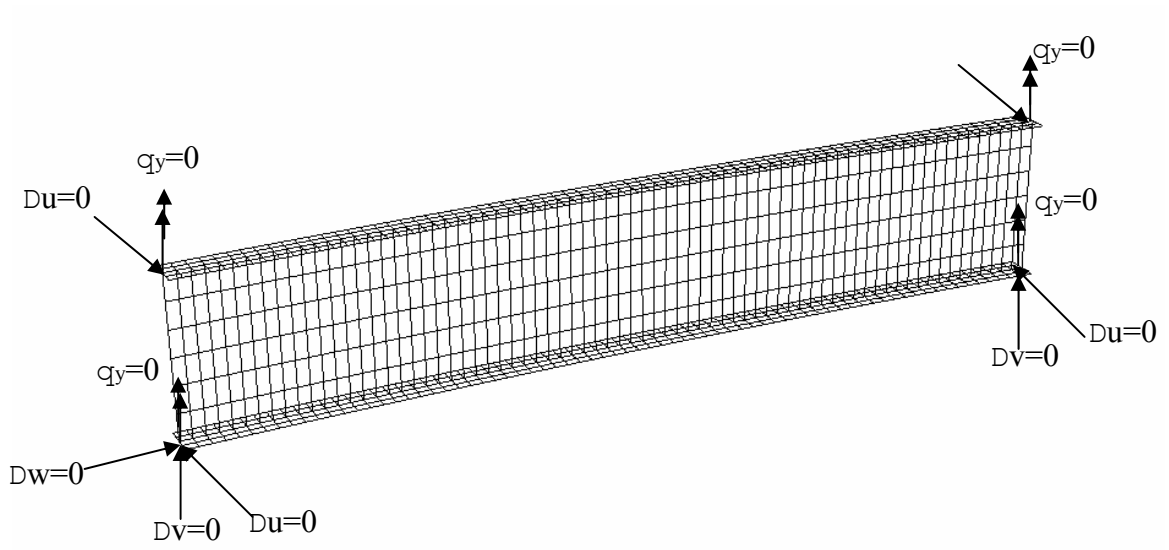


Figure 7.11 Boundary Condition of Beam for Analysis of Sectional Deformation

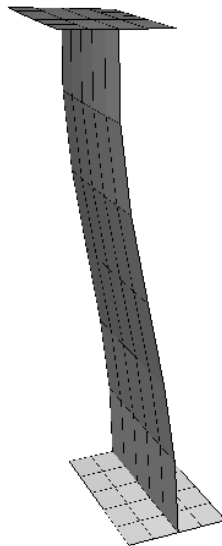


Figure 7.12 Deformation Shape of Beam Segment at the mid span

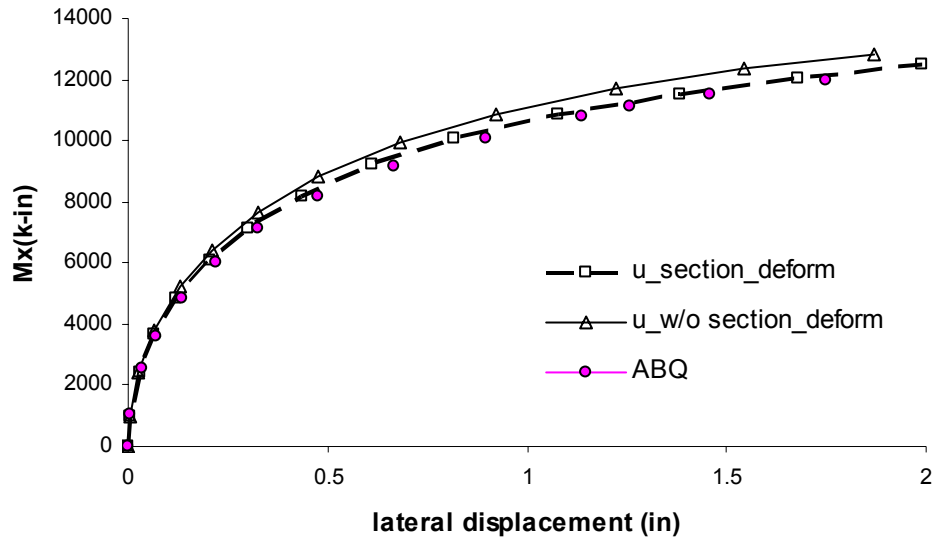


Figure 7.13 Lateral Displacement of Cross Section with Low I_ω/K_T ratio, Effect of Sectional Deformation

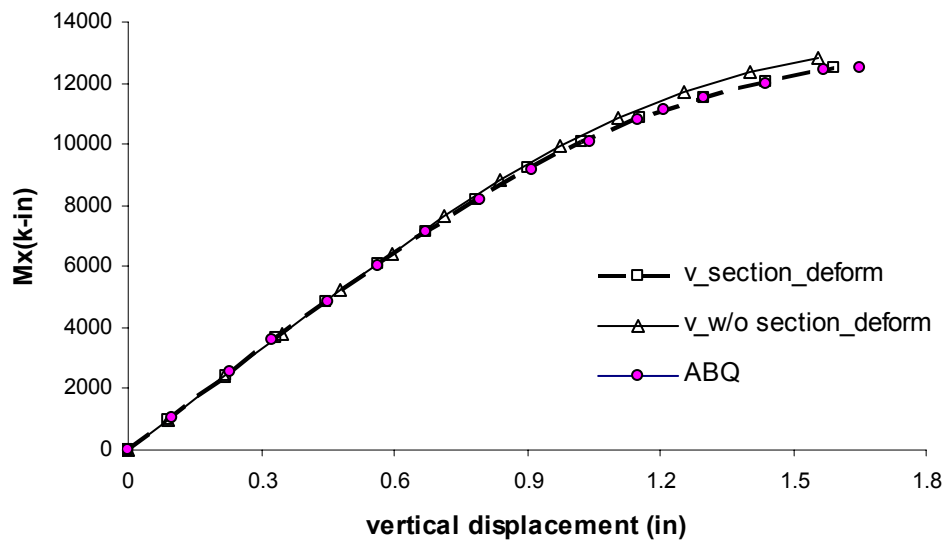


Figure 7.14 Vertical Displacement of Cross Section with Low I_ω/K_T ratio, Effect of Sectional Deformation

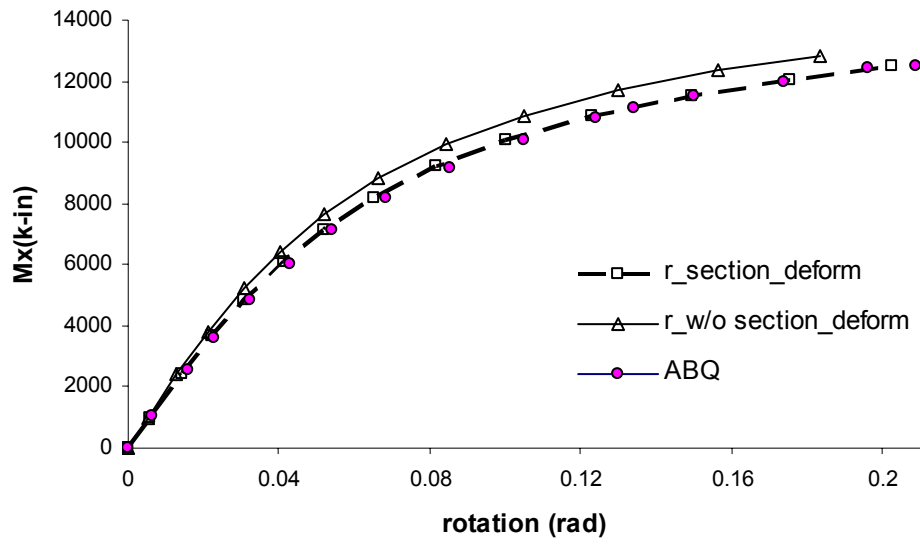


Figure 7.15 Rotation of Cross Section with Low I_{ω}/K_T ratio, Effect of Sectional Deformation

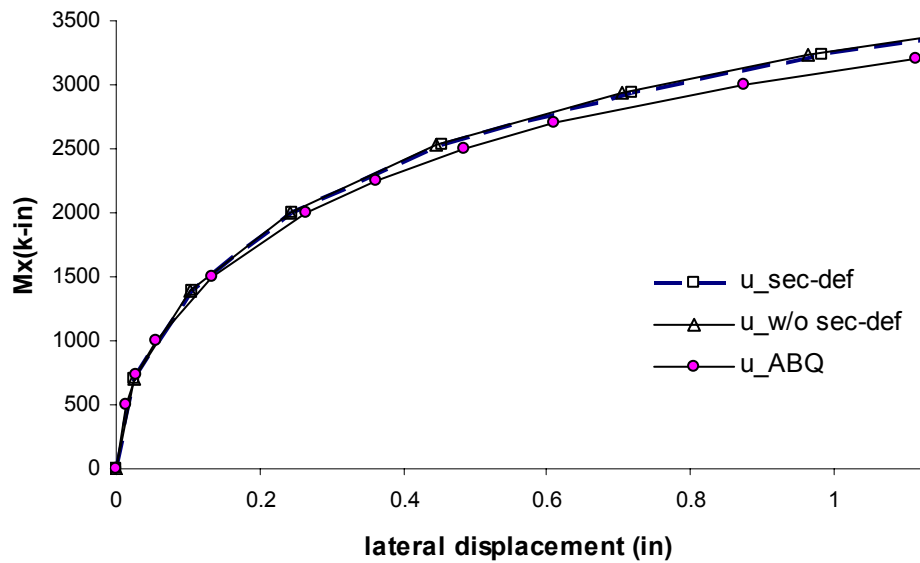


Figure 7.16 Lateral Displacement of Cross Section with High I_{ω}/K_T ratio, Effect of Sectional Deformation

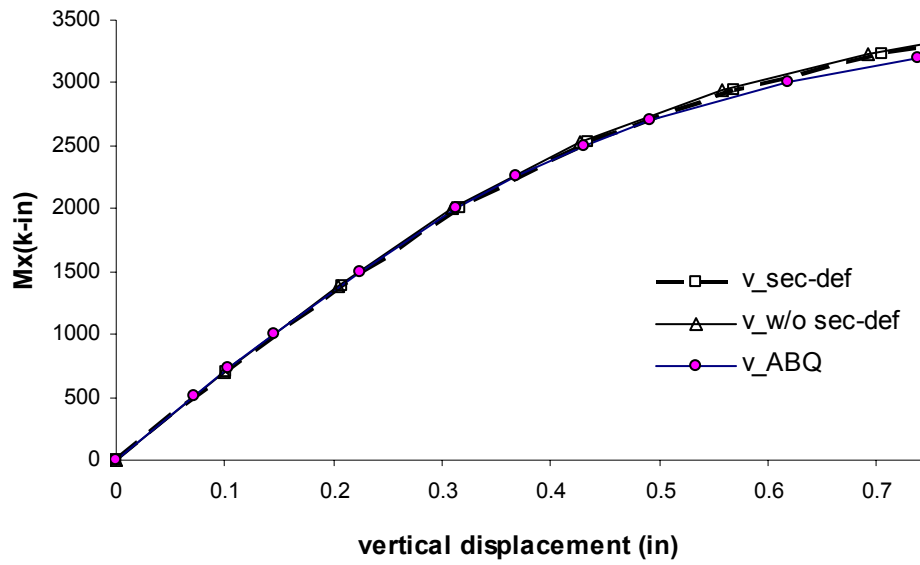


Figure 7.17 Vertical Displacement of Cross Section with High I_ω/K_T ratio Section, Effect of Sectional Deformation

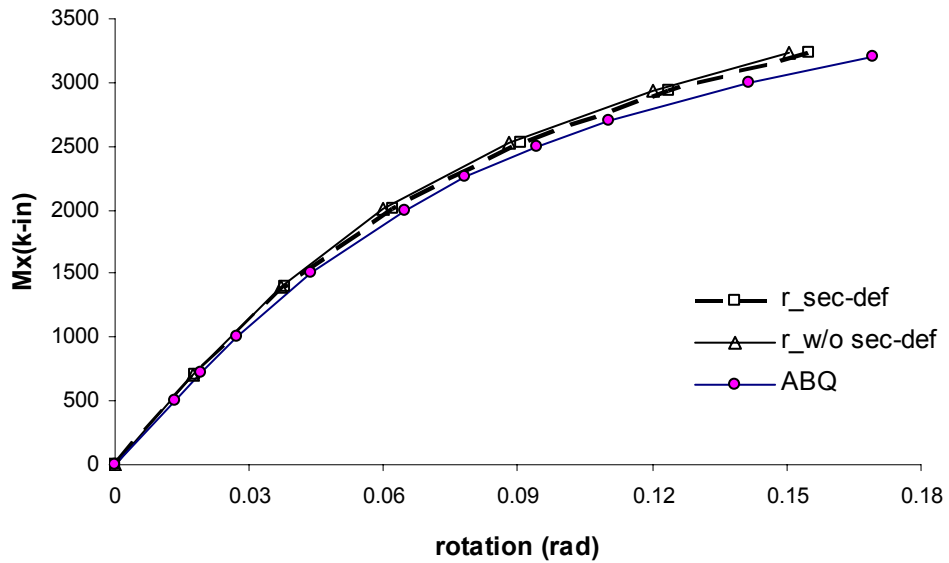


Figure 7.18 Rotation of Cross Section with High I_ω/K_T ratio, Effect of Sectional Deformation

8. Equation for Maximum Stress of Symmetrical I-Beams

8.1 Need for an Equation

In both the procedure of traditional allowable stress design and the procedure of load and resistance factor design (LRFD), an equation for maximum stress in the flange of beams is required. Current equations for flange stresses of curved beam do not include the effects of large displacement, large rotation and P- Δ effect. A new equation is needed.

An ideal equation should include all the relevant parameters which affect the determination of stresses, yet the equation should not be too cumbersome to use. One relatively simple form of the equation is to apply an amplification factor for a curved beam to the stress equation of the corresponding straight beam. However, due to the complexity of internal forces in curved beams, the expression of the amplification factor can not be derived directly from the strains of Chapter 3 and the differential equations of Chapter 4. Consequently, it is most efficient to adopt the procedure of conducting a parametric study using the line element of Chapter 5 and then deriving a stress equation through a regression analysis. But because external applied loads to curved beams usually generate coupled moments of Mx and Bi-moment, and their proportion depends on the beam geometry, it is almost impossible to derive a single stress equation. At the least, a set of stress equations for Mx and Bi-moment are needed. In the following, the procedure of developing a stress equation for a beam with a doubly symmetrical cross section under Mx is presented.

The primary assumption used in parametric study and regression analysis is that the parameters are independent and a simple equation can be derived by linear regression as:

$$Y = b_0 + b_1X_1 + b_2X_2 + b_3X_3 + \dots \quad 8.1$$

Or by non-linear regression as:

$$Y = b_0 + b_1X_1 + b_2X_2 + b_3X_3 + b_{12}X_1X_2 + b_{13}X_1X_3 \dots \quad 8.2$$

Where: X_i is an independent parameter

b_i is coefficient of the parameter

8.2 Selection of independent Parameters

Seven parameters are considered for the equation of maximum stress of curved beams with a doubly symmetrical cross section. These parameters are the flange width and thickness (b and t_f), the web plate depth and thickness (d and t_w), the span length and radius (L and R) and the yield strength of the beam steel. The geometrical parameters are rearranged as non-dimensional parameters.

L/R , the ratio of length to radius,

L/b , the ratio of length to width of flange

d/b , the ratio of depth of web to width of flange

b/t_f , the ratio of width to thickness of flange, b/t_f and

d/t_w , the ratio of depth and thickness of web

Through the preliminary case study, it is determined that the primary parameters for nonlinear behavior are L/b and L/R . The ratio d/t_w of depth to thickness of web is not a dominant parameter from the results of Chapters 6 and 7, and is not considered in the parametric study.

The ranges of major parameters L/R , L/b , d/b and b/t_f for the parametric study are listed in Table 8.1. These values are derived from design specifications and practical considerations.

To investigate whether the selected parameters are independent, several basic cases are analyzed first. The sectional properties of the basic beams are listed in Table 8.2. The basis beam has the most stocky cross section in the range of parameters in Table 8.1. Beams Lcomp1, Lcomp2, Lcomp3 and Lcomp4 have the same parameter values but different cross sectional dimensions. Beam Lcomp5 has a high value of d/b ratio for comparison. Results of analyzing these five cases are shown in Figure 8.1. The ordinate $M_x/M_{x,y}$ represents the external bending moment normalized by the yield moment $M_{x,y}$ of the cross section produced by vertical bending moment only. Since additional normal stresses are generated by warping, radial bending and sectional deformation, the amplification analyses are continued until the maximum normal stress reaches $1.2\sigma_y$. The abscissa S_n/S_l is the ratio of stress calculated by the nonlinear and the linear analysis. The stress S_l by the linear analysis is calculated from equation 8.3.

$$S_l = \frac{M_x}{I_x} y + \frac{Bi}{I_w} \omega \quad 8.3a$$

where:

$$M_x = M_0 \left[\frac{\left(\sin\left(\frac{L-z}{R}\right) + \sin\left(\frac{z}{R}\right) \right)}{\sin\left(\frac{L}{R}\right)} \right] \quad 8.3b$$

$$Bi = \frac{M_0 R}{1 + (k R)^2} \left[\frac{\left(\sin\left(\frac{L-z}{R}\right) + \sin\left(\frac{z}{R}\right) \right)}{\sin\left(\frac{L}{R}\right)} - \frac{\sinh(k(L-z)) + \sinh(k z)}{\sinh(k L)} \right] \quad 8.3c$$

$$k = \sqrt{\frac{G K_t}{E I_\omega}} \quad 8.3d$$

As shown in Figure 8.1, the curves of stress amplification for beams Lcomp1, Lcomp2, Lcomp3 are practically identical and that for Lcomp4 is very close. This means that the major parameters L/R , L/b , d/b and b/t_f in table 8.1 are independent for the parametric study. Another notable result in Figure 8.1 is that these beams with the lowest value of parameters of Table 8.1 generate very low amplification of stress. The highest is being about 1.3%. The difference between linear and nonlinear analysis for

the basis beam is less than 0.5%, and for the next four reference beams is only about 0.8%. All these can practically be ignored.

8.3 Parametric Study

Since the ratio L/b is the dominant parameter on the nonlinear behavior of horizontally curved beams, the regression analysis is started with L/b . Other parameters L/R , d/b and b/t_f are examined in order.

Table 8.3 lists the geometric dimension of five beams with L/b equals to 7, 12, 17, 21 and 25 and L/R , b_f/t_f and d/b at their basic values. The results of analysis by the line element are shown in Figure 8.2. As the value of L/b ratio is increased, the amplification of stress increases rapidly. At the maximum value of $L/b=25$ for beam L_b4 , as the external moment is increased towards the yield moment, the stress calculated by the nonlinear analysis is 35% higher than that by the linear analysis. This result is for the lowest values of the other parameters in their respective range. When the value of these other ratios increased, the amplification is even higher than 35%.

For a systematic study on the effects of all parameters, the five values of L/b ratio, 7, 12, 17, 21, 25, are combined with the following set of values of parameters in this study.

$L/R = 0.1, 0.077, 0.054, 0.031, 0.008$

$b_f/t_f = 10, 12.5, 15, 17.5, 20$

$d/b = 2, 2.5, 3, 3.5, 4.0$.

The combinations of these values of parameters are listed in Tables 8.4 to 8.18. Tables 8.4 to 8.6 are for $L/b=7$, Tables 8.7 to 8.9 for $L/b=25$; and so on. The characteristics of amplification of flange stresses in curved beams as listed in Tables 8.4 to 8.6 are shown in Figures 8.3 to 8.5. The maximum amplification is less than 3.5%. At the low value of $L/b=7$, the effects of curvature (L/R) on the character of amplification are significant, as seen in Fig. 8.3. This implies that L/R ratio is also a primary governing parameter. The effects of d/b are less prominent as shown in Figs 8.5, and the effect of b/t are even less as shown in Fig. 8.4.

Similar characters are observed in the case study for other sets of values of the parameters. Figures 8.6 to 8.8 are for $L/b=12$ with values of other parameters listed in Tables 8.10 to 8.12; Figures 8.9 to 8.11 are for $L/b=17$ with values of other parameters listed in Tables 7.13 to 7.15, and son on. The notable character is that when L/R is 0.008 (LR4 in Figs. 8.6, 8.9, 8.12 and 8.15), the amplification of stress increases nonlinearly with respect to increase of moment. This nonlinear behavior of curved beams with relatively small curvature points out the necessity of considering large displacement, large rotation and $P-\Delta$ effects.

From the results of the parameter study, it is confirmed that all four parameters, L/b , L/R , b/t_f and d/b are independent parameters affecting the nonlinear behavior of curved beams.

8.4 Equation for Maximum Stress

After a regression analysis of the data generated by the parametric study, the following equation is derived for calculating the maximum stress in doubly symmetrical curved I-beams under end moment M_x .

$$\frac{S_{nl}}{S_l} = \left[1 + A * \sinh \left(B * \left(\frac{M_x}{M_{x,y}} \right) \right) \right] \quad \mathbf{8.5a}$$

Where:

$$A = 0.411 + 0.097 * Ln \left[\left(\frac{L}{R} \right) + 0.0136 \right] \quad \mathbf{8.5b}$$

$$B1 = -0.29 + \frac{1}{\left[8.7 / \left(\frac{L}{b} \right) + 0.002 \right]^2} \quad \mathbf{8.5c}$$

$$B2 = \left(-0.031 + \frac{1}{198 / \left(\frac{L}{b} \right) - 3.16} \right) \left(\frac{b}{t} - 20 \right) \quad \mathbf{8.5d}$$

$$B3 = \left(-0.218 + \frac{1}{28 / \left(\frac{L}{b} \right) - 0.503} \right) \left(\frac{d}{b} - 4 \right) \quad \mathbf{8.5e}$$

$$B = B1 + B2 + B3 \quad \mathbf{8.5f}$$

In order to evaluate Equation 8.5, a comparison between the results generated by Equation 8.5 and by the line element analysis is conducted for three beams with different cross sections: cross section 1 for a stocky section, cross section 3 for a slender section and cross section 2 for a section in between. The values of the parameters for the cross sections are the following.

Cross Section 1: $L/b=7$, $L/R=0.08$, $b/t_f=10$, $d/b=2$, $L=35$

Cross Section 2: $L/b=16$, $L/R=0.08$, $b/t_f=15$, $d/b=3$, $L=160$

Cross Section 3: $L/b=25$, $L/R=0.1$, $b/t_f=20$, $d/b=4$, $L=125$

The comparison is made in Figures 8.18 to 8.20 for beams with cross section 1 to 3. As can be conclude from the figures, the developed equation predicts the maximum stress well. Equation 8.5 is developed based on large displacement, large rotation and sectional deformation analysis of horizontally curved beams with doubly symmetric cross sections which conform to AASHTO Specifications. Thus, the equation can readily be used for calculating the maximum stress of such beams under equal end

moments M_x . Similarly, an equation can be developed for the bi-moment. The same procedure of analysis can be applied to singly symmetrical I-shapes for developing corresponding flange stress equations.

Table 8.1 Range of Parameters

Parameter	Range
L/R	0.008 ~ 0.1
L/b	7 ~25
b/t _f	10 ~ 20
d/b	2 ~4

Table 8.2 Reference Cases

	b	d	t _f	t _w	L	R	L/b	L/R	b _f /t _f	d/b
Basis	20	40	2	0.4	140	17500	7	0.008	10	2
Lcomp1	20	60	2	0.6	140	17500	7	0.008	10	3
Lcomp2	5	15	1	0.3	70	8750	7	0.008	10	3
Lcomp3	5	15	0.5	0.15	35	4375	7	0.008	10	3
Lcomp4	10	30	1	0.2	70	8750	7	0.008	10	3
Lcomp5	10	50	1	0.5	70	8750	7	0.008	10	5

Table 8.3 Value of L/b ratio

	b	d	t _f	t _w	L	R	L/b	L/R	b _f /t _f	d/b
Basis	20	40	2	0.4	140	17500	7	0.008	10	2
L_b1	11.67	23.34	1.167	0.234	140	17500	12	0.008	10	2
L_b2	8.24	16.48	0.824	0.16	140	17500	17	0.008	10	2
L_b3	6.67	13.34	0.667	0.13	140	17500	21	0.008	10	2
L_b4	5.6	11.2	0.56	0.11	140	17500	25	0.008	10	2

Table 8.4 Values of L/R ratio L/b =7

	b	d	t _f	t _w	L	R	L/b	L/R	b _f /t _f	d/b
Ref.	20	80	1	0.8	140	1400	7	0.1	20	4
L_R1	20	80	1	0.8	140	1818	7	0.077	20	4
L_R2	20	80	1	0.8	140	2593	7	0.054	20	4
L_R3	20	80	1	0.8	140	4516	7	0.031	20	4
L_R4	20	80	1	0.8	140	17500	7	0.008	20	4

Table 8.5 Values of b_f/t_f ratio with L/b =7

	b	d	t _f	t _w	L	R	L/b	L/R	b_f/t_f	d/b
Ref.	20	80	1	0.8	140	1400	7	0.1	20	4
b_t1	20	80	1.25	0.8	140	1400	7	0.1	17.5	4
b_t2	20	80	1.5	0.8	140	1400	7	0.1	15	4
b_t3	20	80	1.75	0.8	140	1400	7	0.1	12.5	4
b_t4	20	80	2	0.8	140	1400	7	0.1	10	4

Table 8.6 Values of d/b ratio with L/b=7

	b	d	t _f	t _w	L	R	L/b	L/R	b _f /t _f	d/b
Ref.	20	80	2	0.8	140	1400	7	0.1	20	4
d b1	20	70	2	0.7	140	1400	7	0.1	20	3.5
d b2	20	60	2	0.6	140	1400	7	0.1	20	3
d b3	20	50	2	0.5	140	1400	7	0.1	20	2.5
d b4	20	40	2	0.4	140	1400	7	0.1	20	2

Table 8.10 Values of L/R ratio with L/b =12

	b	d	t _f	t _w	L	R	L/b	L/R	b _f /t _f	d/b
Ref.	11.67	46.7	0.58	0.47	140	1400	12	0.1	20	4
L R1	11.67	46.7	0.58	0.47	140	1818	12	0.077	20	4
L R2	11.67	46.7	0.58	0.47	140	2593	12	0.054	20	4
L R3	11.67	46.7	0.58	0.47	140	4516	12	0.031	20	4
L R4	11.67	46.7	0.58	0.47	140	17500	12	0.008	20	4

Table 8.11 Values of b_f/t_f ratio with L/b =12

	b	d	t _f	t _w	L	R	L/b	L/R	b _f /t _f	d/b
Ref.	11.67	46.7	0.58	0.47	140	1400	12	0.1	20	4
b t1	11.67	46.7	0.67	0.47	140	1400	12	0.1	17.5	4
b t2	11.67	46.7	0.78	0.47	140	1400	12	0.1	15	4
b t3	11.67	46.7	0.93	0.47	140	1400	12	0.1	12.5	4
b t4	11.67	46.7	1.17	0.47	140	1400	12	0.1	10	4

Table 8.12 Values of d/b ratio with L/b =12

	b	d	t _f	t _w	L	R	L/b	L/R	b _f /t _f	d/b
Ref.	11.67	46.7	0.58	0.47	140	1400	12	0.1	20	4
d b1	11.67	40.9	0.58	0.41	140	1400	12	0.1	20	3.5
d b2	11.67	35	0.58	0.35	140	1400	12	0.1	20	3
d b3	11.67	29.2	0.58	0.29	140	1400	12	0.1	20	2.5
d b4	11.67	23.3	0.58	0.23	140	1400	12	0.1	20	2

Table 8.13 Values of L/R ratio with L/b =17

	b	d	t _f	t _w	L	R	L/b	L/R	b _f /t _f	d/b
Ref.	8.24	33	0.41	0.33	140	1400	17	0.1	20	4
L R1	8.24	33	0.41	0.33	140	1818	17	0.077	20	4
L R2	8.24	33	0.41	0.33	140	2593	17	0.054	20	4
L R3	8.24	33	0.41	0.33	140	4516	17	0.031	20	4
L R4	8.24	33	0.41	0.33	140	17500	17	0.008	20	4

Table 8.14 Values of b_f/t_f ratio with $L/b = 17$

	b	d	t_f	t_w	L	R	L/b	L/R	b_f/t_f	d/b
Ref.	8.24	33	0.41	0.33	140	1400	17	0.1	20	4
b t1	8.24	33	0.47	0.33	140	1400	17	0.1	17.5	4
b t2	8.24	33	0.55	0.33	140	1400	17	0.1	15	4
b t3	8.24	33	0.66	0.33	140	1400	17	0.1	12.5	4
b t4	8.24	33	0.82	0.33	140	1400	17	0.1	10	4

Table 8.15 Values of d/b ratio with $L/b = 17$

	b	d	t_f	t_w	L	R	L/b	L/R	b_f/t_f	d/b
Ref.	8.24	33	0.41	0.33	140	1400	17	0.1	20	4
d b1	8.24	28.8	0.41	0.29	140	1400	17	0.1	20	3.5
d b2	8.24	24.7	0.41	0.25	140	1400	17	0.1	20	3
d b3	8.24	20.6	0.41	0.21	140	1400	17	0.1	20	2.5
d b4	8.24	16.5	0.41	0.17	140	1400	17	0.1	20	2

Table 8.16 Values of L/R ratio with $L/b = 21$

	b	d	t_f	t_w	L	R	L/b	L/R	b_f/t_f	d/b
Ref.	6.67	26.7	0.33	0.27	140	1400	21	0.1	20	4
L R1	6.67	26.7	0.33	0.27	140	1818	21	0.077	20	4
L R2	6.67	26.7	0.33	0.27	140	2593	21	0.054	20	4
L R3	6.67	26.7	0.33	0.27	140	4516	21	0.031	20	4
L R4	6.67	26.7	0.33	0.27	140	17500	21	0.008	20	4

Table 8.17 Values of b_f/t_f ratio with $L/b = 21$

	b	d	t_f	t_w	L	R	L/b	L/R	b_f/t_f	d/b
Ref.	6.67	26.7	0.33	0.27	140	1400	21	0.1	20	4
b t1	6.67	26.7	0.38	0.27	140	1400	21	0.1	17.5	4
b t2	6.67	26.7	0.44	0.27	140	1400	21	0.1	15	4
b t3	6.67	26.7	0.53	0.27	140	1400	21	0.1	12.5	4
b t4	6.67	26.7	0.67	0.27	140	1400	21	0.1	10	4

Table 8.18 Values of d/b ratio with $L/b = 21$

	b	d	t_f	t_w	L	R	L/b	L/R	b_f/t_f	d/b
Ref.	6.67	26.7	0.33	0.27	140	1400	21	0.1	20	4
d b1	6.67	23.3	0.33	0.23	140	1400	21	0.1	20	3.5
d b2	6.67	20	0.33	0.2	140	1400	21	0.1	20	3
d b3	6.67	16.7	0.33	0.17	140	1400	21	0.1	20	2.5
d b4	6.67	13.3	0.33	0.13	140	1400	21	0.1	20	2

Table 8.7 Values of L/R ratio with L/b =25

	b	d	t _f	t _w	L	R	L/b	L/R	b _f /t _f	d/b
Ref.	5.6	22.4	0.28	0.22	140	1400	25	0.1	20	4
L R1	5.6	22.4	0.28	0.22	140	1818	25	0.077	20	4
L R2	5.6	22.4	0.28	0.22	140	2593	25	0.054	20	4
L R3	5.6	22.4	0.28	0.22	140	4516	25	0.031	20	4
L R4	5.6	22.4	0.28	0.22	140	17500	25	0.008	20	4

Table 8.8 Values of b_f/t_f ratio with L/b =25

	b	d	t _f	t _w	L	R	L/b	L/R	b_f/t_f	d/b
Ref.	5.6	22.4	0.28	0.22	140	1400	25	0.1	20	4
b t1	5.6	22.4	0.32	0.22	140	1400	25	0.1	17.5	4
b t2	5.6	22.4	0.37	0.22	140	1400	25	0.1	15	4
b t3	5.6	22.4	0.45	0.22	140	1400	25	0.1	12.5	4
b t4	5.6	22.4	0.56	0.22	140	1400	25	0.1	10	4

Table 8.9 Values of d/b ratio with L/b ratio =25

	b	d	t _f	t _w	L	R	L/b	L/R	b _f /t _f	d/b
Ref.	5.6	22.4	0.28	0.22	140	1400	25	0.1	20	4
d b1	5.6	19.6	0.28	0.196	140	1400	25	0.1	20	3.5
d b2	5.6	16.8	0.28	0.168	140	1400	25	0.1	20	3
d b3	5.6	14.0	0.28	0.14	140	1400	25	0.1	20	2.5
d b4	5.6	11.2	0.28	0.112	140	1400	25	0.1	20	2

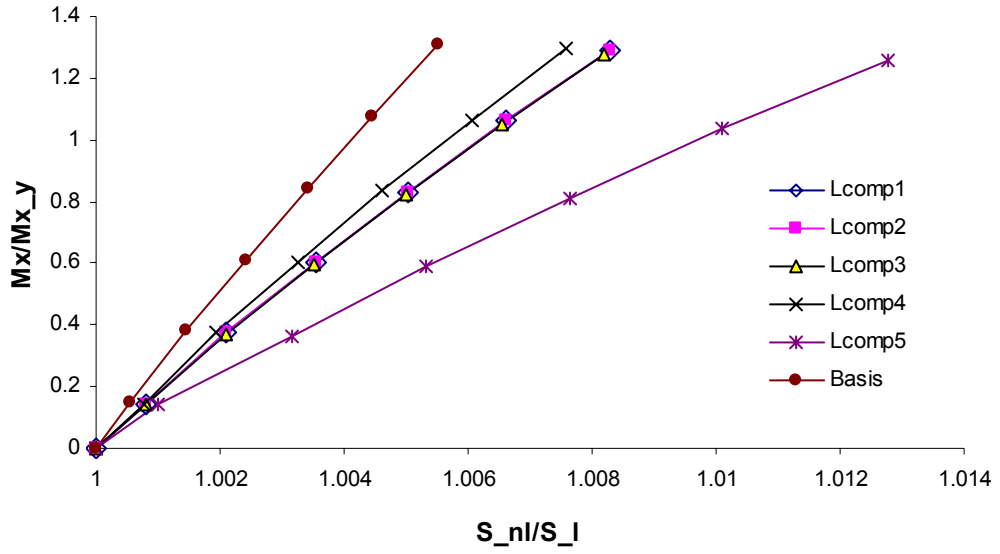


Figure 8.1 Amplification of Reference Beams

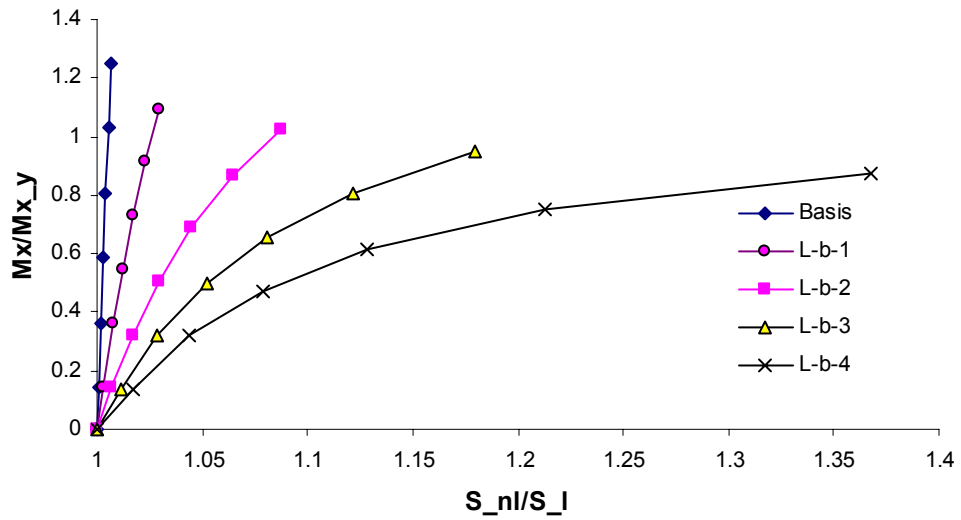


Figure 8.2 Amplification Character of L/b

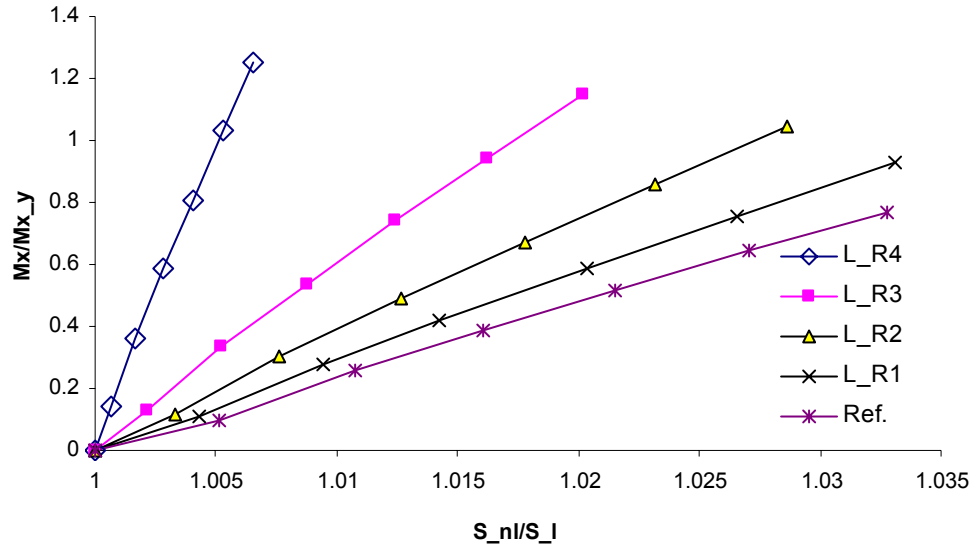


Figure 8.3 Effects of L/R on Amplification, L/b=7

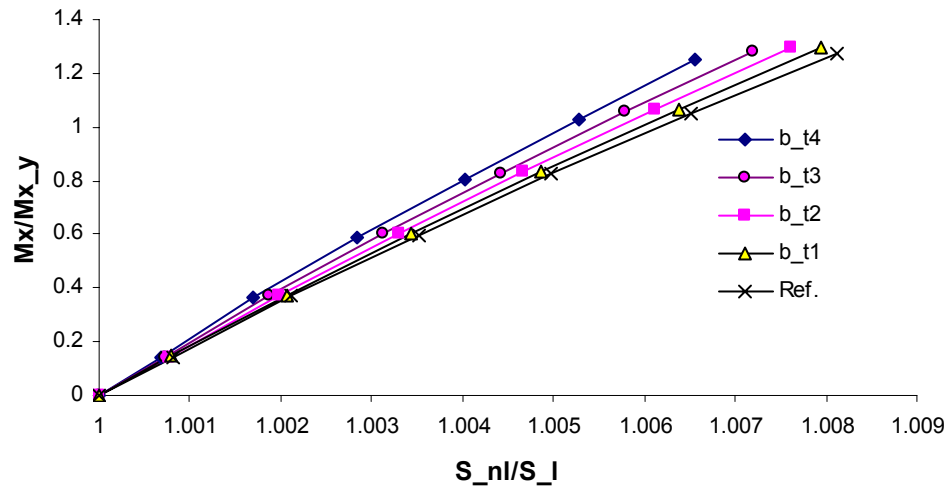


Figure 8.4 Effects of b/t on Amplification, L/b=7

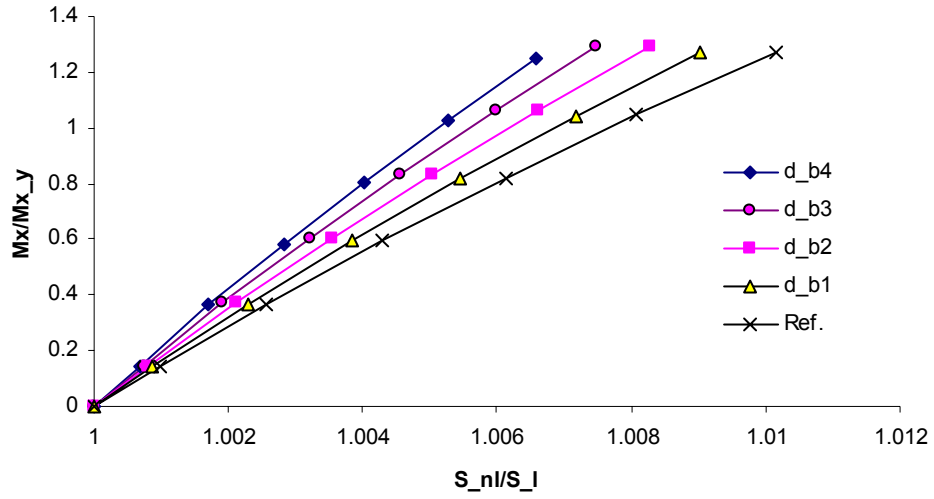


Figure 8.5 Effects of d/b on Amplification, $L/b=7$

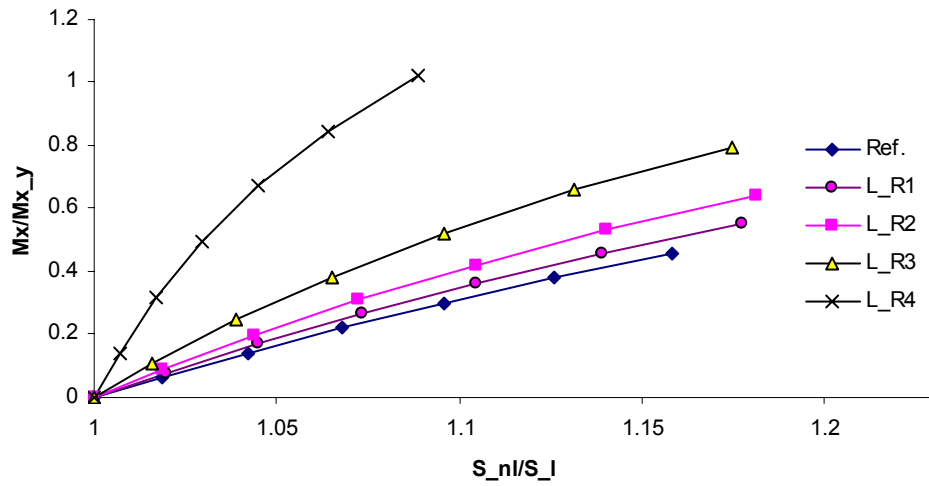


Figure 8.6 Effects of L/R on Amplification, $L/b=12$

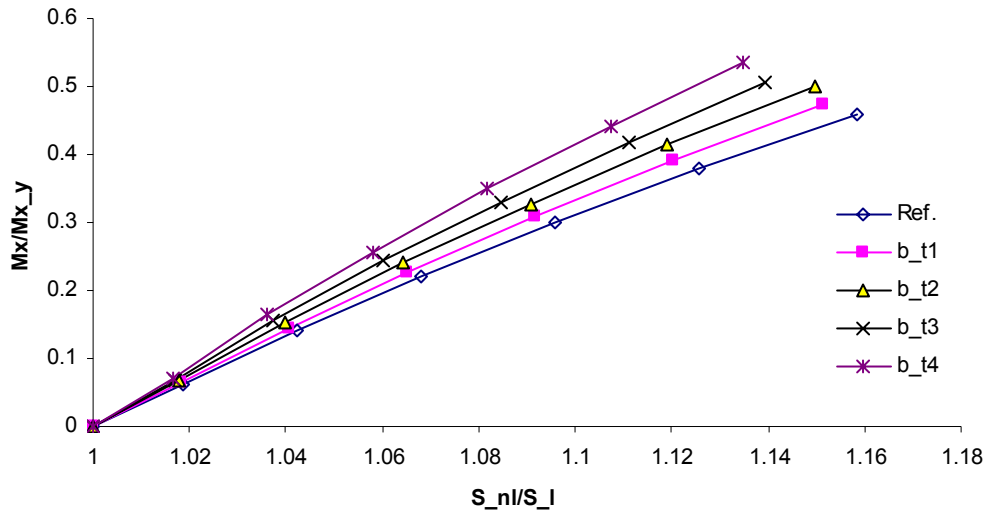


Figure 8.7 Effects of b/t on Amplification, $L/b=12$

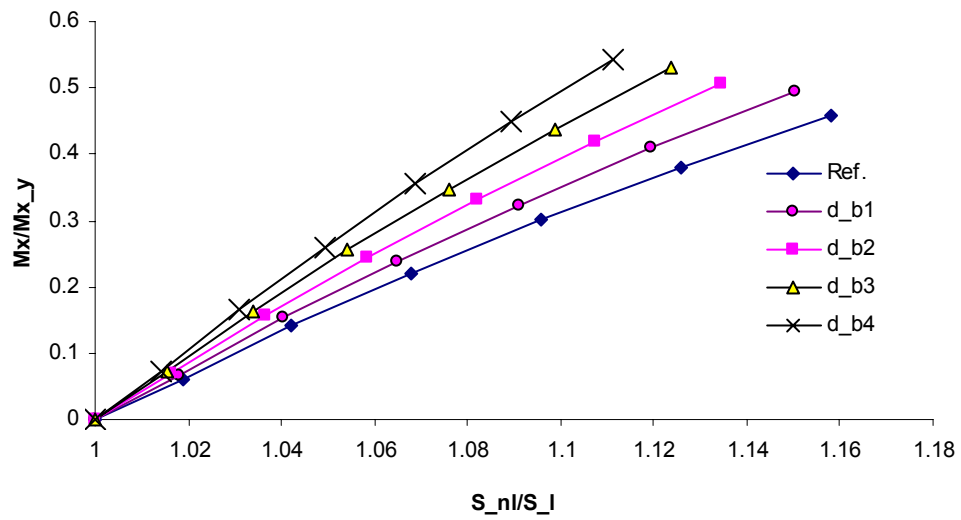


Figure 8.8 Effects of d/b on Amplification, $L/b=12$

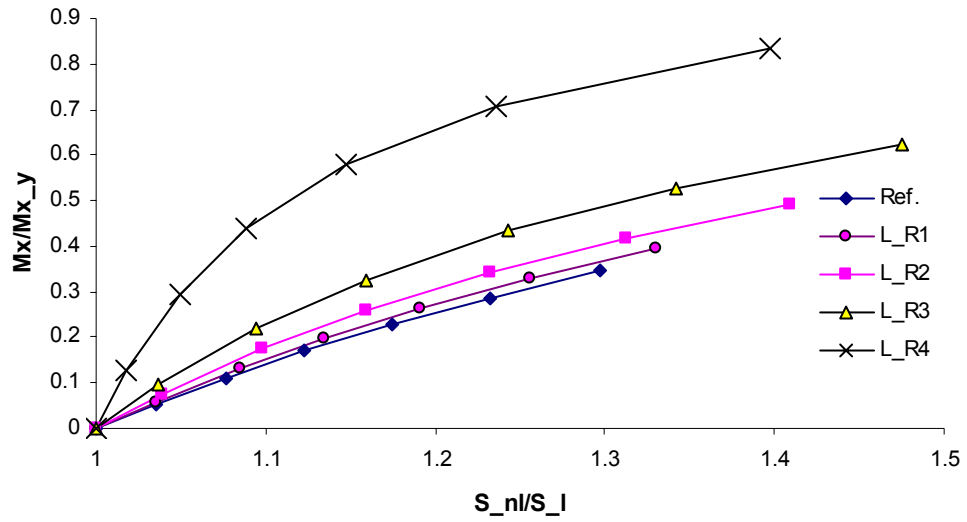


Figure 8.9 Effects of L/R on Amplification, L/b=17

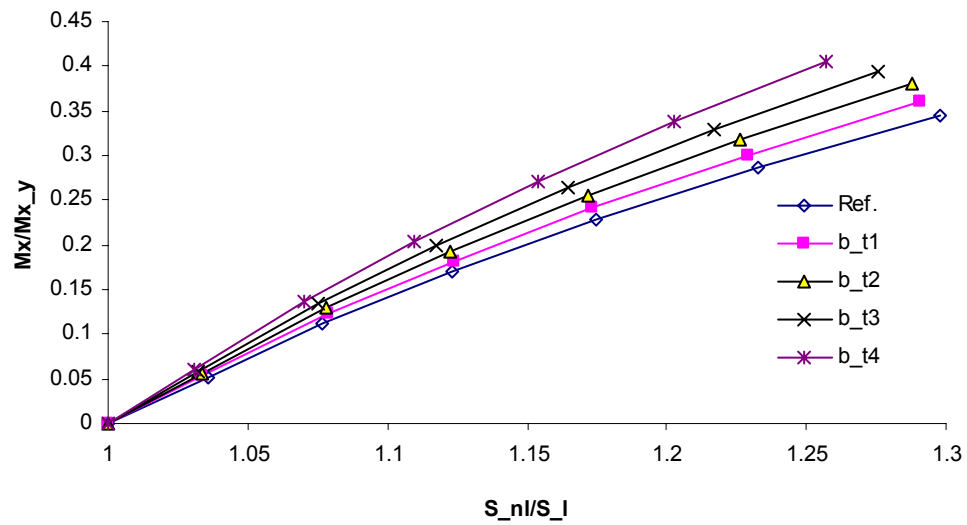


Figure 8.10 Effects of b/t on Amplification, L/b=17

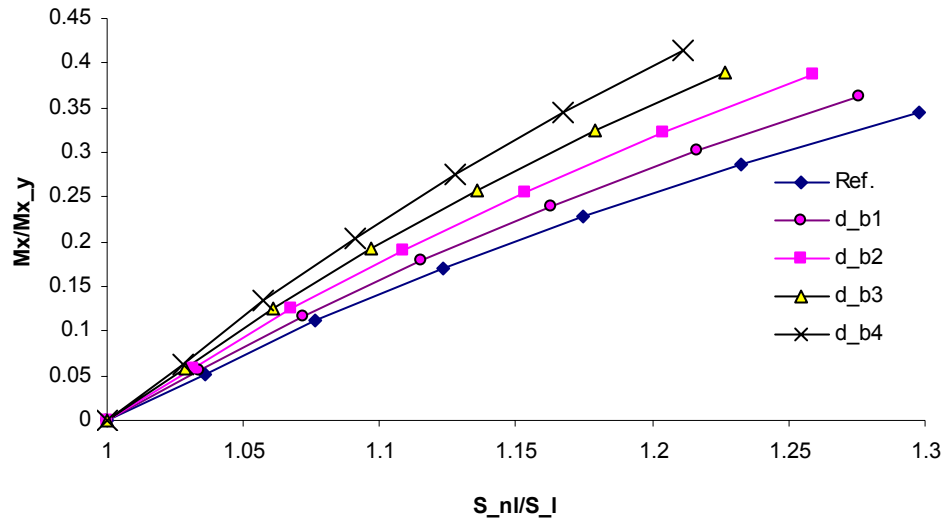


Figure 8.11 Effects of d/b on Amplification, L/b=17

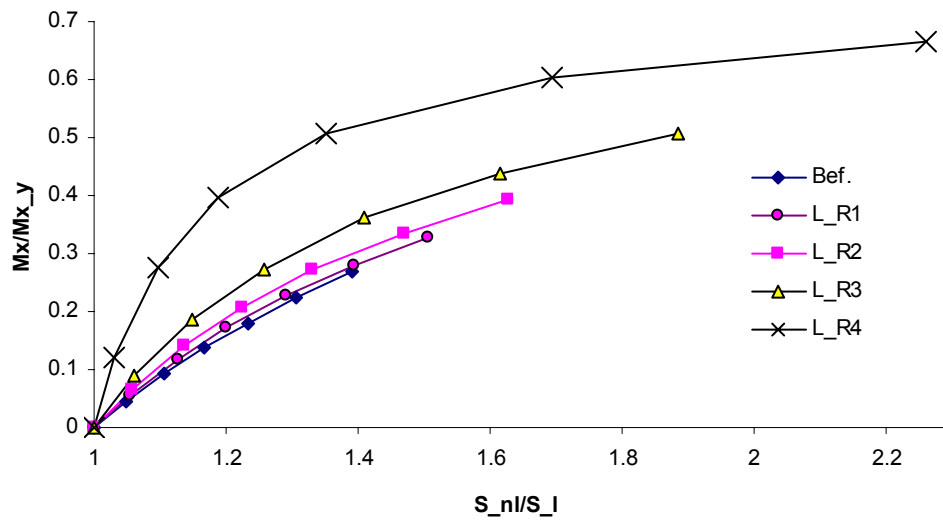


Figure 8.12 Effects of L/R on Amplification, L/b=21

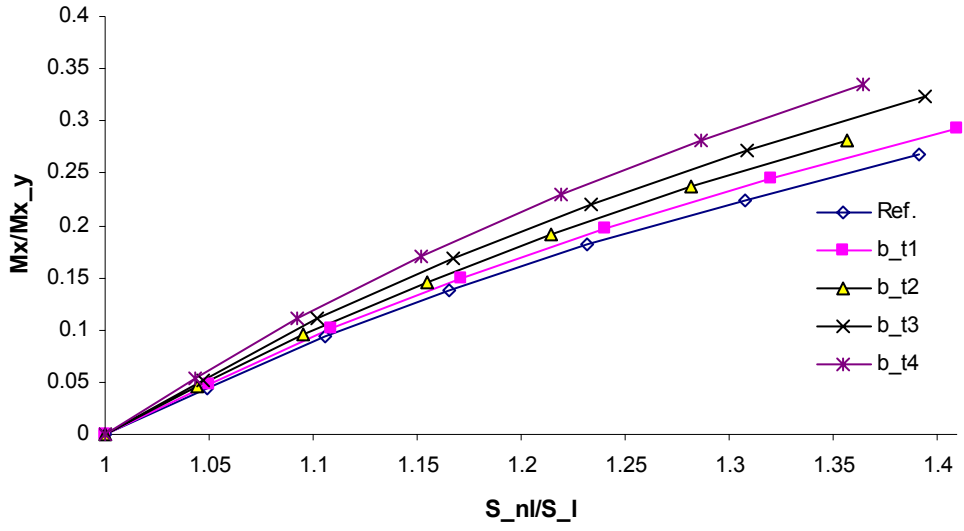


Figure 8.13 Effects of b/t on Amplification, $L/b=21$

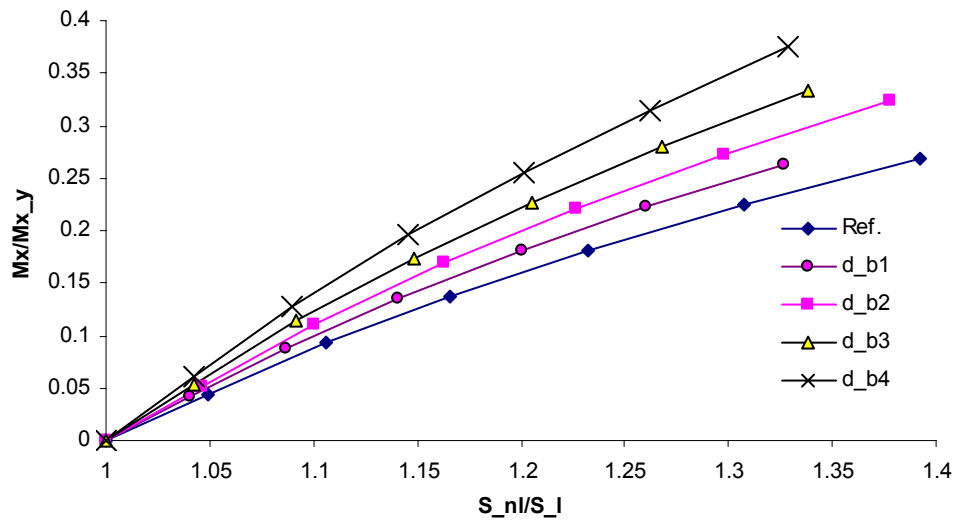


Figure 8.14 Effects of d/b on Amplification, $L/b=21$

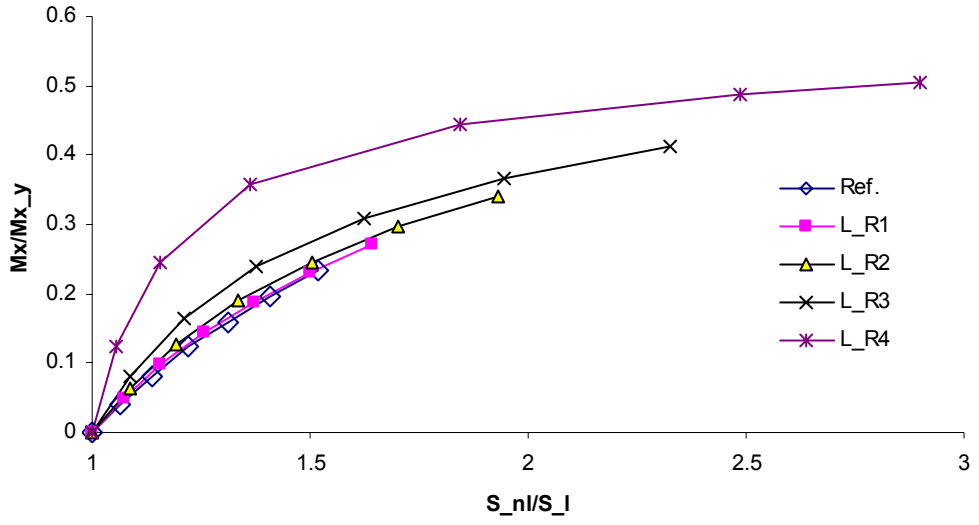


Figure 8.15 Effects of L/R on Amplification, $L/b=25$

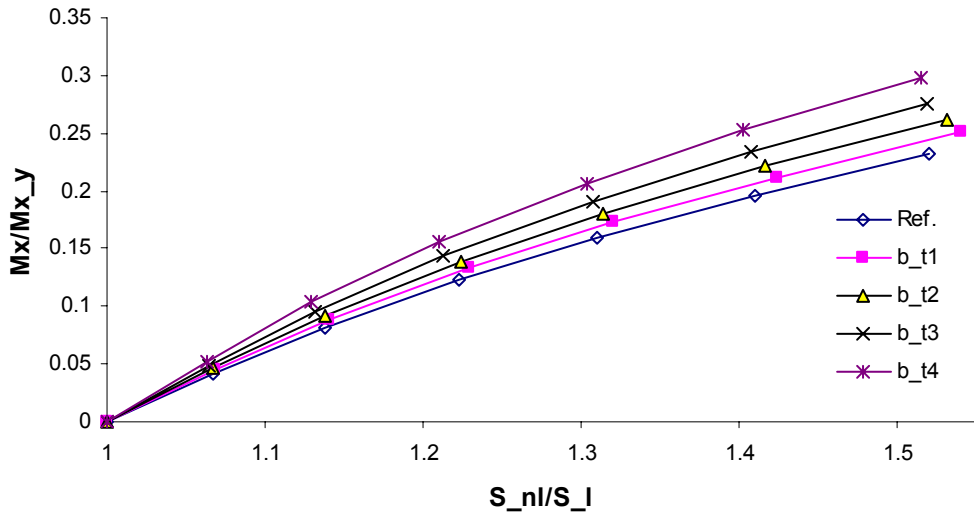


Figure 8.16 Effects of b/t on Amplification, $L/b=25$

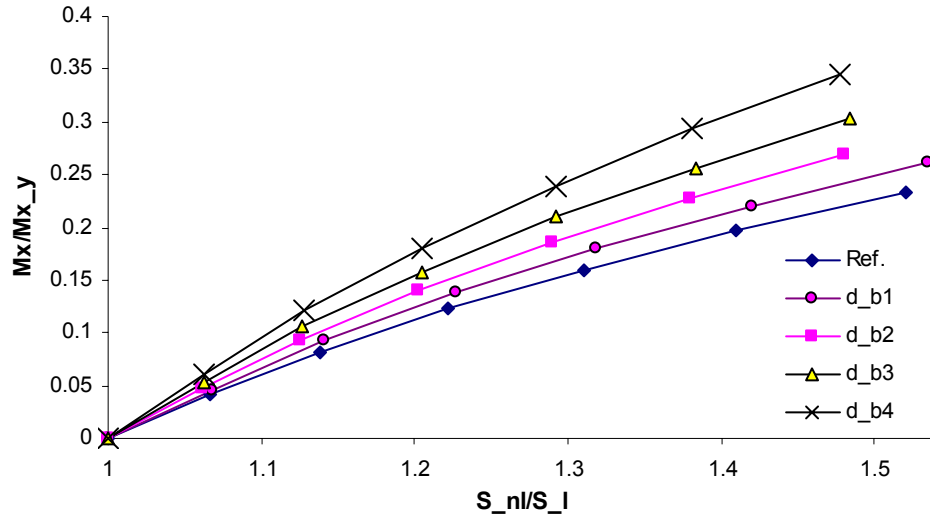


Figure 8.17 Effects of d/b on Amplification, L/b=25

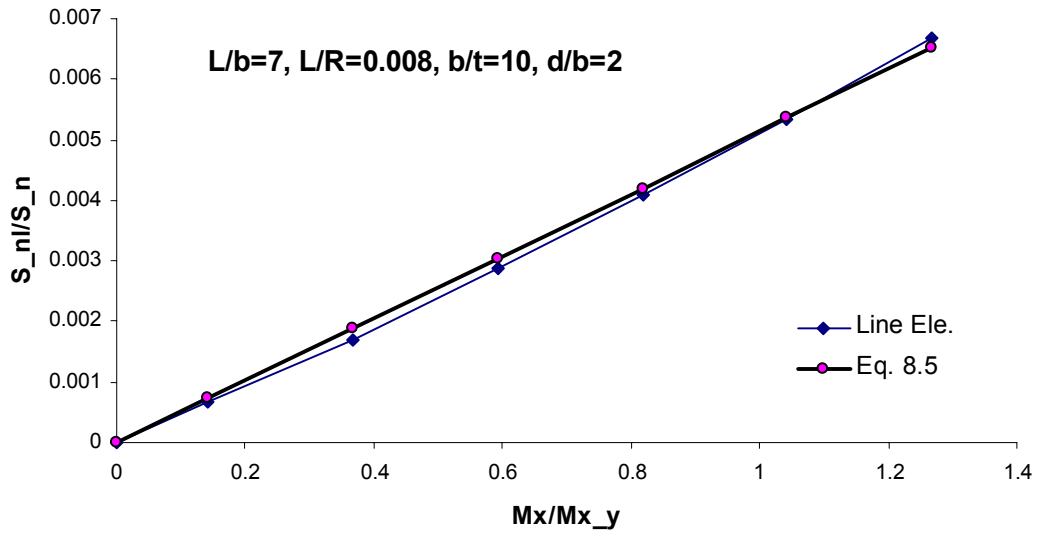


Figure 8.18 Comparisons of Line Element and Regression Analysis, Section 1

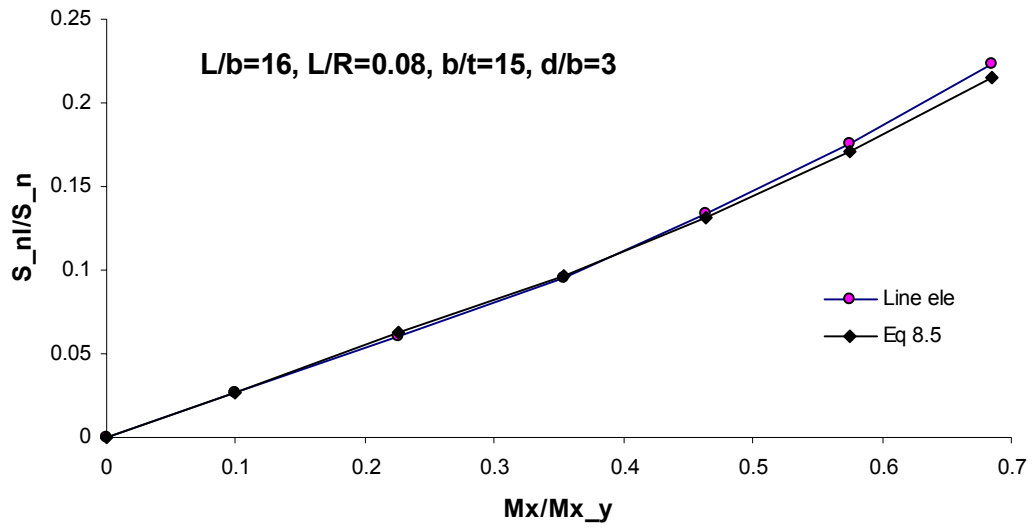


Figure 8.19 Comparisons of Line Element and Regression Analysis, Section 2

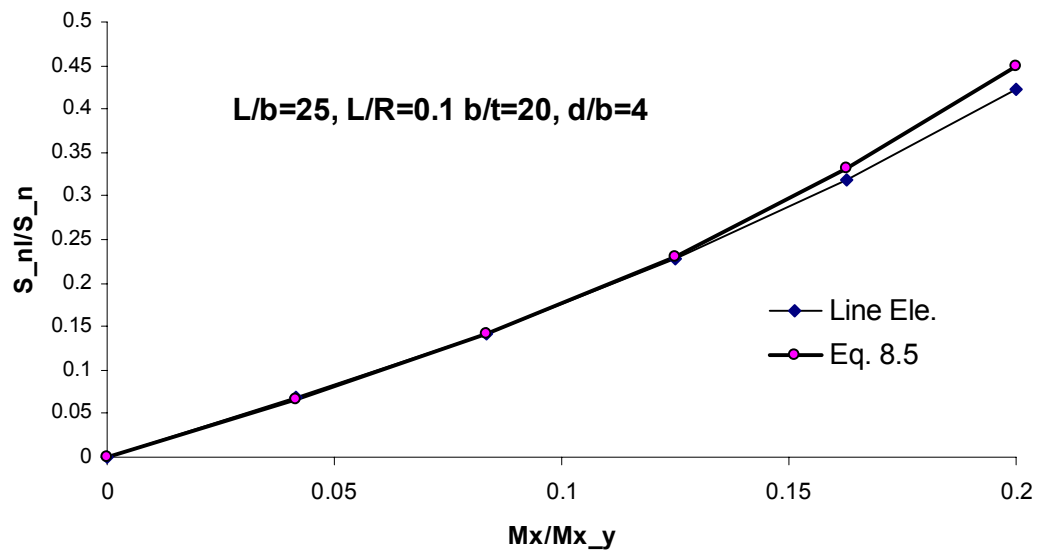


Figure 8.20 Comparisons of Line Element and Regression Analysis, Section 3

9. Summary and Conclusion

9.1 Summary

In this study, an analytical study associated with the nonlinear response of thin-walled open-section horizontally curved beam has been conducted. In chapter 3, simplified strains based on various levels of commonly used approximations have been derived. The approximations are following:

- a) The nonlinear term divided by R^2 and higher can be ignored.
- b) $(R-x)/R$ can be simplified as 1.0.
- c) The nonlinear terms divided by R can be ignored
- d) With the assumption of small rotation, trigonometric functions can be simplified by the first term of Taylor expansions.

A sensitivity study has been conducted to investigate the effects of different levels of approximation. Since the inclusion of rotation is essential in attaining an acceptable accuracy for curved beams, considering the effects of large displacements and large rotations is necessary. In Chapter 4, an incremental analysis for large deflection is developed using total Lagrangian formulation. The analysis includes warping of the cross section, sectional deformation and p-delta effect. In order to overcome difficulties in the derivation of differential equations with reference to both centroidal and shear center axes, formulas based on a single reference line are developed through proper rotational transformation. Exact solutions of displacement and warping have been obtained for linear differential equations for beams under several loading and boundary conditions.

The solution of nonlinear differential equations is impossible for spatially curved beams under general loading and boundary conditions. A finite line element with a suitable form of governing equation is established in Chapter 5. In an effort to overcome numerical difficulties for an efficient interpolation function, a shape function has been developed for the line element based on generalized linear strains. The line element has eight modes of deformation including stretching, twisting, bending, warping and sectional deformation.

For the evaluation of the line element, load-displacement curves of several beams with different cross sections and under several loading cases have been developed and compared with those by a three dimensional finite element analysis in Chapter 6. To transform the classical boundary conditions into the three-dimensional finite element model, two boundary constraints for rigid systems and free-to-deform conditions have been developed. These boundary systems provide upper and lower bound load-deflection curves. In Chapter 7, the contributions of large rotation, sectional deformation and p-delta effect on the non-linear behavior of horizontally curved beams are investigated by using the line element. In Chapter 8, an equation for calculating the maximum stress in the flanges when the beam is under equal end moment M_x is developed from regression analysis. This equation includes the effect of large displacement, large rotation and sectional deformation.

9.2. Conclusions

Based on the analysis and comparison of results from large rotation analysis, small rotation analysis, linear analysis and finite element analysis, the following conclusions can be made.

- (i) The different levels of approximation do not affect much the load-displacement behavior of horizontally curved beams (Chapter 3 and Chapter 6). Therefore, simplified strains can be used for derivation of equations.
- (ii) In the flange, computed stresses considering large displacement and large rotation are much higher than those based on linear analysis far before yielding. The difference can be as high as one third or more. Sometimes the signs of stresses are even reversed (Chapter 6). Therefore linear analysis is not adequate for stress calculation of horizontally curved beam.
- (iii) For beams with cross section of low I_w/K_T ratio, the reduction of Saint-Venant torsional resistance caused by the web deformation directly affects the total torsional moment resistance. The magnitude is dependent on the cross sectional properties (Chapter 7). Therefore the effects of sectional deformation should be considered for such beams.
- (iv) Twist rotation and the associated P-delta effect of curved beams occur as soon as an external force is applied. This effect on the behavior of horizontally curved beams is very significant and induces large displacement of the beam (Chapter 7). Therefore P-delta effect has to be considered.
- (v) By introducing proper rotational characteristics of cross sections, equations based on one reference line produces results identical to those based on two-reference lines (Chapter 4). Therefore, with additional cross sectional properties, the equations for doubly symmetric sections can be used for non-symmetric cross sections.
- (vi) The primary nonlinear behavior comes from the coupling between displacement and twist rotation. Analysis based on small rotation and large displacement does not provide accurate results (Chapter 7). In order to predict accurately the nonlinear behavior of horizontally curved beams, large rotation analysis has to be used.
- (vii) The line element for analysis of curved beams can be used for any thin-walled open cross section and beam boundary conditions to provide accurate results (Chapter 7). Also, since the line element is formulated considering sectional deformation, the element can be used for both stocky and slender cross sections.

- (viii) As an example of procedure, an equation is developed for maximum stresses in thin-walled, doubly symmetric, open cross section of horizontally curved beam under vertical bending, (Chapter 8). The equation is derived by a parametric study using the line element and a regression analysis.

9.3 Potential Future Work

- (i) In the current study, the equation for maximum stress in curved beams handles only doubly symmetric cross sections under vertical bending. The modification of this equation for singly symmetric cross sections should be examined. Modification of the equation or development of new equations should also be made for beams under different loading cases.
- (ii) All the derivation and analysis in the current study are within the elastic range of material properties. Studies based on not only geometrical nonlinearity but also material nonlinearity are recommended
- (iii) Since the design of horizontally curved beam is governed not only by deformation but also by ultimate strength, studies on ultimate strength considering displacement, rotation, and cross sectional deformation, are necessary.
- (iv) Only limited experimental studies have been conducted and most are on horizontally curved beams with doubly symmetric cross section. Additional experiments as well as studies on beams with singly symmetric cross sections are necessary.

10. REFERENCES

1. Argyris, J. (1982) "An Excursion into Large Rotations," *Computer Method in Applied Mechanics and Engineering*, 32, 85-155
2. Austin, W. J. (1971) "In-Plane Bending and Buckling of Arches," *Journal of the Structural Division*, ASCE, 97, 1575-1592
3. Austin, W. J. (1975) "Elastic Buckling of Arches Under Symmetrical Loading," *Journal of the Structural Division*, ASCE, 102, 1085-1095
4. Badawy, Hammouda E. I. (1977) "Plastic Analysis of Curved Beams under Point Loads," *Journal of the Structural Division*, ASCE, 103, 1429-1445
5. Bathe, K.J. (1996) *Finite Element Procedures*, Prentice-Hall, Inc. A Simon & Schuster Company, New Jersey
6. Bradford, M. A. (1988) "Distortional Instability of Fabricated Monosymmetric I-Beams," *Computer & Structures*, 29, 715-724
7. Bull, J. W. (1990) *Finite Element Applications to Thin-Walled Structures*, Elsevier Science Publishers, New York, NY
8. Culver, C. (1965) "Biaxial Bending of Terminally Loaded Elastic Members", *Ph.D. Dissertation*, Lehigh University, Bethlehem, Pennsylvania
9. Culver, C. and Mozer, J. (1970) "Horizontally Curved Highway Bridges – Stability of Curved Box Girders," *Report No. B1*, U.S. Department of Transportation Federal Highway Administration
10. DaDeppo, D. A. and R. Schmidt (1974) "Large Deflections and Stability of Hingeless Circular Arches Under Interacting Loads," *Journal of Applied Mechanics*, ASME, 41, 989-994
11. Culver, C. and Mozer, J. (1971) "Horizontally Curved Highway Bridges – Stability of Curved Box Girders," *Report No. B2*, U.S. Department of Transportation Federal Highway Administration
12. Davidson, J. S. (1996) "Local Buckling of Curved I-Girder Flanges," *Journal of the Structural Division*, ASCE, 122, 936-947
13. Dabrowski, R. (1968) "Curved Thin Walled Girders – Theory and Analysis," Translated by C.V. Amerongen, Cement and Concrete Association

14. Fujii, Fumio (1988) "Field Transfer Matrix for Nonlinear Curved Beams," *Journal of the Structural Division*, ASCE, 114, 675-692
15. Fukumoto, Y. and Nishada, S. (1981) "Ultimate Load Behavior of Curved I-Beams," *Journal of the Engineering Mechanics Division*, ASCE, 107, 367-385
16. Gottffeld, H. Die Berechnung Raumllich gekrummter stahlbrucken. (The analysis of spatically curved Ssteel bridges.) Die. Bautechnik. 1932. P. 715.
17. Galambos, T.V. (1968) *Prentice-Hall International Series in Theoretical and Applied Mechanics – Structural Analysis and Design Series*, Prentice-Hall, CANADA
18. Gendy, A. S. (1991) "On the Finite Element Analysis of the Spatial Response of Curved Beams with Arbitrary Thin-Walled Sections," *Computer & Structures*, 44, 639-652
19. Gendy, A. S. (1992) "Development of Effective Models for Nonlinear Static Dynamic, and Stability Analysis of Thin-Walled Structures," *Ph.D. Dissertation*, University of Akron
20. Goldberg, John E. (1952) "Torsion of I-Type and H-Type Beams," *ASCE Transactions*, 771-793
21. Goodier, J. N. and Barton, M. V. (1944) "The Effect of Web Deformation on the Torsion of I-Beams," *Journal of Applied Mechanics, Transactions of the American Society of Mechanical Engineers*, 66, A35-A40
22. "Guide Specification for the Design of Horizontally Curved Highway Bridges," American Association of State, Highway and Transportation Officials, Inc., Washington D. C., 2003
23. "Guidelines for the Design of Horizontally Curved Girder Bridges", The Hanshin Expressway Public Corporation, 1988 (English translation)
24. Gummadi, L. N. B. (1997) "Nonlinear Analysis of Beams and Arches Undergoing Large rotations," *Journal of the Engineering Mechanics Division*, ASCE, 123, 394-398
25. Harrison, H. B. (1970). "In-plane stability of parabolic arches." *Journal of the Structural Division*, ASCE, 108, 195-205

26. Howson, W. P. (1999) "Exact Out-of-Plane Natural Frequencies of Curved Timoshenko Beams," *Journal of the Engineering Mechanics Division*, ASCE, 125, 19-24
27. Huddleston, J. V. (1968) "Finite Deflections and Snap-Through of High Circular Arches," *Journal of Applied Mechanics*, ASME, 35, 763-769
28. Kang Young-Jong and Yoo (1992) "Nonlinear Theory of Thin-Walled Curved Beams and Finite Element Formulation," *Ph.D. Dissertation*, Auburn University, Auburn, Alabama
29. Kang, Young J. and Yoo (1994) "Thin-Walled Curved Beams. I: Formulation of Nonlinear Equation," *Journal of the Engineering Mechanics Division*, ASCE, 120, 2072-2101
30. Kang, Young J. (1994) "Thin-Walled Curved Beams. II: Analytical Solutions for Buckling of Arches," *Journal of the Engineering Mechanics Division*, ASCE, 120, 2102-2125
31. Kang, Kijun (1996) "Vibration Analysis of Horizontally Curved Beams with Warping Using DQM," *Journal of the Structural Division*, ASCE, 122, 657-662
32. Kim, M. (2000) "Spatial Stability of nonsymmetric Thin-Walled Curved Beams I: Analytical Approach," *Journal of the Engineering Mechanics Division*, ASCE, 126, 497-505
33. Kim, M. (2000) "Spatial Stability of nonsymmetric Thin-Walled Curved Beams II: Numerical Approach" *Journal of the Engineering Mechanics Division*, ASCE, 126, 506-514
34. Krahula, Joseph L. (1988) "Castigliano's Method for Warped Thin Curved Beams," *Journal of the Engineering Mechanics Division*, ASCE, 114, 1581-1584
35. Kuo, Shyh-Rong (1991) "New Theory on Buckling of Curved Beams," *Journal of the Engineering Mechanics Division*, ASCE, 117, 1689-1717
36. Lin, W. Y. and Hsiao, K. M. (2001) "Co-rotational Formulation for Geometric Nonlinear Analysis of Doubly Symmetric Thin-Walled Beams," *Comput. Methods Appl. Mech. Engrg.*, 190, 6023-6052
37. Love, A. E. H. *A Treatise on the Mathematical Theory of Elasticity*, 4th ed., Dover Publications, New York, N.Y.

38. McManus, Paul F. (1969) "Horizontally Curved Girders-State of the Art," *Journal of the Structural Division*, ASCE, 95, 853-870
39. McManus P. F. (1971) "Lateral Buckling of Curved Plate Girders," *Ph.D. Dissertation*, Carnegie-Mellon University, Pittsburgh, Pennsylvania Murray, David W. (1974) "Technique for Formulating Beam Equations," *Journal of the Engineering Mechanics Division*, ASCE, 101, 561-572
40. Mozer, J. and Culver, C. (1970) "Horizontally Curved Highway Bridges Stability of Curved Plate Girders," *Report No. P1*, U.S. Department of Transportation Federal Highway Administration
41. Mozer, J., Ohlson, R. and Culver, C. (1971) "Horizontally Curved Highway Bridges Stability of Curved Plate Girders," *Report No. P2*, U.S. Department of Transportation Federal Highway Administration
42. Mozer, J. and Culver, C. (1973) "Horizontally Curved Highway Bridges Stability of Curved Plate Girders," *Report No. P3*, U.S. Department of Transportation Federal Highway Administration
43. Nakai, H. and Yoo, C.H. (1988) *Analysis and Design of Curved Steel Bridges*, McGraw-Hill, New York
44. Ojalvo. (1968) "Buckling of Naturally Curved and Twisted Beams," *Journal of the Engineering Mechanics Division*, ASCE, 94, 1067-1087.
45. Ojalvo, M (1977) "Effect of Warping Restraints on I-Beam Buckling," *Journal of the Structural Division*, ASCE, 103, 2351-2361
46. Paavola, J. (1992) "A Finite Element Technique for Thin-Walled Girders," *Computer & Structures*, 44, 159-175
47. Palani G. S. (1992) "Finite Element Analysis of Thin-Walled Curved Beams Made of Composites," *Journal of the Structural Division*, ASCE, 118, 2039-2062
48. Pantazopoulou, S. J. (1992) "Low-Order Interpolation Functions for Curved Beams," *Journal of the Engineering Mechanics Division*, ASCE, 118, 329-350
49. Papangelis, T. P., and Trahair, N. S. (1987a) "Flexural-Torsional Buckling of Arches," *Journal of the Structural Division*, ASCE, 113, 889-906
50. Papangelis, T. P., and Trahair, N. S. (1987b) "Flexural-Torsional Buckling tests on arches," *Journal of the Structural Division*, ASCE, 113, 1433-1443

51. Pi, Yong Lin (1991) "Prebuckling Deflections and Lateral Buckling I: Theory," *Journal of the Structural Division*, ASCE, 118, 2949-2966
52. Pi, Yong Lin (1994) "Nonlinear Inelastic Analysis of Steel Beam-Columns. I: Theory," *Journal of the Engineering Mechanics Division*, ASCE, 120, 2041-2061
53. Pi, Yong-Lin (1994) "Prebuckling Deformations and Flexural-Torsional Buckling of Arches," *Research Report*, R695, Sch. Civ Mining Engrg, The Uni. Sydney, Australia
54. Pi, Yong-Lin and Trahair, N. S. (1994) "Three Dimensional Nonlinear Analysis of Elastic Arches," *Research Report*, R703, Sch. Civ Mining Engrg, The Uni. Sydney, Australia
55. Pi, Yong-Lin and Trahair, N. S. (1995) "Prebuckling Deformation and Flexural-Torsional Buckling of Arches," *Journal of the Structural Division*, ASCE, 121, 1313-1322
56. Pi, Yong-Lin (1996), "In-Plane Inelastic Buckling and Strength of Steel Arches" *Journal of the Structural Division*, ASCE, 122, 734-747
57. Pi, Yong-Lin and Trahair, N. S. (1996) "Nonlinear Elastic Behavior of I-Beams Curved in Plane," *Research Report*, R734, Sch. Civ Mining Engrg, The Uni. Sydney, Australia
58. Pi, Yong-Lin (1997) "Nonlinear Elastic Behavior of I-Beams Curved In Plan," *Journal of the Structural Division*, ASCE, 123, 1201-1209
59. Pi, Yong-Lin (1997) "Out-of-Plane Inelastic Buckling and Strength of Steel Arces," *Research Report*, R737, Sch. Civ Mining Engrg, The Uni. Sydney, Australia
60. Pi, Yong-Lin (1998) "Inelastic Lateral Buckling Strength and Design of Steel Arches," *Research Report*, R764, Sch. Civ Mining Engrg, The Uni. Sydney, Australia
61. Pi, Yong-Lin (1999) "In-Plane Buckling and Design of Steel Arches" *Journal of the Structural Division*, ASCE, 125, 1291-1298
62. Pi, Yong-Lin (2000) "Inelastic analysis and Behavior of Steel I-Beams Curved in Plane," *Journal of the Structural Division*, ASCE, 126, 772-779

63. Pi, Yong-Lin (2000) "Distortion and Warping at Beam Supports," *Journal of the Structural Division*, ASCE, 126, 1279-1287
64. Pi, Yong-Lin (2001) "Strength Design of Steel I-Section Beams Curved in Plane," *Journal of the Structural Division*, ASCE, 127, 639-646
65. Qaqish, Samih (1991) " Buckling Behavior of Elastic Circular Arches," *Journal of the Structural Division*, ASCE, 117, 2659-2680
66. Rajasekaran S. and Padmanabhan, E. (1982) " Discussion of Flexural-Torsional Stability of Curved Beams," *Journal of the Engineering Mechanics Division*, ASCE, 108, 144-149
67. Rajasekaran, S. and Padmanabhan, E. (1989) "Equation of Curved Beams," *Journal of the Engineering Mechanics Division*, ASCE, 115, 1094-1111
68. Reddy, J. N. (1992) *Energy and Variational Methods in Applied Mechanics – with introduction to the Finite Element Method*, John Wiley & Sons, New York
69. Saint-Venant (1843) "Memoire sur le calcul de la resistance et la flexion des pieces solides a simple ou a double courbure, en prenant simultanement en consideration les divers efforts auxquels eiles peuvent entre soumises dans tous les sens," *Compts-Rendus, l'Academie des Sciences de Paris*, vol. 17.
70. Shanmugam, N. E. (1995) "Experimental Study on Steel Beams Curved in Plan," *Journal of the Structural Division*, ASCE, 121, 249-259
71. Sheinman, I. (1982) "Large Deflectio of Curved Beam with Shear Deformation," *Journal of the Engineering Mechanics Division*, ASCE, 637-647
72. Shinke, t., zui, H., and Namita, Y. (1975). "Analysis of in-plane elasto-plastic buckling and load carrying capacity of arches." *Proc. Japan Soc. of Civ. Engrs.*, Tokyo, Japan, No. 244, 57-70.
73. Simpson, M. D. (1999) "Analytical Investigation of Curved Steel Girder Behavior," *Ph.D. Dissertation*, University of Toronto, Toronto, CANADA
74. Smith, C. V. (1969) "Effect of Shear and Load Behavior on Ring Stability," *Journal of the Engineering Mechanics Division*, ASCE, 95, 559-569
75. Sutjahjo, Edhi (1988) "Integrated Bending Field Finite Element for Curved Beams," *Journal of the Engineering Mechanics Division*, ASCE, 114, 1497-1511

76. Timoshenko, S. P., and Gere, J. M. (1961) *Theory of elastic stability*, McGraw Hill, New York, N. Y.
77. Trahair, Nicholas S. (1973) "Effect of Major Curvature on I-Beam Stability," *Journal of the Engineering Mechanics Division*, ASCE, 99, 85-98
78. Trahair, N. S. (1987) "Flexural-Torsional Buckling of Mono-symmetric Arches," *Journal of the Structural Division*, ASCE, 113, 2271-2288
79. Umanskii, A. A. *Mechanical Engineering*. Moscow, 1948, Vol.1, Part 2, Chapter IV. P. 346.
80. Usami, T., and Kuh, S. Y. (1980) "Large Displacement Theory of Thin-walled Curved Members and Its Application to Lateral-Torsional Buckling Analysis of Circular Arches," *Int. J. Solids Structures*, 16, 71-95
81. Vacharajittiphan, Porpan (1973) "Warping And Distortion at I-Section Joints," *Journal of the Structural Division*, ASCE, 100, 547-564
82. Vacharajittiphan, Porpan (1975) "Flexural-Torsional Buckling of Curved Members," *Journal of the Structural Division*, ASCE, 101, 1223-1238
83. Vlasov, V. Z. (1961) *Thin-Walled Elastic Beams*, 2nd Ed., National Science Foundation, Washington, D. C.
84. Wang, Tung-Ming (1988) "Stiffness Coefficients of Noncircular Curved Beams," *Journal of the Structural Division*, ASCE, 114, 1689-1699
85. Wang, Tung-Ming (1992) "Fixed-End Moments and Thrusts of Planar Curved Beams," *Journal of the Structural Division*, ASCE, 118, 324-331
86. Wei, Ber-Lin (1998) "The Static In-Plane Strength of Welded Steel Plate I-Girders Under Bending," *Ph.D. Dissertation*, Lehigh University, Bethlehem, Pennsylvania
87. Wicks, P. J. (1991) "General Equations for Buckling of Thin, Shallow Arches of Any Shape," *Journal of the Engineering Mechanics Division*, ASCE, 117, 225-240
88. Xanthakos, Petros P. (1994) *Theory and Design of Bridges*, John Wiley & Sons, New York
89. Yang, Yeong-Bin and Kuo, S. R. (1986) "Static Stability of Curved Thin-Walled Beams," *Journal of the Engineering Mechanics Division*, ASCE, 112, 821-841

90. Yang, Yeong-Bin, and Kuo, S. R. (1987) "Effect of Curvature on Stability of Curved Beams," *Journal of the Structural Division*, ASCE, 113, 1185-1202
91. Yang, Yeong-Bin (1989) "Curved Beam Elements for Nonlinear Analysis," *Journal of the Engineering Mechanics Division*, ASCE, 115, 840-855
92. Yang, Yeong-Bin (1991) "Use of Straight-Beam Approach to Study Buckling of Curved Beams," *Journal of the Structural Division*, ASCE, 117, 1963-1978
93. Yang, Yeong-Bin and Kuo, S.R. (1994) *Theory & Analysis of Nonlinear Framed Structures*, Simon & Schuster (Asia) Pte Ltd, Singapore
94. Yoo, Chai Hong (1980) "Matrix Formulation of Curved Girders," *Journal of the Engineering Mechanics Division*, ASCE, 105, 971-988
95. Yoo, Chai Hong (1982) "Flexural-Torsional Stability of Curved Beams," *Journal of the Engineering Mechanics Division*, ASCE, 108, 1351-1369
96. Yoo, Chai Hong (1983) "Elastic Stability of Curved Members," *Journal of the Structural Division*, ASCE, 109, 2922-2940
97. Yoo, Chai Hong (1984) "Buckling of Curved Beams with In-Plane Deformation," *Journal of the Structural Division*, ASCE, 100, 291-300
98. Yoo, Chai H., Kang, Y. J., Davidson, James S., (1996) "Buckling Analysis of Curved Beams By Finite-Element Discretization," *Journal of the Engineering Mechanics Division*, ASCE, 122, 762-770
99. Yoshida, Hiroshi (1983) "Ultimate Strength Analysis of Curved I-Beams," *Journal of the Engineering Mechanics Division*, ASCE, 109, 192-214